MSFC MPR-SAT-FE-71-1

cy

GEORGE C. MARSHALL SPACE FLIGHT CENTER

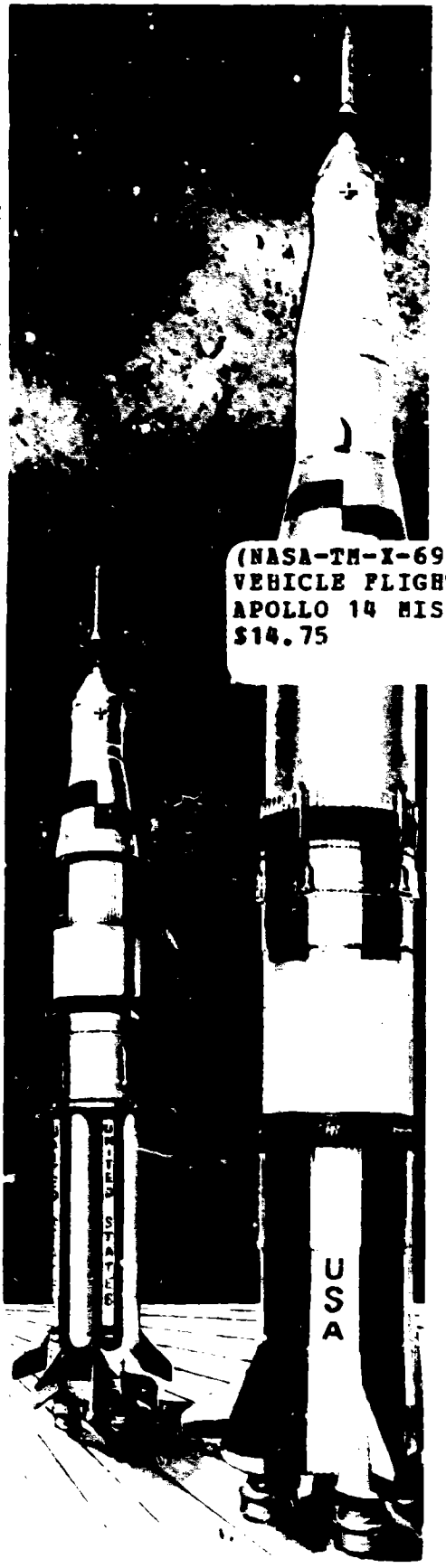

SATURN

MPR-SAT-FE-71-1

APRIL 1, 1971

(NASA-TM-X-69536) SATURN 5 LAUNCH VEHICLE FLIGHT EVALUATION REPORT-AS-509 APOLLO 14 MISSION (NASA) 253 p HC $14.75 CSCL 22C

N73-33824

Unclas G3/30 19847

SATURN V LAUNCH VEHICLE FLIGHT EVALUATION REPORT-AS-509 APOLLO 14 MISSION

NOV 1973 RECEIVED NASA STI FACILITY INPUT BRANCH

PREPARED BY

SATURN FLIGHT EVALUATION WORKING GROUP

NASA

NATIONAL AERONAUTICS AND SPACE ADMINISTRATION

GEORGE C. MARSHALL SPACE FLIGHT CENTER

MPR-SAT-FE-71-1

SATURN V LAUNCH VEHICLE

FLIGHT EVALUATION REPORT - AS-509

APOLLO 14 MISSION

PREPARED BY

SATURN FLIGHT EVALUATION WORKING GROUP

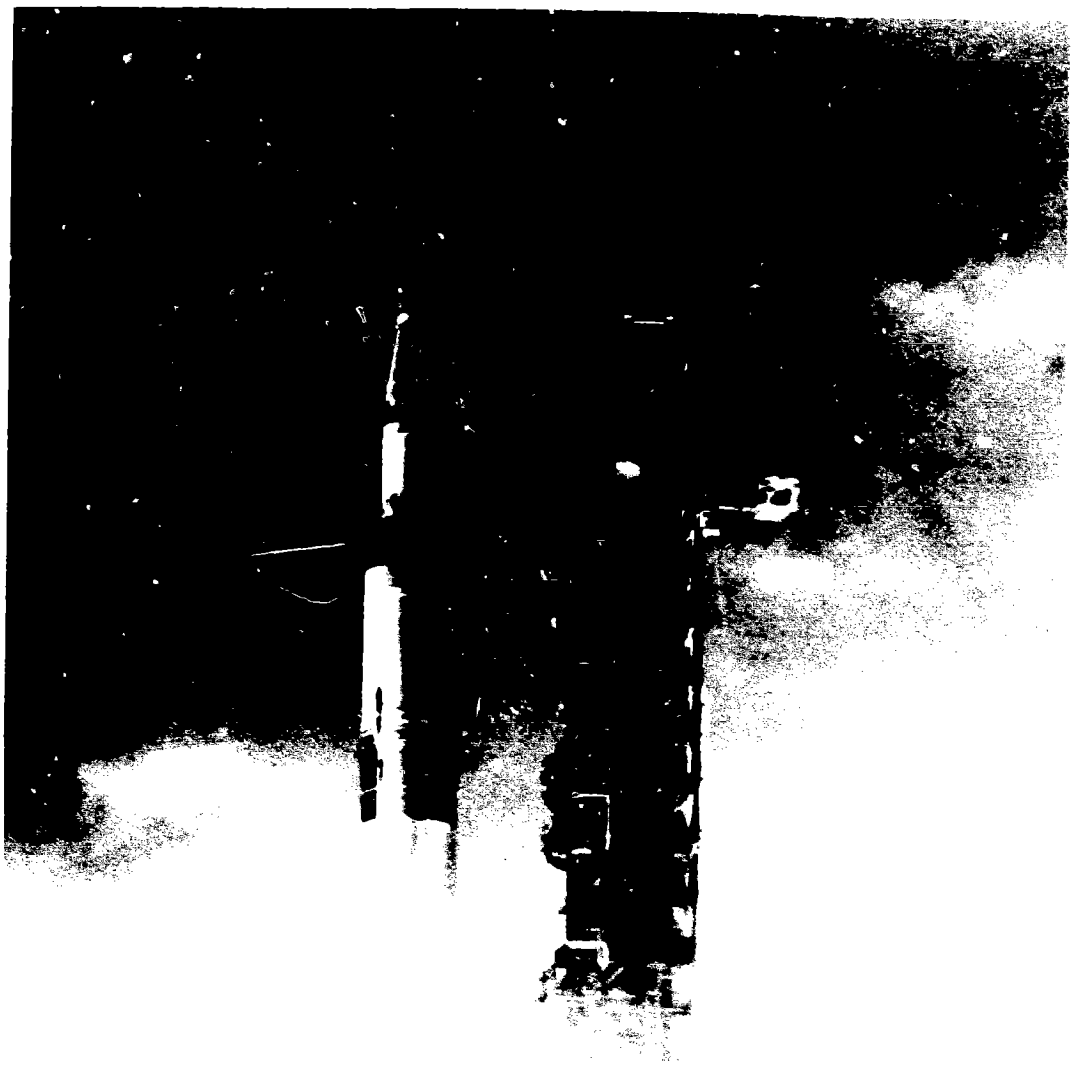

AS-509 Launch Vehicle

MPR-SAT-FE-71-1

SATURN V LAUNCH VEHICLE FLIGHT EVALUATION REPORT - AS-509

APOLLO 14 MISSION

BY

Saturn Flight Evaluation Working Group
George C. Marshall Space Flight Center

ABSTRACT

Saturn V AS-509 (Apollo 14 Mission) was launched at 16:03:02.00 Eastern Standard Time (EST) on January 31, 1971, from Kennedy Space Center, Complex 39, Pad A. Launch was originally scheduled for 15:23:00.00 EST; however, the count was held for approximately 40 minutes because of weather conditions in the launch area. The vehicle lifted off on a launch azimuth of 90 degrees east of north and rolled to a flight azimuth of 75.558 degrees east of north. The launch vehicle successfully placed the manned spacecraft in the planned translunar injection coast mode. The S-IVB/IU impacted the lunar surface within the planned target area. Preliminary assessment of data indicates that the inflight electrophoretic separation, composites casting and flow and convection demonstration were successful.

All Mandatory and Desirable Objectives of this mission for the launch vehicle were accomplished except the precise determination of the lunar impact point. It is expected that this will be accomplished at a later date. No failures, anomalies, or deviations occurred that seriously affected the mission.

Any questions or comments pertaining to the information contained in this report are invited and should be directed to:

Director, George C. Marshall Space Flight Center
Huntsville, Alabama 35812
Attention: Chairman, Saturn Flight Evaluation Working Group, S&E-CSE-LA (Phone 205-453-2462)

PRECEDING PAGE BLANK NOT FILMED

TABLE OF CONTENTS

		Page
TABLE OF CONTENTS		iii
LIST OF ILLUSTRATIONS		vi
LIST OF TABLES		ix
ACKNOWLEDGEMENT		xi
ABBREVIATIONS		xii
MISSION PLAN		xv
FLIGHT SUMMARY		xviii
MISSION OBJECTIVES ACCOMPLISHMENT		xxiv
FAILURES, ANOMALIES AND DEVIATIONS		xxv
SECTION 1 - INTRODUCTION		
1.1	Purpose	1-1
1.2	Scope	1-1
SECTION 2 - EVENT TIMES		
2.1	Summary of Events	2-1
2.2	Variable Time and Commanded Switch Selector Events	2-1
SECTION 3 - LAUNCH OPERATIONS		
3.1	Summary	3-1
3.2	Prelaunch Milestones	3-1
3.3	Countdown Events	3-1
3.4	Propellant Loading	3-1
3.4.1	RP-1 Loading	3-1
3.4.2	LOX Loading	3-3
3.4.3	LH_2 Loading	3-4
3.5	Insulation	3-4
3.6	Ground Support Equipment	3-4
3.6.1	Ground/Vehicle Interface	3-4
3.6.2	MSFC Furnished Ground Support Equipment	3-5
SECTION 4 - TRAJECTORY		
4.1	Summary	4-1
4.2	Trajectory Evaluation	4-1
4.2.1	Ascent Phase	4-1
4.2.2	Parking Orbit Phase	4-4
4.2.3	Injection Phase	4-8
4.2.4	Post TLI Phase	4-9
SECTION 5 - S-IC PROPULSION		
5.1	Summary	5-1
5.2	S-IC Ignition Transient Performance	5-1
5.3	S-IC Mainstage Performance	5-3
5.4	S-IC Engine Shutdown Transient Performance	5-3
5.5	S-IC Stage Propellant Management	5-5
5.6	S-IC Pressurization Systems	5-6
5.6.1	S-IC Fuel Pressurization System	5-6
5.6.2	S-IC LOX Pressurization System	5-7
5.7	S-IC Pneumatic Control Pressure System	5-8
5.8	S-IC Purge Systems	5-9
5.9	S-IC POGO Suppression System	5-9
5.10	S-IC Hydraulic System	5-9
SECTION 6 - S-II PROPULSION		
6.1	Summary	6-1
6.2	S-II Chilldown and Buildup Transient Performance	6-2
6.3	S-II Mainstage Performance	6-4
6.4	S-II Shutdown Transient Performance	6-6
6.5	S-II Propellant Management	6-8
6.6	S-II Pressurization System	6-11
6.6.1	S-II Fuel Pressurization System	6-11
6.6.2	S-II LOX Pressurization System	6-12
6.7	S-II Pneumatic Control Pressure System	6-16
6.8	S-II Helium Injection System	6-18
6.9	POGO Suppression System	6-18
6.10	S-II Hydraulic System	6-20
SECTION 7 - S-IVB PROPULSION		
7.1	Summary	7-1
7.2	S-IVB Chilldown and Buildup Transient Performance for First Burn	7-2

TABLE OF CONTENTS (CONTINUED)

		Page
7.3	S-IVB Mainstage Performance For First Burn	7-4
7.4	S-IVB Shutdown Transient Performance for First Burn	7-4
7.5	S-IVB Parking Orbit Coast Phase Conditioning	7-4
7.6	S-IVB Chilldown and Buildup Transient Performance for Second Burn	7-6
7.7	S-IVB Mainstage Performance for Second Burn	7-10
7.8	S-IVB Shutdown Transient Performance for Second Burn	7-10
7.9	S-IVB Stage Propellant Management	7-10
7.10	S-IVB Pressurization System	7-13
7.10.1	S-IVB Fuel Pressurization System	7-13
7.10.2	S-IVB LOX Pressurization System	7-17
7.11	S-IVB Pneumatic Control Pressure System	7-18
7.12	S-IVB Auxiliary Propulsion System	7-21
7.13	S-IVB Orbital Safing Operations	7-21
7.13.1	Fuel Tank Safing	7-23
7.13.2	LOX Tank Dumping and Safing	7-23
7.13.3	Cold Helium Dump	7-25
7.13.4	Ambient Helium Dump	7-27
7.13.5	Stage Pneumatic Control Sphere Safing	7-28
7.13.6	Engine Start Tank Safing	7-28
7.13.7	Engine Control Sphere Safing	7-28
7.14	Hydraulic System	7-26
SECTION 8 - STRUCTURES		
8.1	Summary	8-1
8.2	Total Vehicle Structures Evaluation	8-2
8.2.1	Longitudinal Loads	8-2
8.2.2	Bending Moments	8-2
8.2.3	Vehicle Dynamic Characteristics	8-3
8.3	POGO Limiting Backup Cutoff System	8-10
SECTION 9 - GUIDANCE AND NAVIGATION		
9.1	Summary	9-1
9.1.1	Performance of the Guidance and Navigation System as Implemented in the Flight Program	9-1
9.1.2	Guidance and Navigation System Components	9-1
9.2	Guidance Comparisons	9-1
9.3	Navigation and Guidance Scheme Evaluation	9-7
9.3.1	Variable Launch Azimuth	9-8
9.3.2	First Boost Period	9-10
9.3.3	Earth Parking Orbit	9-10
9.3.4	Second Boost Period	9-12
9.3.5	Post TLI Period	9-12
9.4	Guidance System Component Evaluation	9-13
9.4.1	LVDC and LVDA Performance	9-13
9.4.2	ST-124M-3 Stabilized Platform Subsystem	9-14
SECTION 10 - CONTROL AND SEPARATION		
10.1	Summary	10-1
10.2	S-IC Control System Evaluation	10-1
10.3	S-II Control System Evaluation	10-5
10.4	S-IVB Control System Evaluation	10-5
10.4.1	Control System Evaluation During First Burn	10-9
10.4.2	Control System Evaluation During Parking Orbit	10-10
10.4.3	Control System Evaluation During Second Burn	10-10
10.4.4	Control System Evaluation After S-IVB Second Burn	10-11
10.5	Instrument Unit Control Components Evaluation	10-15
10.6	Separatic	10-15
SECTION 11 - ELECTRICAL NETWORKS AND EMERGENCY DETECTION SYSTEM		
11.1	Summary	11-1
11.2	S-IC Stage Electrical System	11-1
11.3	S-II Stage Electrical System	11-2
11.4	S-IVB Stage Electrical System	11-3
11.5	Instrument Unit Electrical System	11-3
11.6	Saturn V Emergency Detection System (EDS)	11-6
SECTION 12 - VEHICLE PRESSURE ENVIRONMENT		
12.1	Summary	12-1
12.2	Base Pressures	12-1
12.2.1	S-IC Base Pressures	12-1
12.2.2	S-II Base Pressures	12-1
SECTION 13 - VEHICLE THERMAL ENVIRONMENT		
13.1	Summary	13-1
13.2	S-IC Base Heating	13-1
13.3	S-II Base Heating	13-3
13.4	Vehicle Aeroheating Thermal Environment	13-7
SECTION 14 - ENVIRONMENTAL CONTROL SYSTEMS		
14.1	Summary	14-1
14.2	S-IC Environmental Control	14-1
14.3	S-II Environmental Control	14-2
14.4	IU Environmental Control	14-2
14.4.1	Thermal Conditioning System	14-2
14.4.2	ST-124M-3 Gas Bearing System (GBS)	14-6
SECTION 15 - DATA SYSTEMS		
15.1	Summary	15-1
15.2	Vehicle Measurements Evaluation	15-1
15.3	Airborne VHF Telemetry Systems Evaluation	15-2
15.3.1	Performance Summary	15-2
15.3.2	Loss of DP1-A0 Analog Data	15-3
15.3.3	Loss of M0060-603 Guidance Computer Word	15-10
15.3.4	DP-1 Telemetry RF Output Power Fluctuations	15-11

TABLE OF CONTENTS (CONTINUED)

		Page
15.4	C-Band Radar System Evaluation	15-13
15.5	Secure Range Safety Command Systems Evaluation	15-13
15.6	Command and Communication System Evaluation	15-15
15.7	Ground Engineering Cameras	15-15
SECTION 16 - MASS CHARACTERISTICS		
16.1	Summary	16-1
16.2	Mass Evaluation	16-1
SECTION 17 - LUNAR IMPACT		
17.1	Summary	17-1
17.2	Time Base 8 Maneuvers	17-1
17.3	Trajectory Evaluation	17-2
17.4	Lunar Impact Condition	17-2
17.5	Tracking	17-3
SECTION 18 - SPACECRAFT SUMMARY		18-1
SECTION 19 - APOLLO 14 INFLIGHT DEMONSTRATIONS		
19.1	Summary	19-1
19.2	Electrophoretic Separation Demonstration	19-1
19.3	Composites Casting Demonstration	19-2
19.4	Heat Flow and Convection Demonstration	19-3
APPENDIX A - ATMOSPHERE		
A.1	Summary	A-1
A.2	General Atmospheric Conditions at Launch Time	A-1
A.3	Surface Observations at Launch Time	A-1
A.4	Upper Air Measurements	A-3
A.4.1	Wind Speed	A-5
A.4.2	Wind Direction	A-5
A.4.3	Pitch Wind Component	A-5
A.4.4	Yaw Wind Component	A-5
A.4.5	Component Wind Shears	A-5
A.4.6	Extreme Wind Data in the High Dynamic Region	A-5
A.5	Thermodynamic Data	A-13
A.5.1	Temperature	A-13
A.5.2	Atmospheric Pressure	A-13
A.5.3	Atmospheric Density	A-13
A.5.4	Optical Index of Refraction	A-13
A.6	Comparison of Selected Atmospheric Data for Saturn V Launches	A-13
APPENDIX B - AS-509 SIGNIFICANT CONFIGURATION CHANGES		
B.1	Introduction	B-1

LIST OF ILLUSTRATIONS

Figure		Page
2-1	Ground Station Time to Vehicle Time Conversion	2-3
4-1	Ascent Trajectory Position Comparison	4-2
4-2	Ascent Trajectory Space-Fixed Velocity and Flight Path Angle Comparisons	4-3
4-3	Ascent Trajectory Acceleration Comparison	4-3
4-4	Dynamic Pressure and Mach Number Comparisons	4-4
4-5	Ground Track	4-9
4-6	Injection Phase Space-Fixed Velocity and Flight Path Angle Comparisons	4-10
4-7	Injection Phase Acceleration Comparison	4-11
5-1	S-IC LOX Start Box Requirements	5-2
5-2	S-IC Engines Thrust Buildup	5-2
5-3	S-IC Stage Propulsion Performance	5-4
5-4	S-IC Stage Fuel Tank Ullage Pressure	5-7
5-5	S-IC LOX Tank Ullage Pressure	5-8
6-1	S-II Engine Start Tank Performance	6-5
6-2	S-II Engine Pump Inlet Start Requirements	6-5
6-3	S-II Steady State Operation	6-7
6-4	S-II Outboard Engine Chamber Pressure Decay	6-10
6-5	S-II Fuel Tank Ullage Pressure	6-12
6-6	S-II Fuel Pump Inlet Conditions	6-13
6-7	S-II LOX Tank Ullage Pressure	6-14
6-8	S-II Oxidizer Manifold Pressure and Regulator Potentiometer Profiles	6-15
6-9	S-II LOX Tank Pressurization Regulator	6-16
6-10	S-II LOX Pump Inlet Conditions	6-17
6-11	S-II LOX Center Engine Feedline Accumulator and Helium Injection System	6-18
6-12	S-II Center Engine LOX Feedline Accumulator Bleed System Performance	6-19
6-13	S-II Center Engine LOX Feedline Accumulator Fill Transient	6-20
6-14	S-II Center Engine LOX Feedline Accumulator Helium Supply System Performance	6-21
7-1	S-IVB Start Box and Run Requirements - First Burn	7-3
7-2	S-IVB Steady-State Performance - First Burn	7-5
7-3	S-IVB CVS Performance - Coast Phase	7-7
7-4	S-IVB Ullage Conditions During Repressurization Using O_2/H_2 Burner	7-8
7-5	S-IVB O_2/H_2 Burner Thrust and Pressurant Flowrate	7-8
7-6	S-IVB Start Box and Run Requirements - Second Burn	7-9
7-7	S-IVB Steady-State Performance - Second Burn	7-11
7-8	S-IVB LH_2 Ullage Pressure - First Burn and Parking Orbit	7-14
7-9	S-IVB LH_2 Ullage Pressure - Second Burn and Translunar Coast	7-15
7-10	S-IVB Fuel Pump Inlet Conditions - First Burn	7-16
7-11	S-IVB Fuel Pump Inlet Conditions - Second Burn	7-16
7-12	S-IVB LOX Tank Ullage Pressure - First Burn and Earth Parking Orbit	7-17
7-13	S-IVB LOX Pump Inlet Conditions - First Burn	7-19
7-14	S-IVB LOX Pump Inlet Conditions - Second Burn	7-19
7-15	S-IVB Cold Helium Supply History	7-20

LIST OF ILLUSTRATIONS (CONTINUED)

Figure		Page
7-16	APS Helium Bottle Conditions	7-22
7-17	S-IVB LOX Dump and Orbital Safing Sequence	7-25
7-18	S-IVB LOX Tank Ullag Pressure - Second Burn and Translunar Coast	7-26
7-19	S-IVB LOX Dump Parameter Histories	7-27
8-1	Longitudinal Acceleration at IU During Thrust Buildup and Launch	8-2
8-2	Longitudinal Load at Time of Maximum Bending Moment, CECO and OECO	8-3
8-3	Bending Moment Distribution at Time of Maximum Bending Moment	8-4
8-4	IU Accelerometer Response During S-IC Burn	8-5
8-5	Longitudinal Acceleration at IU at S-IC CECO and OECO	8-6
8-6	AS-509/AS-508 Acceleration and Pressure Oscillations During S-II Burn (8 to 20 Hz Filter)	8-7
8-7	AS-509 Pump Inlet Pressure and Thrust Pad Acceleration Oscillations During Accumulator Fill Transient (0 to 110 Hertz Filter)	8-8
8-8	S-II Engine 1 LOX Pump Inlet Pressure Contourgram/NPSP Comparison	8-9
8-9	G-Switch Performance	8-11
9-1	Trajectory and ST-124M-3 Platform Velocity Comparison Boost-to-EPO (Trajectory Minus Guidance)	9-2
9-2	Trajectory and ST-124M-3 Platform Velocity Comparison at S-IVB Second Burn (Trajectory Minus Guidance)	9-3
9-3	LH_2 Continuous Vent Thrust During Parking Orbit	9-6
9-4	Attitude Commands During Boost-to-EPO	9-11
9-5	Attitude Commands During S-IVB Second Burn	9-11
9-6	Switch Selector Bit 5 Driver Monitor Circuit	9-15
9-7	Accelerometer Head Deflections	9-16
10-1	Pitch and Yaw Plane Dynamics During S-IC Burn	10-3
10-2	Angle-of-Attack During S-IC Burn	10-6
10-3	Total Angle-of-Attack at Q-Ball	10-7
10-4	Pitch and Yaw Plan Attitude Errors During S-II Burn	10-8
10-5	Pitch and Yaw Attitude Errors During S-IVB First Burn	10-9
10-6	Pitch Attitude Error During Parking Orbit	10-11
10-7	Pitch and Yaw Attitude Errors During S-IVB Second Burn	10-12
10-8	Pitch Attitude Error During Translunar Coast	10-14
11-1	S-IVB Stage Forward No. 1 Battery Voltage and Current	11-4
11-2	S-IVB Stage Forward No. 2 Battery Voltage and Current	11-4
11-3	S-IVB Stage Aft No. 1 Battery Voltage and Current	11-5
11-4	S-IVB Stage Aft No. 2 Battery Voltage and Current	11-5
11-5	IU Battery 6D10 Voltage, Current, and Temperature	11-8
11-6	IU Battery 6D20 Voltage, Current, and Temperature	11-9
11-7	IU Battery 6D30 Voltage, Current, and Temperature	11-10
11-8	IU Battery 6D40 Voltage, Current, and Temperature	11-11
12-1	S-IC Base Heat Shield Differential Pressure	12-2
12-2	S-II Heat Shield Forward Face Pressure	12-2
12-3	S-II Thrust Cone Pressure	12-3
12-4	S-II Heat Shield Aft Face Pressure	12-3
13-1	S-IC Base Region Total Heating Rate	13-2
13-2	S-IC Base Region Gas Temperature	13-2
13-3	S-IC Ambient Gas Temperature Under Engine Cocoon	13-3
13-4	S-II Heat Shield Aft Heat Rate	13-4
13-5	S-II Heat Shield Recovery Temperature	13-5
13-6	S-II Heat Shield Aft Radiation Heat Rate	13-6
13-7	Forward Location of Separated Flow on S-IC Stage	13-8
14-1	IU TCS Coolant Control Temperature	14-2
14-2	IU Sublimator Performance During Ascent	14-3
14-3	IU TCS Hydraulic Performance	14-4
14-4	IU TCS GN_2 Sphere Pressure	14-5
14-5	Selected IU Component Temperatures	14-6
14-6	IU Inertial Platform GN_2 Pressures	14-7
14-7	IU GBS GN_2 Sphere Pressure	14-8
15-1	VHF Telemetry Coverage Summary	15-9
15-2	DP1-A0 270 Multiplexer Analog Data	15-11
15-3	6D31 Bus Voltage	15-12
15-4	6D30 Battery Current	15-12
15-5	C-Band Radar Coverage Summary	15-14
15-6	CCS Coverage Summary	15-16
17-1	Accumulated Longitudinal Velocity Change During Time Base 8	17-3
17-2	Lunar Impact Trajectory Radius and Space-Fixed Velocity Profiles	17-5

LIST OF ILLUSTRATIONS (CONTINUED)

Figure		Page
17-3	Comparison of Lunar Impact Points	17-6
17-4	Summary of CCS Tracking Data Used for Post TLI Orbit	17-8
A-1	Surface Weather Map Approximately 9 Hours Before Launch of AS-509	A-2
A-2	500 Millibar Map Approximately 9 Hours Before Launch of AS-509	A-3
A-3	Scalar Wind Speed at Launch Time of AS-509	A-6
A-4	Wind Direction at Launch Time of AS-509	A-7
A-5	Pitch Wind Velocity Component (W_X) at Launch Time of AS-509	A-8
A-6	Yaw Wind Velocity Component (W_Z) at Launch Time of AS-509	A-9
A-7	Pitch (S_X) and Yaw (S_Z) Component Wind Shears at Launch Time of AS-509	A-10
A-8	Relative Deviation of Temperature and Pressure from the PRA-63 Reference Atmosphere, AS-509	A-14
A-9	Relative Deviation of Density and Absolute Deviation of the Index of Refraction from the PRA-63 Reference Atmosphere, AS-509	A-15

LIST OF TABLES

Table		Page
1	Mission Objectives Accomplishment	
2	Summary of Deviations	
2-1	Time Base Summary	2-3
2-2	Significant Event Times Summary	2-4
2-3	Variable Time and Command Switch Selector Events	2-10
3-1	AS-509/Apollo 14 Prelaunch Milestones	3-2
4-1	Comparison of Significant Trajectory Events	4-5
4-2	Comparison of Cutoff Events	4-6
4-3	Comparison of Separation Events	4-7
4-4	Parking Orbit Insertion Conditions	4-8
4-5	Translunar Injection Conditions	4-11
5-1	S-IC Individual Standard Sea Level Engine Performance	5-5
5-2	S-IC Stage Propellant Mass History	5-6
6-1	S-II Engine Performance	6-8
6-2	S-II Engine Performance Shifts	6-9
6-3	AS-509 Flight S-II Propellant Mass History	6-11
7-1	S-IVB Steady-State Performance - First Burn (STDV +130-Second Time Slice at Standard Altitude Conditions)	7-6
7-2	S-IVB Steady-State Performance - Second Burn (STDV +200-Second Time Slice at Standard Altitude Conditions)	7-12
7-3	S-IVB Stage Propellant Mass History	7-13
7-4	S-IVB APS Propellant Consumption	7-24
8-1	S-II Engine No. 1 Peak Response Summary for Post CECO 11 Hertz Oscillations	8-8
9-1	Inertial Platform Velocity Comparisons (PACSS 12 Coordinate System)	9-4
9-2	Guidance Comparisons (PACSS 13)	9-5
9-3	Contributing Factors to Space Fixed Component Differences (OMPT - VD)	9-7
9-4	State Vector Differences at Translunar Injection	9-8
9-5	AS-509 Guidance System Accuracy	9-9
9-6	Parking Orbit Insertion Parameters	9-12
9-7	Translunar Injection Parameters	9-13
10-1	Maximum Control Parameters During S-IC Flight	10-2
10-2	AS-509 Liftoff Misalignment Summary	10-4
10-3	Maximum Control Parameters During S-II Burn	10-8
10-4	Maximum Control Parameters During S-IVB First Burn	10-10
10-5	Maximum Control Parameters During S-IVB Second Burn	10-13
11-1	S-IC Stage Battery Power Consumption	11-1
11-2	S-II Stage Battery Power Consumption	11-2
11-3	S-IVB Stage Battery Power Consumption	11-6
11-4	IU Battery Power Consumption	11-7
15-1	AS-509 Measurement Summary	15-2
15-2	AS-509 Flight Measurements Waived Prior to Flight	15-3
15-3	AS-509 Measurement Malfunctions	15-4
15-4	AS-509 Questionable Flight Measurements	15-7
15-5	AS-509 Launch Vehicle Telemetry Links	15-8
15-6	Command and Communication System Command History, AS-509	15-17
16-1	Total Vehicle Mass--S-IC Burn Phase--Kilograms	16-3
16-2	Total Vehicle Mass--S-IC Burn Phase--Pounds Mass	16-3

LIST OF TABLES (CONTINUED)

Table		Page
16-3	Total Vehicle Mass--S-II Burn Phase--Kilograms	16-4
16-4	Total Vehicle Mass--S-II Burn Phase--Pounds Mass	16-4
16-5	Total Vehicle Mass--S-IVB First Burn Phase--Kilograms	16-5
16-6	Total Vehicle Mass--S-IVB First Burn Phase--Pounds Mass	16-5
16-7	Total Vehicle Mass-S-IVB Second Burn Phase--Kilograms	16-6
16-8	Total Vehicle Mass--S-IVB Second Burn Phase--Pounds Mass	16-6
16-9	Flight Sequence Mass Summary	16-7
16-10	Mass Characteristics Comparison	16-9
17-1	Lunar Targeting Maneuvers	17-4
17-2	Geocentric O Parameters Following A'S Lunar Impact Burn	17-5
17-3	S-IVB/IU Lunar Impact Parameters	17-7
17-4	Summary of Lunar Impact Times	17-7
17-5	S-IVB/IU CCS Tracking Network	17-8
19-1	Specimen List and Abbreviated Procedure	19-5
A-1	Surface Observations at AS-509 Launch Time	A-2
A-2	Solar Radiation . AS-509 Launch Time, Launch Pad 39A	A 4
A-3	Systems Used to Measure Upper Air Wind Data for AS-509	A-4
A-4	Maximum Wind Speed in High Dynamic Pressure Region for Apollo/Saturn 501 through Apollo/Saturn 509 Vehicles	A-11
A-5	Extreme Wind Shear Values in the High Dynamic Pressure Region for Apollo/Saturn 501 through Apollo/Saturn 509 Vehicles	A-12
A-6	Selected Atmospheric Observations for Apollo/Saturn 501 through Apollo/Saturn 509 Vehicle Launches at Kennedy Space Center, Florida	A-16
B-1	S-IC Significant Configuration Changes	B-1
B-2	S-II Significant Configuration Changes	B-2
B-3	S-IVB Significant Configuration Changes	B-2
B-4	IU Significant Configuration Changes	B-3
B-5	Spacecraft Significant Configuration Changes	B-4

ACKNOWLEDGEMENT

This report is published by the Saturn Flight Evaluation Working Group, composed of representatives of Marshall Space Flight Center, John F. Kennedy Space Center, and MSFC's prime contractors, and in cooperation with the Manned Spacecraft Center. Significant contributions to the evaluation have been made by:

George C. Marshall Space Flight Center

Science and Engineering

Central Systems Engineering
Aero-Astrodynamics Laboratory
Astrionics Laboratory
Computation Laboratory
Astronautics Laboratory

Program Management

John F. Kennedy Space Center

Manned Spacecraft Center

The Boeing Company

McDonnell Douglas Astronautics Company

International Business Machines Company

North American Rockwell/Space Division

North American Rockwell/Rocketdyne Division

ABBREVIATIONS

ACN	Ascension Island
ACS	Alternating Current Power Supply
ALSEP	Apollo Lunar Surface Experiments Package
ANT	Antigua
AOS	Acquisition of Signal
APS	Auxiliary Propulsion System
ARIA	Apollo Range Instrument Aircraft
ASC	Accelerometer Signal Conditioner
BDA	Bermuda
CIF	Central Instrumentation Facility
CCS	Command and Communications System
CDDT	Countdown Demonstration Test
CECO	Center Engine Cutoff
CG	Center of Gravity
CM	Command Module
CNV	Cape Kennedy
CRO	Carnarvon
CRP	Computer Reset Pulse
CSM	Command and Service Module
CT4	Cape Telemetry 4
CVS	Continuous Vent System
CYI	Grand Canary Island
DDAS	Digital Data Acquisition System
DEE	Digital Events Evaluator
DNA	Deoxyribonucleic Acid
DO	Desirable Objective
DOM	Data Output Multiplexer
DTS	Data Transmission System
EBW	Exploding Bridge Wire
ECO	Engine Cutoff
ECP	Engineering Change Proposal
ECS	Environmental Control System
EDS	Emergency Detection System
EMR	Engine Mixture Ratio
EPO	Earth Parking Orbit
ESC	Engine Start Command
EST	Eastern Standard Time
ETC	Goddard Experimental Test Center
ETW	Error Time Word
EVA	Extra-Vehicular Activity
FCC	Flight Control Computer
FM/FM	Frequency Modulation/ Frequency Modulation
FRT	Flight Readiness Test
GBI	Grand Bahama Island
GBS	Gas Bearing System
GFCV	GOX Flow Control Valve

ABBREVIATIONS (CONTINUED)

GDS	Goldstone
GG	Gas Generator
GOX	Gaseous Oxygen
GRR	Guidance Reference Release
GSE	Ground Support Equipment
GSFC	Goddard Space Flight Center
GTK	Grand Turk Island
GWM	Guam
HAW	Hawaii
HDA	Holddown Arm
HFCV	Helium Flow Control Valve
HSK	Honeysuckle Creek
IGM	Iterative Guidance Mode
IMU	Inertial Measurement Unit
IU	Instrument Unit
KSC	Kennedy Space Center
LET	Launch Escape Tower
LH_2	Liquid Hydrogen
LM	Lunar Module
LMR	Launch Mission Rule
LOI	Lunar Orbit Insertion
LOS	Loss of Signal
LOX	Liquid Oxygen
LUT	Launch Umbilical Tower
LV	Launch Vehicle
LVDA	Launch Vehicle Data Adapter
LVDC	Launch Vehicle Digital Computer
LVGSE	Launch Vehicle Ground Support Equipment
MAD	Madrid
MAP	Message Acceptance Pulse
MCC-H	Mission Control Center - Houston
MILA	Merritt Island Launch Area
ML	Mobile Launcher
MO	Mandatory Objective
MOV	Main Oxidizer Valve
MR	Mixture Ratio
MRCV	Mixture Ratio Control Valve
MSC	Manned Spacecraft Center
MSFC	Marshall Space Flight Center
MSFN	Manned Space Flight Network
MSS	Mobile Service Structure
MTF	Mississippi Test Facility
M/W	Methanol Water
NPSP	Net Positive Suction Pressure
NPV	Nonpropulsive Vent
NASA	National Aeronautics and Space Administration
OAT	Overall Test
OCP	Orbital Correction Program
OECO	Outboard Engine Cutoff
OFSO	Overfill Shutoff Sensor
OMPT	Postflight Trajectory
OT	Operational Trajectory
PAFB	Patrick Air Force Base
PCM	Pulse Code Modulation
PCM/FM	Pulse Code Modulation/ Frequency Modulation
PEA	Platform Electronics Assembly

ABBREVIATIONS (CONTINUED)

PIO	Process Input/Output
POI	Parking Orbit Insertion
PMR	Programed Mixture Ratio
PRA	Patrick Reference Atmosphere
PTCS	Propellant Tanking Computer System
PU	Propellant Utilization
RF	Radiofrequency
RFI	Radiofrequency Interference
RMS	Root Mean Square
RP-1	Designation for S-IC Stage Fuel (kerosene)
SA	Service Arm
SC	Spacecraft
SCFM	Standard Cubic Feet per Minute
SCIM	Standard Cubic Inch per Minute
SLA	Spacecraft/LM Adapter
SM	Service Module
SPS	Service Propulsion System
SRSCS	Secure Range Safety Command System
SSDO	Switch Selector and Discrete Output Register
STDV	Start Tank Discharge Valve
SV	Space Vehicle
TCS	Thermal Conditioning System
TD&E	Transposition, Docking and Ejection
TEI	Transearth Injection
TEX	Corpus Christi (Texas)
TLI	Translunar Injection
TMR	Triple Module Redundant
TSM	Tail Service Mast
TVC	Thrust Vector Control
UCR	Unsatisfactory Condition Report
USB	Unified S-Band
UT	Universal Time
VA	Volt Amperes
VAN	Vanguard (ship)
VHF	Very High Frequency
Z	Zulu Time (equivalent to UT)

MISSION PLAN

The AS-509 flight (Apollo 14 Mission) is the ninth flight in the Apollo/Saturn V flight program, the fourth lunar landing mission, and the second landing planned for the lunar highlands. The planned mission and landing are to accomplish the objectives originally assigned to the aborted Apollo 13 Mission. The primary mission objectives are: a) perform selenological inspection, survey, and sampling of materials in a preselected region of the Fra Mauro formation; b) deploy and activate the Apollo Lunar Surface Experiments Package (ALSEP); c) develop man's capability to work in the lunar environment; and d) obtain photographs of candidate exploration sites. The crew consists of Alan B. Shepard, Jr. (Mission Commander), Stuart A. Roosa (Command Module Pilot), and Edgar B. Mitchell (Lunar Module Pilot).

The AS-509 Launch Vehicle (LV) is composed of the S-IC-9, S-II-9, and S-IVB-509 stages, and Instrument Unit (IU)-509. The Spacecraft (SC) consists of SC/Lunar Module (LM) Adapter (SLA)-17, Command and Service Module (CSM)-110, and LM-8.

Vehicle launch from Complex 39A at Kennedy Space Center (KSC) is along a 90 degree azimuth with a roll to a flight azimuth of approximately 75.6 degrees measured east of true north. Vehicle mass at ignition is 6,508,444 lbm.

The S-IC stage powered flight is approximately 165 seconds; the S-II stage provides powered flight for approximately 390 seconds. The S-IVB stage burn of approximately 141 seconds inserts the S-IVB/IU/SLA/LM/CSM into a circular 100 n mi altitude (referenced to the earth equatorial radius) Earth Parking Orbit (EPO). Vehicle mass at orbit insertion is 301,108 lbm.

At approximately 10 seconds after EPO insertion, the vehicle is aligned with the local horizontal. Continuous hydrogen venting is initiated shortly after EPO insertion and the LV and CSM systems are checked in preparation for the Translunar Injection (TLI) burn. During the second or third revolution in EPO, the S-IVB stage is restarted and burns for approximately 356 seconds. This burn injects the S-IVB/IU/SLA/LM/CSM into a free-return, translunar trajectory.

Within 15 minutes after TLI, the vehicle initiates an inertial attitude hold for CSM separation, docking and LM ejection. Following the attitude freeze, the CSM separates from the LV and the SLA panels are jettisoned. The CSM then transposes and docks to the LM. After docking, the CSM/LM is spring ejected from the S-IVB/IU. Following separation of the combined CSM/LM from the S-IVB/IU, the S-IVB/IU will perform a yaw maneuver and an 80-second burn of the S-IVB Auxiliary Propulsion System (APS) ullage engines to propel the S-IVB/IU a safe distance away from the spacecraft. Subsequent to the completion of the S-IVB/IU evasive maneuver, the S-IVB/IU is placed on a trajectory such that it will impact the lunar surface in the vicinity of the Apollo 12 landing site. The impact trajectory is achieved by propulsive venting of liquid hydrogen (LH_2), dumping of liquid oxygen (LOX) and by firing the APS engines. The S-IVB/IU impact will be recorded by the seismograph deployed during the Apollo 12 mission. S-IVB/IU lunar impact is predicted at approximately 82 hours 24 minutes after launch.

Three in-flight demonstrations designed to demonstrate the effects of a Zero-G environment will be flown on Apollo 14. These include an electrophoretic separation demonstration, a composites casting demonstration and a heat flow and convection demonstration. These self-contained experiments will be activated by the astronauts during the translunar/transearth coast periods.

During the three day translunar coast, the astronauts will perform star-earth landmark sightings, Inertial Measurement Unit (IMU) alignments, general lunar navigation procedures and possibly four midcourse corrections. One of these maneuvers will transfer the SC into a low-periselenum non-free-return translunar trajectory at approximately 28 hours after TLI. At approximately 82 hours and 38 minutes, a Service Propulsion System (SPS), Lunar Orbit Insertion (LOI) burn of approximately 367 seconds inserts the CSM/LM into a 57 by 170 n mi altitude parking orbit.

Approximately two revolutions after LOI, a 21.4-second SPS burn will adjust the orbit into a 10 by 58 n mi altitude. The LM is entered by astronauts Shepard and Mitchell, and checkout is accomplished. During the twelfth revolution in orbit, at 104.5 hours, the LM separates from the CSM and prepares for the lunar descent. The CSM is then inserted into a 56 by 63 n mi altitude orbit using a 3.8 second SPS burn. The LM descent propulsion system is used to brake the LM into the proper landing trajectory and maneuver the LM during descent to the lunar surface.

Following lunar landing, two 4.25-hour Extravehicular Activity (EVA) time periods are scheduled during which the astronauts will explore the lunar surface, examine the LM exterior, photograph the lunar terrain, and deploy scientific instruments. The total stay time on the lunar

surface is open-ended, with a planned maximum of 35 hours, depending upon the outcome of current lunar surface operations planning and of real-time operational decisions. After the EVA, the astronauts prepare the LM ascent propulsion system for lunar ascent.

The CSM performs a plane change approximately 24 hours before lunar ascent. At approximately 142.4 hours, the ascent stage inserts the LM into a 9 by 51 n mi altitude lunar orbit. At approximately 144 hours the rendezvous and docking with the CSM are accomplished.

Following docking, equipment transfer, and decontamination procedures, the LM ascent stage is jettisoned and targeted to impact the lunar surface between Apollo 12 and Apollo 14 landing sites. Seismometer readings will be provided from both sites. Following LM ascent stage deorbit burn, the CSM performs a plane change to photograph future landing sites. Photographing and landmark tracking will be performed during revolutions 40 through 44. Transearth Injection (TEI) is accomplished at the end of revolution 46 at approximately 167 hours and 29 minutes with a 135-second SPS burn.

During the 73-hour transearth coast, the astronauts will perform navigation procedures, star-earth-moon sightings, and possibly three midcourse corrections. The Service Module (SM) will separate from the Command Module (CM) 15 minutes before reentry. Splashdown will occur in the Pacific Ocean approximately 216 hours and 42 minutes after liftoff.

After the recovery operations, a biological quarantine is imposed on the crew and CM. An incubation period of 18 days from splashdown (21 days from lunar ascent) is required for the astronauts. The hardware incubation period is the time required to analyze certain lunar samples.

FLIGHT SUMMARY

The seventh manned Saturn V Apollo space vehicle, AS-509 (Apollo 14 Mission) was launched at 16:03:02 Eastern Standard Time (EST) on January 31, 1971 from Kennedy Space Center, Complex 39, Pad A. The launch was scheduled for 15:23:00 EST but was delayed approximately 40 minutes because of weather conditions in the launch area. The basic performance of the launch vehicle was satisfactory and this ninth launch of the Saturn V/ Apollo successfully performed all mandatory and desirable objectives. All aspects of the S-IVB/IU lunar impact objective were accomplished successfully except for precise determination of the impact point. Preliminary assessments indicate that the final impact solution will satisfy the mission objective.

The ground systems supporting countdown and launch performed satisfactorily. System component failures and malfunctions requiring corrective action were corrected during countdown without causing unscheduled holds. Propellant tanking was accomplished satisfactorily. Damage to the pad, Launch Umbilical Tower (LUT) and support equipment was minor.

The vehicle was launched on an azimuth 90 degrees east of north. A roll maneuver was initiated at 12.8 seconds that placed the vehicle on a flight azimuth of 75.558 degrees east of north. The trajectory parameters from launch to TLI were close to nominal. Earth parking orbit insertion conditions were achieved 1.72 seconds earlier than nominal at a heading angle 0.071 degree less than nominal. TLI was achieved 4.99 seconds earlier than nominal. The trajectory parameters at Command and Service Module (CSM) separation deviated from nominal since the event occurred 181.0 seconds later than predicted.

All S-IC propulsion systems performed satisfactorily. Stage site thrust (averaged from time zero to Outboard Engine Cutoff [OECO]) was 0.65 percent higher than predicted. Total propellant consumption rate was 0.42 percent higher than predicted with the consumed Mixture Ratio (MR) 0.94 percent higher than predicted. Specific impulse was 0.23 percent higher than predicted. Total propellant consumption from Holddown Arm (HDA) release to OECO was low by 0.15 percent. Center Engine Cutoff (CECO) was initiated by the Instrument Unit (IU) as planned. Outboard engine cutoff, initiated by LOX low level sensors, occurred 0.94 second earlier than predicted. The LOX residual at OECO was 42,570 lbm compared to the predicted 42,257 lbm. The fuel residual at OECO was 32,312 lbm compared to the predicted

31,630 lbm. This was the first flight which incorporated a venturi in the LOX pressurization system to replace the GOX Flow Control Valve (GFCV). The system performed satisfactorily and all performance requirements were met, although the LOX ullage pressure drifted below the minimum predicted level at 140 seconds.

S-IC hydraulic system performance was normal throughout the flight.

The S-II propulsion system performed satisfactorily throughout the flight. CECO occurred as planned and OECO occurred 2.15 seconds later than predicted. The later than predicted OECO was a result of lower than predicted flowrates during the low Engine Mixture Ratio (EMR) portion of the flight. Total stage thrust at the standard time slice (61 seconds after S-II Engine Start Command [ESC]) was 0.25 percent below predicted. Total propellant flowrate, including pressurization flow, was 0.12 percent below predicted and stage specific impulse was 0.19 percent below predicted at the standard time slice. Stage propellant mixture ratio was 0.18 percent above predicted. Engine thrust buildup and cutoff transients were normal. A center engine LOX feedline accumulator was installed for the first time on this flight as a POGO suppression device. The accumulator system was effective in suppressing POGO type oscillations. The propellant management system performance was satisfactory throughout propellant loading and flight. However, during the helium injection at T-4 hours, the LOX Overfill Shutoff (OFSO) sensor indicated wet approximately 15 percent of each minute. At this time an investigation was made to determine if a time period violation of the Launch Mission Rule (LMR) might occur later during terminal sequence. The investigation indicated that this would not be a problem, and propellant loading operations were continued and progressed without incident. The new pneumatically actuated engine Mixture Ratio Control Valves (MRCV) were used for the first time in flight and operated satisfactorily. The performance of the LH_2 tank pressurization system was satisfactory and within predicted limits. The LOX tank pressurization system operated sufficiently to satisfy all mission objectives; however, the LOX ullage pressure was below that predicted near the end of S-II flight. The low LOX ullage pressure is attributed to restricted flow through the LOX tank pressurization regulator subsequent to LOX step pressurization. The regulator is being replaced with an orifice for AS-510 and subsequent stages. Engine servicing operations, required to condition the engines, were satisfactorily accomplished. Engine start tank conditions were marginal at S-II ESC because of the lower start tank relief valve settings caused by warmer than usual start tank temperatures. These warmer temperatures were a result of the hold prior to launch. Revised hold option procedures are under consideration for AS-510. The recirculation, helium injection, and valve actuation systems performed satisfactorily.

S-II hydraulic system performance was normal throughout the flight.

The S-IVB stage J-2 engine operated satisfactorily throughout the operational phase of first and second burn and had normal shutdowns. S-IVB first burntime was 4.1 seconds less than predicted. Approximately 2.4 seconds of the shorter burntime can be attributed to higher S-IVB performance. The remainder can be attributed to the S-IC and S-II stage performance and the change in the flight azimuth. The engine performance during first burn, as determined from standard altitude reconstruction analysis, deviated from the predicted Start Tank Discharge Valve (STDV) open +130-second time slice by 1.48 percent for thrust and 0.14 percent for specific impulse. The S-IVB stage first burn Engine Cutoff (ECO) was initiated by the Launch Vehicle Digital Computer (LVDC) at 700.56 seconds. The Continuous Vent System (CVS) adequately regulated LH_2 tank ullage pressure at an average level of 19.2 psia during orbit, and the Oxygen/Hydrogen (O_2/H_2) burner satisfactorily achieved LH_2 and LOX tank repressurization for restart. Engine restart conditions were within specified limits. The restart at full open Propellant Utilization (PU) valve position was successful. S-IVB second burntime was 5.5 seconds less than predicted. The engine performance during second burn, as determined from the standard altitude reconstruction analysis, deviated from the predicted STDV +200-second time slice by 1.57 percent for thrust and 0.14 percent for specific impulse. Second burn ECO was initiated by the LVDC at 9263.24 seconds (02:34:23.24). A small shift in LOX chilldown flowrate and pump differential pressure observed during boost has been determined to be due to vehicle induced longitudinal dynamics. Subsequent to second burn, the stage propellant tanks and helium spheres were safed satisfactorily. Sufficient impulse was derived from LOX dump, LH_2 CVS operation and Auxiliary Propulsion System (APS) ullage burn to achieve a successful lunar impact within the planned target area. The APS pressurization system operated normally throughout the flight except for a helium leak in Module No. 1 from 5 to 7 hours. The magnitude and duration of this leak was not large enough to present any problems.

S-IVB hydraulic system performance was satisfactory during the entire mission.

The structural loads experienced during the S-IC boost phase were well below design values. The maximum bending moment occurred at the S-IC LOX tank and was 45 percent of the design value. Thrust cutoff transients experienced by AS-509 were similar to those of previous flights. The maximum longitudinal dynamic responses at the IU were ± 0.25 g at S-IC CECO and ± 0.35 g at OECO. The magnitudes of the thrust cutoff responses are considered normal. During S-IC stage boost, 4 to 5 hertz oscillations were detected beginning at approximately 100 seconds. The maximum amplitude measured at the IU was ± 0.06 g. Oscillations in the 4 to 5 hertz range have been observed on previous flights and are considered

to be normal vehicle response to flight environment. POGO did not occur during S-IC boost. The S-II stage center engine LOX feedline accumulator successfully inhibited the 14 to 16 hertz POGO oscillations experienced on previous flights. A peak response of ±0.6 g was measured on engine No. 5 gimbal pad during steady state engine operation. As on previous flights, low amplitude 11 hertz oscillations were experienced near the end of S-II burn. Peak engine No. 1 gimbal pad response was ±0.16 g. POGO did not occur during S-II boost. The POGO limiting backup cutoff system performed satisfactorily during prelaunch and flight operation. The structural loads experienced during the S-IVB stage burns were well below design values. During first burn the S-IVB experienced low amplitude, 16 to 20 hertz oscillations. The amplitudes measured on the gimbal block were comparable to previous flights and well within the expected range of values. Similarly, S-IVB second burn produced intermittent low amplitude oscillations in the 12 to 14 hertz frequency range which peaked near second burn cutoff.

The guidance and navigation system performed satisfactorily in the accomplishment of all mission objectives. The ST-124M-3 inertial platform, the Launch Vehicle Data Adapter (LVDA), and the LVDC performance was satisfactory. LVDA telemetry, however, indicated one hardware measurement failure. The LVDA internal hardware monitor of the switch selector register driver status did not indicate the correct state of the bit 5 driver. This is a measurement for telemetry only; performance of the driver and all associated switch selector functions was unaffected and satisfactory.

The AS-509 control system, which was essentially the same as that of AS-508, performed satisfactorily. The Flight Control Computer (FCC), Thrust Vector Control (TVC) System, and APS satisfied all requirements for vehicle attitude control during the flight. Bending and slosh dynamics were adequately stabilized. The prelaunch programed yaw, roll, and pitch maneuvers were properly executed during S-IC boost. During the maximum dynamic pressure region of flight, the launch vehicle experienced winds that were less than 95-percentile January winds. The maximum average pitch and yaw engine deflections were in the maximum dynamic pressure region. S-IC/S-II first and second plane separations were accomplished with no significant attitude deviations. Related data indicate that the S-IC retromotors performed as expected. At Iterative Guidance Mode (IGM) initiation, a pitchup transient occurred similar to that seen on previous flights. The S-II retromotors and S-IVB ullage motors performed as expected and provided a normal S-II/S-IVB separation. Satisfactory control of the vehicle was maintained during first and second S-IVB burns and during coast in Earth Parking Orbit (EPO). During the CSM separation from the S-IVB/IU and during the Transposition, Docking, and Ejection (TD&E) maneuver, the control system maintained the vehicle in a fixed inertial attitude to provide a stable docking platform. Following TD&E, S-IVB/IU attitude control was maintained during the evasive maneuver, the maneuver to lunar impact attitude, and the LOX dump and APS burn.

The AS-509 launch vehicle electrical systems and Emergency Detection System (EDS) performed satisfactorily throughout all phases of flight. Operation of the batteries, power supplies, inverters, Exploding Bridge Wire (EBW) firing units and switch selectors was normal.

Vehicle base pressure and base thermal environments, in general, were similar to those experienced on earlier flights. The environmental control system performance was satisfactory.

All elements of the data system performed satisfactorily throughout flight except the IU telemetry system. The DP1-A0 270 multiplexer data and the 410K multiplexer data were lost at 0.409 second and at 10,955.861 seconds (03:02:35.861), respectively. In addition the DP-1 telemetry RF output measurement changed abruptly several times during the flight. The vehicle measurement reliability was 95.5 percent. Telemetry performance was normal except for the noted problems. Radio-frequency (RF) propagation was generally good, though the usual problems due to flame effects and staging were experienced. Usable VHF data were received until 18,360 seconds (05:06:00). The Secure Range Safety Command Systems (SRSCS) on the S-IC, S-II and S-IVB stages were ready to perform their functions properly, on command, if flight conditions during the launch phase had required destruct. The system properly safed the S-IVB on a command transmitted from Bermuda (BDA) at 710.2 seconds. The performance of the Command and Communication System (CCS) was excellent. Usable CCS telemetry data were received until 53,039 seconds (14:43:59) when the telemetry subcarrier was inhibited. Carnarvon (CRO), Goldstone (GDS), Hawaii (HAW), Honeysuckle (HSK), and Merritt Island Launch Area (MILA) were receiving CCS signal carrier until S-IVB/IU lunar impact. Good tracking data were received from the C-Band radar, with BDA indicating final Loss of Signal (LOS) at 28,950 seconds (08:02:30). The 65 ground engineering cameras provided good data during the launch.

All aspects of the S-IVB/IU Lunar Impact objective were accomplished successfully except the precise determination of the impact point. The final impact solution is expected to satisfy the mission objective. At 297,472.17 seconds (82:37:52.17) (actual time of occurrence at the moon) the S-IVB/IU impacted the lunar surface at approximately 8.07 degrees south latitude and 26.04 degrees west longitude, which is approximately 294 kilometers (159 n mi) from the target of 1.596 degrees south latitude and 33.25 degrees west longitude. Impact velocity was 2543 m/s (8343 ft/s). The mission objectives were to maneuver the S-IVB/IU such that it would have at least a 50 percent probability of impacting the lunar surface within 350 kilometers (189 n mi) of the target, and to determine the actual impact point within 5 kilometers (2.7 n mi), and the time of impact within 1 second.

Three inflight demonstrations designed to demonstrate the effects of a Zero g environment were flown on Apollo 14. These included an electrophoretic separation demonstration, a composites casting demonstration and a heat flow and convection demonstration. Preliminary assessment of the data indicates that all demonstrations were successful. The degree of success will be determined when final data are received and evaluated.

MISSION OBJECTIVES ACCOMPLISHMENT

Table 1 presents the MSFC Mandatory Objectives and Desirable Objectives as defined in the "Saturn V Apollo 14/AS-509 Mission Implementation Plan," MSFC Document PM-SAT-8010.7 (Rev. A), dated January 15, 1971. An assessment of the degree of accomplishment of each objective is shown. Discussion supporting the assessment can be found in other sections of this report as shown in Table 1.

Table 1. Mission Objectives Accomplishment

NO.	MSFC MANDATORY OBJECTIVES (MO) AND DESIRABLE OBJECTIVES (DO)	DEGREE OF ACCOMPLISHMENT	DISCREPANCIES	PARAGRAPH IN WHICH DISCUSSED
1	Launch on a flight azimuth between 72 and 96 degrees and insert the S-IVB/IU/SC into the planned circular earth parking orbit (MO).	Complete	None	4.1, 9.1.1
2	Restart the S-IVB during either the second or third revolution and inject the S-IVB/IU/SC onto the planned translunar trajectory (MO).	Complete	None	4.2.3, 7.6
3	Provide the required attitude control for the S-IVB/IU/SC during TDBE (MO).	Complete	None	10.4.4
4	Perform an evasive maneuver after ejection of the CSM/LM from the S-IVB/IU (DO).	Complete	None	10.4.4
5	Impact the S-IVB/IU on the lunar surface within 350 kilometers of lat. 1°35'45.6" S, long. 33°15' W (DO).	Complete	None	17.4
6	Determine actual impact point within 5 kilometers and time of impact within one second (DO).	Probably Complete	Analysis Not Complete	17.4
7	After final LV/SC separation, vent and dump the remaining gases and propellants to safe the S-IVB/IU (DO).	Complete	None	7.13
-	Verify the operation of the LOX feedline accumulator system installed on the S-II stage center engine.	Complete	None	6.9, 8.2

FAILURES, ANOMALIES AND DEVIATIONS

Evaluation of the launch vehicle data revealed no failure, no anomalies, and four deviations. The deviations are summarized in Table 2.

Table 2. Summary of Deviations

ITEM	VEHICLE SYSTEM	DEVIATION	PROBABLE CAUSE	SIGNIFICANCE	PARAGRAPH REFERENCE
1	S-II Propulsion	LOX tank ullage pressure below minimum predicted level near end of S-II burn.	(1) Failure of the LOX pressurization regulator to open fully when required, and (2) to a lesser degree the J-2 engine heat exchangers flowing at saturated conditions.	None. Ullage pressure was well above level to satisfy engine NPSP requirements. Regulator will be replaced with orifice effective AS-510 and subsequent.	6.6.2
2	IU Telemetry	DP1-A0 270 multiplexer data were lost at 0.4 secon and for the remainder of flight.	Under investigation.	Probably none, although loss of the 270 multiplexer data (59 measurements) impacted the total performance analysis of the vehicle.	15.3.2
3	IU Telemetry	410K multiplexer data were lost at 10,95o seconds and for the remainder of flight.	Under investigation.	Probably none, although loss of the 410k multiplexer data impacted the performance analysis of the guidance computer.	15.3.3
4	IU LVDA	Loss of LVDA switch selector register driver status measurement.	Switch selector bit 5 driver monitor circuit inoperative between pickoff point and common data output multiplexer input gate	None. This measurement is used for switch selector error analysis and was not needed this flight.	9.4.1

SECTION 1

INTRODUCTION

1.1 PURPOSE

This report provides the National Aeronautics and Space Administration (NASA) Headquarters, and other interested agencies, with the launch vehicle evaluation results of the AS-509 flight (Apollo 14 Mission). The basic objective of flight evaluation is to acquire, reduce, analyze, evaluate and report on flight data to the extent required to assure future mission success and vehicle reliability. To accomplish this objective, actual flight failures and deviations are identified, their causes determined, and information made available for corrective action.

1.2 SCOPE

This report contains the performance evaluation of the major launch vehicle systems, with special emphasis on failures and deviations. Summaries of launch operations and spacecraft performance are included.

The official George C. Marshall Space Flight Center (MSFC) position at this time is represented by this report. It will not be followed by a similar report unless continued analysis or new information should prove the conclusions presented herein to be significantly incorrect. Reports covering major subjects and special subjects will be published as required.

SECTION 2

EVENT TIMES

2.1 SUMMARY OF EVENTS

Range zero time, the basic time reference for this report is 16:03:02 Eastern Standard Time (EST) (21:03:02 Universal Time [UT]) January 31, 1971. Range time is the elapsed time from range zero time and, unless otherwise noted, is the time used throughout this report. All data, except as otherwise defined, presented in "Range Time" are the times at which the data were received at the telemetry ground station, i.e., actual time of occurrence at the vehicle plus telemetry transmission time. The Time-From-Base times are presented as elapsed vehicle time from start of time base. Vehicle time is the Launch Vehicle Digital Computer (LVDC) clock time. Figure 2-1 shows the conversion between ground station time and vehicle time.

Vehicle times for each time base used in the flight sequence program and the signal for initiating each time base are presented in Table 2-1. Ground station times for each timebase are the same as those shown in Table 2-1, except that T_8 is 21,840.53 (06:04:00.53). Start times of T_0, T_1 and T_2 were nominal. T_3, T_4 and T_5 were initiated approximately 1.0 second early, 2.2 seconds late and 1.7 seconds early, respectively, due to variations in the stage burn times. These variations are discussed in Sections 5, 6 and 7 of this document. Start times of T_6 and T_7 were 0.3 second late and 4.9 seconds early, respectively. T_8, which was initiated by the receipt of a ground command, started 6392 seconds (01:46:32) late, due to extended Command and Service Module (CSM) docking operations.

A summary of significant events for AS-509 is given in Table 2-2. The predicted times for establishing actual minus predicted times in Table 2-2 were taken from 40M33627B, "Interface Control Document Definition of Saturn SA-507 and Subs Flight Sequence Program" and from the "AS-509 Postlaunch Operational Trajectory," dated February 1, 1971.

2.2 VARIABLE TIME AND COMMAND SWITCH SELECTOR EVENTS

Table 2-3 lists the switch selector events which were issued during the flight, but were not programed for specific times. The water coolant valve open and close switch selector commands were issued based on the

condition of two thermal switches in the Environmental Control System (ECS). The output of these switches was sampled once every 300 seconds beginning nominally at 480 seconds, and a switch selector command was issued to open or close the water valve. The valve was opened if the temperature was too high and was closed if the temperature was too low. Data indicate the water coolant valve responded properly to temperature fluctuations.

Table 2-3 also contains the special sequence of switch selector events which were programed to be initiated by telemetry station acquisition and included the following calibration sequence:

FUNCTION	STAGE	TIME (SEC)
Telemetry Calibrator In-Flight Calibrate ON	IU	Acquisition +60.0
TM Calibrate ON	S-IVB	Acquisition +60.4
TM Calibrate OFF	S-IVB	Acquisition +61.4
Telemetry Calibrator In-Flight Calibrate OFF	IU	Acquisition +65.0

Table 2-1. Time Base Summary

TIME BASE	VEHICLE TIME SECONDS (HR:MIN:SEC)	SIGNAL START
T_0	-16.96	Guidance Reference Release
T_1	0.57	IU Umbilical Disconnect Sensed by LVDC
T_2	135.27	Downrange Velocity $\geq$ 500 m/s at T_1 +134.7 seconds as sensed by LVDC
T_3	164.11	S-IC OECO Sensed by LVDC
T_4	559.05	S-II OECO Sensed by LVDC
T_5	700.79	S-IVB ECO (Velocity) Sensed by LVDC
T_6	8334.17 (02:18:54.17)	Restart Equation Solution
T_7	9263.47 (02:34:23.47)	S-IVB ECO (Velocity) Sensed by LVDC
T_8	21,840.35 (06:04:00.35)	Initiated by Ground Command

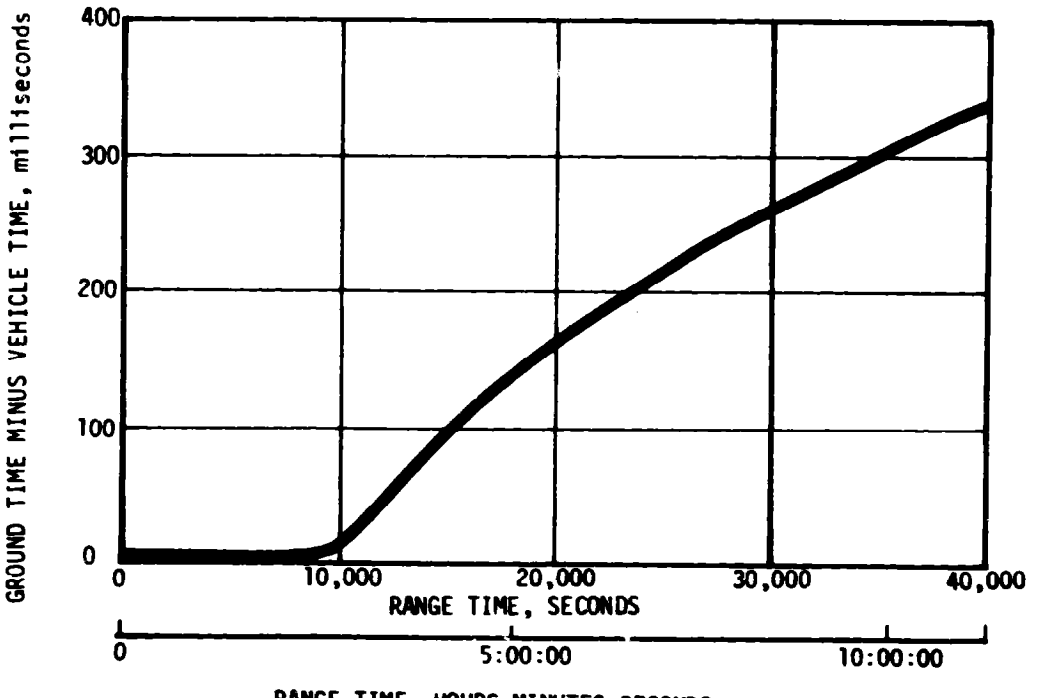

Figure 2-1. Ground Station Time to Vehicle Time Conversion

Table 2-2. Significant Event Times Summary

ITEM	EVENT DESCRIPTION	RANGE TIME		TIME FROM BASE	
		ACTUAL SEC	ACT-PRED SEC	ACTUAL SEC	ACT-PRED SEC
1	GUIDANCE REFERENCE RELEASE (GRR)	-17.0	0.1	-17.5	0.2
2	S-IC ENGINE START SEQUENCE COMMAND (GROUND)	-8.9	0.0	-9.5	0.0
3	S-IC ENGINE NO.5 START	-6.5	0.1	-7.1	0.1
4	S-IC ENGINE NO.1 START	-6.3	0.0	-6.9	0.1
5	S-IC ENGINE NO.3 START	-6.2	0.1	-6.8	0.1
6	S-IC ENGINE NO.2 START	-6.1	0.0	-6.7	0.1
7	S-IC ENGINE NO.4 START	-5.9	0.1	-6.5	0.1
8	ALL S-IC ENGINES THRUST OK	-1.6	-0.1	-2.2	0.0
9	RANGE ZERO	0.0		-0.6	
10	ALL HOLDDOWN ARMS RELEASED (FIRST MOTION)	0.2	0.0	-0.3	0.1
11	IU UMBILICAL DISCONNECT, START OF TIME BASE 1 (T1)	0.6	0.0	0.0	0.0
12	BEGIN TOWER CLEARANCE YAW MANEUVER	2.0	0.4	1.4	0.4
13	END YAW MANEUVER	9.9	0.3	9.3	0.3
14	BEGIN PITCH AND ROLL MANEUVER	12.8	-0.4	12.2	-0.4
15	S-IC OUTBOARD ENGINE CANT	20.5	-0.1	20.0	0.0
16	END ROLL MANEUVER	28.0	-3.2	27.4	-3.2
17	MACH 1	68.0	-1.2	67.4	-1.2
18	MAXIMUM DYNAMIC PRESSURE (MAX Q)	81.0	-4.6	80.4	-4.6
19	S-IC CENTER ENGINE CUTOFF (CECO)	135.14	-0.12	134.57	-0.05
20	START OF TIME BASE 2 (T2)	135.7	0.0	0.0	0.0
21	END PITCH MANEUVER (TILT ARREST)	164.1	0.9	28.8	0.9
22	S-IC OUTBOARD ENGINE CUTOFF (OFCO)	164.10	-0.94	28.83	-0.87
23	START OF TIME BASE 3 (T3)	164.1	-1.0	0.0	0.0

Table 2-2. Significant Event Times Summary (Continued)

ITEM	EVENT DESCRIPTION	RANGE TIME		TIME FROM BASE	
		ACTUAL SEC	ACT-PRED SEC	ACTUAL SEC	ACT-PRED SEC
24	START S-II LH2 TANK HIGH PRESSURE VENT MODE	164.2	-1.0	0.1	0.0
25	S-II LH2 RECIRCULATION PUMPS OFF	164.3	-1.0	0.2	0.0
26	S-II ULLAGE MOTOR IGNITION	164.6	-1.0	0.5	0.0
27	S-IC/S-II SEPARATION COMMAND TO FIRE SEPARATION DEVICES AND RETRO MOTORS	164.8	-1.0	0.7	0.0
28	S-II ENGINE START SEQUENCE COMMAND (ESC)	165.5	-1.0	1.4	0.0
29	S-II ENGINE SOLENOID ACTIVATION (AVERAGE OF FIVE)	165.5	-1.0	1.4	0.0
30	S-II IGNITION-STDV OPEN	166.5	-1.0	2.4	0.0
31	S-II CHILLDOWN VALVES CLOSE	168.4	-1.0	4.3	0.0
32	S-II MAINSTAGE	168.5	-1.0	4.4	0.0
33	S-II ULLAGE MOTOR BURN TIME TERMINATION (THRUST REACHES 75%)	168.7	-1.0	4.6	0.0
34	S-II HIGH (5.5) EMR NO. 1 ON	171.0	-1.0	6.9	0.0
35	S-II HIGH (5.5) EMR NO. 2 ON	171.2	-1.0	7.1	0.0
36	S-II SECOND PLANE SEPARATION COMMAND (JETTISON S-II AFT INTERSTAGE)	194.8	-1.0	30.7	0.0
37	LAUNCH ESCAPE TOWER (LET) JETTISON	200.7	-0.7	36.6	0.2
38	ITERATIVE GUIDANCE MODE (IGM) PHASE 1 INITIATED	205.9	0.1	41.8	1.0
39	S-II LOX STEP PRESSURIZATION	264.1	-1.0	100.0	0.0
40	S-II CENTER ENGINE CUTOFF (CECO)	463.09	-0.96	298.98	-0.02
41	S-II LH2 STEP PRESSURIZATION	464.1	-1.0	300.0	0.0
42	S-II LOW ENGINE MIXTURE RATIO (EMR) SHIFT (ACTUAL)	473.1	-1.5	309.0	-0.5
43	START OF ARTIFICIAL TAU MODE	474.0	2.8	309.9	3.7

Table 2-2. Significant Event Times Summary (Continued)

ITEM	EVENT DESCRIPTION	RANGE TIME		TIME FROM BASE	
		ACTUAL SEC	ACT-PRED SEC	ACTUAL SEC	ACT-PRED SEC
44	END OF ARTIFICIAL TAU MODE	485.1	2.9	321.0	3.8
45	S-II OUTBOARD ENGINE CUTOFF (OECO)	559.05	2.15	394.94	3.09
46	S-II ENGINE CUTOFF INTERRUPT, START OF TIME BASE 4 (T4) (START OF IGM PHASE 3)	559.1	2.2	0.0	0.0
47	S-IVB ULLAGE MOTOR IGNITION	559.9	2.1	0.9	0.0
48	S-II/S-IVB SEPARATION COMMAND TO FIRE SEPARATION DEVICES AND RETRO MOTORS	560.0	2.1	1.0	0.0
49	S-IVB ENGINE START COMMAND (FIRST ESC)	560.1	2.1	1.1	0.0
50	FUEL CHILLDOWN PUMP OFF	561.2	2.1	2.2	0.0
51	S-IVB IGNITION (STDV OPEN)	563.4	2.4	4.3	0.2
52	S-IVB MAINSTAGE	565.9	2.4	6.8	0.2
53	START OF ARTIFICIAL TAU MODE	568.2	3.2	9.7	1.1
54	S-IVB ULLAGE CASE JETTISON	571.8	2.1	12.8	0.0
55	END OF ARTIFICIAL TAU MODE	579.4	6.0	20.4	3.9
56	BEGIN TERMINAL GUIDANCE	667.1	-0.8	108.0	-3.0
57	END IGM PHASE 3	693.2	-1.0	134.1	-3.2
58	BEGIN CHI FREEZE	693.2	-1.0	134.1	-3.2
59	S-IVB VELOCITY CUTOFF COMMAND NO. 1 (FIRST ECO)	700.56	-1.73	-0.27	-0.02
60	S-IVB VELOCITY CUTOFF COMMAND NO. 2	700.66	-1.73	-0.12	-0.02
61	S-IVB ENGINE CUTOFF INTERRUPT, START OF TIME BASE 5 (T5)	700.8	-1.7	0.0	0.0
62	S-IVB APS ULLAGE ENGINE NO. 1 IGNITION COMMAND	701.1	-1.7	0.3	0.0
63	S-IVB APS ULLAGE ENGINE NO. 2 IGNITION COMMAND	701.2	-1.7	0.4	0.0
64	LOX TANK PRESSURIZATION OFF	701.9	-1.8	1.2	0.0
65	PARKING ORBIT INSERTION	710.6	-1.7	9.8	0.0
66	BEGIN MANEUVER TO LOCAL HORIZONTAL ATTITUDE	722.1	-0.3	21.3	1.3

Table 2-2. Significant Event Times Summary (Continued)

ITEM	EVENT DESCRIPTION	RANGE TIME		TIME FROM BASE	
		ACTUAL SEC	ACT-PRED SEC	ACTUAL SEC	ACT-PRED SEC
67	S-IVB CONTINUOUS VENT SYSTEM (CVS) ON	759.7	-1.8	59.0	0.0
68	S-IVB APS ULLAGE ENGINE NO. 1 CUTOFF COMMAND	787.8	-1.7	87.0	0.0
69	S-IVB APS ULLAGE ENGINE NO. 2 CUTOFF COMMAND	787.8	-1.8	87.1	0.0
70	BEGIN ORBITAL NAVIGATION	802.3	-0.2	101.5	1.5
71	BEGIN S-IVB RESTART PREPARATIONS, START OF TIME BASE 6 (T6)	8334.2	0.3	0.0	0.0
72	S-IVB O2/H2 BURNER LH2 ON	8375.4	0.2	41.3	0.0
73	S-IVB O2/H2 BURNER EXCITERS ON	8375.7	0.2	41.6	0.0
74	S-IVB O2/H2 BURNER LOX ON (HELIUM HEATER ON)	8376.1	0.2	42.0	0.0
75	S-IVB CVS OFF	8376.3	0.2	42.2	0.0
76	S-IVB LH2 REPRESSURIZATION CONTROL VALVE ON	8382.2	0.2	48.1	0.0
77	S-IVB LOX REPRESSURIZATION CONTROL VALVE ON	8382.4	0.2	48.3	0.0
78	S-IVB AUX HYDRAULIC PUMP FLIGHT MODE ON	8553.1	0.2	219.0	0.0
79	S-IVB LOX CHILLDOWN PUMP ON	8583.1	0.2	249.0	0.0
80	S-IVB LH2 CHILLDOWN PUMP ON	8588.1	0.2	254.0	0.0
81	S-IVB PREVALVES CLOSED	8593.1	0.2	259.0	0.0
82	S-IVB MIXTURE RATIO CONTROL VALVE OPEN	8784.2	0.2	450.1	0.0
83	S-IVB APS ULLAGE ENGINE NO. 1 IGNITION COMMAND	8830.5	0.3	496.3	0.0
84	S-IVB APS ULLAGE ENGINE NO. 2 IGNITION COMMAND	8830.6	0.3	496.4	0.0
85	S-IVB O2/H2 BURNER LH2 OFF (HELIUM HEATER OFF)	8831.0	0.3	496.8	0.0
86	S-IVB O2/H2 BURNER LOX OFF	8835.4	0.2	501.3	0.0
87	S-IVB LH2 CHILLDOWN PUMP OFF	8903.5	0.2	569.4	0.0

Table 2-2. Significant Event Times Summary (Continued)

ITEM	EVENT DESCRIPTION	RANGE TIME		TIME FROM BASE	
		ACTUAL SEC	ACT-PRED SEC	ACTUAL SEC	ACT-PRED SEC
88	S-IVB LOX CHILLDOWN PUMP OFF	8903.7	0.2	569.6	0.0
89	S-IVB ENGINE RESTART COMMAND (FUEL LEAD INITIATION) (SECOND ESC)	8904.1	0.2	570.0	0.0
90	S-IVB APS ULLAGE ENGINE NO. 1 CUTOFF COMMAND	8907.1	0.2	573.0	0.0
91	S-IVB APS ULLAGE ENGINE NO. 2 CUTOFF COMMAND	8907.2	0.2	573.1	0.0
92	S-IVB SECOND IGNITION (STDV OPEN)	8912.4	0.5	578.2	0.2
93	S-IVB MAINSTAGE	8914.9	0.5	580.7	0.2
94	ENGINE MIXTURE RATIO (EMR) SHIFT	9049.6	0.7	715.5	0.5
95	S-IVB LH2 STEP PRESSURIZATION (SECOND BURN RELAY OFF)	9184.1	0.2	850.0	0.0
96	BEGIN TERMINAL GUIDANCE	9236.1	-2.7	901.9	-3.1
97	BEGIN CHI FREEZE	9260.9	-4.9	926.7	-5.3
98	S-IVB SECOND GUIDANCE CUTOFF COMMAND NO. 1 (SECOND ECO)	9263.24	-5.00	-0.23	-0.03
99	S-IVB SECOND GUIDANCE CUTOFF COMMAND NO. 2	9263.35	-4.99	-0.12	-0.02
100	S-IVB ENGINE CUTOFF INTERRUPT, START OF TIME BASE 7	9263.5	-4.9	0.0	0.0
101	S-IVB CVS ON	9263.9	-5.0	0.5	0.0
102	TRANSLUNAR INJECTION	9273.2	-5.0	9.8	0.0
103	S-IVB CVS OFF	9414.3	-5.0	150.9	0.0
104	BEGIN ORBITAL NAVIGATION	9414.8	-3.6	151.4	1.4
105	BEGIN MANEUVER TO LOCAL HORIZONTAL ATTITUDE	9415.1	-3.3	151.6	1.6
106	BEGIN MANEUVER TO TRANSPOSITION AND DOCKING ATTITUDE (TD&E)	10164.4	-4.1	900.9	0.9
107	CSM SEPARATION	10949.4	181.0	1685.9	185.9
108	CSM DOCK	17816.0	6447.6	8552.4	6452.4

Table 2-2. Significant Event Times Summary (Continued)

ITEM	EVENT DESCRIPTION	RANGE TIME		TIME FROM BASE	
		ACTUAL SEC	ACT-PRED SEC	ACTUAL SEC	ACT-PRED SEC
109	SC/LV FINAL SEPARATION	20834.4	6766.0	11570.8	6770.9
110	START OF TIME BASE 8 (TB)	21840.5	6392.0	0.0	0.0
111	S-IVB APS ULLAGE ENGINE NO. 1 IGNITION COMMAND	21841.7	6392.0	1.2	0.0
112	S-IVB APS ULLAGE ENGINE NO. 2 IGNITION COMMAND	21841.9	6392.0	1.4	0.0
113	S-IVB APS ULLAGE ENGINE NO. 1 CUTOFF COMMAND	21921.7	6392.0	81.2	0.0
114	S-IVB APS ULLAGE ENGINE NO. 2 CUTOFF COMMAND	21921.9	6392.0	81.4	0.0
115	INITIATE MANEUVER TO LOX DUMP ATTITUDE	22423.0	6394.4	582.5	2.4
116	S-IVB CVS ON	22840.5	6391.9	1000.0	0.0
117	BEGIN LOX DUMP	23120.5	6391.9	1280.0	0.0
118	S-IVB CVS OFF	23140.5	6391.9	1300.0	0.0
119	END LOX DUMP	23168.5	6391.9	1328.0	0.0
120	H2 NONPROPULSIVE VENT (NPV) ON	23247.5	6391.9	1407.0	0.0
121	INITIATE MANEUVER TO ATTITUDE REQUIRED FOR FINAL S-IVB APS BURN	31421.0	9792.6	9530.4	3400.6
122	S-IVB APS ULLAGE ENGINE NO. 1 IGNITION COMMAND	32399.0	8970.6	10558.4	2578.6
123	S-IVB APS ULLAGE ENGINE NO. 2 IGNITION COMMAND	32399.2	8970.6	10558.6	2578.6
124	S-IVB APS ULLAGE ENGINE NO. 1 CUTOFF COMMAND	32651.0	8984.6	10810.4	2592.6
125	S-IVB APS ULLAGE ENGINE NO. 2 CUTOFF COMMAND	32651.2	8984.6	10810.6	2592.6
126	S-IVB/IU LUNAR IMPACT	297,473.4 82:37:53.4 (HR:MIN:SEC)	818.5	275,631.8 76:33:51.8 (HR:MIN:SEC)	-5574.7

Table 2-3. Variable Time and Command Switch Selector Events

FUNCTION	STAGE	RANGE TIME (SEC)	TIME FROM BASE (SEC)	REMARKS
Low (4.8) Engine Mixture Ratio No. 1 ON	S-II	472.9	T_3 + 308.8	LVDC Function
Low (4.8) Engine Mixture Ratio No. 2 ON	S-II	473.1	T_3 + 309.0	LVDC Function
Water Coolant Valve CLOSED	IU	780.7	T_5 + 79.9	LVDC Function
Telemetry Calibrator In-Flight Calibrate OFF	IU	1075.0	T_5 + 374.2	Acquisition by Canary Rev. 1
Telemetry Calibrator In-Flight Calibrate ON	IU	3198.0	T_5 +2497.2	Acquisition by Carnarvon Rev. 1
TM Calibrate ON	S-IVB	3198.4	T_5 +2497.6	Acquisition by Carnarvon Rev. 1
TM Calibrate OFF	S-IVB	3199.4	T_5 +2498.6	Acquisition by Carnarvon Rev. 1
Telemetry Calibrator In-Flight Calibrate OFF	IU	3203.0	T_5 +2502.2	Acquisition by Carnarvon Rev. 1
Telemetry Calibrator In-Flight Calibrate ON	IU	3670.0	T_5 +2969.2	Acquisition by Honeysuckle Rev. 1
TM Calibrate ON	S-IVB	3670.4	T_5 +2969.6	Acquisition by Honeysuckle Rev. 1
TM Calibrate OFF	S-IVB	3671.4	T_5 +2970.6	Acquisition by Honeysuckle Rev. 1
Telemetry Calibrator In-Flight Calibrate OFF	IU	3675.0	T_5 +2974.2	Acquisition by Honeysuckle Rev. 1
Water Coolant Valve OPEN	IU	5580.4	T_5 +4879.7	LVDC Function
Water Coolant Valve CLOSED	IU	5880.5	T_5 +5179.7	LVDC Function

Table 2-3. Variable Time and Command Switch Selector Events (Continued)

FUNCTION	STAGE	RANGE TIME (SEC)	TIME FROM BASE (SEC)	REMARKS
Telemetry Calibrator In-Flight Calibrate ON	IU	6742.0	T_5 +6041.2	Acquisition by Canary Rev. 2
TM Calibrate ON	S-IVB	6742.4	T_5 +6041.6	Acquisition by Canary Rev. 2
TM Calibrate OFF	S-IVB	6745.4	T_5 +6044.6	Acquisition by Canary Rev. 2
Telemetry Calibrator In-Flight Calibrate OFF	IU	6749.0	T_5 +6048.2	Acquisition by Canary Rev. 2
Water Coolant Valve OPEN	IU	12,780.3	T_7 +3516.8	LVDC Function
Start of Time Base 8 (T_8)		21,840.5	T_8 + 0.0	CCS Command
Water Coolant Valve OPEN	IU	24,780.4	T_8 +2939.8	LVDC Function
Water Coolant Valve CLOSED	IU	25,080.5	T_8 +3239.9	LVDC Function
Water Coolant Valve OPEN	IU	26,880.5	T_8 +5039.9	LVDC Function
Water Coolant Valve CLOSED	IU	27,180.5	T_8 +5339.9	LVDC Function

SECTION 3

LAUNCH OPERATIONS

3.1 SUMMARY

The ground systems supporting the AS-509/Apollo 14 countdown and launch performed satisfactorily. System component failures and malfunctions requiring corrective action were corrected during countdown without causing unscheduled holds. Propellant tanking was accomplished satisfactorily. The launch was scheduled for 15:23:00 Eastern Standard Time (EST); however, there was a 40 minute 2 second hold at T-8 minutes 2 seconds due to weather conditions in the launch area. Launch occurred at 16:03:02 EST on January 31, 1971 from pad 39A of the Kennedy Space Center, Saturn complex. Damage to the pad, Launch Umbilical Tower (LUT) and support equipment was considered minimal.

3.2 PRELAUNCH MILESTONES

A chronological summary of prelaunch milestones for the AS-509 launch is contained in Table 3-1.

3.3 COUNTDOWN EVENTS

The AS-509/Apollo 14 terminal countdown was picked up at T-28 hours on January 30, 1971 at 01:00:00 EST. Scheduled holds were initiated at T-9 hours for a duration of 9 hours 23 minutes and at T-3 hours 30 minutes for a duration of 1 hour. An unscheduled hold of 40 minutes 2 seconds occurred at T-8 minutes 2 seconds due to high overcast and rain. As a result of this hold the flight azimuth was changed from 72.067 degrees to 75.558 degrees. Launch occurred at 16:03:02 EST January 31, 1971 from pad 39A of the Kennedy Space Center, Saturn Launch Complex.

3.4 PROPELLANT LOADING

3.4.1 RP-1 Loading

The RP-1 system successfully supported countdown and launch without incident. S-IC stage replenishment was accomplished at T-13 hours, and level adjust and fill line inert at about T-1 hour. A replenish operation was performed because lower than expected ambient temperature reduced the S-IC load to a marginal level.

Table 3-1. AS-509/Apollo 14 Prelaunch Milestones

DATE	ACTIVITY OR EVENT
November 19, 1969	Command and Service Module (CSM) -110 Arrival
December 24, 1969	Lunar Module (LM) -8 Arrival
January 11, 1970	S-IC-9 Stage Arrival
January 14, 1970	S-IC Erection on Mobile Launcher (ML) -2
January 20, 1970	S-IVB-509 Stage Arrival
January 21, 1970	S-II-9 Stage Arrival
March 31, 1970	Spacecraft/Lunar Module Adapter (SLA) -17 Arrival
May 6, 1970	Instrument Unit (IU) -509 Arrival
May 12, 1970	S-II Erection
May 13, 1970	S-IVB Erection
May 14, 1970	IU Erection
June 4, 1970	Launch Vehicle (LV) Electrical Systems Test
July 7, 1970	LV Propellant Dispersion/Malfunction Overall Test (OAT) Complete
October 21, 1970	LV Service Arm OAT
November 4, 1970	Spacecraft (SC) Erection
November 9, 1970	Space Vehicle (SV)/ML Transfer to Pad 39A
December 13, 1970	SV Electrical Mate
December 14, 1970	SV OAT No. 1 (Plugs In)
December 19, 1970	SV Flight Readiness Test (FRT) Completed
January 8, 1971	RP-1 Loading
January 18, 1971	Countdown Demonstration Test (CDDT) Completed (Wet)
January 19, 1971	CDDT Completed (Dry)
January 31, 1971	SV Terminal Countdown Started
January 31, 1971	SV Launch

The mast cutoff valve (A18651) opened shortly after liftoff when Tail Service Mast (TSM) power was secured allowing RP-1 piping in Mobile Launcher (ML) room 4A to be contaminated by fill line residuals. This condition has occurred after all launches to date. ECN 74408, effective AS-510, will correct the problem by replacing the present mast cutoff valve with one that remains in the last commanded position when power is removed.

3.4.2 LOX Loading

The LOX system supported countdown and launch satisfactorily. The fill sequence began with S-IVB fill command at 06:09 EST on January 31 and was completed 2 hours 37 minutes later with all stage replenish normal at 08:46 EST.

The S-IVB LOX tank Propellant Utilization (PU) probe assembly was replaced prior to launch countdown due to problems encountered during Countdown Demonstration Test (CDDT). There was no performance degradation in LOX loading with the replacement probe.

S-II LOX loading was normal and was performed on time in the primary mode by the Propellant Tanking Computer System (PTCS). At T-4 hours, during propulsion helium injection/accumulator test, the LOX tank overfill point sensor was indicating wet approximately 15 percent of each minute. This occurrence created concern regarding a possible time period violation of the propellant launch mission rule requirements. After conducting a special 30-minute helium injection test, a real time change to the Launch Mission Rule (LMR) requirements of 2.0 percent to 2.7 percent was obtained (any single excursion above 2.7 percent is to be disregarded). In addition, the S-II LOX replenish flow was manually controlled to insure that the LOX loading redline would be met. Manual controlling of the S-II LOX replenish flow provided the means of eliminating excursions of the LOX flight mass so that the redline would not be exceeded at initiation of terminal sequence.

The S-IC LOX tank vent and relief valve was replaced prior to launch as a result of out-of-specification operation during CDDT. No problems were observed with the replacement valve during prelaunch or flight operations. Disassembly and failure analysis of the removed valve indicated the problem to be lubricant in the solenoid valve which controls operation of the vent valve. The cause of this problem appears to be unrelated to a similar problem reported on AS-508 which was attributed to binding in the valve, due to interferences caused by thermal gradients and manufacturing tolerances "stack-up". The AS-509 problem is considered closed with removal of lubricated solenoid valves from AS-510 and subsequent vehicles and from the spares storeroom. The AS-508 problem is still under study.

3.4.3 LH_2 Loading

The LH_2 system successfully supported countdown and launch. The fill sequence began with start of S-II loading at 08:57 EST, January 31, 1971, and was completed 84 minutes later when all stage replenish was established at 10:21 EST. S-II replenish was automatic until terminated with terminal countdown start at T-187 seconds. S-IVB replenish was automatic until T-3 hours when a manual override was initiated to obtain data for use in the event of a PU system failure. Automatic replenish was again established and continued until T-1 hour 25 minutes. A manual override was again initiated, this time at the request of S-IVB. Manual replenish was then continued through terminal countdown start.

3.5 INSULATION

The performance of the S-II-9 stage insulation, including Ground Support Equipment (GSE) purge and vacuum systems, was satisfactory in all respects. The forward bulkhead uninsulated area and the J-ring area purge pressures and flows were satisfactory. The common bulkhead was evacuated to approximately 0.5 psia, well below the redline value.

Total heat to the liquid hydrogen in flight is estimated as 65,000 Btu which is well below the 209,000 Btu allowable.

Following CDDT a minimal number of defects were identified in the external insulation system including four cork debonds, five coating blisters, and four foam divots. Repairs were accomplished within the allotted schedule time. All repairs could have been made if a 24-hour turnaround was required, provided access to the stage was available.

Following CDDT, cracks and debonds were found in a limited area in the ablative paint-type insulation on the inside of the interstage. Repairs were made prior to launch. The cause of the defects has not been determined; however, test programs are continuing to determine both the cause and corrective action.

During the launch countdown, observation by operational television indicated that the insulation performed in a satisfactory manner.

3.6 GROUND SUPPORT EQUIPMENT

3.6.1 Ground/Vehicle Interface

In general, performance of the ground service systems supporting all stages of the launch vehicle was satisfactory. Overall damage to the pad, LUT, and support equipment from the blast and flame impingement was considered minimal. Detailed discussion of the GSE is contained in KSC Apollo/Saturn V (AS-509) "Ground Support Evaluation Report."

The PTCS satisfactorily supported countdown and launch operations. There was no damage and only one problem noted. A printed circuit board in the S-IVB LOX auto computer drawer was replaced.

The Data Transmission System (DTS) satisfactorily supported countdown and launch. There was no damage and only one problem noted. The LH_2 transfer line preconditioner vent valve secondary solenoid command did not function when the Firing Room No. 2 switch was activated.

The Environmental Control System (ECS) performed satisfactorily throughout countdown and launch. Changeover from air to GN_2 purge was made at 05:03 EST, 20 minutes prior to the end of the T-9 hour hold. Purge GN_2 flow was continued after launch until approximately 20 minutes in order to obtain data on low pressure GN_2 line volume and ECS flow at reduced supply pressures. All launch vehicle and spacecraft specifications were met. There were no system failures.

The holddown arms and Service Arm Control Switches (SACS) satisfactorily supported countdown and launch. All holddown arms released pneumatically within a 4 millisecond period. The retraction and explosive release lanyard pull was accomplished in advance of ordnance actuation with a 36 millisecond margin. SACS primary switches closed within 6 milliseconds of each other at 418 and 424 milliseconds after commit. The SACS secondary switches were 16 milliseconds apart at 1.070 and 1.086 seconds after commit.

Overall performance of the TSM was satisfactory. Mast retraction times were nominal; 2.168 seconds for TSM 1-2, 2.496 seconds for TSM 3-2, and 2.131 seconds for TSM 3-4, measured from umbilical plate separation to mast retracted.

The Service Arms (S/A 1 through 8) satisfactorily supported launch and caused no countdown holds or delays.

3.6.2 MSFC Furnished Ground Support Equipment

The S-IC mechanical GSE supported countdown and launch satisfactorily. System damage was slight and only one minor problem was noted. During application of S-IC hydraulics at about T-22 hours a slight leak was noted in the pump No. 1 upper servo cylinder supply line. The leak was isolated to a faulty O-ring seal which was replaced per NCR 259691 when hydraulics were removed at about T-20 hours. The system then performed satisfactorily through liftoff without further incident.

The S-IC GSE satisfactorily supported countdown and launch. There were no failures or anomalies and only minor damage.

All ground power and battery equipment supported satisfactorily from the start of precount through launch. All systems performed within acceptable limits and there was no significant launch damage.

At T-50 hours during S-IC flight battery activation, it was found that four cell vent caps could not be installed with normal torque (2-3 in.-lb). The cell caps were installed using 6 in.-lb of torque. The cell caps were removed and the battery vent holes and caps were inspected. No damage was found. The caps were reinstalled using the normal torque value of 2-3 in.-lb. For additional assurance that no damage had occurred, the voltages of the battery and the individual cells were monitored for 15 hours with all voltages normal. It was decided that the problem experienced with the cell caps was not cause for rejection if the batteries could pass all requirements of activation. The batteries passed all other requirements, were used for flight and performed satisfactorily. No corrective action is planned.

The hazardous gas detection system became active during countdown operations at 05:00 EST and satisfactorily supported GN_2 changeover, LOX and LH_2 propellant loading operations, and the remainder of countdown. No valid oxygen or hydrogen detections were recorded during countdown operations except for air intrusion into the S-IC aft area, which has been observed on all launches.

Following installation of S-IVB stage batteries and application of stage power at T-23 hours 43 minutes, battery heating was noted which appeared to be a failure of the primary heater thermal switch in forward battery No. 2. Battery temperature indication reached 101.6°F which was higher than the previous battery lab temperature indication of 94°F. Replacement of the battery was accomplished at T-21 hours 7 minutes resulting in a 10 minute delay to the power transfer test; however, no hold was required. The replacement battery exhibited a similar initial temperature response followed by normal temperature cycling. Subsequent laboratory testing of the replaced battery demonstrated that the battery was being controlled by the temperature controller in a normal manner, and the battery was redesignated as a backup battery.

During IU battery activation, it was found that cell No. 8 of the 6D20 battery was installed with reversed polarity by the manufacturer. The defective battery was replaced by a new battery which corrected the problem.

During battery activation, it was found that the vent valve on the 6D40 battery would not hold pressure at 10 psig. The vent valve should hold pressure up to 10 psig, and vent at pressures greater than 10 psig. The defective valve was replaced with a new item and retested, correcting the problem.

At T-5 hours it was observed on the Digital Events Evaluator (DEE) -6 printout that UT and the Countdown Clock (CDC) time seconds transmission was offset by 271 milliseconds. The CDC lagged the UT by 271 milliseconds. The first several Saturn V vehicles were launched prior to a clock model that synchronized UT and CDC time and had

similar offsets. It is suspected that this offset was caused by not performing a complete count clock reinitialization after the timing units were switched on the morning of January 31, 1971. A decision was made to use "as is" for launch and the count proceeded.

SECTION 4

TRAJECTORY

4.1 SUMMARY

The vehicle was launched on an azimuth 90 degrees east of north. A roll maneuver was initiated at 12.8 seconds that placed the vehicle on a flight azimuth of 75.558 degrees east of north. The reconstructed trajectory was generated by merging the following four trajectory segments: the ascent phase, the parking orbit phase, the injection phase, and the post Translunar Injection (TLI) phase. The analysis for each phase was conducted separately with appropriate end point constraints to provide trajectory continuity. Available C-Band radar and Unified S-Band (USB) tracking data plus telemetered guidance velocity data were used in the trajectory reconstruction.

The trajectory parameters from launch to TLI were close to nominal. Earth parking orbit insertion conditions were achieved 1.72 seconds earlier than nominal at a heading angle 0.071 degree less than nominal. TLI was achieved 4.99 seconds earlier than nominal. The trajectory parameters at Command and Service Module (CSM) separation deviated from nominal since the event occurred 181.0 seconds later than predicted.

4.2 TRAJECTORY EVALUATION

4.2.1 Ascent Phase

The ascent phase spans the interval from guidance reference release through parking orbit insertion. The ascent trajectory was established by using telemetered guidance velocities as generating parameters to fit tracking data from five C-Band stations and two S-Band stations. Approximately 25 percent of the C-Band tracking data and 60 percent of the S-Band tracking data were eliminated due to inconsistencies. An investigation to explain the high percentage of S-Band data inconsistencies is being conducted. The launch phase portion of the ascent phase, (liftoff to approximately 20 seconds), was established by constraining integrated telemetered guidance accelerometer data to the best estimate trajectory.

Actual and nominal altitude, surface range, and crossrange for the ascent phase are presented in Figure 4-1. Actual and nominal space-fixed velocity and flight path angle during ascent are shown in Figure 4-2. Actual and nominal comparisons of total inertial accelerations are shown in Figure 4-3. The maximum acceleration during S-IC burn was 3.82 g.

Mach number and dynamic pressure are shown in Figure 4-4. These parameters were calculated using meteorological data measured to an altitude of 59.0 kilometers (31.9 n mi). Above this altitude the measured data were merged into the U.S. Standard Reference Atmosphere.

Actual and nominal values of parameters at significant trajectory event times, cutoff events, and separation events are shown in Tables 4-1, 4-2, and 4-3, respectively.

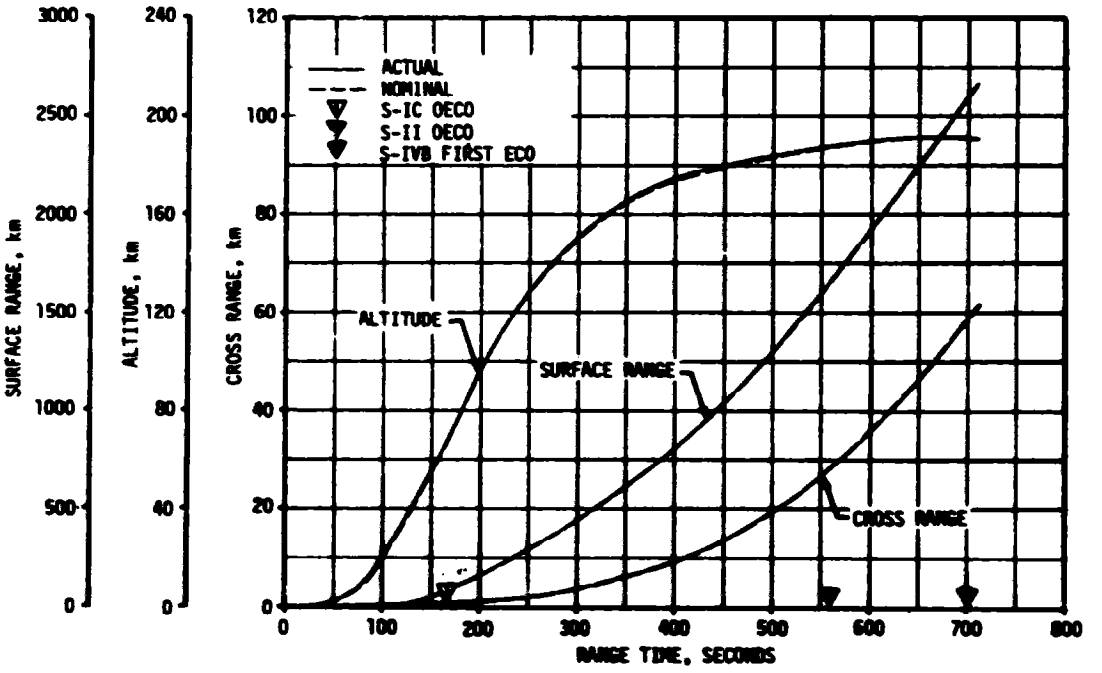

Figure 4-1. Ascent Trajectory Position Comparison

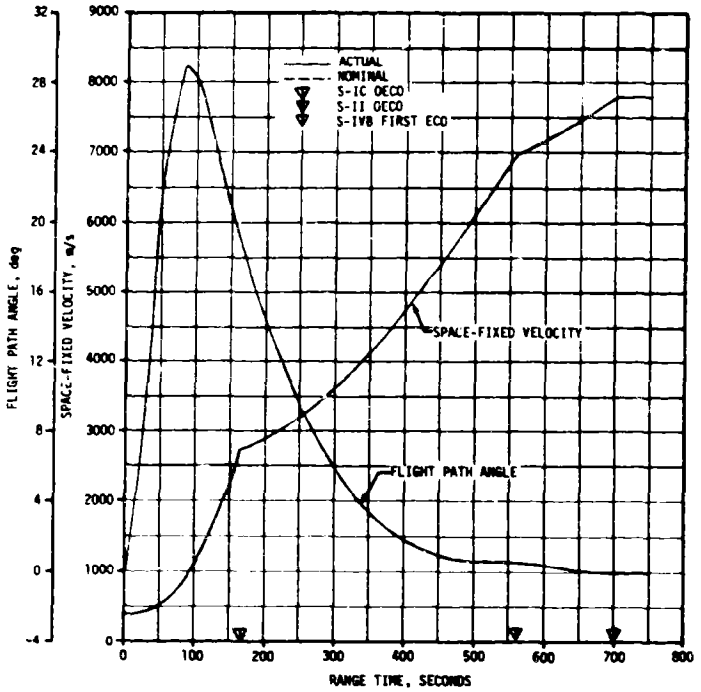

Figure 4-2. Ascent Trajectory Space-Fixed Velocity and Flight Path Angle Comparisons

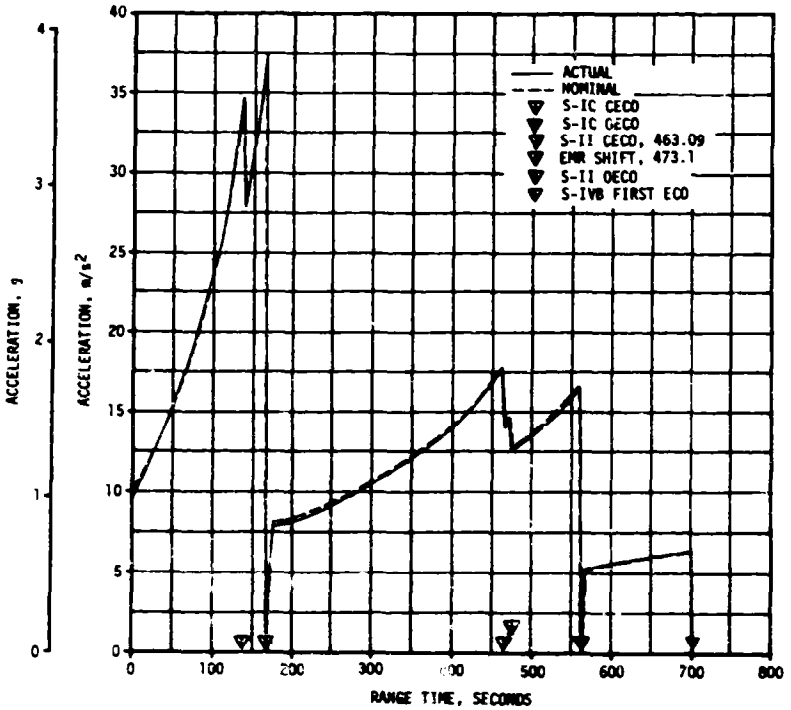

Figure 4-3. Ascent Trajectory Acceleration Comparison

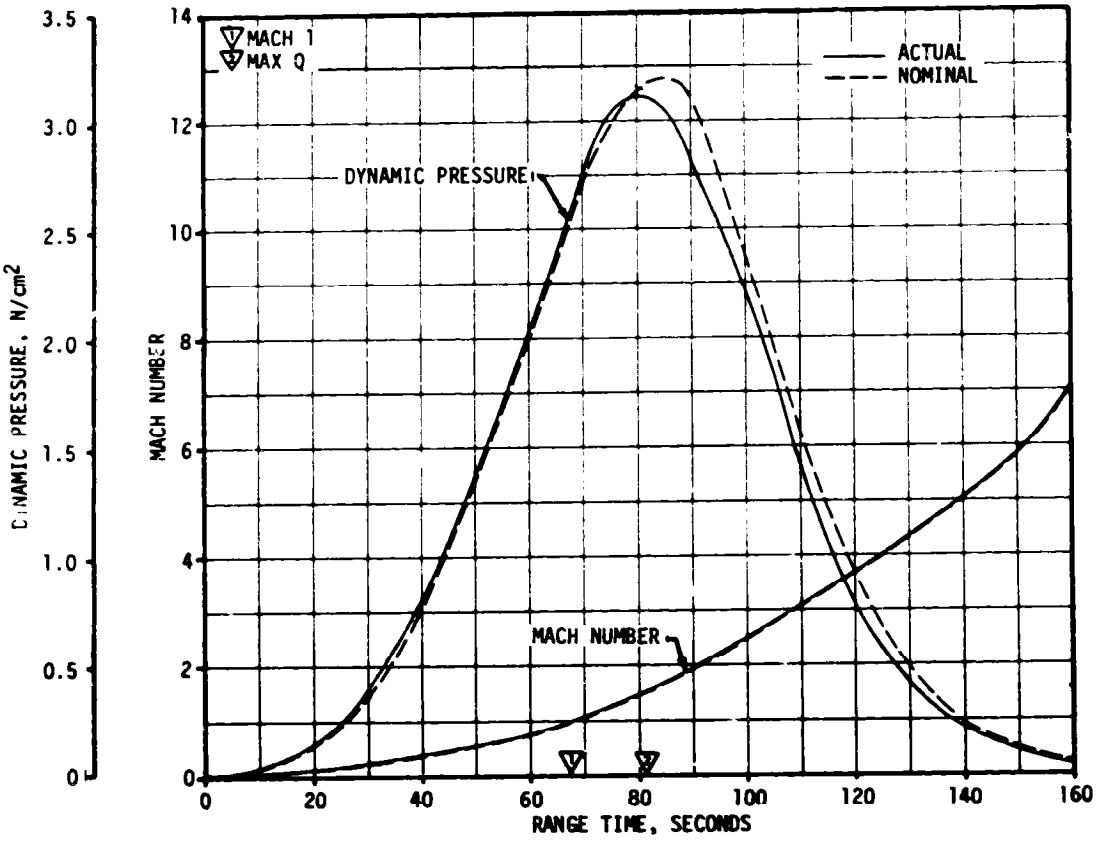

Figure 4-4. Dynamic Pressure and Mach Number Comparisons

4.2.2 Parking Orbit Phase

Orbital tracking was conducted by the NASA Manned Space Flight Network (MSFN). Three C-Band stations and three S-Band stations furnished seven data passes for use in determining the parking orbit trajectory.

The parking orbit trajectory was obtained by integrating a comprehensive orbit model with corrected insertion conditions forward to 8810 seconds (02:26:50). The insertion conditions, as determined by the Orbital Correction Program (OCP), were obtained by a differential correction procedure which adjusted the estimated insertion conditions to fit the tracking data in accordance with the weights assigned to the data. The venting model used was derived from telemetered guidance velocity data from the ST-124M-3 guidance platform.

Table 4-1. Comparison of Significant Trajectory Events

EVENT	PARAMETER	ACTUAL	NOMINAL	ACT-NOM
First Motion	Range Time, sec	0.2	0.2	0.0
	Total Inertial Acceleration, m/s^2	10.34	10.43	-0.09
	(ft/s^2)	(33.92)	(34.22)	(-0.30)
	(g)	(1.05)	(1.06)	(-0.01)
Mach 1	Range Time, sec	68.0	69.2	-1.2
	Altitude, km	8.0	8.0	0.0
	(n mi)	(4.3)	(4.3)	(0.0)
Maximum Dynamic Pressure	Range Time, sec	81.0	85.6	-4.6
	Dynamic Pressure, N/cm^2	3.14	3.19	-0.05
	(lbf/ft^2)	(655.80)	(666.25)	(-10.45)
	Altitude, km	12.3	13.6	-1.3
	(n mi)	(6.6)	(7.3)	(-0.7)
Maximum Total Inertial Acceleration: S-IC	Range Time, sec	164.18	164.24	-0.06
	Acceleration, m/s^2	37.46	37.13	0.33
	(ft/s^2)	(122.90)	(121.82)	(1.08)
	(g)	(3.82)	(3.79)	(0.03)
S-II	Range Time, sec	463.17	464.05	-0.88
	Acceleration, m/s^2	17.71	17.81	-0.10
	(ft/s^2)	(58.10)	(58.43)	(-0.33)
	(g)	(1.81)	(1.82)	(-0.01)
S-IVB 1st Burn	Range Time, sec	700.66	702.38	-1.72
	Acceleration, m/s^2	6.59	6.49	0.10
	(ft/s^2)	(21.62)	(21.29)	(0.33)
	(g)	(0.67)	(0.66)	(0.01)
S-IVB 2nd Burn	Range Time, sec	9,263.34	9,268.33	-4.99
	Acceleration, m/s^2	14.07	13.77	0.30
	(ft/s^2)	(46.16)	(45.18)	(0.98)
	(g)	(1.43)	(1.40)	(0.03)
Maximum Earth-Fixed Velocity: S-IC	Range Time, sec	164.59	165.55	-0.96
	Velocity, m/s	2,369.8	2,364.2	5.6
	(ft/s)	(7,774.9)	(7,756.6)	(18.3)
S-II	Range Time, sec	560.07	557.99	2.08
	Velocity, m/s	6,575.9	6,570.4	5.5
	(ft/s)	(21,574.5)	(21,556.4)	(18.1)
S-IVB 1st Burn	Range Time, sec	710.56	712.28	-1.72
	Velocity, m/s	7,382.8	7,383.3	-0.5
	(ft/s)	(24,221.8)	(24,223.4)	(-1.6)
S-IVB 2nd Burn	Range Time, sec	9,263.67	9,268.44	-4.77
	Velocity, m/s	10,422.3	10,413.9	8.4
	(ft/s)	(34,193.9)	(34,166.3)	(27.6)

NOTE: Range Times used are times of occurrence at the vehicle, see Figure 2-1.

Table 4-2. Comparison of Cutoff Events

PARAMETER	ACTUAL	NOMINAL	ACT-NOM	ACTUAL	NOMINAL	ACT-NOM
	S-1C CECO (ENGINE SOLENOID)			S-1C OECO (ENGINE SOLENOID)		
Range Time, sec	135.14	135.26	-0.12	164.10	165.04	-0.94
Altitude, km (n mi)	43.0 (23.2)	42.1 (22.7)	0.9 (0.5)	67.3 (36.3)	66.9 (36.1)	0.4 (0.2)
Surface Range, km (n mi)	44.8 (24.2)	43.7 (23.6)	1.1 (0.6)	94.7 (51.1)	94.7 (51.1)	0.0 (0.0)
Space-Fixed Velocity, m/s (ft/s)	1,915.2 (6,283.5)	1,892.6 (6,209.3)	22.6 (74.2)	2,734.8 (8,972.4)	2,729.8 (8,956.0)	5.0 (16.4)
Flight Path Angle, deg	23.554	23.626	-0.072	19.584	19.504	0.080
Heading Angle, deg	79.228	79.164	0.064	78.468	78.390	0.078
Cross Range, km (n mi)	0.4 (0.2)	0.1 (0.1)	0.3 (0.1)	0.7 (0.4)	0.3 (0.2)	0.4 (0.2)
Cross Range Velocity, m/s (ft/s)	7.0 (23.0)	3.8 (12.5)	3.2 (10.5)	13.5 (44.3)	9.8 (32.2)	3.7 (12.1)
	S-II CECO (ENGINE SOLENOID)			S-II OECO (ENGINE SOLENOID)		
Range Time, sec	463.09	464.05	-0.96	559.05	556.90	2.15
Altitude, km (n mi)	181.7 (98.1)	180.6 (97.5)	1.1 (0.6)	188.1 (101.6)	187.3 (101.1)	0.8 (0.5)
Surface Range, km (n mi)	1,101.4 (594.7)	1,102.9 (595.5)	-1.5 (-0.8)	1,650.0 (890.9)	1,634.3 (882.5)	15.7 (8.4)
Space-Fixed Velocity, m/s (ft/s)	5,655.4 (18,554.5)	5,669.4 (18,600.4)	-14.0 (-45.9)	6,981.7 (22,905.8)	6,976.2 (22,887.8)	5.5 (18.0)
Flight Path Angle, deg	0.829	0.851	-0.022	0.621	0.669	-0.048
Heading Angle, deg	82.809	82.876	-0.067	85.784	85.733	0.051
Cross Range, km (n mi)	14.9 (8.0)	14.6 (7.9)	0.3 (0.1)	28.0 (15.1)	27.9 (15.1)	0.1 (0.0)
Cross Range Velocity, m/s (ft/s)	106.3 (348.8)	112.7 (369.8)	-6.4 (-21.0)	172.7 (566.6)	176.1 (577.8)	-3.4 (-11.2)
	S-IVB 1ST GUIDANCE CUTOFF SIGNAL			S-IVB 2ND GUIDANCE CUTOFF SIGNAL		
Range Time, sec	700.56	702.28	-1.72	9,263.24	9,268.23	-4.99
Altitude, km (n mi)	190.9 (103.1)	190.9 (103.1)	0.0 (0.0)	318.2 (171.8)	326.3 (176.2)	-8.1 (-4.4)
Surface Range, km (n mi)	2,604.4 (1,406.3)	2,614.4 (1,411.7)	-10.0 (-5.4)			
Space-Fixed Velocity, m/s (ft/s)	7,790.6 (25,559.7)	7,791.4 (25,562.3)	(-0.8) (-2.6)	10,832.9 (35,541.0)	10,826.1 (35,518.7)	6.8 (22.3)
Flight Path Angle, deg	-0.004	-0.001	-0.003	7.047	7.183	-0.136
Heading Angle, deg	91.245	91.317	-0.072	65.881	65.843	0.038
Cross Range, km (n mi)	58.7 (31.7)	59.8 (32.3)	-1.1 (-0.6)			
Cross Range Velocity, m/s (ft/s)	264.5 (867.8)	267.1 (876.3)	-2.6 (-8.5)			
Eccentricity				0.9712	0.9711	0.0001
C_3*, m^2/s^2 (ft^2/s^2)				-1,742,882 (-18,760,227)	-1,765,681 (-18,790,355)	2,799 (30,128)
Inclination, deg				30.821	30.812	0.009
Descending Node, deg				117.372	117.399	-0.027

NOTE: Range Times used are times of occurrence at the vehicle, see Figure 2-1.

* C_3 is twice the specific energy of orbit

$$C_3 = V^2 - \frac{2\mu}{R}$$

where V = Inertial Velocity
μ = Gravitational Constant
R = Radius vector from center of earth

Table 4-3. Comparison of Separation Events

PARAMETER	ACTUAL	NOMINAL	ACT-NOM
		S-IC/S-II SEPARATION	
Range Time, sec	164.8	165.8	-1.0
Altitude, km (n mi)	67.9 (36.7)	[illegible] (36.[illegible])	0.4 (0.3)
Surface Range, km (n mi)	96.1 (51.9)	[illegible] (51.9)	-0.1 (0.0)
Space-Fixed Velocity, m/s (ft/s)	2,744.6 (9,004.6)	2,739.7 (8,988.5)	4.9 (16.1)
Flight Path Angle, deg	19.494	19.404	0.090
Heading Angle, deg	78.467	78.390	0.077
Cross Range, km (n mi)	0.7 (0.4)	0.3 (0.2)	0.4 (0.2)
Cross Range Velocity, m/s (ft/s)	13.6 (44.6)	9.9 (32.5)	3.7 (12.1)
Geodetic Latitude, deg N	28.815	28.819	-0.004
Longitude, deg E	-79.649	-79.649	(0.0)
		S-II/S-IVB SEPARATION	
Range Time, sec	560.0	557.9	2.1
Altitude, km (n mi)	188.2 (101.6)	187.3 (101.1)	0.9 (0.5)
Surface Range, km (n mi)	1,656.0 (894.2)	1,640.6 (885.9)	15.4 (8.3)
Space-Fixed Velocity, m/s (ft/s)	6,985.2 (22,917.3)	6,979.8 (22,899.6)	5.4 (17.7)
Flight Path Angle, deg	0.612	0.659	-0.047
Heading Angle, deg	85.818	85.769	0.049
Cross Range, km (n mi)	28.2 (15.2)	28.0 (15.1)	0.2 (0.1)
Cross Range Velocity, m/s (ft/s)	173.2 (568.2)	176.6 (579.4)	-3.4 (-11.2)
Geodetic Latitude, deg N	31.030	31.017	0.013
Longitude, deg E	-63.681	-63.842	0.161
		S-IVB/CSM SEPARATION	
Range Time, sec	10,949.4	10,768.4	181.0
Altitude, km (n mi)	7,943.8 (4,289.3)	6,964.3 (3,760.4)	979.5 (528.9)
Space-Fixed Velocity, m/s (ft/s)	7,346.1 (24,101.4)	7,619.7 (24,999.0)	-273.6 (-897.6)
Flight Path Angle, deg	46.812	44.891	1.921
Heading Angle, deg	65.393	64.157	1.236
Geodetic Latitude, deg N	19.215	17.451	1.764
Longitude, deg E	-153.447	-156.588	3.141

NOTE: Range Times used are times of occurrence at the vehicle, see Figure 2-1.

The actual and nominal parking orbit insertion parameters are presented in Table 4-4. The ground track from insertion to S-IVB/CSM separation is given in Figure 4-5.

The S-Band range rate and X-Angle observations from first pass, Corpus Christi, Carnarvon, the Canary Islands and second pass Carnarvon, were not used in the OCP solutions because of inconsistencies with the C-Band radars. All S-Band data from Goldstone and second pass Canary Islands were deleted from the solution because of inconsistencies.

4.2.3 Injection Phase

The injection phase was generated by the integration of the telemetered guidance accelerometer data. These accelerometer data were initialized from a parking orbit state vector at 8810 seconds (02:26:50) and were constrained to a state vector at TLI obtained from the post-TLI trajectory. The S-Band tracking data available during the early portion

Table 4-4. Parking Orbit Insertion Conditions

PARAMETER	ACTUAL	NOMINAL	ACT-NOM
Range Time, sec	710.56	712.28	-1.72
Altitude, km (n mi)	190.9 (103.1)	190.9 (103.1)	0.0 (0.0)
Space-Fixed Velocity, m/s (ft/s)	7,792.5 (25,565.9)	7,793.1 (25,567.9)	-0.6 (-2.0)
Flight Path Angle, deg	-0.003	-0.001	-0.002
Heading Angle, deg	91.656	91.727	-0.071
Inclination, deg	31.120	31.114	0.006
Descending Node, deg	117.455	117.429	0.026
Eccentricity	0.0002	0.0000	0.0002
Apogee*, km (n mi)	185.3 (100.1)	185.2 (100.0)	0.1 (0.1)
Perigee*, km (n mi)	183.2 (98.9)	185.0 (99.9)	-1.8 (-1.0)
Period, min	88.18	88.19	-0.01
Geodetic Latitude, deg N	31.246	31.236	0.010
Longitude, deg E	-52.983	-52.878	-0.105

NOTE: Range Times used are times of occurrence at the vehicle, see Figure 2-1.
*Based on a spherical earth of radius 6,378.165 km (3,443.934 n mi).

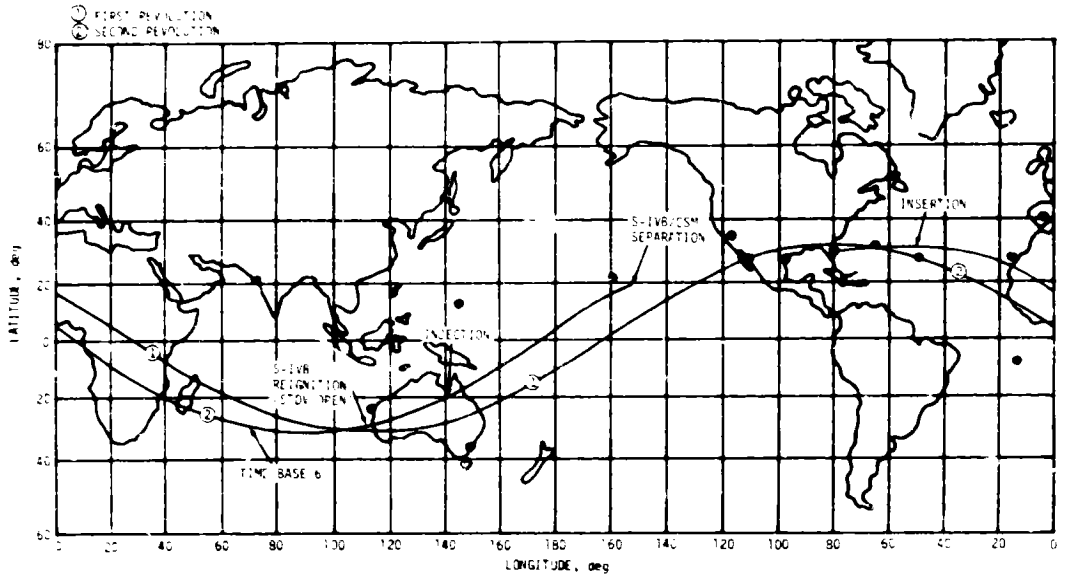

Figure 4-5. Ground Track

of the injection phase were not used in the trajectory reconstruction because the data were inconsistent with parking orbit and translunar orbit tracking solutions.

Comparisons between the actual and nominal space-fixed velocity and flight path angle are shown in Figure 4-6. The actual and nominal total inertial acceleration comparisons are presented in Figure 4-7. The space-fixed velocity was greater than nominal with deviations more noticeable towards the end of the time period. The actual and nominal targeting parameters at S-IVB second guidance cutoff are presented in Table 4-2.

4.2.4 Post TLI Phase

The post TLI trajectory spans the interval from translunar injection to S-IVB/CSM separation. Tracking data from one C-Band station (Merritt Island) and three S-Band stations (Goldstone, Guam, and Hawaii) were utilized in the reconstruction of this trajectory segment. The post TLI trajectory reconstruction utilizes the same methodology as outlined in paragraph 4.2.2. The actual and nominal translunar injection conditions are compared in Table 4-5. The S-IVB/CSM separation conditions are presented in Table 4-3.

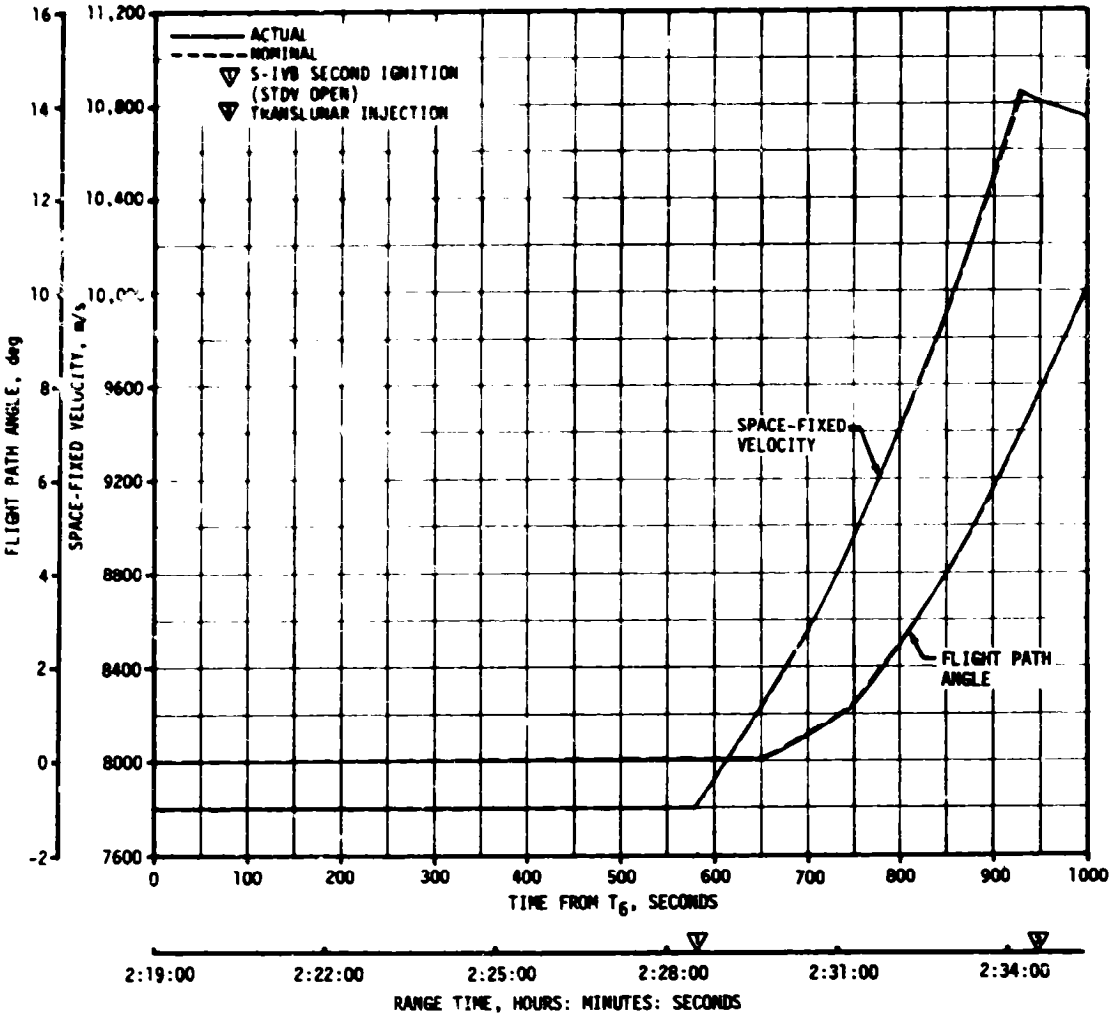

Figure 4-6. Injection Phase Space-Fixed Velocity and Flight Path Angle Comparisons

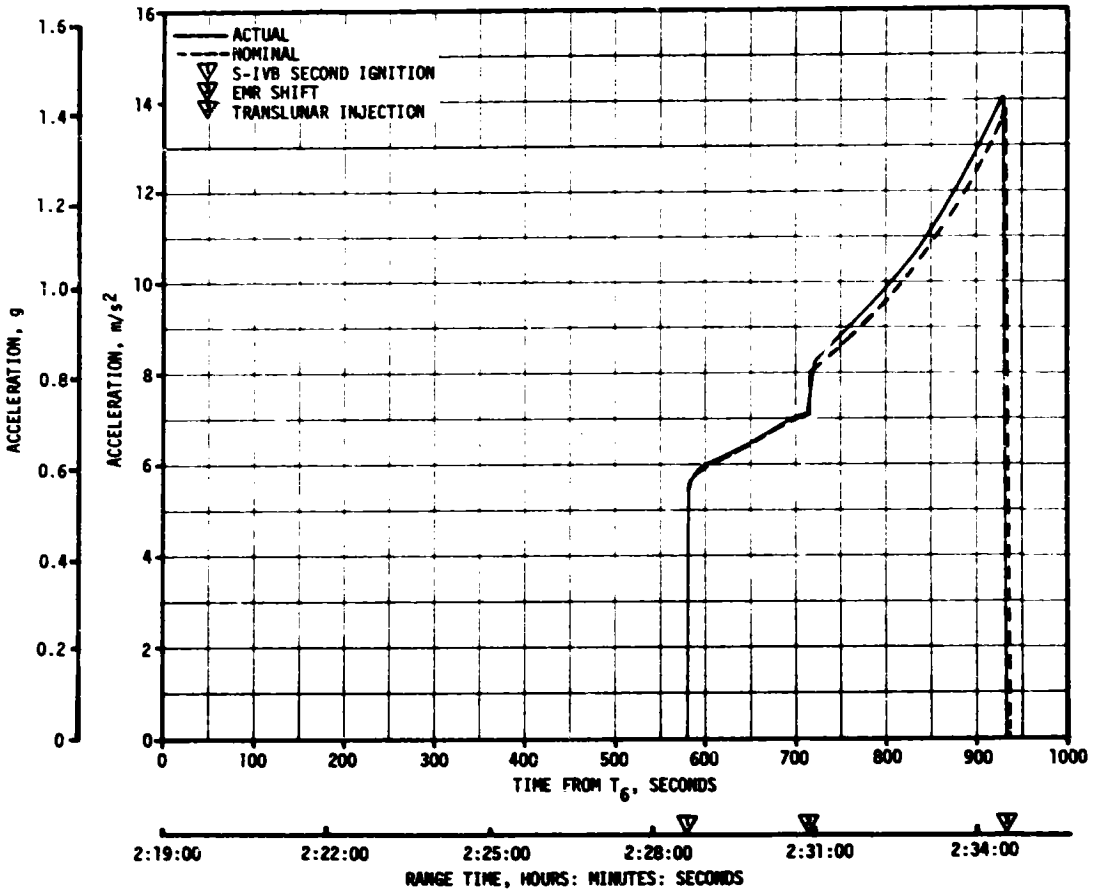

Figure 4-7. Injection Phase Acceleration Comparison

Table 4-5. Translunar Injection Conditions

PARAMETER	ACTUAL	NOMINAL	ACT-NOM
Range Time, sec	9,273.24	9,278.23	-4.99
Altitude, km (n mi)	331.8 (179.2)	340.1 (183.6)	-8.3 (-4.4)
Space-Fixed Velocity, m/s (ft/s)	10,824.7 (35,514.1)	10,818.1 (35,492.5)	6.6 (21.6)
Flight Path Angle, deg	7.481	7.633	-0.152
Heading Angle, deg	65.592	65.546	0.046
Inclination, deg	30.813	30.812	0.001
Descending Node, deg	117.358	117.400	-0.042
Eccentricity	0.9722	0.9723	-0.0001
C_3, m^2/s^2 (ft^2/s^2)	-1,678,092 (-18,062,833)	-1,673,540 (-18,013,836)	-4,552 (-48,997)

NOTE: Range Times used are times of occurrence at the vehicle, see Figure 2-1.

SECTION 5

S-IC PROPULSION

5.1 SUMMARY

All S-IC propulsion systems performed satisfactorily. Stage site thrust (averaged from time zero to Outboard Engine Cutoff [OECO]) was 0.65 percent higher than predicted. Total propellant consumption rate was 0.42 percent higher than predicted with the consumed Mixture Ratio (MR) 0.94 percent higher than predicted. Specific impulse was 0.23 percent higher than predicted. Total propellant consumption from Holddown Arm (HDA) release to OECO was low by 0.15 percent.

Center Engine Cutoff (CECO) was initiated by the Instrument Unit (IU) at 135.1 seconds as planned. Outboard engine cutoff, initiated by LOX low level sensors, occurred at 164.10 seconds which was 0.94 second earlier than predicted. The LOX residual at OECO was 42,570 lbm compared to the predicted 42,257 lbm. The fuel residual at OECO was 32,312 lbm compared to the predicted 31,630 lbm.

This was the first flight which incorporated a venturi in the LOX pressurization system to replace the GOX Flow Control Valve (GFCV). The system performed satisfactorily and all performance requirements were met, although the LOX ullage pressure drifted below the minimum predicted level at 140 seconds.

S-IC hydraulic system performance was normal throughout the flight.

5.2 S-IC IGNITION TRANSIENT PERFORMANCE

The fuel pump inlet preignition pressure was 45.9 psia and within F-1 Engine Model Specification limits of 43.3 to 110 psia.

The LOX pump inlet preignition pressure and temperature were 81.7 psia and -287.3°F and were within the F-1 Engine Model Specification limits, as shown in Figure 5-1.

The planned 1-2-2 start was attained. Engine position starting order was 5, 1-3, and 2-4. By definition, two engines are considered to start together if their combustion chamber pressures reach 100 psig in a 100-millisecond time period. Thrust buildup rates were as expected, as shown in Figure 5-2.

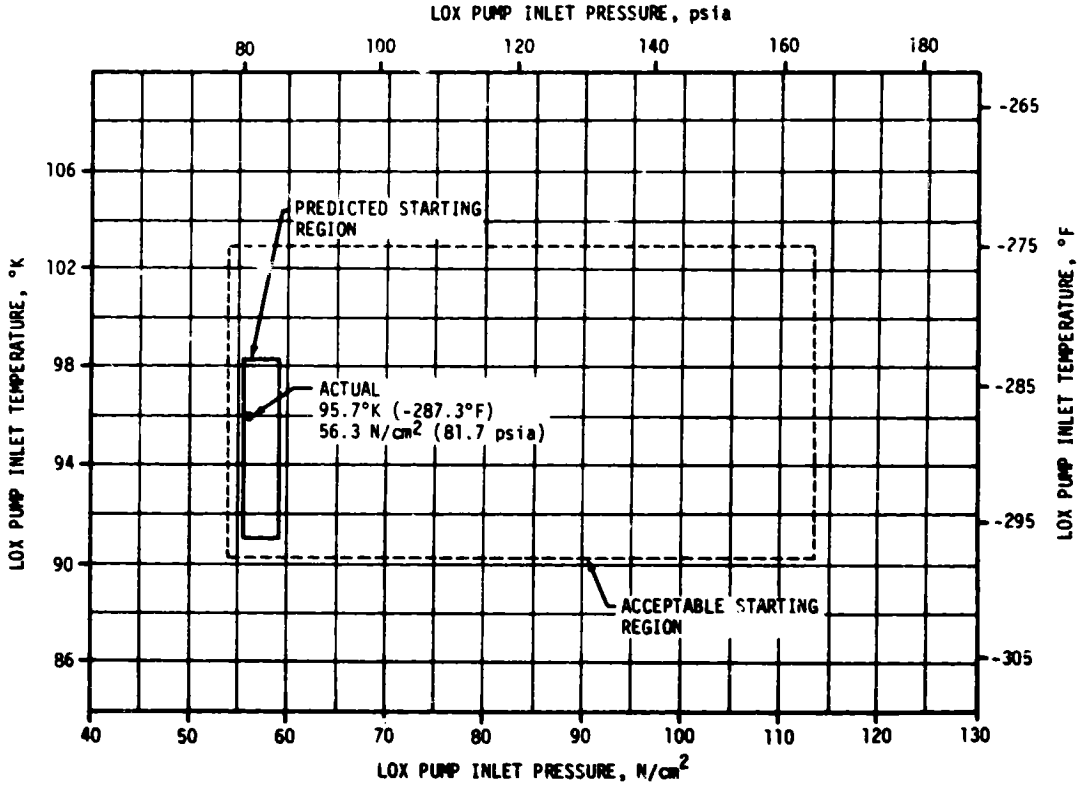

Figure 5-1. S-IC LOX Start Box Requirements

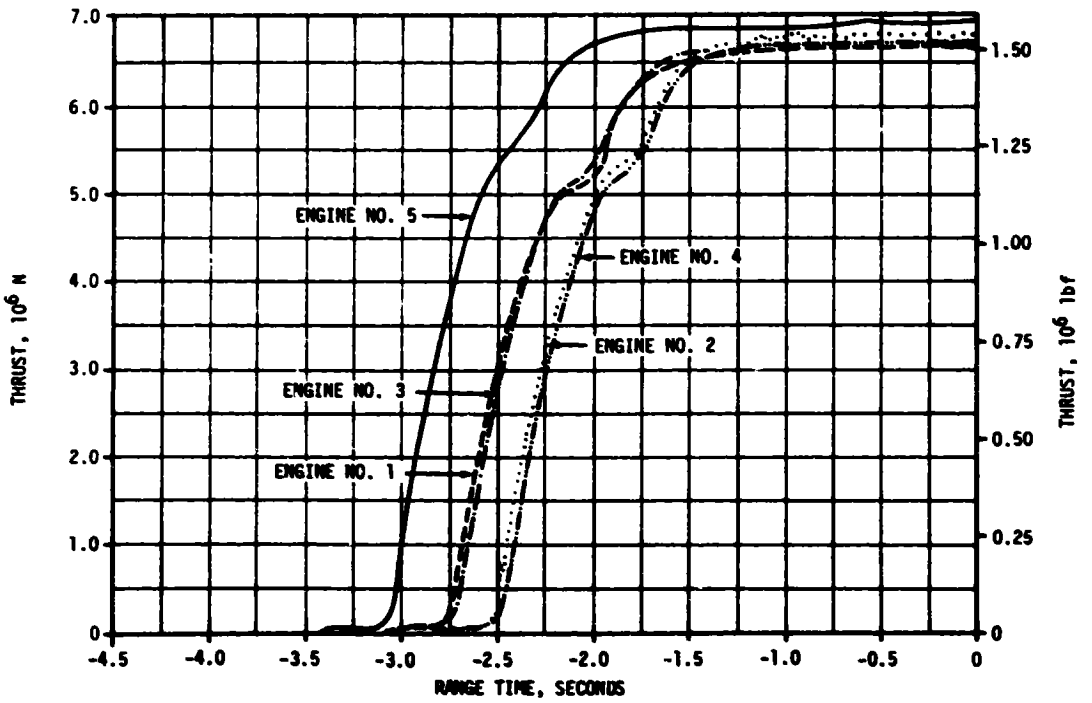

Figure 5-2. S-IC Engines Thrust Buildup

5.3 S-IC MAINSTAGE PERFORMANCE

S-IC stage propulsion performance was satisfactory. The stage site thrust (averaged from time zero to OECO) was 0.65 percent higher than predicted. Total propellant consumption rate was 0.42 percent higher than predicted and the total consumed mixture ratio was 0.94 percent higher than predicted. The specific impulse was 0.23 percent higher than predicted. Total propellant consumption from HDA release to OECO was low by 0.15 percent. See Figure 5-3.

The higher than predicted site performance was due to (1) lower than predicted fuel density, and (2) use of an updated LOX density subroutine in the math model after the final prediction was computed. The lower fuel density was due to a lower than nominal batch density and a higher than predicted fuel temperature. The change in the LOX density subroutine incorporated a change in the Bureau of Standards LOX Density Tables (Standard used in S-IC Propulsion Analysis) which reflected a slightly higher density.

For comparison of F-1 engine flight performance with predicted performance, the flight performance has been analytically reduced to standard conditions and compared to the predicted performance which is based on ground firings and also reduced to standard conditions. These values are shown in Table 5-1 and are at the 35 to 38-second time slice. The largest thrust deviation from the predicted value was -13 Klbf for engine No. 2. Engines No. 3, 4 and 5 had lower thrust than predicted by 4, 2 and 9 Klbf, respectively. Engine No. 1 was high by 3 Klbf. Engines No. 2 and 4 were below the engine acceptance test minimum of 1500 Klbf at 1497 Klbf and 1494 Klbf, respectively. The average of all five engines was 1501 Klbf, but caused no problems, especially since the average flight (site) thrust was on the high side due to lower than expected fuel density. The F-1 engines for AS-510 and subs have been reorficed since being static fired and their performance levels targeted for 1,522 Klbf (F-1 ECP 612).

5.4 S-IC ENGINE SHUTDOWN TRANSIENT PERFORMANCE

Thrust decay of the F-1 engines was normal. Cutoff impulse, measured from cutoff signal to zero thrust was 682,522 lbf-s for the center engine and 2,664,436 lbf-s for all outboard engines.

Center engine cutoff, initiated by a signal from the IU, was at 135.1 seconds as planned. Outboard engine cutoff, initiated by LOX low level sensors, occurred at 164.10 seconds which was 0.94 second earlier than the nominal predicted time of 165.04 seconds. This is a small difference compared to the predicted 3-sigma limits of +5.61, and -4.08 seconds.

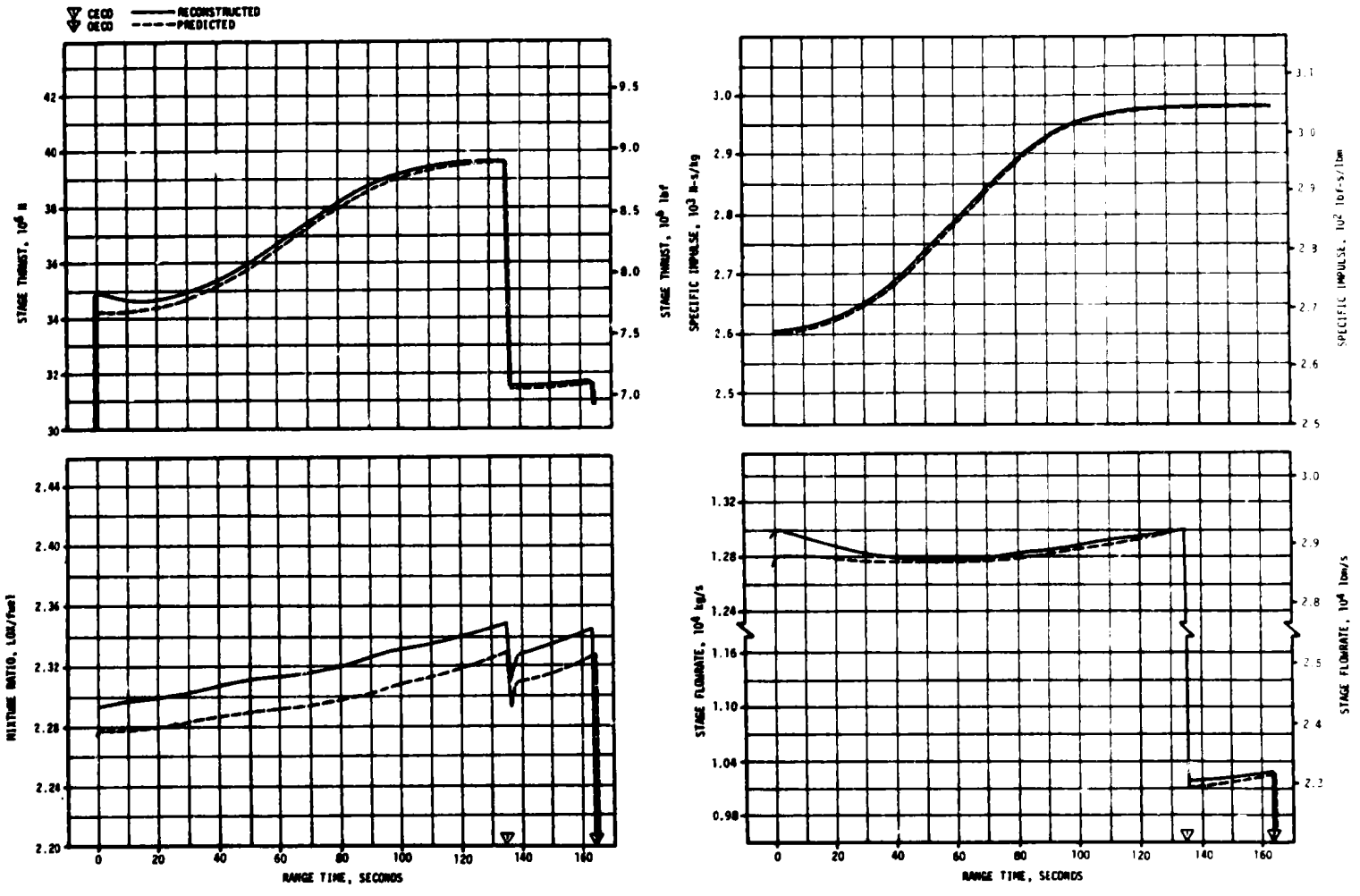

Figure 5-3. S-IC Stage Propulsion Performance

Table 5-1. S-IC Individual Standard Sea Level Engine Performance

PARAMETER	ENGINE	PREDICTED	RECONSTRUCTION ANALYSIS	DEVIATION PERCENT	AVERAGE DEVIATION PERCENT
Thrust, 10^3 lbf	1	1504	1507	0.199	
	2	1510	1497	-0.860	
	3	1505	1501	-0.266	-0.331
	4	1496	1494	-0.134	
	5	1514	1505	-0.594	
Specific Impulse, lbf-s/lbm	1	264.7	264.7	0	
	2	264.2	263.9	-0.114	
	3	265.0	264.9	-0.038	-0.053
	4	264.3	264.3	0	
	5	265.1	264.8	-0.113	
Total Flowrate lbm/s	1	5684	5692	0.141	
	2	5713	5672	-0.717	
	3	5677	5664	-0.228	-0.290
	4	5661	5652	-0.159	
	5	5712	5684	-0.490	
Mixture Ratio LOX/Fuel	1	2.266	2.262	-0.177	
	2	2.276	2.270	-0.264	
	3	2.280	2.275	-0.219	-0.211
	4	2.260	2.255	-0.221	
	5	2.241	2.237	-0.178	

NOTE: Performance levels were reduced to standard sea level and pump inlet conditions. Data were taken from the 35 to 38-second time slice.

5.5 S-IC STAGE PROPELLANT MANAGEMENT

Outboard engine cutoff was initiated by the LOX low level sensors as planned and resulted in residual propellants being very close to the predicted values. The residual LOX at OECO was 42,570 lbm compared to the predicted value of 42,257 lbm. The fuel residual at OECO was 32,312 lbm compared to the predicted value of 31,630 lbm. A summary of the propellants remaining at major event times is presented in Table 5-2.

Table 5-2. S-IC Stage Propellant Mass History

EVENT	PREDICTED, LBM		LEVEL SENSOR DATA, LBM		RECONSTRUCTED, LBM	
	LOX	FUEL	LOX	FUEL	LOX	FUEL
Ignition Command	3,306,116	1,438,188	-	1,428,561	3,312,769	1,428,561
Holddown Arm Release	3,239,986	1,419,569	3,254,139	1,407,728	3,244,149	1,409,389
CECO	524,730	239,453	511,940	232,883	513,984	233,870
OECO	42,257	31,630	36,702	32,629	42,570	32,312
Separation	37,362	29,266	-	-	37,507	29,867
Zero Thrust	37,017	28,714	-	-	36,795	29,176

NOTE: Predicted and reconstructed values do not include pressurization gas so they will compare with level sensor data.

5.6 S-IC PRESSURIZATION SYSTEMS

5.6.1 S-IC Fuel Pressurization System

The fuel tank pressurization system performed satisfactorily keeping ullage pressure within acceptable limits during flight. Helium Flow Control Valves (HFCV) 1 through 4 opened as planned and HFCV 5 was not required.

The low flow prepressurization system was commanded on at -97 seconds. The low flow system was cycled on a second time at -2.9 seconds. High flow pressurization, accomplished by the onboard pressurization system, performed as expected. Helium Flow Control Valve No. 1 was commanded on at -2.7 seconds and was supplemented by the high flow prepressurization system until umbilical disconnect.

Fuel tank ullage pressure was within the predicted limits throughout flight as shown in Figure 5-4. Helium Flow Control Valves 2, 3, and 4 were commanded open during flight by the switch selector within acceptable limits. Helium bottle pressure was 3125 psia at -2.8 seconds and decayed to 475 psia at OECO. Total helium flowrate and heat exchanger performance were as expected.

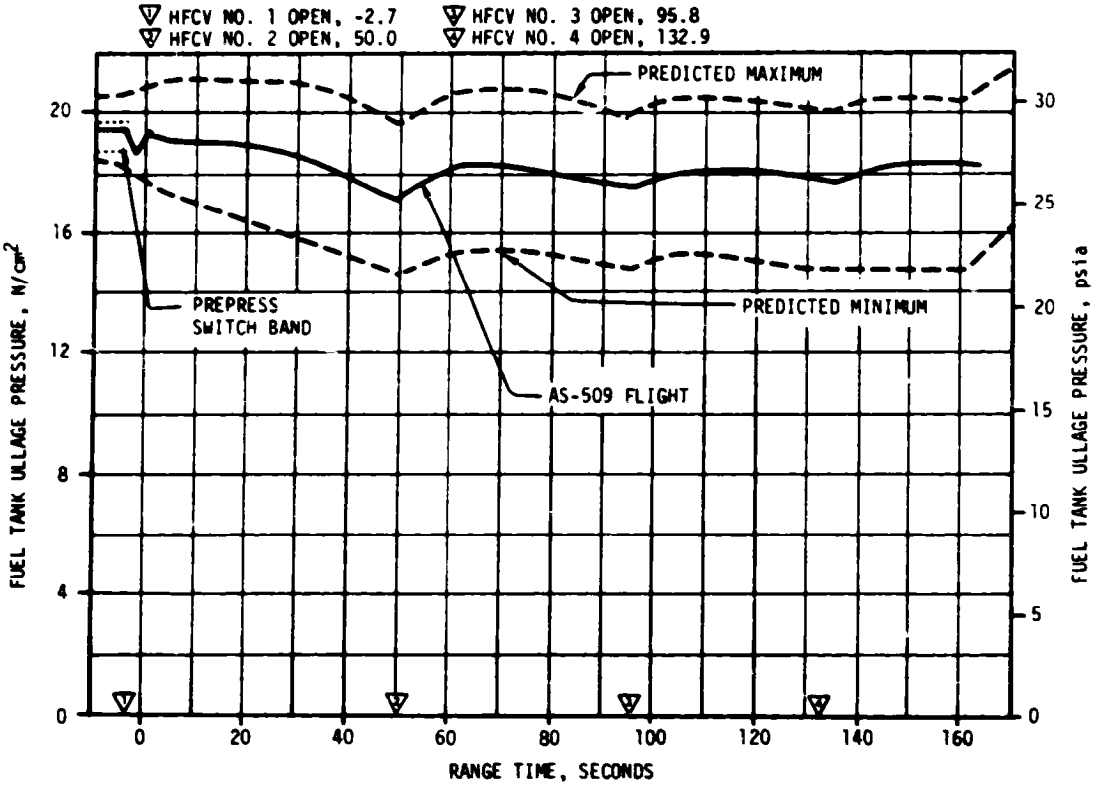

Figure 5-4. S-IC Stage Fuel Tank Ullage Pressure

Fuel pump inlet pressure was maintained above the required minimum Net Positive Suction Pressure (NPSP) during flight.

5.6.2 S-IC LOX Pressurization System

The LOX pressurization system performed satisfactorily and all performance requirements were met. The ground prepressurization system maintained ullage pressure within acceptable limits until launch commit. The on-board pressurization system which included a venturi in place of the GOX Flow Control Valve (GFCV) performed satisfactorily during flight.

The prepressurization system was initiated at -72 seconds. Ullage pressure increased to the prepressurization switch band and flow was terminated at -57.7 seconds. The low flow system was cycled on three additional times at -42.5, -21.4 and -5.1 seconds. At -4.7 seconds the high flow system was commanded on and maintained ullage pressure within acceptable limits until launch commit.

This was the first flight with ECP 3003 incorporated which replaced the GFCV with a venturi. Ullage pressure was maintained within the predicted limits until center engine cutoff. See Figure 5-5. Although

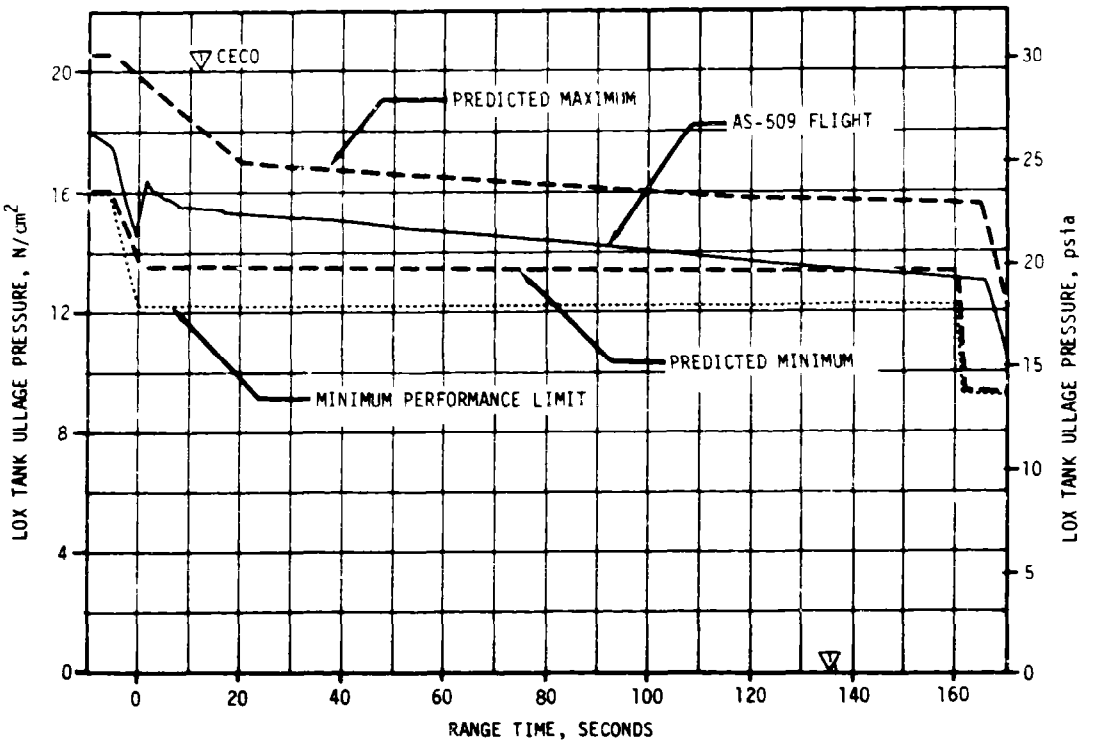

Figure 5-5. S-IC LOX Tank Ullage Pressure

ullage pressure decreased to slightly below the prediction after CECO, it was still well above the pressure required to prevent flash boiling. The maximum GOX flowrate to the tank after the initial transient was 46.9 lbm/s at CECO. The performance of the heat exchangers was as expected.

The LOX pump inlet pressure met the minimum required NPSP requirement throughout flight.

During the Countdown Demonstration Test (CDDT), the S-IC LOX tank vent and relief valve exceeded operation specifications on closing time. The vent and relief valve and its associated solenoid valve were removed and replaced with new ones. No problem was encountered with the replacement valves during prelaunch operations or during flight. See paragraph 3.4.2 for additional details.

5.7 S-IC PNEUMATIC CONTROL PRESSURE SYSTEM

The control pressure system functioned satisfactorily throughout the S-IC flight.

Sphere pressure was 3000 psia at liftoff and remained steady until CECO when it decreased to 2877 psia. The decrease was due to center engine prevalve actuation. There was a further decrease to 2506 psia after OECO.

5.8 S-IC PURGE SYSTEMS

Performance of the purge systems was satisfactory during the 164-second flight.

The turbopump LOX seal storage sphere pressure of 3000 psia was within the preignition limits of 2700 to 3300 psia. The pressure decayed to 2545 psia from liftoff to OECO.

5.9 S-IC POGO SUPPRESSION SYSTEM

The POGO suppression system performed satisfactorily during S-IC flight.

Outboard LOX prevalve temperature measurements indicated that the prevalve cavities were filled with gas prior to liftoff as planned. The four resistance thermometers behaved during the AS-509 flight similarly to the AS-508 flight. In the outboard lines, the temperature measurements were cold momentarily at liftoff indicating that LOX sloshed on the probes. They remained warm (off scale high) through flight, indicating helium was in the prevalve. At cutoff, the increased pressure forced LOX into the prevalves once more. The two thermometers in the center engine prevalve were cold, indicating LOX in this valve as planned.

5.10 S-IC HYDRAULIC SYSTEM

The performance of the S-IC hydraulic system was satisfactory. All servoactuator supply pressures were within required limits. The engine control system return pressures were within predicted limits, and the engine hydraulic control system valves operated as planned.

SECTION 6

S-II PROPULSION

6.1 SUMMARY

The S-II propulsion system performed satisfactorily throughout the flight. The S-II Engine Start Command (ESC), as sensed at the engines, occurred at 165.5 seconds. Center Engine Cutoff (CECO) occurred as planned at 463.09 seconds and Outboard Engine Cutoff (OECO) occurred at 559.05 seconds giving an outboard engine operation time of 393.6 seconds or 3.2 seconds longer than predicted. The later than predicted OECO was a result of a lower than predicted flowrate during the low Engine Mixture Ratio (EMR) portion of the flight.

Total stage thrust at the standard time slice (61 seconds after S-II ESC) was 0.25 percent below predicted. Total propellant flowrate, including pressurization flow, was 0.12 percent below predicted and stage specific impulse was 0.19 percent below predicted at the standard time slice. Stage propellant mixture ratio was 0.18 percent above predicted. Engine thrust buildup and cutoff transients were normal.

A center engine LOX feedline accumulator was installed for the first time on this flight as a POGO suppression device. The operation of the accumulator system was effective in suppressing POGO type oscillations.

The propellant management system performance was satisfactory throughout propellant loading and flight. However, during the helium injection at T-4 hours, the LOX Overfill Shutoff (OFSO) sensor indicated wet approximately 15 percent of each minute. At this time an investigation was made to determine if a time period violation of the Launch Mission Rule (LMR) might occur later during terminal sequence. The investigation indicated that this would not be a problem and propellant loading operations were continued and progressed without incident. The new pneumatically actuated engine Mixture Ratio Control Valves (MRCV) were used for the first time in flight and operated satisfactorily.

The performance of the LH_2 tank pressurization system was satisfactory and within predicted limits. The LOX tank pressurization system operated sufficiently to satisfy all mission objectives; however, the LOX ullage pressure was below that predicted near the end of S-II flight. The low LOX ullage pressure is attributed primarily to restricted flow through the LOX tank pressurization regulator subsequent to LOX step pressurization at 264.1 seconds. The regulator is being replaced with an orifice on AS-510 and subsequent S-II stages.

Engine servicing operations, required to condition the engines, were satisfactorily accomplished. Engine start tank conditions were marginal at S-II ESC because of lower start tank relief valve settings caused by warmer than usual start tank temperatures. These warmer temperatures were a result of the hold prior to launch. Revised hold option procedures are under consideration for AS-510.

The recirculation, helium injection, and valve actuation systems performed satisfactorily.

S-II hydraulic system performance was normal throughout the flight.

6.2 S-II CHILLDOWN AND BUILDUP TRANSIENT PERFORMANCE

The engine servicing operations required to condition the engines prior to engine start were satisfactorily accomplished. Thrust chamber temperatures were within predicted limits at both prelaunch and engine start. Thrust chamber chilldown requirements were -200°F maximum at prelaunch commit and -150°F maximum at engine start. Thrust chamber temperatures ranged between -281 and -253°F at prelaunch commit and between -220 and -199°F at engine start. Thrust chamber temperature warmup rates during S-IC boost agreed closely with those experienced on previous flights.

Both temperature and pressure conditions of the J-2 engine start tanks were within the required prelaunch and engine start boxes as shown in Figure 6-1. Initial start tank pressurization normally occurs after thrust chamber chill is initiated resulting in nominal start tank temperatures at the time of vent valve closure of approximately -310°F. During initial start tank pressurization the temperature increases from 30 to 40°F and would normally read approximately -270 to -260°F. However, as a result of initiating countdown hold option No. 2 prior to thrust chamber chill, lockup temperatures were between -240 and -225°F or about 40°F warmer than usual.

Total time elapsed between start tank pressurization and S-II engine start including hold time, countdown time, and S-IC boost, was approximately 2550 seconds (00:42:30). During the hold, the start tank temperature increased approximately 85°F. Between pressurization and liftoff the start tanks were vented (using ground emergency vents) at least five times each in order to maintain start tank pressures below 1280 psia (which corresponds to the lowest relief valve setting) to prevent actuation of the relief valves. The actual relief valve settings vary inversely with the start tank temperatures; therefore, as a result of the initial pressurization occurring at a warmer temperature and the subsequent start tank warmup during the hold, the relief valve settings apparently were lower than 1280 psia. Engines No. 1, 2, and 4 start tank vent and relief valves relieved after liftoff at least one time

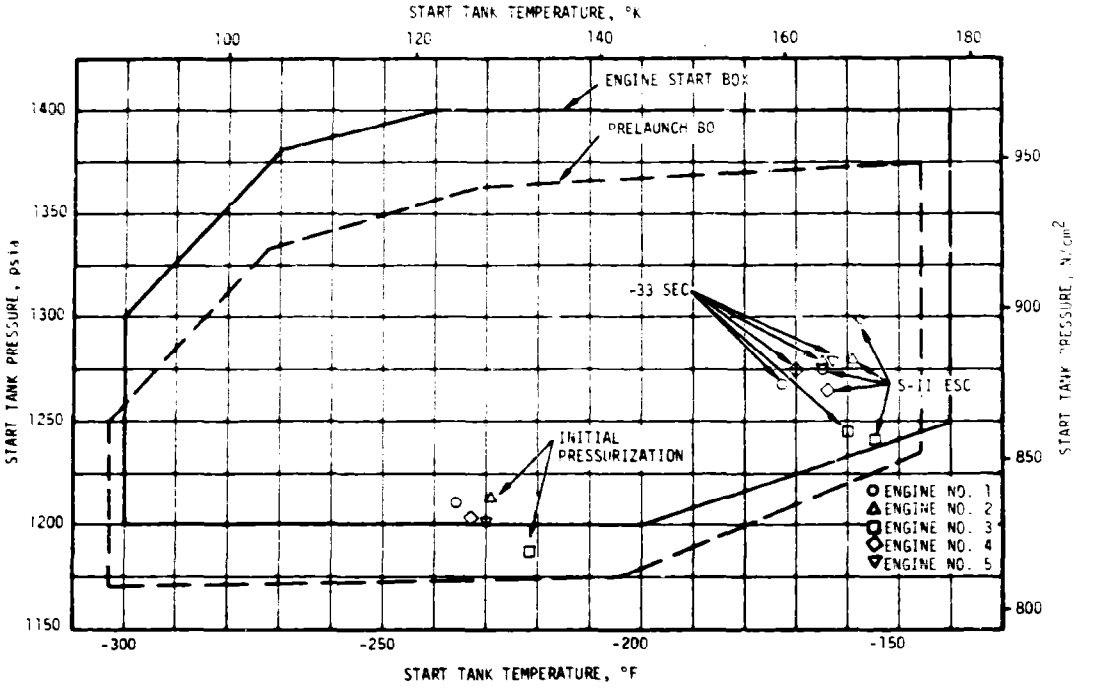

Figure 6-1. S-II Engine Start Tank Performance

prior to engine start. Engine No. 3 appeared to be relieving prior to liftoff and through S-IC boost. Although this venting is not desirable, it is considered by the engine contractor to be expected with such an increase in start tank temperature.

Prior to the AS-509 launch a prediction had been generated regarding the length of time available between start tank pressurization and exceeding the temperature redline requirements. This prediction was based upon data gathered during a special 30-minute hold test conducted on S-II-13 at Mississippi Test Facility (MTF) and extrapolated to represent maximum Kennedy Space Center (KSC) capability. A maximum time of 4200 seconds (01:10:00) was indicated between tank pressurization and liftoff. This, of course, would equate to a "hold" duration of 3720 seconds (01:02:00) since the final 480 seconds are required for the terminal count.

This prediction was not conservative in that it did not consider large engine to engine temperature differences or the possibility that start tank pressurization would occur prior to initiating thrust chamber chill. Unfortunately, both of these eventualities took place during the engine

conditioning period resulting in the warmest engine measuring -221°F as opposed to the prediction base of -258°F. This resulted in a reduction of the maximum pressurized time from 4200 seconds (01:10:00) to 2820 seconds (00:47:00). Actual time between pressurization and liftoff was 2400 seconds (00:40:00) so that a margin of 420 seconds was still available.

Both aspects of the J-2 engine start tank problem (limited hold duration and relief valve operation at warmer temperatures) will be resolved for AS-510 countdown by changes to the existing hold options. A procedure patterned after the new S-IVB procedure featuring a shortened start tank chilldown recycle will be devised and tested during the AS-510 Countdown Demonstration Test (CDDT). The intent of the new procedure will be to maintain or increase hold capability, maintain present count pickup point at -480 seconds without requiring advance warnings, and restrict hold operation to areas of the start tank pressure-temperature envelope that preclude relief valve operation at lower pressures.

As presently envisioned these objectives will require changes to the Launch Mission Rules both in the area of functional sequence and redlines.

All engine helium tank pressures were within the prelaunch and engine start limits of 2800 to 3450 psia. Engine helium tank pressures ranged between 3070 and 3035 psia prior to launch (at -19 seconds) and between 3170 and 3115 psia at S-II ESC. Helium tanks were vented five times during the hold period using the ground vent solenoids.

The LOX and LH_2 recirculation systems used to chill the feed ducts, turbopumps, and other engine components performed satisfactorily during prelaunch and S-IC boost. Engine pump inlet temperatures and pressures at engine start were well within the requirements as shown in Figure 6-2. The LOX pump discharge temperatures at S-II ESC were approximately 15.1°F subcooled, well below the 3°F subcooling requirement.

Prepressurization of the propellant tanks was accomplished satisfactorily. Ullage pressures at S-II ESC were 40.19 psia for LOX and 28.8 psia for LH_2.

S-II ESC was received at 165.5 seconds and the Start Tank Discharge Valve (STDV) solenoid activation signal occurred 1.0 second later. The engine thrust buildup was satisfactory and within the required thrust buildup envelope. All engines reached their mainstage levels (pressure switch pickup) within 2.87 seconds after S-II ESC.

6.3 S-II MAINSTAGE PERFORMANCE

The propulsion reconstruction analysis showed that stage performance during mainstage operation was satisfactory. A comparison of predicted and reconstructed performance of thrust, specific impulse, total flowrate,

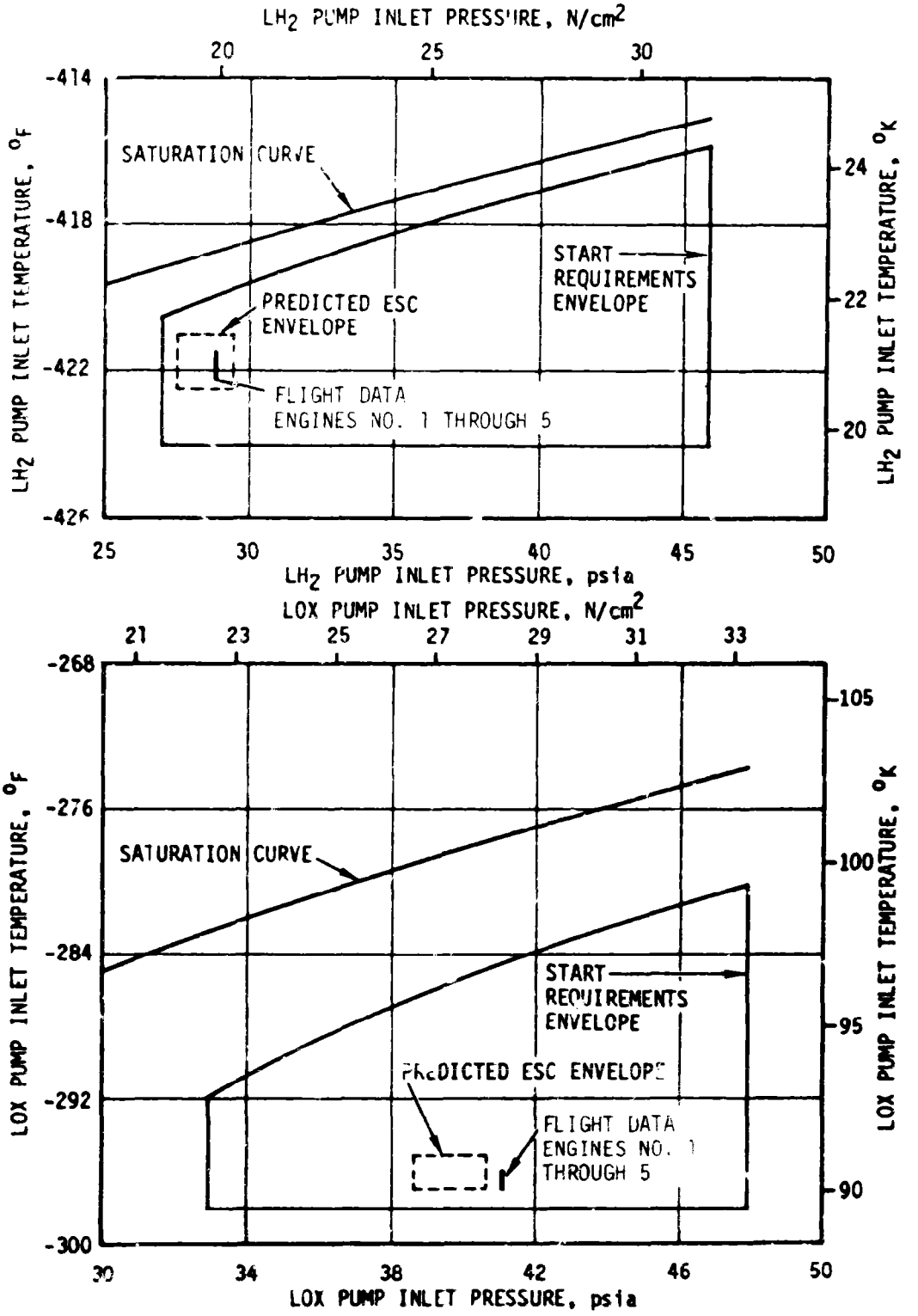

Figure 6-2. S-II Engine Pump Inlet Start Requirements

and mixture ratio versus time is shown in Figure 6-3. Stage performance during the high EMR portion of flight (prior to CECO) was very close to predicted. At the time of ESC +61 seconds, total stage thrust was 1,164,464 lbf which is 2931 lbf (0.25 percent) below the preflight prediction. Total propellant flowrate, including pressurization flow, was 2753.4 lbm/s, 0.12 percent below predicted. Stage specific impulse, including the effect of pressurization gas flowrate, was 422.9 lbf-s/lbm, 0.19 percent below predicted. Stage propellant mixture ratio was 0.18 percent above predicted.

Center engine cutoff was initiated at ESC +297.6 seconds as planned and reduced total stage thrust by 236,932 lbf to a level of 924,939 lbf. The EMR shift from high to low occurred 307.6 seconds after ESC; 0.5 seconds earlier than predicted. The change of EMR resulted in further stage thrust reduction and at ESC +380.3 seconds, the total stage thrust was 776,070 lbf; thus, a decrease in thrust of 148,869 lbf was indicated between high and low EMR operation. S-II burn duration was 393.6 seconds, which was 3.2 seconds longer than predicted.

Individual J-2 engine performance data are presented in Table 6-1 for the ESC +61 second time slice. Good correlation between predicted and reconstructed flight performance is indicated by the small deviations. The performance levels shown in Table 6-1 have not been adjusted to standard J-2 altitude conditions and do not include the effects of pressurization flow.

Typical minor engine performance shifts occurred during the burn period and are attributed to shifts in the Gas Generator (GG) oxidizer system resistance (see Table 6-2).

6.4 S-II SHUTDOWN TRANSIENT PERFORMANCE

S-II OECO was initiated by the stage LOX depletion cutoff system as planned. The LOX depletion cutoff system again included a 1.5 second delay timer. As in previous flights (AS-504 and subs), this resulted in engine thrust decay (observed as a drop in thrust chamber pressure) prior to receipt of the cutoff signal. The precutoff decay was somewhat greater than experienced on AS-508 and was due to a higher EMR at OECO. The high EMR was due to incorporation of the new two-position MRCV which operates nominally at a low EMR of 4.8, where the old valve was set nominally at 4.5.

Again, the largest thrust chamber pressure decay was noted on engine No. 1 with first indications of performance change visible at 0.68 second prior to the cutoff signal. See Figure 6-4. Total pressure decay on engine No. 1 was 230 psi while the other three outboard engines were approximately 115 psi over this interval.

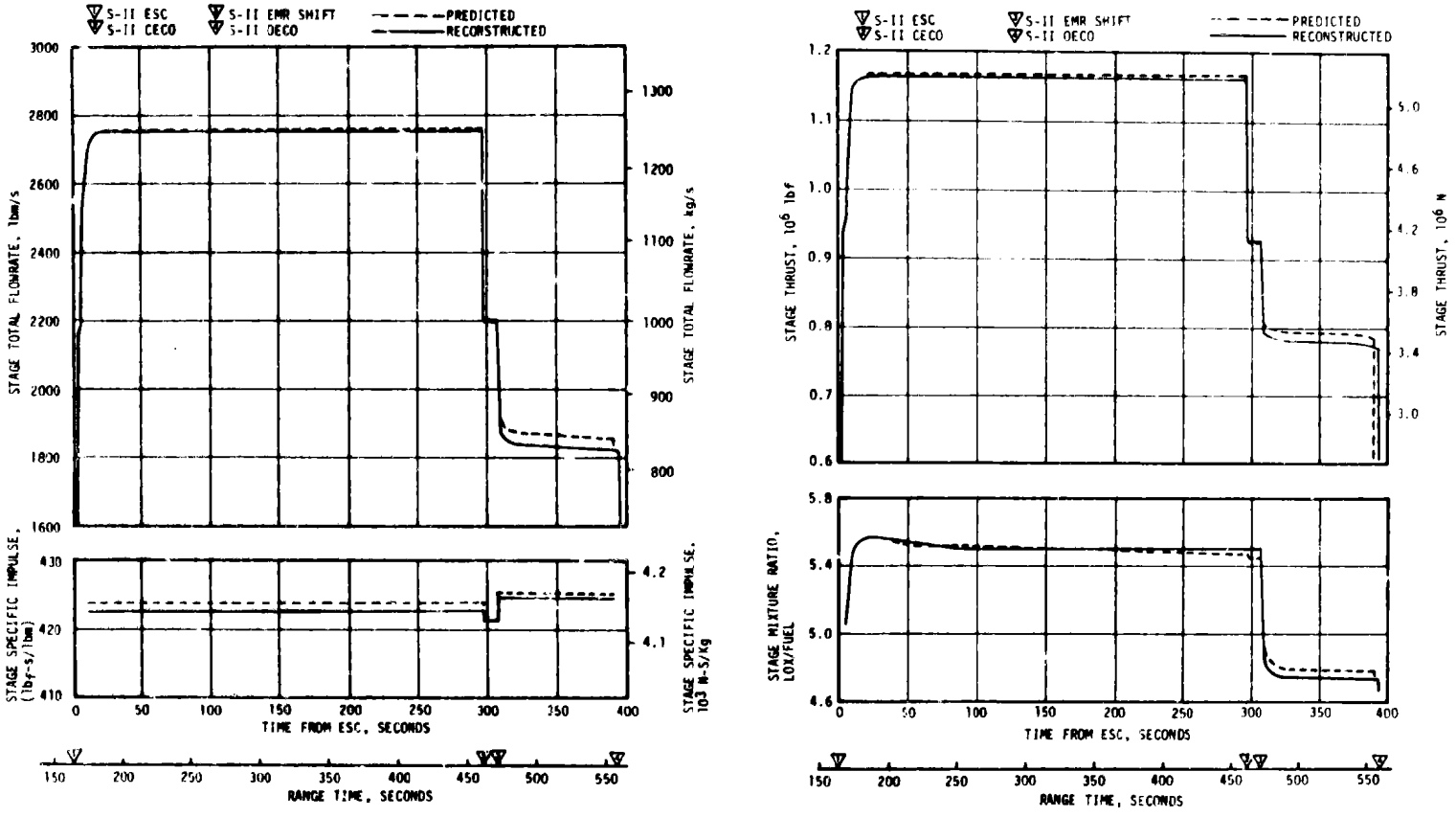

Figure 6-3. S-II Steady State Operation

Table 6-1. S-II Engine Performance

PARAMETER	ENGINE POSITION	PREDICTED	RECONSTRUCTED	PERCENT INDIVIDUAL DEVIATION	PERCENT AVERAGE DEVIATION
Thrust, lbf	1	230,660	229,897	-0.33	
	2	233,552	233,264	-0.12	
	3	233,446	233,146	-0.13	-0.25
	4	232,739	231,111	-0.70	
	5	236,998	237,046	0.02	
Specific Impulse, lbf-s/lbm	1	423.8	423.3	-0.12	
	2	425.1	424.1	-0.24	
	3	425.6	424.8	-0.19	-0.13
	4	424.3	424.1	-0.05	
	5	426.2	426.0	-0.05	
Engine Flowrate, lbm/s	1	544.2	543.1	-0.20	
	2	549.5	550.0	0.10	
	3	548.6	548.8	0.03	-0.13
	4	548.5	544.9	-0.65	
	5	556.1	556.4	0.06	
Engine Mixture Ratio, LOX/Fuel	1	5.55	5.56	0.18	
	2	5.53	5.57	0.72	
	3	5.54	5.56	0.36	0.43
	4	5.56	5.60	0.72	
	5	5.50	5.51	0.18	

NOTE: Performance Levels at ESC +61 seconds. Values do not include effect of pressurization flow.

At S-II OECO total thrust was down to 580,478 lbf. Stage thrust dropped to 5 percent of this level within 0.58 second. The stage cutoff impulse through the 5 percent thrust level is estimated to be 120,576 lbf-s.

6.5 S-II PROPELLANT MANAGEMENT

Flight and ground loading performance of the propellant management system was nominal and all parameters were within expected limits. The S-II stage employed an open-loop Propellant Utilization (PU) system utilizing fixed, open-loop commands from the Instrument Unit (IU) to drive the new two-position pneumatically operated MRCV. Open-loop PU is also planned for use on subsequent vehicles.

The facility Propellant Tanking Control System (PTCS) and the propellant management system properly controlled S-II loading and replenishment. However, at the start of the first period of helium injection (-4 hours),

Table 6-2. S-II Engine Performance Shifts

ENGINE POSITION	PERFORMANCE SHIFT (MAGNITUDE AND TIME OF OCCURRENCE)	REMARKS
1	-1400 lbf run-to-run shift in thrust from engine acceptance.	Shift in Gas Generator (GG) oxidizer system resistance.
4	-1300 lbf in-run thrust shift at 277 seconds.	Shift in GG oxidizer system resistance.
4	+1500 lbf in-run thrust shift at 309 seconds.	Shift in GG oxidizer system resistance.
NOTE: None of the shifts are considered to be unusual in either magnitude or cause.		

as part of the accumulator test, the LOX Overfill Shutoff (OFSO) sensor indicated wet approximately 15 percent of each minute. LOX replenish flow was then terminated, and an investigation made to determine if a time period violation of the propellant Launch Mission Rule (LMR) might occur. The investigation revealed that this would not be a problem and the LOX replenish flow was resumed and continued without incident. See paragraph 3.4.2 for additional details.

Open-loop control of engine mixture ratio during flight was successfully accomplished with the MRCV. At engine start command, helium pressure drove the valves to the engine start position corresponding to the 4.8 EMR. The No. 1 high EMR (5.5) command was received at ESC +5.5 seconds as planned. Helium pressure was thereby relieved and the return spring moved the valves to the high EMR position providing a nominal EMR of 5.50 for the first phase of the Programed Mixture Ratio (PMR).

The shift to low EMR, as seen at the engines, occurred at ESC +307.6 seconds (0.5 second earlier than predicted). The average EMR at the low step was 4.78 as compared to a predicted of 4.83. However, this was within the 2-sigma ±0.06 mixture ratio tolerance.

Outboard engine cutoff was initiated by the LOX tank propellant depletion system (with a 1.5-second OECO time delay) 2.2 seconds later than predicted due primarily to the lowered propellant flowrates at low EMR. The open-loop PU error at OECO was approximately -375 lbm LH_2 versus a 3-sigma tolerance of ±2500 lbm LH_2. Based on flowmeter and point sensor system data, propellant residuals in the tanks at OECO were 1213 lbm LOX and 2960 lbm LH_2 (versus 1802 lbm LOX and 3441 lbm LH_2 predicted). These lower than predicted residuals resulted from the use of a 4.8 EMR at OECO for the first time.

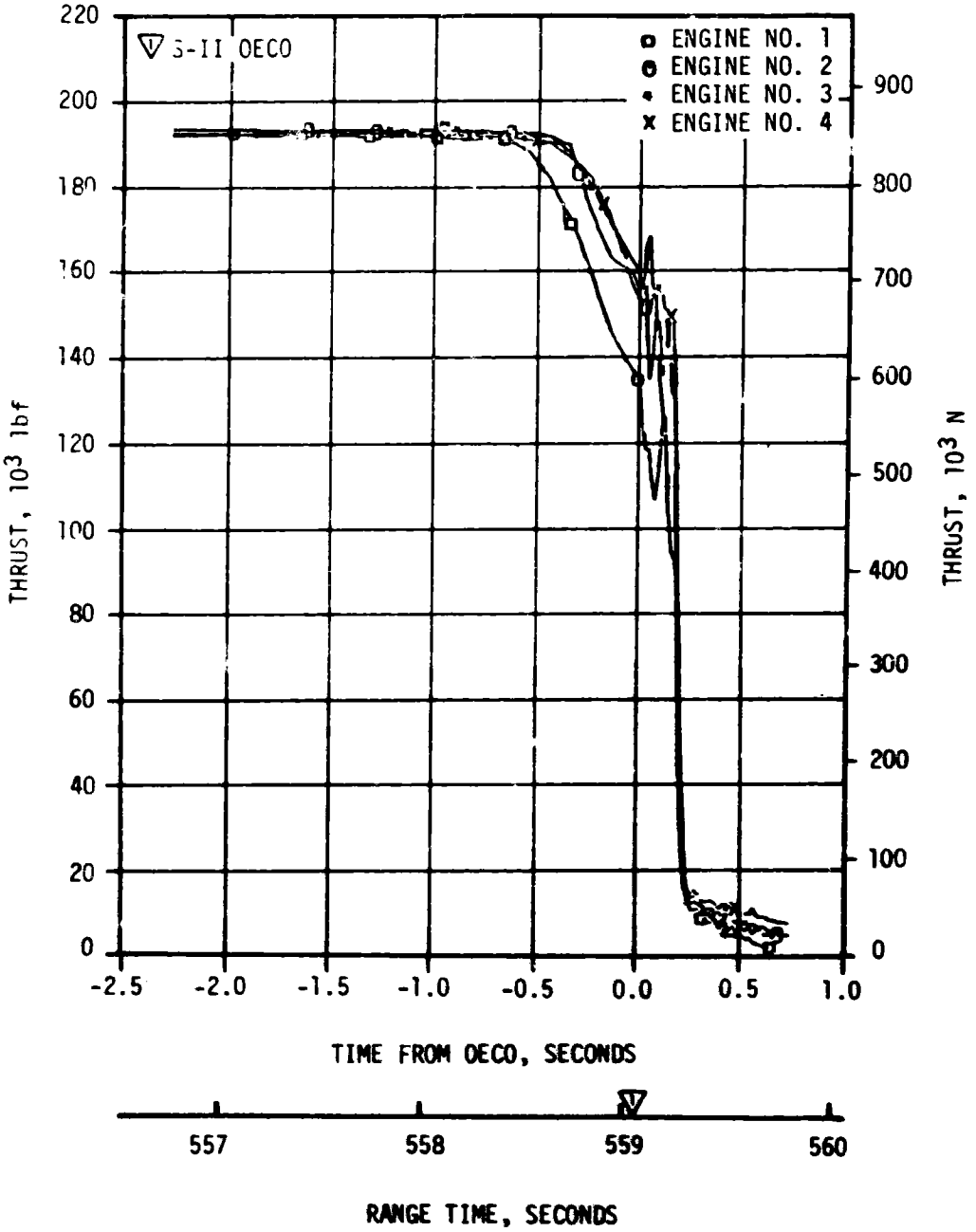

Figure 6-4. S-II Outboard Engine Chamber Pressure Decay

Table 6-3 presents a comparison of propellant masses as measured by the PU probes and engine flowmeters. The best estimate propellant mass is based on integration of flowmeter data utilizing the propellant residuals determined from point sensor data. Best estimates of propellant mass loaded correlates with the postlaunch computer reconstruction of the flight. These mass values were 0.04 percent more than predicted for LOX and 0.31 percent less than predicted for LH_2.

Table 6-3. AS-509 Flight S-II Propellant Mass History

EVENT	PREDICTED, LBM (TRAJECTORY)		PU SYSTEM ANALYSIS, LBM		ENGINE FLOW - METER INTEGRATION (BEST ESTIMATE), LBM	
	LOX	LH_2	LOX	LH_2	LOX	LH_2
Liftoff	835,531	159,427	834,430	159,785	835,859	159,001
S-II ESC	835,531	159,413	836,078	159,058	835,859	158,986
S-II PU Valve Step Cmd	134,069	31,093	132,374	30,675	131,918	30,507
2% Point Sensor	16,046	4,298	16,231	4,288	16,046	4,298
S-II OECO	1,802	3,441	2,319	2,975	1,213	2,960
S-II Residual After Thrust Decay	1,515	3,326	Data Not Usable	Data Not Usable	1,009	2,873

NOTE: Table is based on mass in tanks and sump only. Propellant trapped external to tanks and LOX sump is not included.

6.6 S-II PRESSURIZATION SYSTEM

6.6.1 S-II Fuel Pressurization System

LH_2 tank ullage pressure, actual and predicted, is presented in Figure 6-5 for autosequence, S-IC boost, and S-II boost. The LH_2 vent valves were closed at -93.1 seconds and the ullage volume pressurized at 35.0 psia in 20.8 seconds. One makeup cycle was required at -51.6 seconds. The vent valves modulated during S-IC boost, controlling tank pressure; however, no main poppet operation of the vent valves was evident.

Differential pressure across the vent valve was kept below the low-mode upper limit of 29.5 psi. Ullage pressure at engine start was 28.8 psia exceeding the minimum engine start requirement of 27 psia. The LH_2 tank vent valves were switched to the high vent mode 1.25 seconds prior to S-II engine start.

LH_2 tank ullage pressure remained slightly below its predicted value during S-II mainstage operation prior to step pressurization. The indicated ullage pressure was comparable to the pressure in this interval during the S-II-9 static firing.

The LH_2 tank regulator was commanded open at 464.1 seconds and ullage pressure increased to 32.05 psia. The vent valves started to vent at 491.9 seconds and continued to vent throughout the remainder of the S-II burn. Ullage pressure remained within the high mode vent range of 30.5 to 33.0 psia.

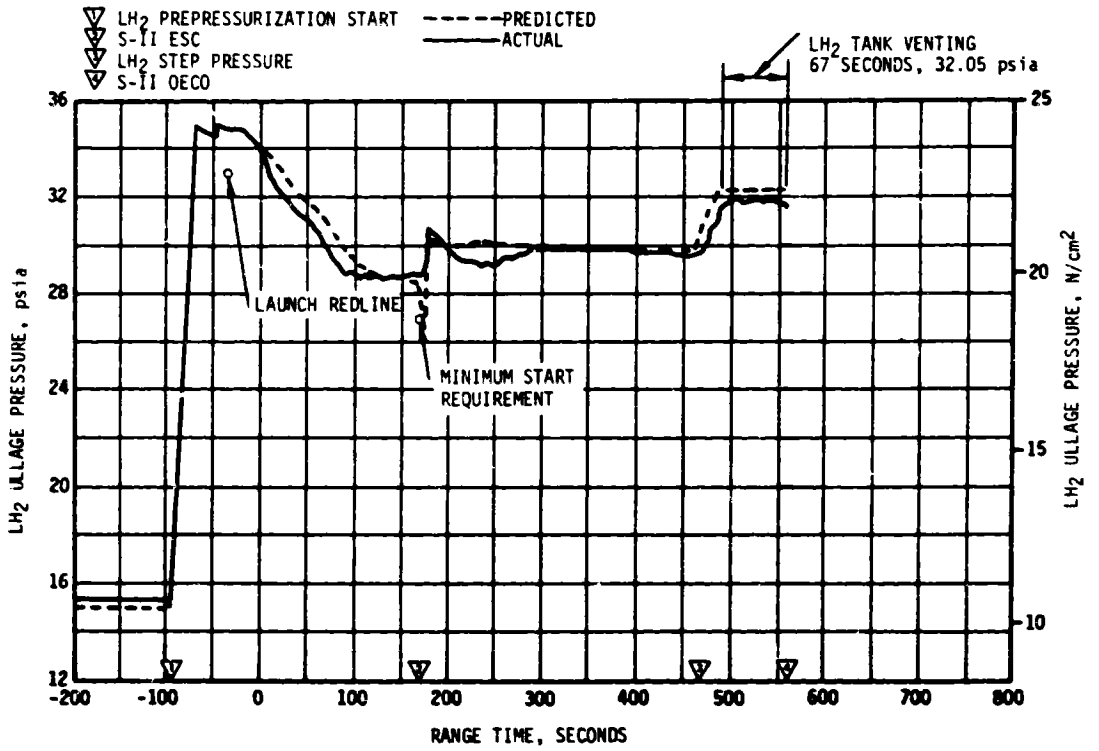

Figure 6-5. S-II Fuel Tank Ullage Pressure

Figure 6-6 shows LH_2 total inlet pressure, temperature and Net Positive Suction Pressure (NPSP) for the J-2 engines. The parameters were close to predicted values. Fuel pump inlet pressure was maintained above the required minimum NPSP throughout the S-II burn period.

6.6.2 S-II LOX Pressurization System

Although the S-II LOX pressurization system operated sufficiently to satisfy all mission objectives, the LOX tank ullage pressure differed from what was predicted (see Figure 6-7). The deviation was caused by (1) the LOX pressurization regulator failing to open fully when required, and (2) the effect of saturated GOX pressurant from the J-2 engine heat exchangers.

As seen in Figure 6-7, the LOX ullage pressure did not increase as rapidly as predicted after the LOX step pressurization command. The LOX pressure regulator potentiometer and oxidizer manifold pressure measurements were used to conclude that the slow pressure rise was a

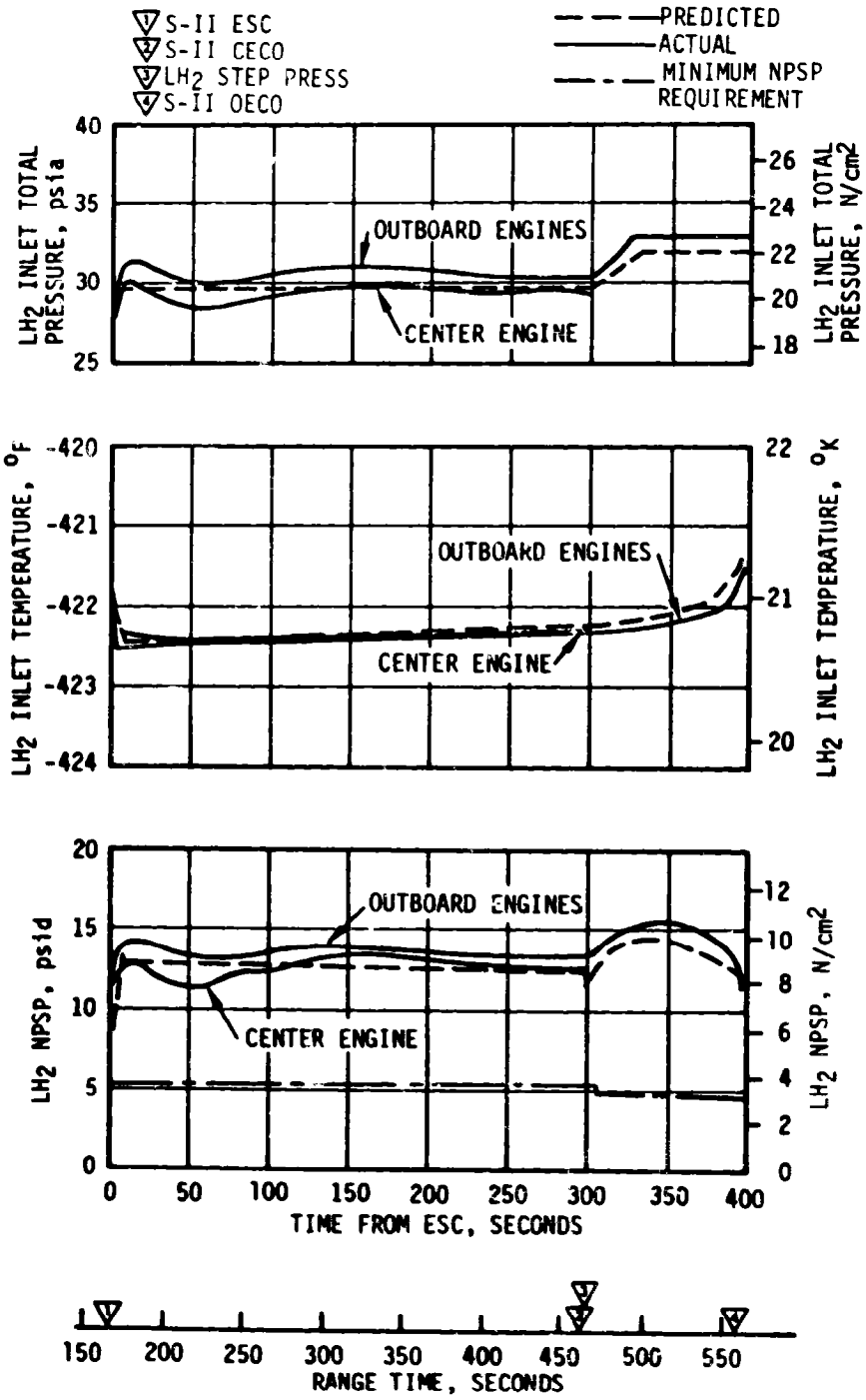

Figure 6-6. S-II Fuel Pump Inlet Conditions

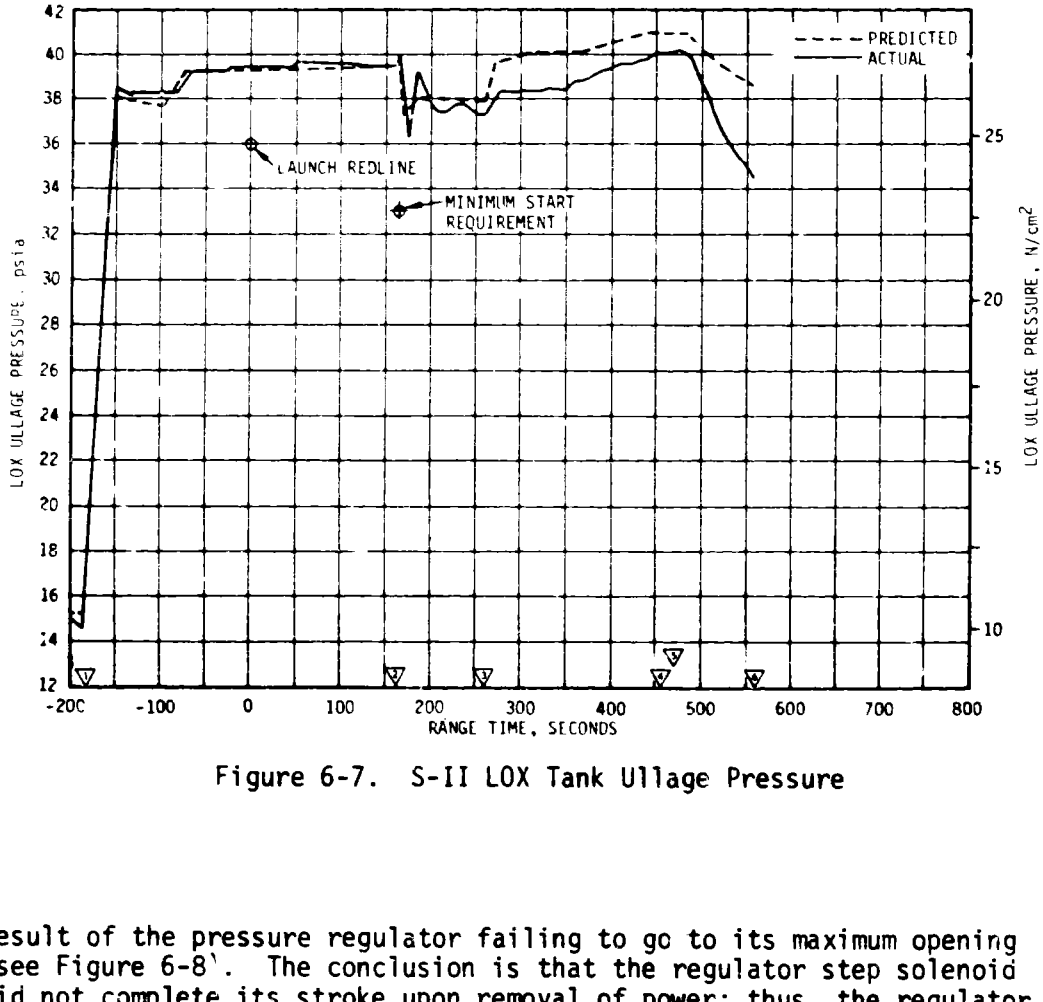

Figure 6-7. S-II LOX Tank Ullage Pressure

result of the pressure regulator failing to go to its maximum opening (see Figure 6-8). The conclusion is that the regulator step solenoid did not complete its stroke upon removal of power; thus, the regulator butterfly could not fully open. The cause has not been determined, but its effect was that the mechanical advantage the bias portion of the regulator has on the regulator power bellows was not completely nullified, thus a force due to pressure was still attempting to hold the regulator butterfly at its minimum opening (see Figure 6-9).

Because the regulator was only partially open, it required less mass (approximately 325 lbm less) at a warmer temperature to have the ullage pressure near the predicted pressure level at EMR step. Upon shifting to low EMR, the regulator inlet pressure dropped below the minimum required pressure (450 psia) necessary to keep the bias portion on the regulator active. When the bias portion became inactive, the regulator power bellows lost its force term tending to hold the butterfly closed and permitted the butterfly to go to its maximum opening.

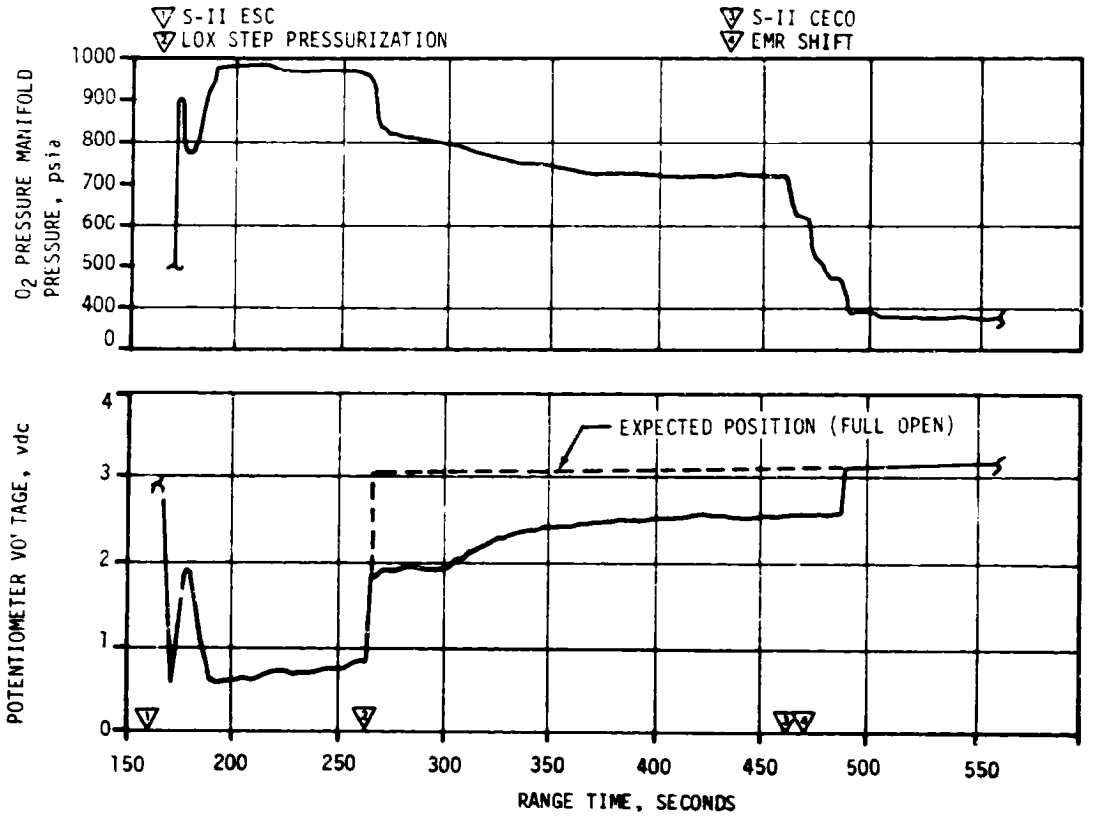

Figure 6-8. S-II Oxidizer Manifold Pressure and Regulator Potentiometer Profiles

The pressure decay after EMR step was amplified due to the GOX pressurant entering the LOX ullage system at colder than predicted temperatures. If the regulator had operated properly, the ullage pressure decay would have been more than predicted (1.8 psi more) but not as much pressure decay as was experienced.

In summary, the slow pressure rise after LOX step pressurization was the result of the pressure regulator not opening fully. The lower than predicted ullage pressure after EMR step was the result of the low incoming pressurant temperature in combination with ullage conditions generated by the partially opened regulator.

The possibility of the regulator problem recurring on subsequent flights has been eliminated with S-II stage ECP No. 6425, effective AS-510 and subsequent, which replaces the LOX tank pressurization regulator with a fixed orifice.

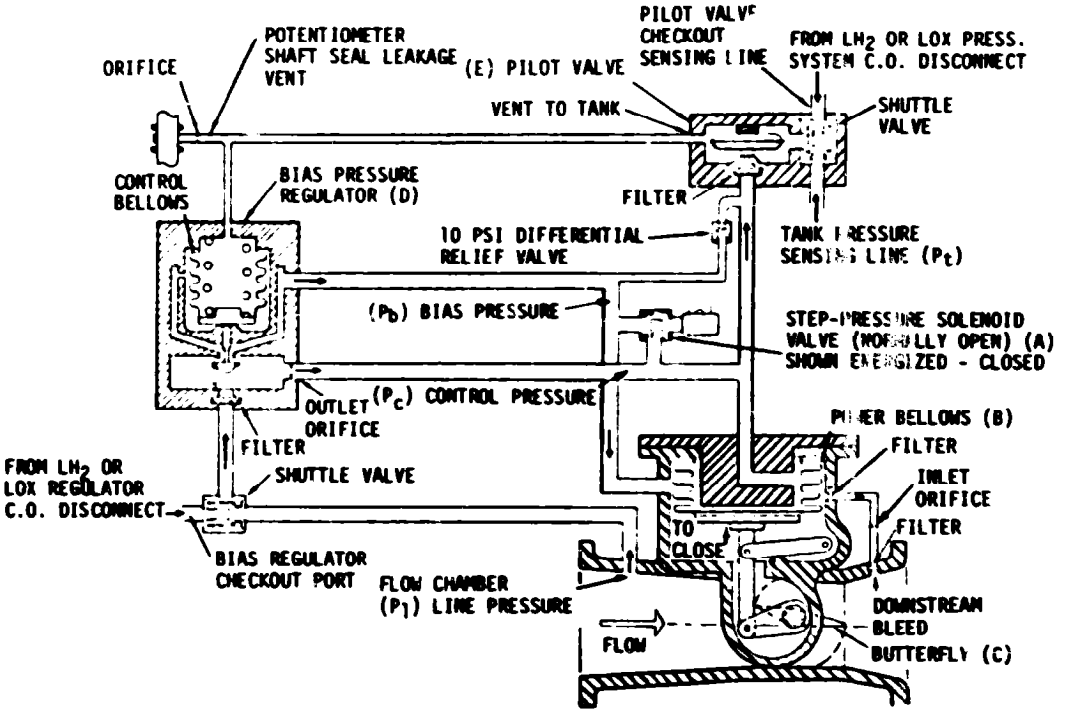

Figure 6-9. S-II LOX Tank Pressurization Regulator

Though the ullage pressure was lower than predicted, it was sufficient to meet NPSP requirements except for the final 0.5 second of mainstage which is to be expected. At cutoff, the ullage pressure had decayed to 34.4 psia.

LOX engine inlet total pressure, temperature and NPSP are presented in Figure 6-10 for the S-II burn phase.

6.7 S-II PNEUMATIC CONTROL PRESSURE SYSTEM

The pneumatic control system functioned satisfactorily throughout the S-IC and S-II boost periods. Bottle pressure was 3010 psia at -30 seconds and due to normal valve activities during S-II burn, decayed to approximately 2640 psia after S-II OECO.

Regulator outlet pressure during flight remained at a constant 710 psia, except for the expected momentary pressure drops when the recirculation or prevalves were actuated closed just after engine start, at CECO and OECO.

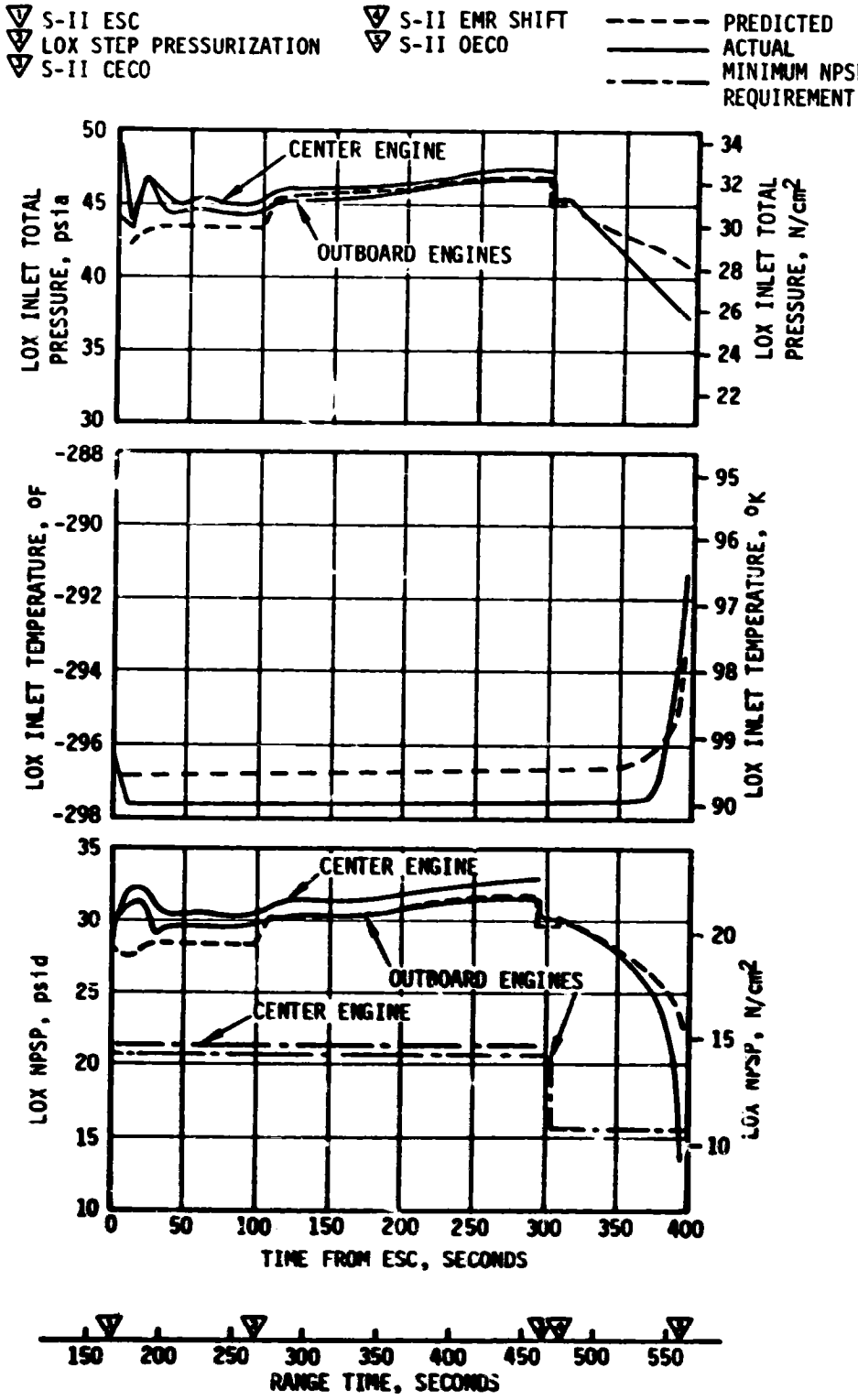

Figure 6-10. S-II LOX Pump Inlet Conditions

6.8 S-II HELIUM INJECTION SYSTEM

The performance of the helium injection system was satisfactory. The supply bottle was pressurized to 3010 psia prior to liftoff and by ESC the pressure was 1730 psia as compared to 700 psia at S-II-8 ESC. The pressure at ESC was higher for S-II-9 due to the addition of another 1.5 ft^3 supply bottle to the helium injection system for servicing the center engine feedline accumulator. Helium injection average total flow-rate during supply bottle blowdown (-30 to 163 seconds) was 65 SCFM.

6.9 POGO SUPPRESSION SYSTEM

A center engine LOX feedline accumulator was installed for the first time on this flight as a POGO suppression device. Propulsion/structural analysis indicates that the accumulator did suppress the S-II POGO oscillations. See paragraph 8.2.3 for complete details. A schematic of the POGO suppression system is shown in Figure 6-11.

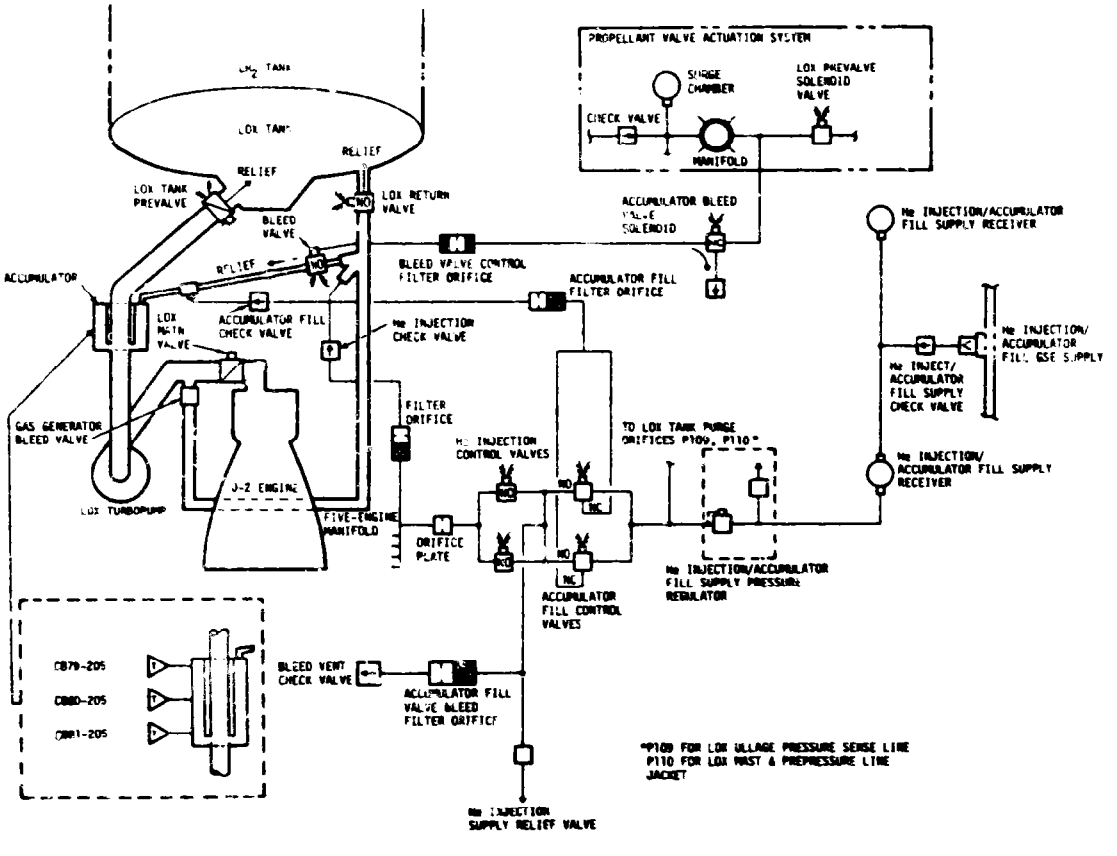

Figure 6-11. S-II LOX Center Engine Feedline Accumulator and Helium Injection System

The accumulator bleed system must maintain subcooled LOX in the accumulator through S-IC boost and S-II engine start. This requirement is accomplished by LOX flowing through a 3/4-inch line from the top of the accumulator to the center engine LOX recirculation return line. There is also a shutoff valve in this bleed line that is used to terminate the bleed flow 1.0 second prior to S-II engine start. Figure 6-12 shows the required accumulator temperature at S-II engine start, the predicted temperatures during S-IC boost, and the actual temperatures experienced during the AS-509 flight. As can be seen, the maximum allowable temperature of -281.5°F at engine start was more than adequately met (-294.5°F).

The accumulator fill system is required to displace the LOX in the accumulator with helium soon after engine start. The accumulator fill must be completed in 5 to 7 seconds after its initiation and must be maintained until CECO. This is accomplished by opening two parallel solenoid valves (one at engine start plus 4.1 seconds and the other engine start plus 4.3 seconds) and initiating a helium flow of 0.0045 to 0.0060 lbm/s from two 1.5 ft^3 bottles (pressurized to 2800 to 3100 psia prior to LOX helium injection), through a regulator, and then into the accumulator. This flow is terminated at CECO by closing the two fill solenoids.

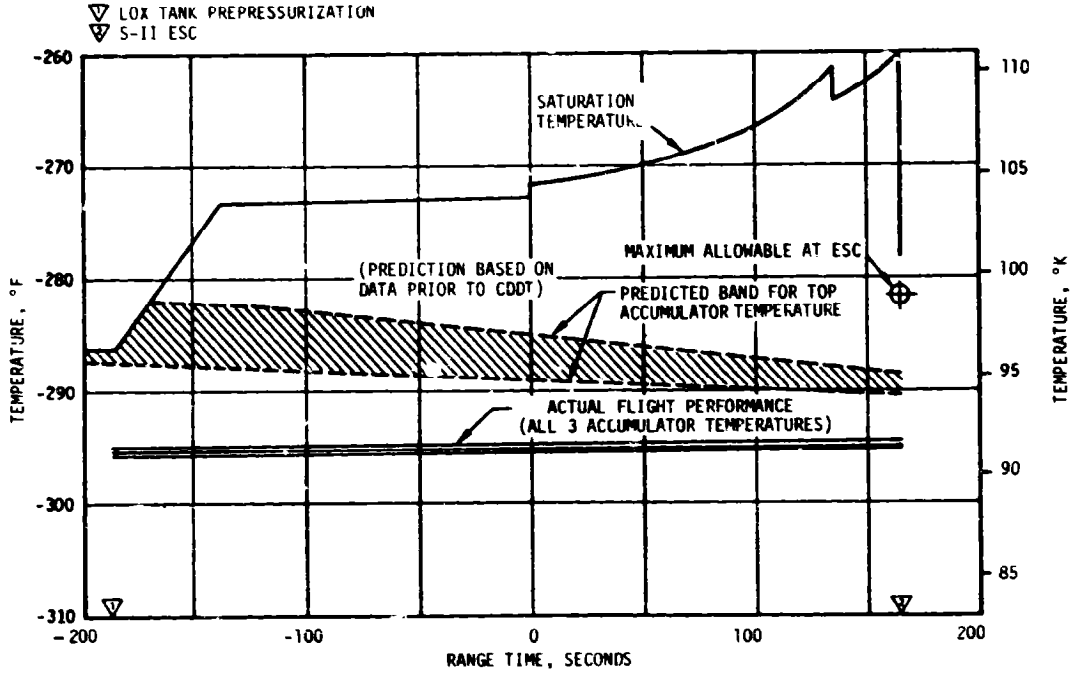

Figure 6-12. S-II Center Engine LOX Feedline Accumulator Bleed System Performance

Figure 6-13 shows accumulator LOX level versus time during the fill transient as determined from the time the three accumulator temperature probes indicated dry. Based on these data, the accumulator was full of helium 6.3 seconds after the start of fill, thus meeting the 5 to 7 second fill time requirement. After the accumulator was filled with helium (just after engine start), it remained in that state until CECO when the helium flow was terminated and LOX backed up into the accumulator due to the post-CECO feedline pressure buildup. There was no sloshing or abnormal liquid level behavior observed in the accumulator while the center engine was operating. Figure 6-14 shows the performance of the helium supply portion of the accumulator fill system.

6.10 S-II HYDRAULIC SYSTEM

S-II hydraulic system performance was normal throughout the flight. System supply and return pressures, reservoir volumes, and system fluid temperatures were within predicted ranges. All servoactuators responded to commands with good precision. The maximum engine deflection was

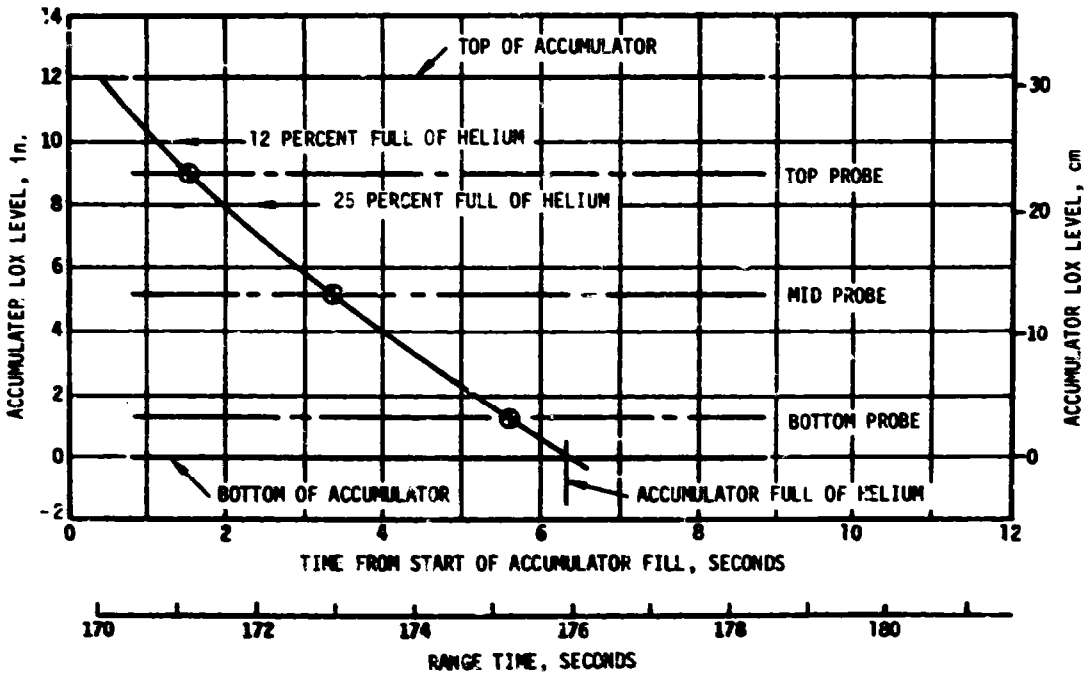

Figure 6-13. S-II Center Engine LOX Feedline Accumulator Fill Transient

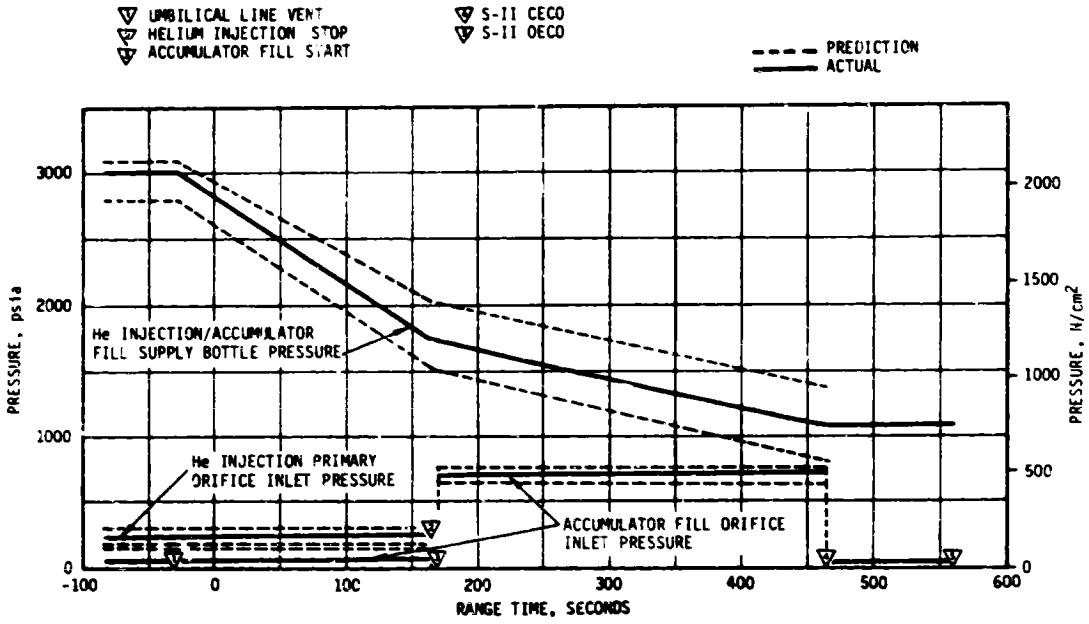

Figure 6-14. S-II Center Engine LOX Feedline Accumulator Helium Supply System Performance

approximately 1.4 degrees in pitch on engine No. 4 in response to the separation and engine start transients. Actuator loads were well within design limits. The maximum actuator load was approximately 9,700 lbf for the yaw actuator of engine No. 1 and occurred during initiation of Iterative Guidance Mode (IGM).

There was no evidence of the engine No. 2 system accumulator lockup valve leakage that was encountered during Flight Readiness Test (FRT) and CDDT.

The engine No. 3 accumulator reservoir manifold assembly was replaced prior to launch countdown due to reservoir piston seal leakage. The replacement unit performed satisfactorily in countdown and flight.

SECTION 7

S-IVB PROPULSION

7.1 SUMMARY

The J-2 engine operated satisfactorily throughout the operational phase of first and second burn and had normal shutdowns. S-IVB first burntime was 157.2 seconds which was 4.1 seconds less than predicted. Approximately 2.4 seconds of the shorter burntime can be attributed to higher S-IC performance. The remainder can be attributed to the S-IC and S-II stage performance and the change in the flight azimuth. The engine performance during first burn, as determined from standard altitude reconstruction analysis, deviated from the predicted Start Tank Discharge Valve (STDV) open +130-second time slice by 1.48 percent for thrust and 0.14 percent for specific impulse. The higher than predicted performance can be attributed primarily to a decrease in gas generator system resistance. The S-IVB stage first burn Engine Cutoff (ECO) was initiated by the Launch Vehicle Digital Computer (LVDC) at 700.56 seconds.

The Continuous Vent System (CVS) adequately regulated LH_2 tank ullage pressure at an average level of 19.2 psia during orbit, and the Oxygen/Hydrogen (O_2/H_2) burner satisfactorily achieved LH_2 and LOX tank repressurization for restart. Engine restart conditions were within specified limits. The restart at full open Propellant Utilization (PU) valve position was successful.

S-IVB second burntime was 350.8 seconds which was 5.5 seconds less than predicted. The engine performance during second burn, as determined from the standard altitude reconstruction analysis, deviated from the predicted STDV +200-second time slice by 1.57 percent for thrust and 0.14 percent for specific impulse. The higher than predicted performance is attributed to the same reason as for first burn. Second burn ECO was initiated by the LVDC at 9263.24 seconds (02:34:23.24).

A small shift in LOX chilldown flowrate and pump differential pressure observed during boost has been determined to be due to vehicle-induced longitudinal dynamics.

Subsequent to second burn, the stage propellant tanks and helium spheres were safed satisfactorily. Sufficient impulse was derived from LOX dump, LH_2 CVS operation and Auxiliary Propulsion System (APS) ullage burn to achieve a successful lunar impact within the planned target area.

The APS pressurization system performed nominally throughout the flight except for a helium leak in Module No. 1 from 5 to 7 hours. The average leakage was about 70 Standard Cubic Inches/Minute (SCIM). The magnitude and duration of this leak was not large enough to present any problems.

The S-IVB hydraulic system performance was satisfactory during the entire mission.

7.2 S-IVB CHILLDOWN AND BUILDUP TRANSIENT PERFORMANCE FOR FIRST BURN

The thrust chamber temperature at launch was well below the maximum allowable redline limit of -130°F. At S-IVB first burn Engine Start Command (ESC), the temperature was -141°F, which was within the requirement of -189.6 ±110°F.

The chilldown and loading of the engine Gaseous Hydrogen (GH_2) start tank and pneumatic control bottle prior to liftoff was satisfactory.

A 40 minute hold for adverse weather conditions occurred during terminal count. A countdown recycle was avoided by utilizing the start tank rechill sequence which was developed during the AS-509 Countdown Demonstration Test (CDDT). When the count was picked up (at -482 seconds) the start tank vent and supply valves were opened, allowing cold flow through the tank. Adequate chilldown was achieved in 93 seconds, and start tank conditions were well within acceptable limits at liftoff. The engine control sphere was vented three times during hold to maintain acceptable pressure levels.

The engine control sphere pressure and temperature at liftoff were 3040 psia and -165°F. At first burn ESC the start tank conditions were within the required region of 1525 ±75 psia and -170 ±30°F for start. The discharge was completed and the refill initiated at first burn ESC +3.8 seconds. The refill was satisfactory and in good agreement with the acceptance test.

The propellant recirculation systems operation, which was continuous from before liftoff until just prior to first ECS, was satisfactory. Start and run box requirements for both fuel and LOX were met, as shown in Figure 7-1. At first ESC the LOX pump inlet temperature was -295.5°F and the LH_2 pump inlet temperature was -421.8°F. A small downward shift in LOX chilldown flowrate and pump delta P, observed from approximately 124 to 174 seconds during boost, has been determined to be due to vehicle-induced longitudinal dynamics. This response was noted during pump qualification vibration testing and is not considered a problem.

The first burn start transient was satisfactory. The thrust buildup was within the established limits. This buildup was similar to the thrust buildups observed on AS-506 through AS-508. The Mixture Ratio Control (MRC)

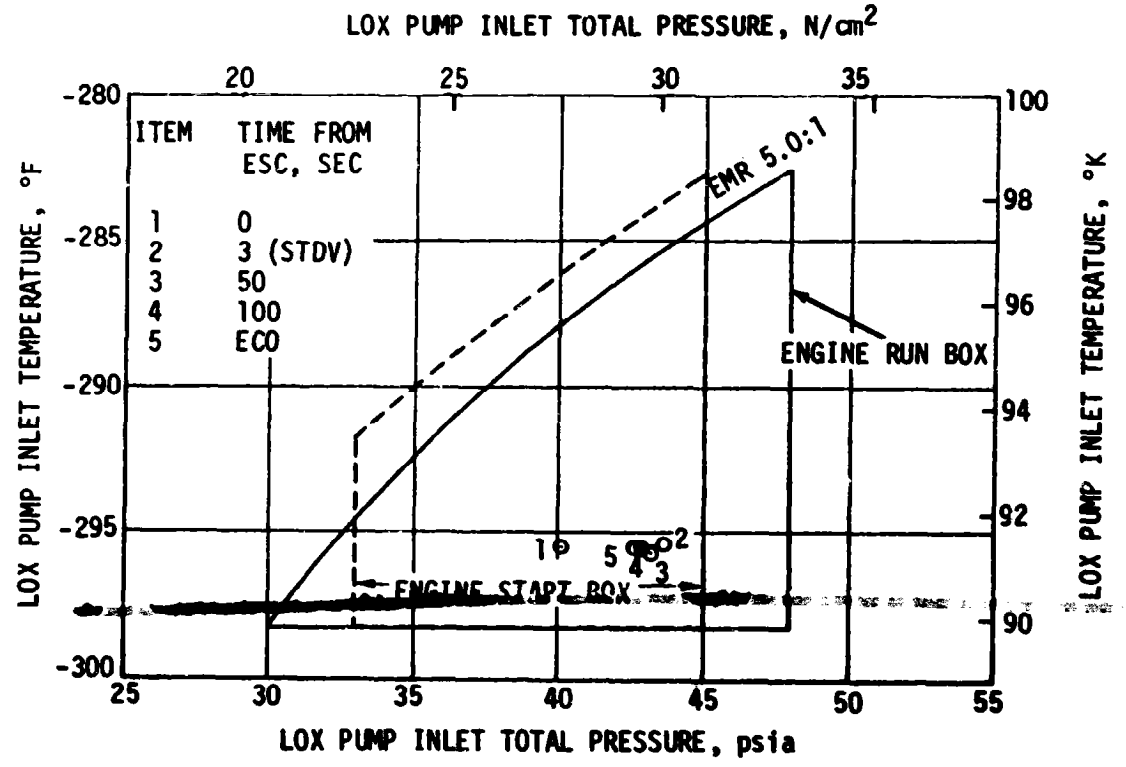

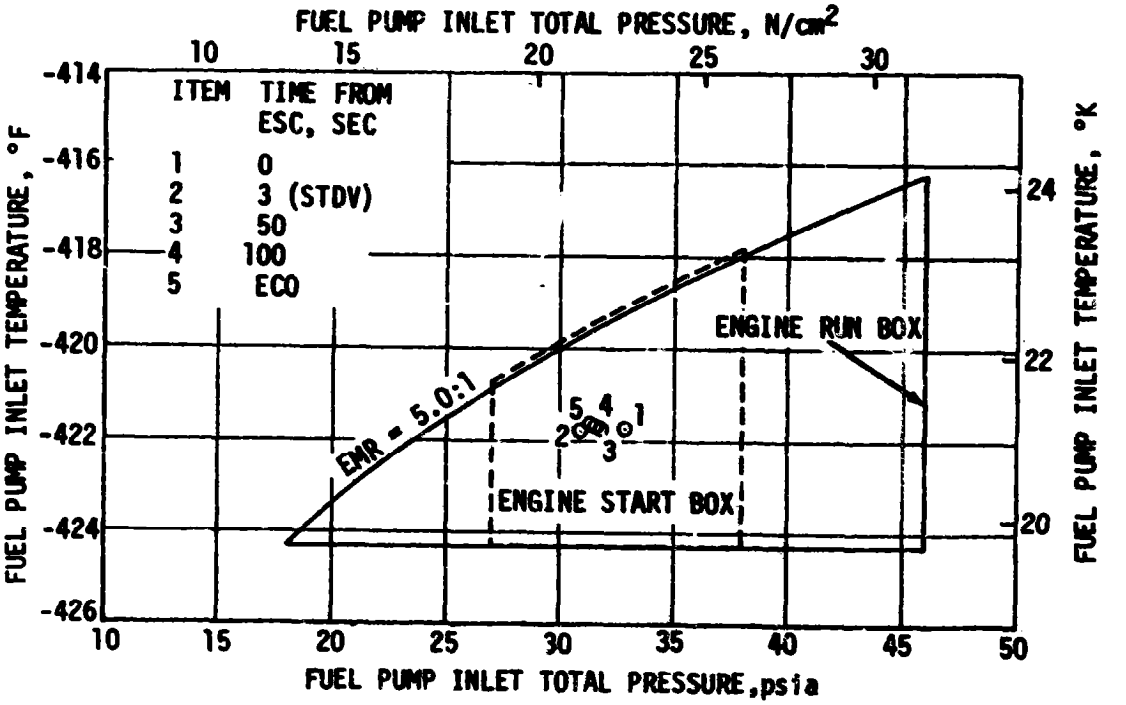

Figure 7-1. S-IVB Start Box and Run Requirements - First Burn

valve was in the closed position prior to first start and performance indicates it remained closed during first burn. The total impulse from STDV open to STDV open +2.5 seconds was 193,080 lbf-s for first start.

First burn fuel lead followed the predicted pattern and resulted in satisfactory conditions as indicated by the thrust chamber temperatures and the associated fuel injector temperatures.

7.3 S-IVB MAINSTAGE PERFORMANCE FOR FIRST BURN

The propulsion reconstruction analysis showed that the stage performance during mainstage operation was satisfactory. A comparison of predicted and actual performance of thrust, specific impulse, total flowrate, and Mixture Ratio (MR) versus time is shown in Figure 7-2. Table 7-1 shows the thrust, specific impulse, flowrates and MR deviations from the predicted at the STDV +130-second time slice.

A mixture ratio control valve setting 2 degrees higher than predicted would correspond to the observed thrust but not the observed mixture ratio. Reconstructed propellant ratio usage indicates that the MR profile was very near to predicted. Therefore, the higher performance at the predicted mixture ratio can be attributed primarily to a decrease in gas generator system resistance.

The performance of the J-2 engine helium control system was satisfactory during mainstage operation. The engine control bottle was connected to the stage ambient repressurization bottles, therefore, there was little pressure decay. Helium usage is estimated as 0.30 lbm during first burn.

7.4 S-IVB SHUTDOWN TRANSIENT PERFORMANCE FOR FIRST BURN

S-IVB ECO was initiated at 700.56 seconds by a guidance velocity cutoff command which resulted in a 4.1-second less than predicted burntime. Approximately 2.4 seconds of the shorter burntime can be attributed to higher S-IVB performance. The remainder can be attributed to S-IC and S-II stage performance and the change in flight azimuth.

The ECO transient was satisfactory. The total cutoff impulse to zero percent of rated thrust was 44,300 lbf-s which was 1720 lbf-s lower than predicted. Cutoff occurred with the MRC valve in the 5.0 position.

7.5 S-IVB PARKING ORBIT COAST PHASE CONDITIONING

The LH_2 CVS performed satisfactorily, maintaining the fuel tank ullage pressure at an average level of 19.2 psia. This was well within the 18 to 21 psia band of the inflight specification.

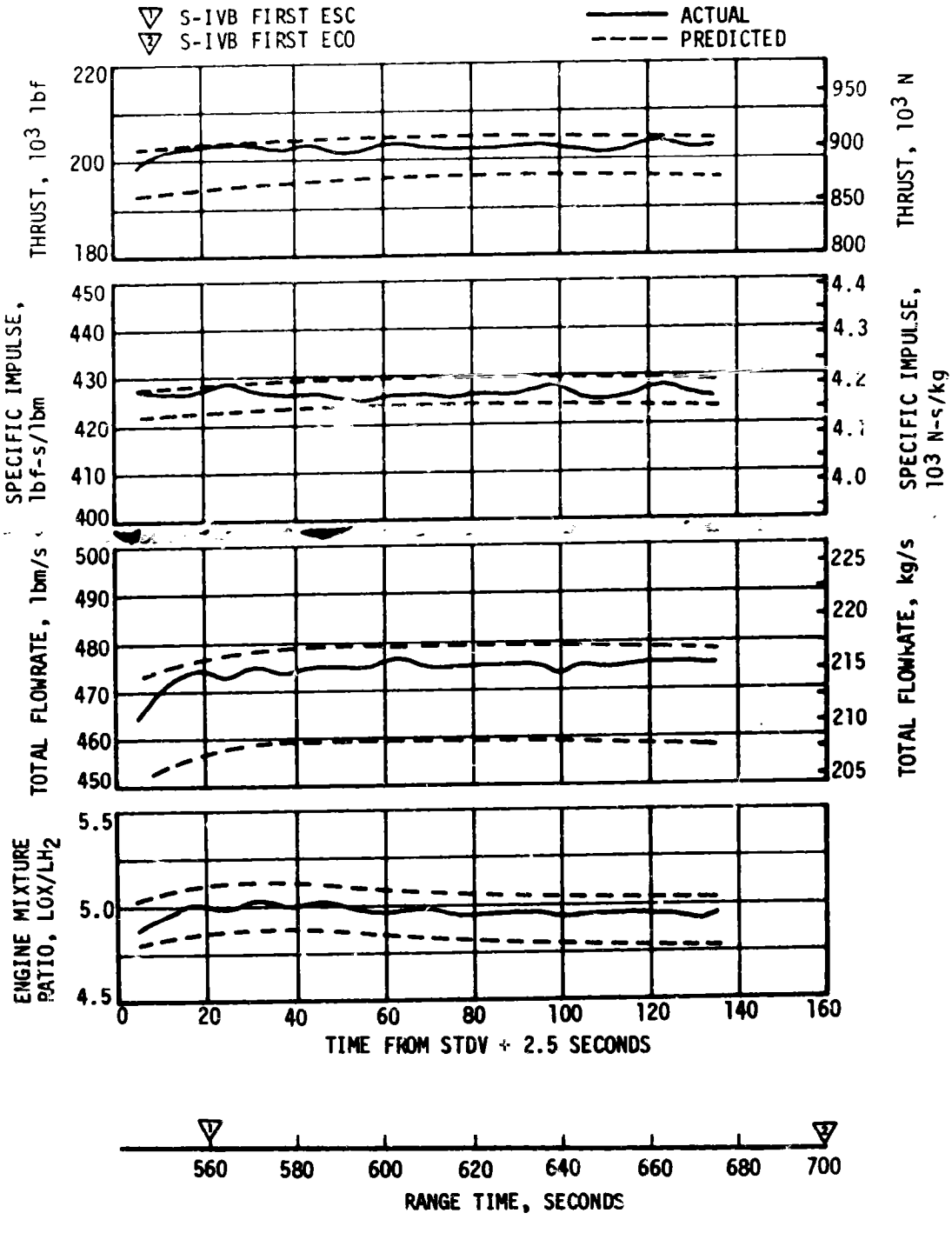

Figure 7-2. S-IVB Steady-State Performance - First Burn

Table 7-1. S-IVB Steady-State Performance - First Burn
(STDV +130-Second Time Slice at Standard Altitude Conditions)

PARAMETER	PREDICTED	RECONSTRUCTION	FLIGHT DEVIATION	PERCENT DEVIATION FROM PREDICTED
Thrust, lbf	198,627	201,572	2945	1.483
Specific Impulse, lbf-s/lbm	426.5	427.1	0.6	0.141
LOX Flowrate, lbm/s	386.78	392.14	5.36	1.386
Fuel Flowrate, lbm/s	78.95	79.80	0.85	1.077
Engine Mixture Ratio, LOX/Fuel	4.899	4.914	0.015	0.306

The continuous vent regulator was activated at 759.7 seconds and was terminated at 8376.3 seconds. The CVS performance is shown in Figure 7-3. The thrust between 5400 seconds and the end of CVS operation was above the predicted level because the orbital heat input was higher than expected.

Calculations based on estimated temperatures indicate that the mass vented during parking orbit was 1935 lbm and that the boiloff mass was 2242 lbm.

7.6 S-IVB CHILLDOWN AND BUILDUP TRANSIENT PERFORMANCE FOR SECOND BURN

Repressurization of the LOX and LH_2 tanks was satisfactorily accomplished by the O_2/H_2 burner. Helium heater "ON" command was initiated at 8376.1 seconds. The LH_2 repressurization control valves were opened at burner "ON" +6.1 seconds and the fuel tank was repressurized from 19.2 to 30.5 psia in 186 seconds. There were 25.9 lbm of cold helium used to repressurize the LH_2 tank. The LOX repressurization control valves were opened at burner "ON" +5.3 seconds and the LOX tank was repressurized from 35.8 to 39.8 psia in 152 seconds. There were 4.7 lbm of helium used to repressurize the LOX tank. LH_2 and LOX ullage pressures are shown in Figure 7-4. The burner continued to operate for a total of 454.9 seconds providing nominal propellant settling forces. The performance of the AS-509 O_2/H_2 burner was satisfactory as shown in Figure 7-5.

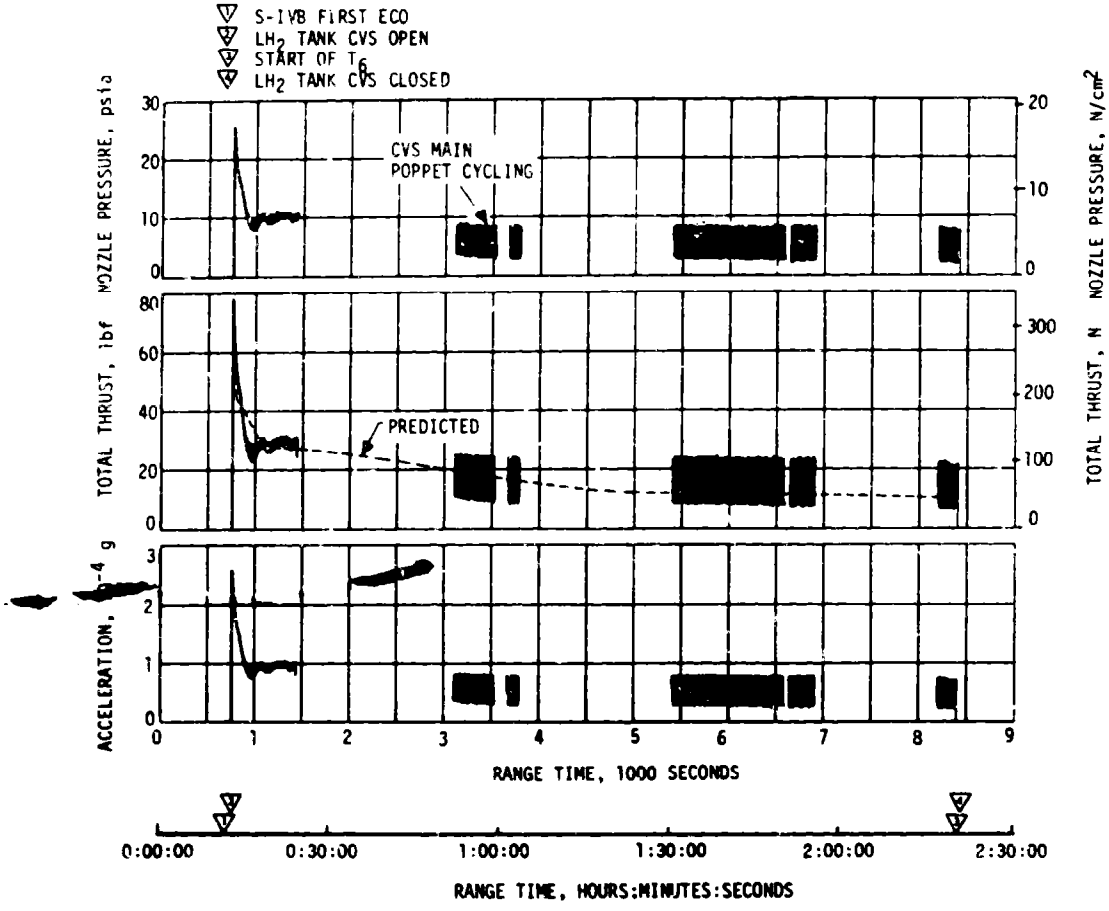

Figure 7-3. S-IVB CVS Performance - Coast Phase

The S-IVB LOX recirculation system satisfactorily provided conditioned oxidizer to the J-2 engine for restart. The LOX and fuel pump inlet conditions are plotted in the start and run boxes in Figure 7-6. At second ESC, the LOX and fuel pump inlet temperatures were -294.9°F and -419.6°F, respectively. Fuel recirculation system performance was adequate and conditions at the pump inlet were satisfactory at second STDV open. Second burn fuel lead generally followed the predicted pattern and resulted in satisfactory conditions as indicated by thrust chamber temperature and the associated fuel injector temperature. Since J-2 start system performance was nominal during coast and restart, no helium recharge was required from the LOX ambient repressurization system (bottle No. 2). The start tank performed satisfactorily during second burn blowdown and recharge sequence. The engine start tank was recharged properly and maintained sufficient pressure during coast. The engine control sphere first burn gas usage was as predicted; the ambient helium spheres recharged the control sphere to a nominal level for restart.

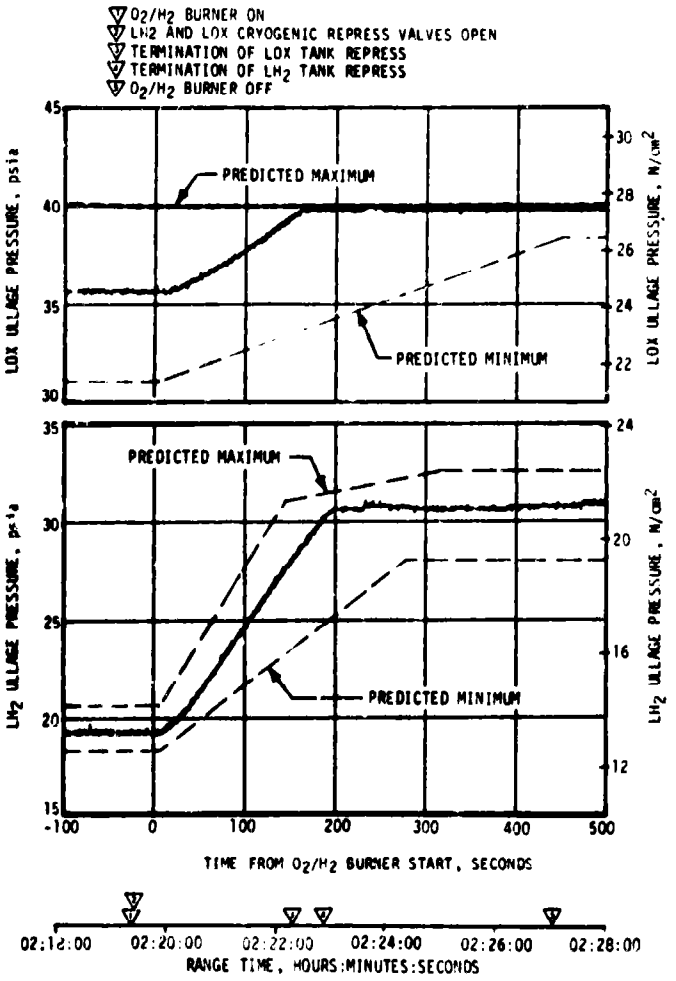

Figure 7-4. S-IVB Ullage Conditions During Repressurization Using O_2/H_2 Burner

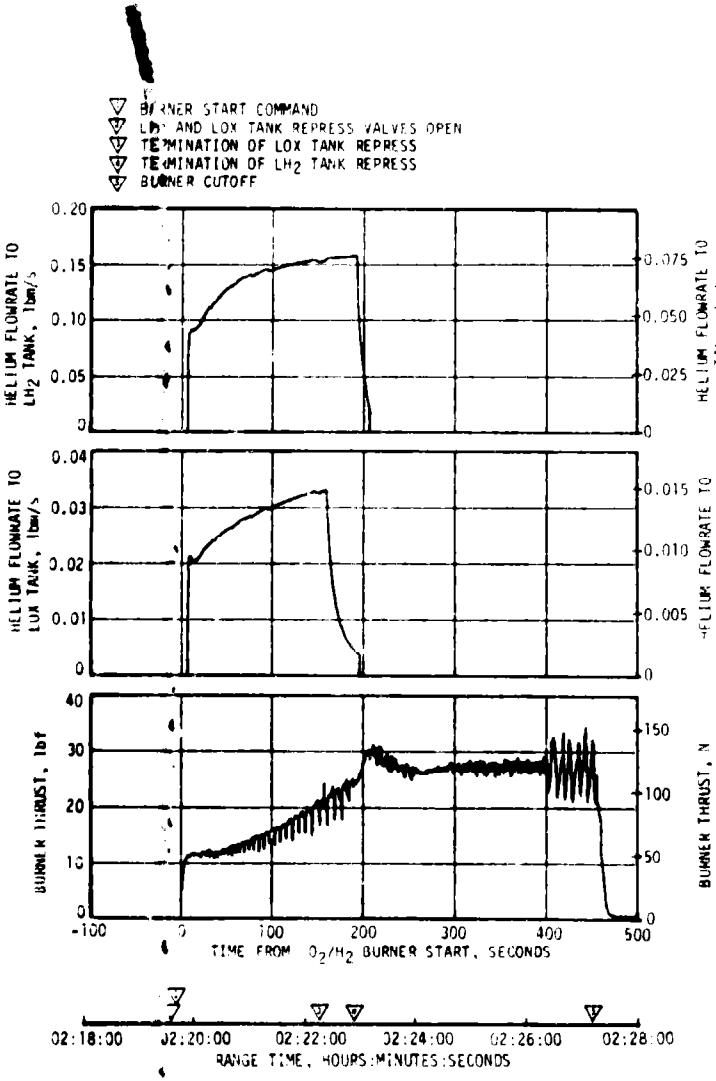

Figure 7-5. S-IVB O_2/H_2 Burner Thrust and Pressurant Flowrate

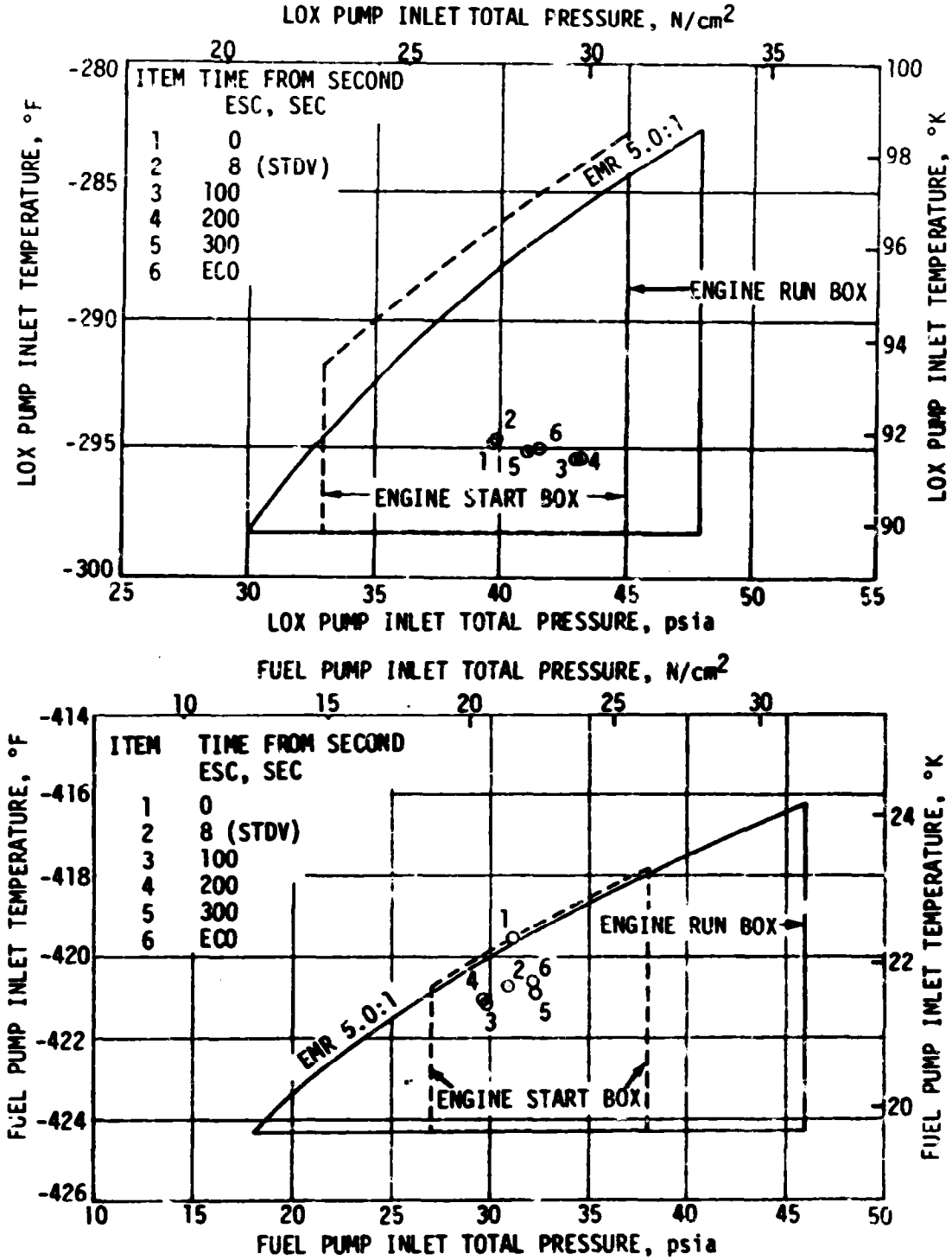

Figure 7-6. S-IVB Start Box and Run Requirements - Second Burn

The second burn start transient was satisfactory. The thrust buildup was within the limits set by the engine manufacturer and was similar to the thrust buildup on AS-506 through AS-508. The MRC valve was in the proper full open (4.5 MR) position prior to the second start. The total impulse from STDV open to STDV open +2.5 seconds was 188,600 lbf-s.

The helium control system performed satisfactorily during second burn mainstage. There was little pressure decay during the burn due to the connection to the stage repressurization system. An estimated 1.1 lbm of helium was consumed during second burn.

7.7 S-IVB MAINSTAGE PERFORMANCE FOR SECOND BURN

The propulsion reconstruction analysis showed that the stage performance during mainstage operation was satisfactory.

The second burntime was also shorter than predicted. This can be primarily attributed to the higher than predicted S-IVB performance.

A comparison of predicted and actual performance of thrust, specific impulse, total flowrate, and mixture ratio versus time is shown in Figure 7-7. Table 7-2 shows the thrust, specific impulse, flowrates, and MR deviations from the predicted at the STDV +200-second time slice. This time slice performance is the standardized altitude performance which is comparable to the first burn slice at STDV +130 seconds. The 200-second time slice thrust for second burn was 1.57 percent higher than predicted. Specific impulse performance for second burn was 0.14 percent higher than predicted. The higher performance during second burn is attributed to the same reason as for first burn. The MRC valve position measurement G0017-401 can only be used as a gross measurement. This measurement during second burn was erratic after returning to the closed position. However, engine performance simulations do not substantiate any MRC valve movement.

7.8 S-IVB SHUTDOWN TRANSIENT PERFORMANCE FOR SECOND BURN

S-IVB second ECO was initiated at 9263.24 seconds by a guidance velocity cutoff command for a burntime of 350.8 seconds. The burntime was 5.5 seconds less than predicted.

The ECO transient was satisfactory. The total cutoff impulse to zero thrust was 45,629 lbf-s, which was 1291 lbf-s lower than predicted. Cutoff occurred with the MRC valve in the full closed (5.0 MR) position.

7.9 S-IVB STAGE PROPELLANT MANAGEMENT

This was the first S-IVB stage to use the pneumatically operated two-position mixture ratio control valve. Since this valve is no longer tied into the PU electronics assembly, the propellant management analysis discussion contained herein will deal only with propellant loading and consumption.

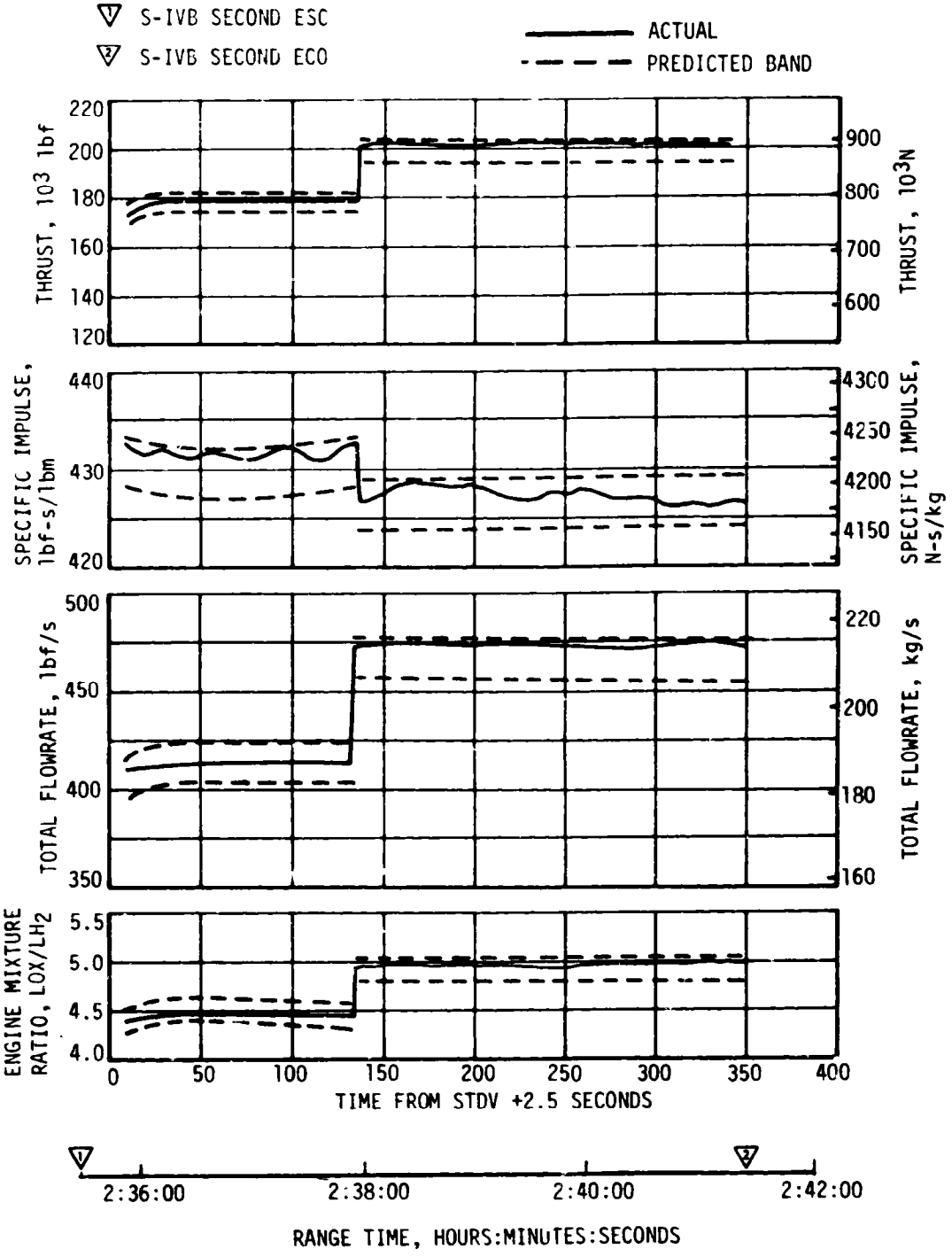

Figure 7-7. S-IVB Steady-State Performance - Second Burn

Table 7-2. S-IVB Steady-State Performance - Second Burn
(STDV +200-Second Time Slice at Standard Altitude Conditions)

PARAMETER	PREDICTED	RECONSTRUCTION	FLIGHT DEVIATION	PERCENT DEVIATION FROM PREDICTED
Thrust, lbf	198,627	201,738	3111	1.566
Specific Impulse, lbf-s/lbm	426.5	427.1	0.6	0.141
LOX Flowrate, lbm/s	386.78	392.47	5.69	1.471
Fuel Flowrate, lbm/s	78.95	79.85	0.90	1.139
Engine Mixture Ratio, LOX/Fuel	4.899	4.915	0.016	0.327

During the CDDT, a problem in the LOX loading system necessitated replacement of the LOX tank PU probe assembly. The replacement probe functioned in a normal manner during prelaunch activities and during flight (reference paragraph 3.4.2).

A comparison of propellant mass values at critical flight events, as determined by various analyses, is presented in Table 7-3. The best estimate full load propellant masses were 0.34 percent greater for LOX and 0.11 percent greater for LH_2 than predicted values. This deviation was well within the required loading accuracy.

Extrapolation of propellant level sensor data to depletion, using the propellant flowrates, indicated that a LOX depletion would have occurred approximately 13.3 seconds after second burn velocity cutoff.

During first burn, the MRC valve was positioned at closed position for start and remained there, as programed, for the duration of the burn.

The MRC valve was commanded to the 4.5 MR position 119.9 seconds prior to second ESC. However, the MRC valve did not actually move until it received engine pneumatics at ESC +0.5 second. The MRC valve took less than 250 milliseconds to reach the open (4.5 MR) position.

Table 7-3. S-IVB Stage Propellant Mass History

EVENT	UNITS	PREDICTED		PU INDICATED (CORRECTED)		PU VOLUMETRIC		FLOW INTEGRAL		BEST ESTIMATE	
		LOX	LH_2	LOX	LH_2	LOX	LH_2	LOX	LH_2	LOX	LH_2
S-IC Liftoff	lbm	189,837	43,500	189,884	43,531	190,884	43,726	189,555	43,488	190,473	43,546
First S-IVB Ignition	lbm	189,831	43,499	189,884	43,531	190,884	43,726	189,555	43,488	190,473	43,544
First S-IVB Cutoff	lbm	135,583	32,413	136,375	32,483	137,090	32,588	135,989	32,557	136,815	32,605
Second S-IVB Ignition	lbm	135,346	30,101	136,145	30,422	136,660	30,587	135,753	30,315	136,551	30,428
Second S-IVB Cutoff	lbm	4,791	2,353	5,664	2,658	5,674	2,666	5,742	2,648	5,812	2,672

At second ESC +145.5 seconds, the valve was commanded to the closed position (approximately 5.0 MR) and remained there throughout the remainder of the flight.

7.10 S-IVB PRESSURIZATION SYSTEM

7.10.1 S-IVB Fuel Pressurization System

The LH_2 pressurization system met all of its operational requirements. The LH_2 pressurization system indicated acceptable performance during prepressurization, boost, first burn, coast phase, and second burn.

The LH_2 tank prepressurization command was received at -96.6 seconds and the tank pressurized signal was received 12.8 seconds later. Following the termination of prepressurization, the ullage pressure reached relief conditions, approximately 31.6 psia, and remained at that level until liftoff, as shown in Figure 7-8. A small ullage collapse occurred during the first 25 seconds of boost. The ullage pressure returned to the relief level by 70 seconds due to self pressurization.

During first burn, the average pressurization flowrate was approximately 0.70 lbm/s providing a total flow of 96.4 lbm. All during the burn the ullage pressure was at the relief level, as predicted.

The LH_2 tank was satisfactorily repressurized for restart by the O_2/H_2 burner. The LH_2 ullage pressure was 31.0 psia at second burn ESC, as shown in Figure 7-8. The average second burn pressurization flowrate was 0.71 lbm/s until step pressurization when it increased to 1.38 lbm/s. This provided a total flow of 300.9 lbm during second burn. Significant venting during second burn occurred at second ESC +280 seconds when step

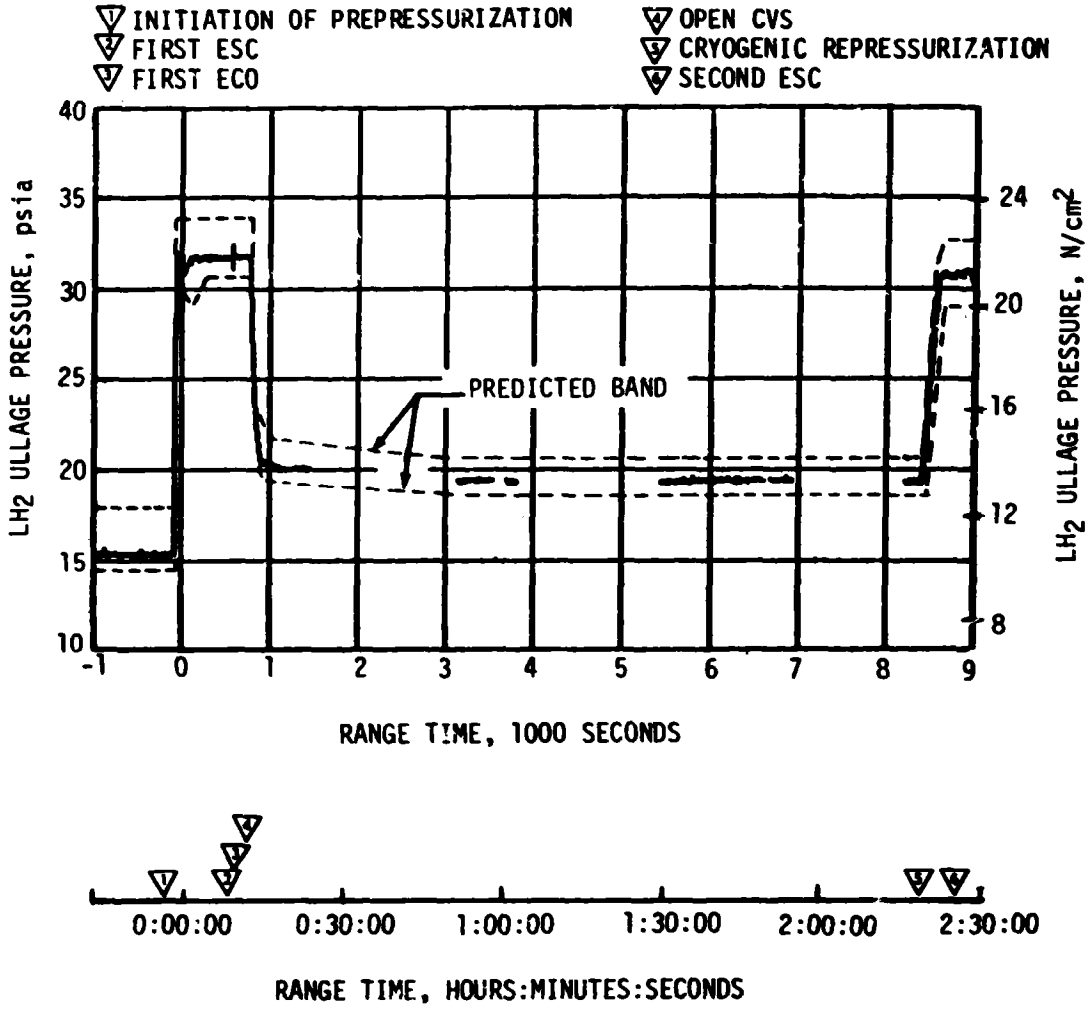

Figure 7-8. S-IVB LH_2 Ullage Pressure - First Burn and Parking Orbit

pressurization was initiated. This behavior was as predicted. The LH_2 ullage pressure during the second burn ECO and translunar coast is shown in Figure 7-9. The delayed third programed vent cycle is discussed in paragraph 7.13.1.

The LH_2 pump inlet Net Positive Suction Pressure (NPSP) was calculated from the pump interface temperature and total pressure. These values indicated that the NPSP at first burn ESC was 15.9 psi. At the minimum point, the NPSP was 7.5 psi above the required value. Throughout the burn, the NPSP had satisfactory agreement with the predicted values. The NPSP at second burn ESC was 5.7 psi which was 1.2 psi above the required value. Figures 7-10 and 7-11 summarize the fuel pump inlet conditions for first and second burns.

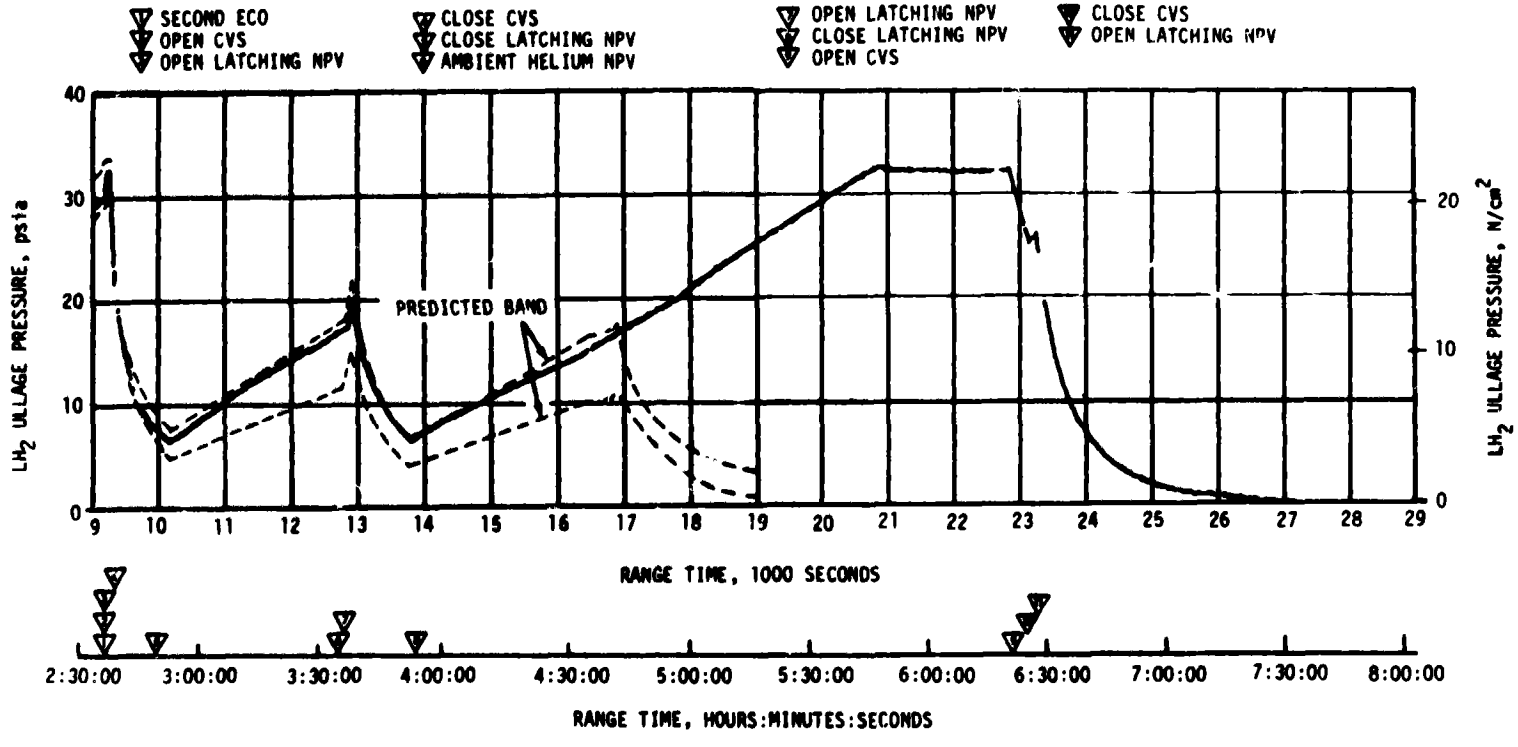

Figure 7-9. S-IVB LH_2 Ullage Pressure - Second Burn and Translunar Coast

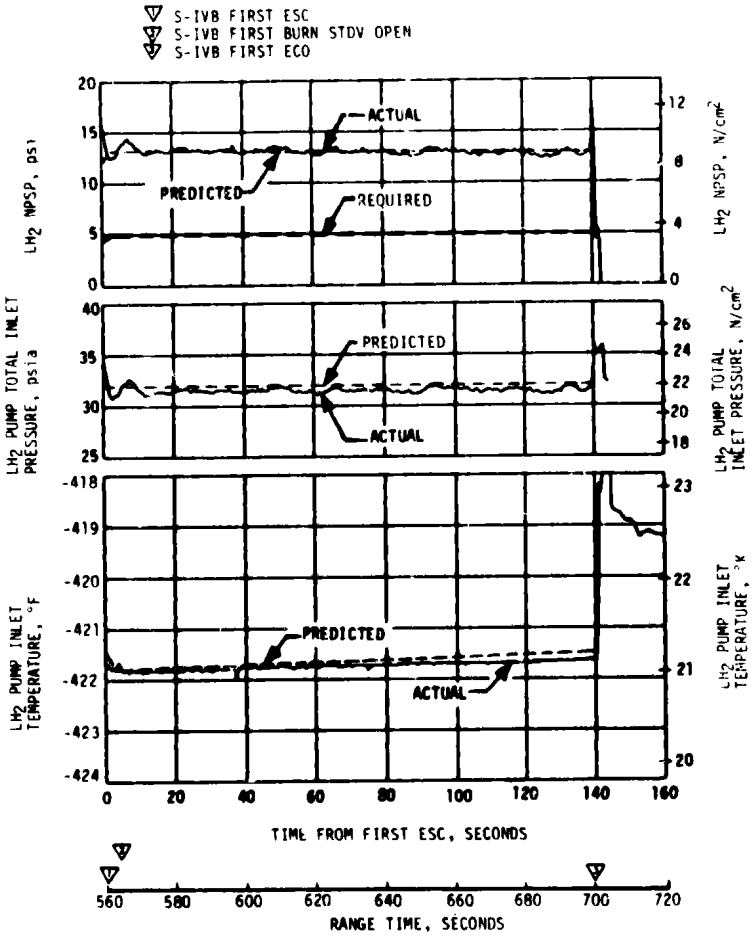

Figure 7-10. S-IVB Fuel Pump Inlet Conditions - First Burn

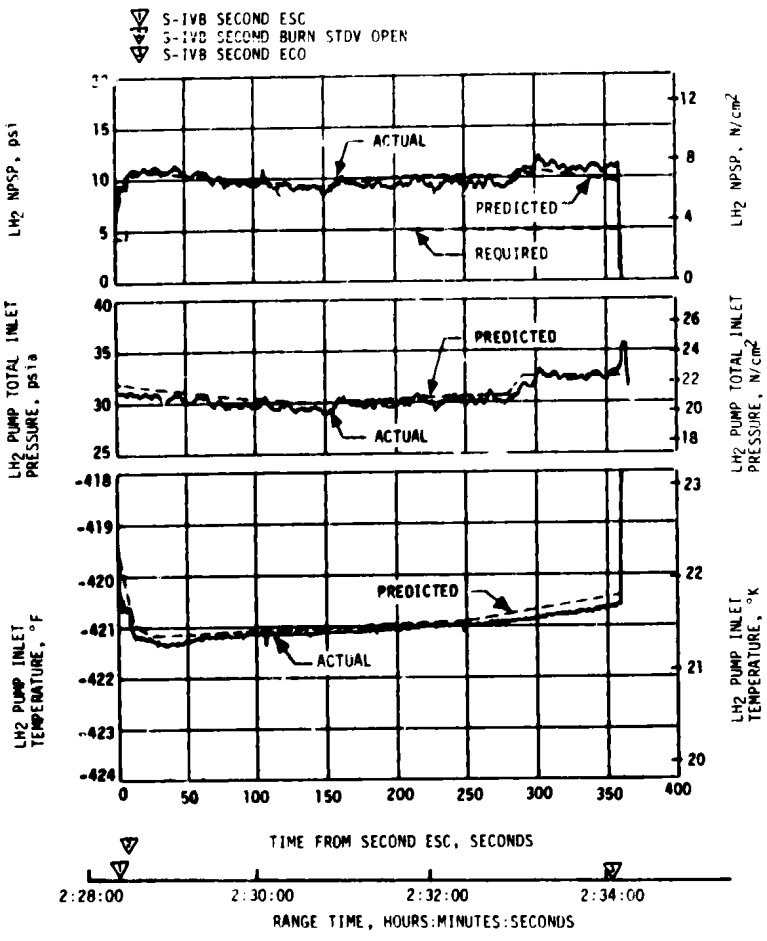

Figure 7-11. S-IVB Fuel Pump Inlet Conditions - Second Burn

7.10.2 S-IVB LOX Pressurization System

LOX tank prepressurization was initiated at -167 seconds and increased the LOX tank ullage pressure from ambient to 40.2 psia within 23 seconds as shown in Figure 7-12. Five makup cycles were required to maintain the LOX tank ullage pressure before the ullage temperature stabilized. At -96 seconds the LOX tank ullage pressure increased from 39.5 to 40.4 psia due to fuel tank prepressurization. The pressure then gradually increased to 42 psia at liftoff.

During boost there was a normal rate of ullage pressure decay caused by an acceleration effect and ullage collapse. No makeup cycles occurred because of an inhibit until after Time Base 4 (T4). LOX tank ullage pressure was 37.9 psia just prior to ESC and was increasing at ESC due to a makeup cycle.

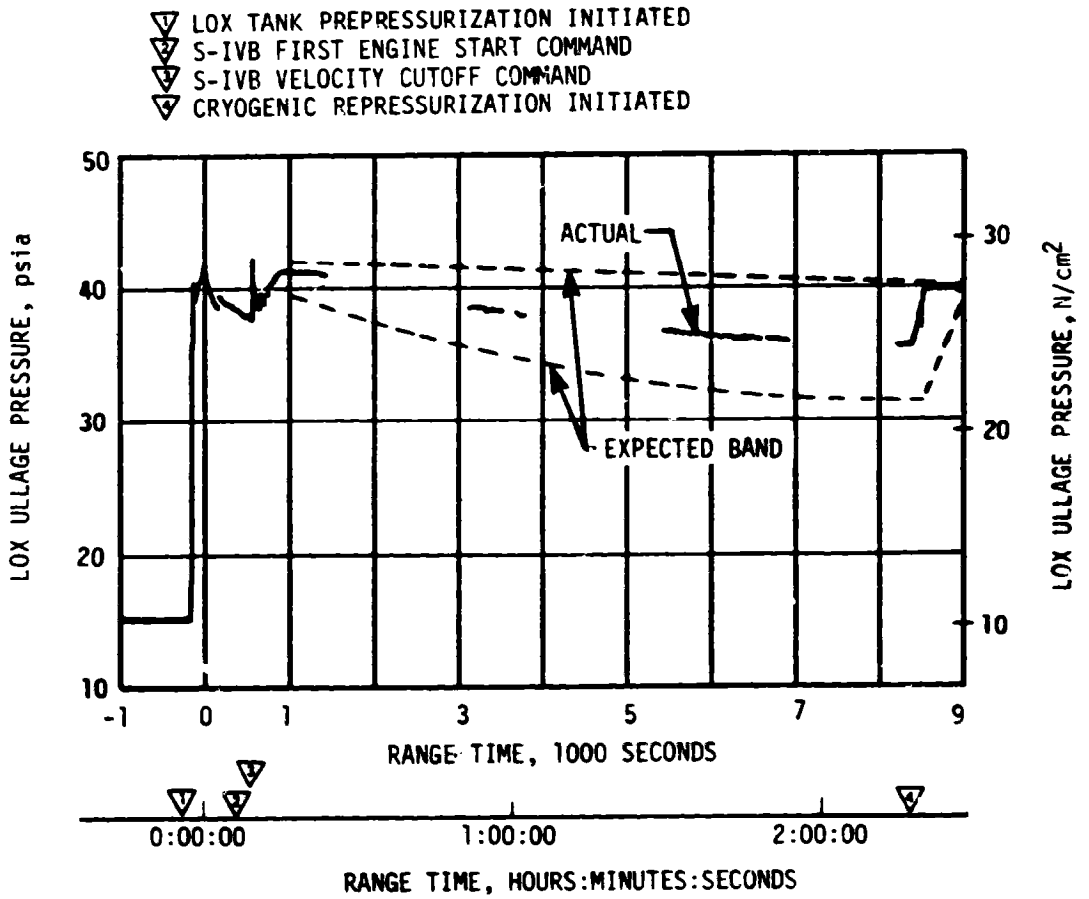

Figure 7-12. S-IVB LOX Tank Ullage Pressure - First Burn and Earth Parking Orbit

During first burn, five over-control cycles were initiated including the programed over-control cycle initiated prior to ESC. The LOX tank pressurization flowrate variation was 0.24 to 0.29 lbm/s during under-control system operation. This variation is normal and is caused by temperature effects. Heat exchanger performance during first burn was satisfactory.

During orbital coast the LOX tank ullage pressure experienced a decay similar to that experienced on the AS-507 flight. This decay was within the predicted band, and was not a problem.

Repressurization of the LOX tank prior to second burn was required and was satisfactorily accomplished by the burner. The tank ullage pressure was 39.8 psia at second ESC and satisfied the engine start requirements.

Pressurization system performance during second burn was satisfactory. There was one over-control cycle as compared to a predicted of from zero to one. Helium flowrate varied between 0.31 to 0.39 lbm/s. Heat exchanger performance was satisfactory.

The LOX NPSP calculated at the interface was 27.2 psi at first burn ESC. The NPSP decreased after start and reached a minimum value of 24.2 psi at 1 second after ESC. This was 11.4 psi above the required NPSP at that time. The LOX pump static interface pressure during first burn followed the cyclic trends of the LOX tank ullage pressure.

The NPSP calculated at the engine interface was 22.5 psi at second burn ESC. At all times during second burn, NPSP was above the required level. Figures 7-13 and 7-14 summarize the LOX pump conditions for first and second burns, respectively. The run requirements for first and second burns were satisfactorily met.

The cold helium supply was adequate to meet all flight requirements. At first burn ESC the cold helium spheres contained 382 lbm of helium. At the end of second burn, the helium mass had decreased to 161 lbm. Figure 7-15 shows helium supply pressure history.

7.11 S-IVB PNEUMATIC CONTROL PRESSURE SYSTEM

The pneumatic control and purge system performed satisfactorily during all phases of the mission. The new series redundant regulation system, which replaced the old pneumatic power control module, performed satisfactorily with the regulator dischage pressure remaining in the center of the 470 ±12 psid band. The dynamic response of the new regulator was superior to the previous regulator, with regulator discharge pressure decrease transients occurring only at the prevalves close command (maximum flow periods).

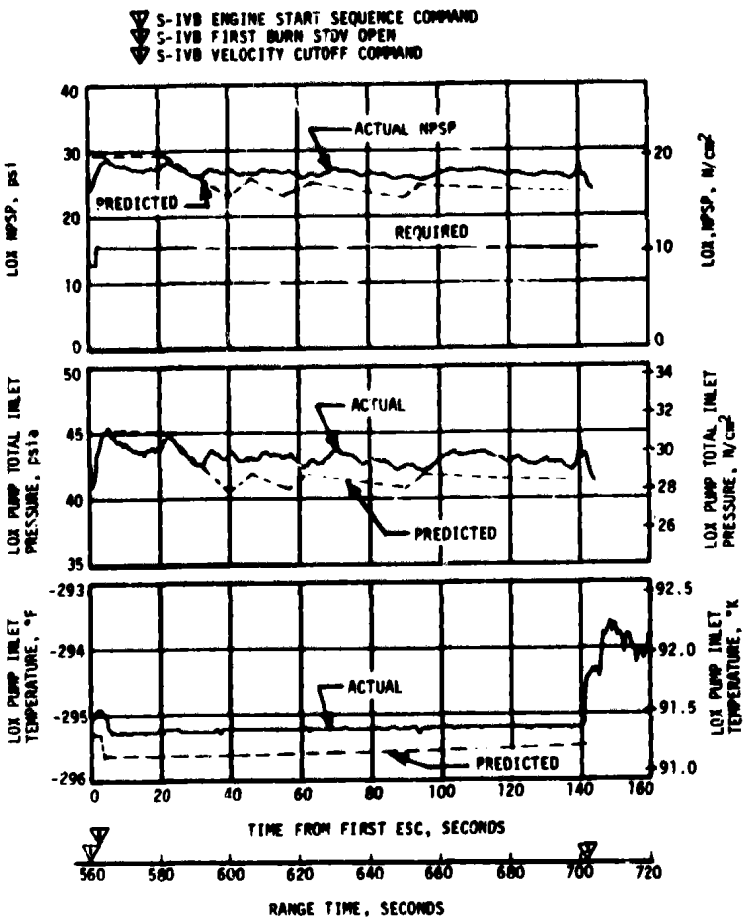

Figure 7-13. S-IVB LOX Pump Inlet Conditions - First Burn

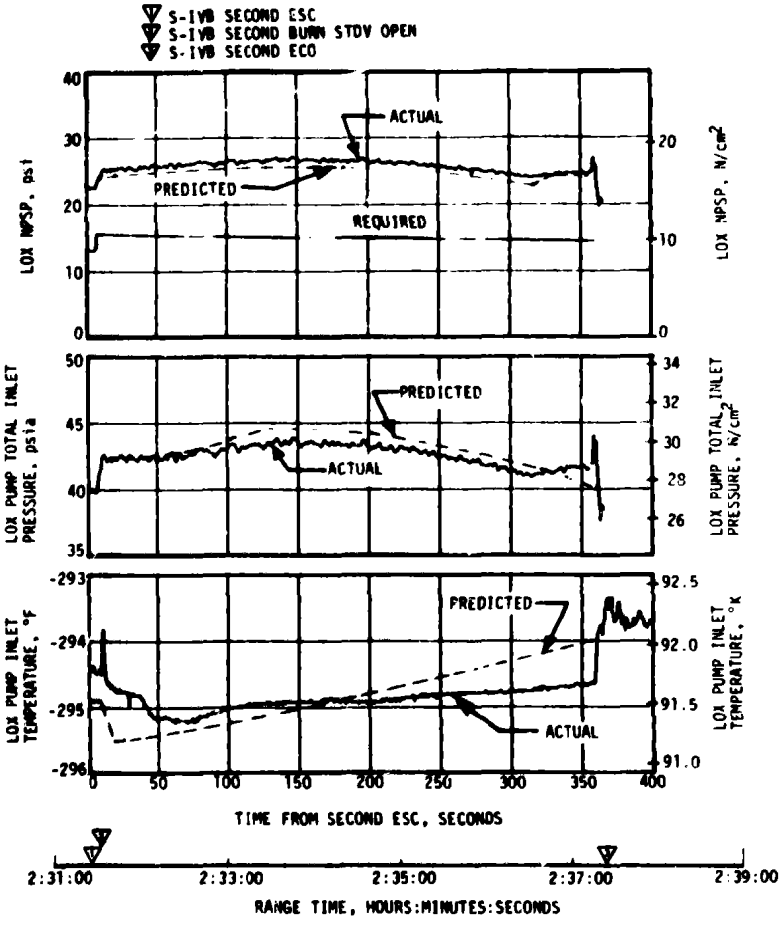

Figure 7-14. S-IVB LOX Pump Inlet Conditions - Second Burn

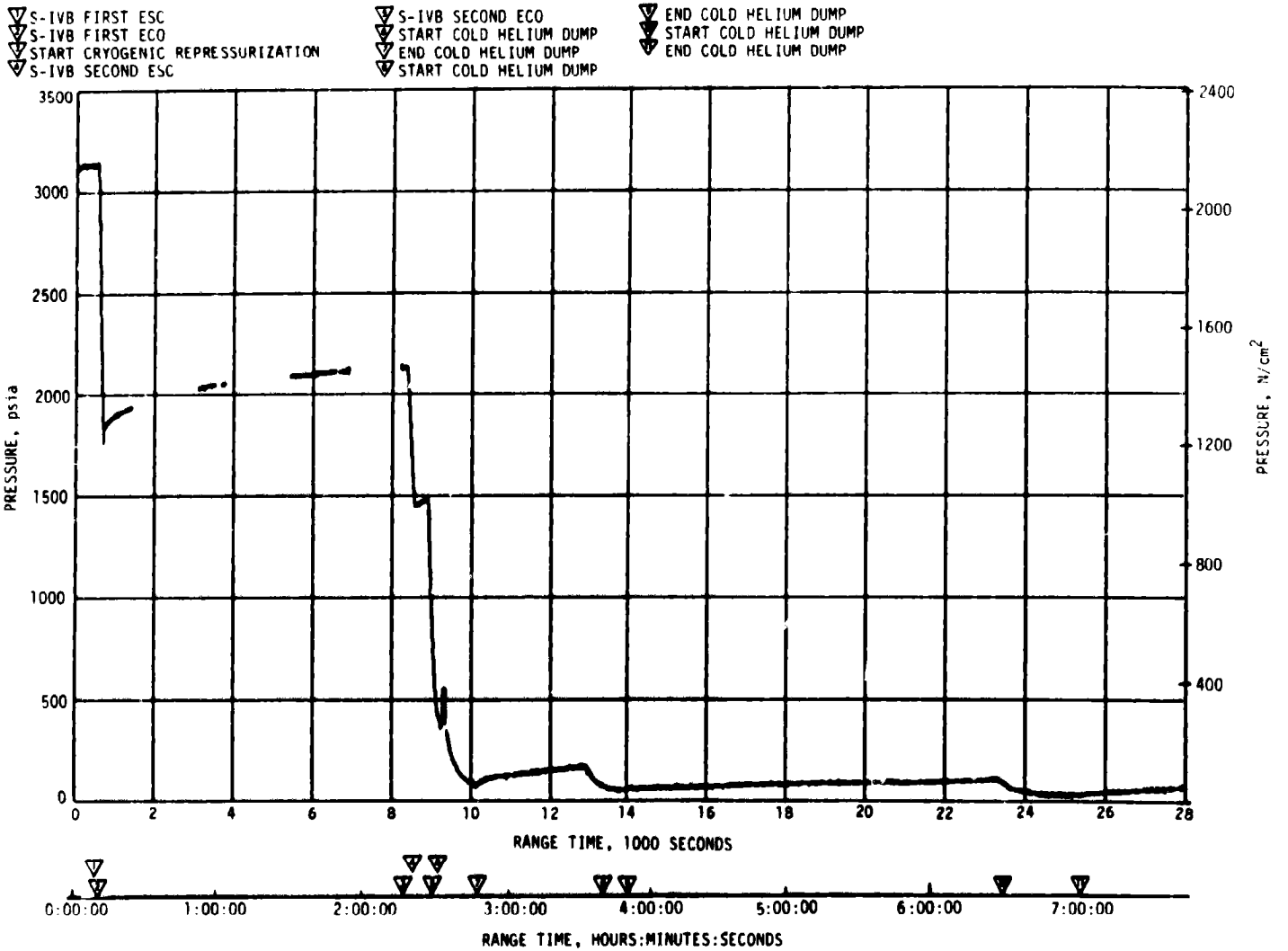

Figure 7-15. S-IVB Cold Helium Supply History

7.12 S-IVB AUXILIARY PROPULSION SYSTEM

The APS pressurization systems demonstrated nominal performance throughout the flight with the exception of a helium leak in Module No. 1. The leak started at approximately 5 hours and continued until approximately 7 hours as shown in Figure 7-16. The average leak rate was about 70 SCIM during this 2 hour period. The total helium leakage was approximately 0.05 lbm which is 5 percent of the quantity loaded. Figure 7-16 shows the helium bottle masses and temperatures for Module No. 1 and 2. As in flights AS-504 and AS-505 when helium leaks were observed, the leak occurred in the cold module when the helium bottle temperature began to decrease. The leak rate for this flight was less than those previously experienced. AS-504 had a leak rate of approximately 235 SCIM while AS-505 had a leak rate of 180 SCIM. The allowable helium leak at liftoff is 60 psi/hr which is equivalent to a 63 SCIM leakage. As in the AS-504 and AS-505 flights there is no way of determining where in the system the leak is occurring. The magnitude and duration of this leak was not large enough to present any problems.

Module No. 1 regulated outlet pressure was maintained between 192 and 201 psia and Module No. 2 regulated outlet pressure between 192 and 198 psia.

The APS ullage pressures in the propellant ullage tanks ranged from 187 to 197 psia.

The oxidizer and fuel supply systems performed as expected during the flight. The propellant temperatures measured in the propellant control modules ranged from 538 to 569°F. The APS propellant usage was as expected. Table 7-4 presents the APS propellant usage during specific portions of the mission.

The performance of the attitude control thrusters and the ullage thrusters was satisfactory throughout the mission. The thruster chamber pressures ranged from 95 to 103 psia. The ullage thrusters successfully completed the three sequenced burns of 86.7 seconds, 76.7 seconds and 80.0 seconds as well as the ground commanded 252-second lunar impact burn. The passive thermal control maneuver was successfully initiated at 42,086 seconds (11:41:26).

7.13 S-IVB ORBITAL SAFING OPERATIONS

The S-IVB high pressure systems were safed following J-2 engine cutoff. The thrust developed during the LOX dump was utilized to provide a velocity change for the lunar impact maneuver. The manner and sequence in which the safing was performed is presented in Figure 7-17.

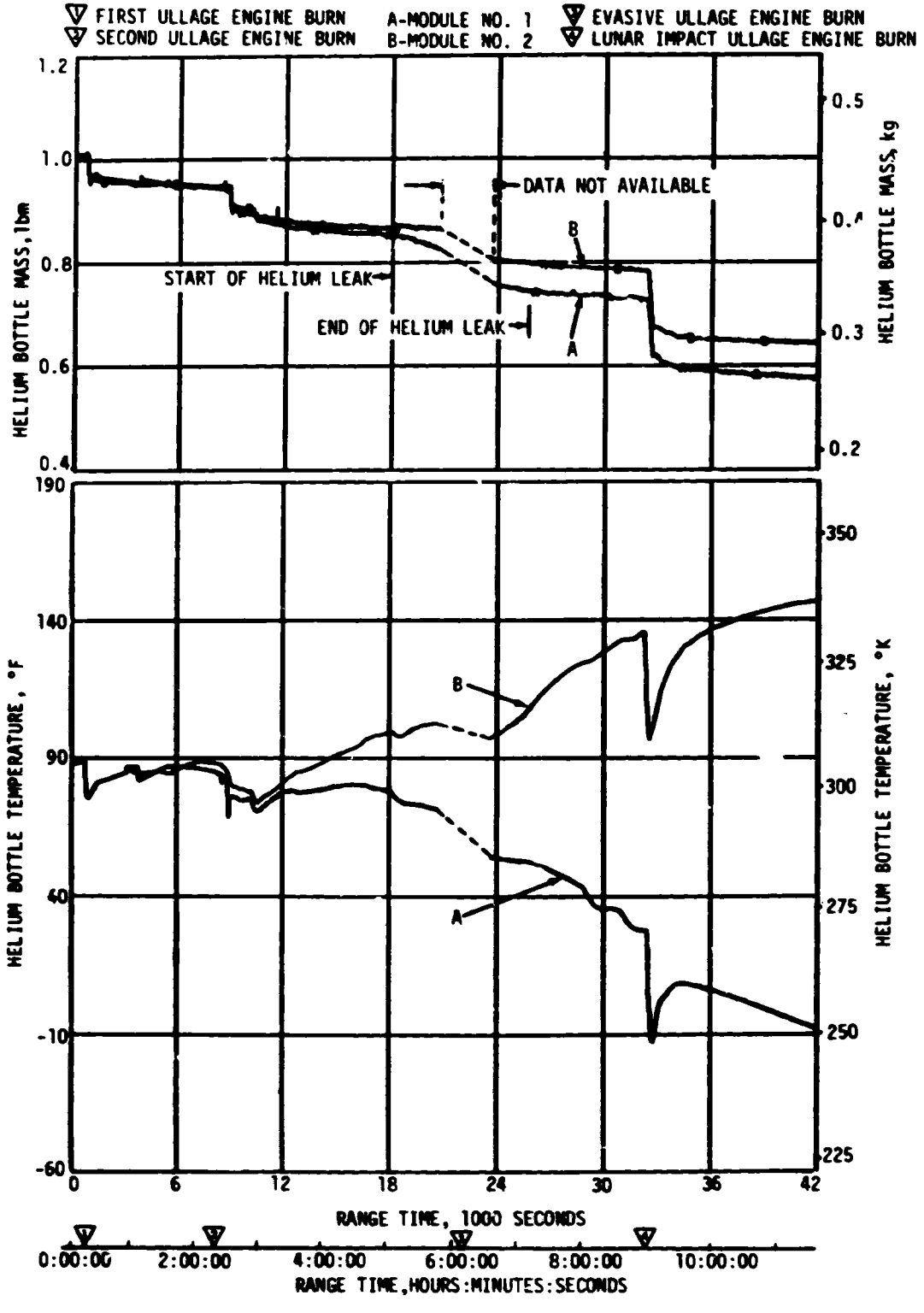

Figure 7-16. APS Helium Bottle Conditions (Sheet 1 of 2)

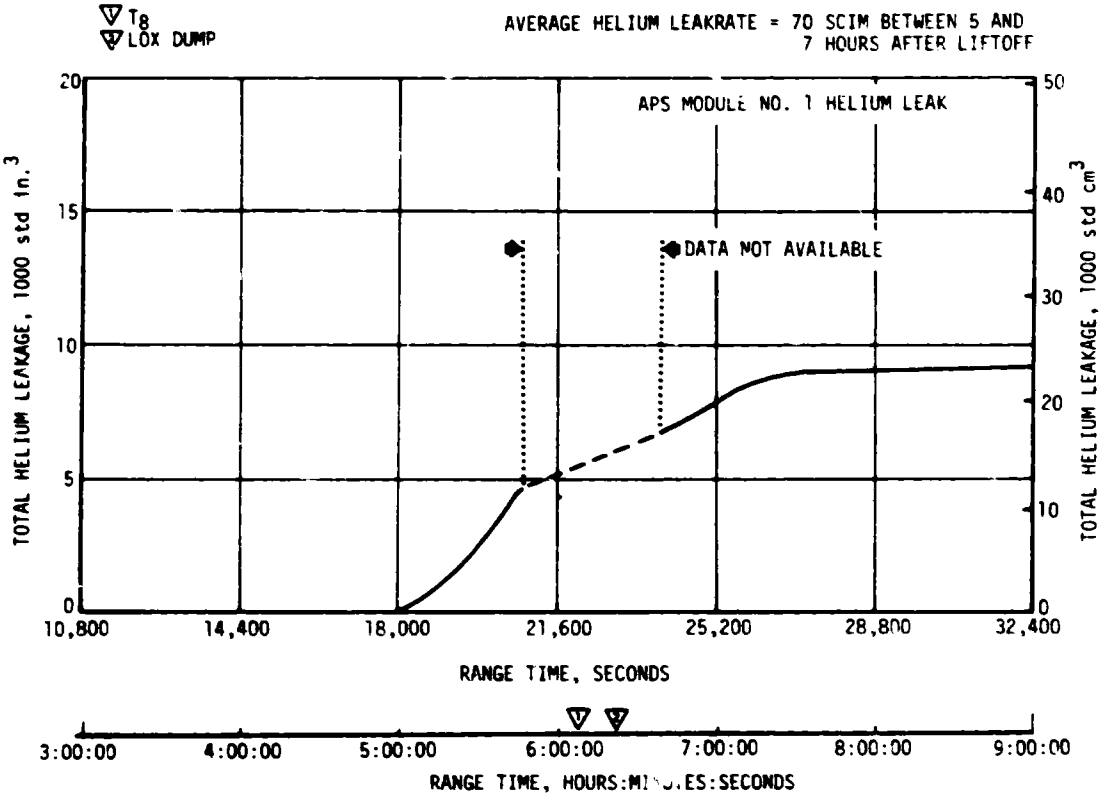

Figure 7-16. APS Helium Bottle Conditions (Sheet 2 of 2)

7.13.1 Fuel Tank Safing

The LH_2 tank was satisfactorily safed by utilizing both the Nonpropulsive Vent (NPV) and the CVS, as indicated in Figure 7-17. The LH_2 tank ullage pressure during safing is shown in Figure 7-9. At second ECO, the LH_2 tank ullage pressure was 32.6 psia and after two programed vent cycles had decayed to 6.8 psia. Due to extended docking operations, the third programed vent cycle was delayed by 6300 seconds, permitting the ullage pressure to increase to the relief level, 32.2 psia, at 20,840 seconds (05:47:20), as shown in Figure 7-9. After approximately 2000 seconds of relief venting, the third vent cycle was initiated and the ullage pressure decayed to 0 psia at 27,000 seconds (07:30:00).

7.13.2 LOX Tank Dumping and Safing

Immediately following second burn cutoff, a programed 150-second vent reduced LOX tank ullage pressure from 39.8 psia to 18.0 psia, as shown in Figure 7-18. Approximately 70 lbm of helium and 125 lbm of GOX were

Table 7 4. S-IVB APS Propellant Consumption

TIME PERIOD	MODULE AT POSITION I		MODULE AT POSITION III	
	OXIDIZER, LBM	FUEL, LBM	OXIDIZER, LBM	FUEL, LBM
Initial Load	204.2	125.9	204.2	125.9
First Burn (Roll Control)	0.7	0.5	0.7	0.5
ECO to End of First APS Ullage Burn	13.4	10.4	13.4	10.4
End of First Ullage Burn to Start of Second Ullage Burn	10.8	3.9	6.9	2.6
Second Ullage Burn	9.5	7.7	10.8	8.7
Second Burn (Roll Control)	1.3	0.9	1.3	0.9
ECO to 20,694 sec	15.6	9.4	15.7	9.6
From 20,694 to 23,572 sec This includes Evasive Ullage Burn and LOX Dump	18.9	13.8	18.9	13.8
From 23,572 sec to Start of Lunar Impact Burn	9.3	5.8	9.7	6.1
Lunar Impact Ullage Burn	31.0	25.7	34.4	27.8
End of Lunar Impact Burn to 41,971 sec	13.2	8.2	10.5	6.6
Total Usage	123.7	86.3	122.3	97.0

vented overboard. As indicated in Figure 7-18 the ullage pressure then rose gradually, due to self-pressurization, to 23.2 psia at the initiation of the Transposition, Docking and Ejection (TD&E) maneuver.

The LOX tank dump was initiated at 23,120.5 seconds (06:25:20.5) and was satisfactorily accomplished. A steady-state liquid flow of 360 gpm was reached within 14 seconds. Gas ingestion did not occur during dump. The LOX residual at the start of dump was 5452 lbm. Calculations indicate

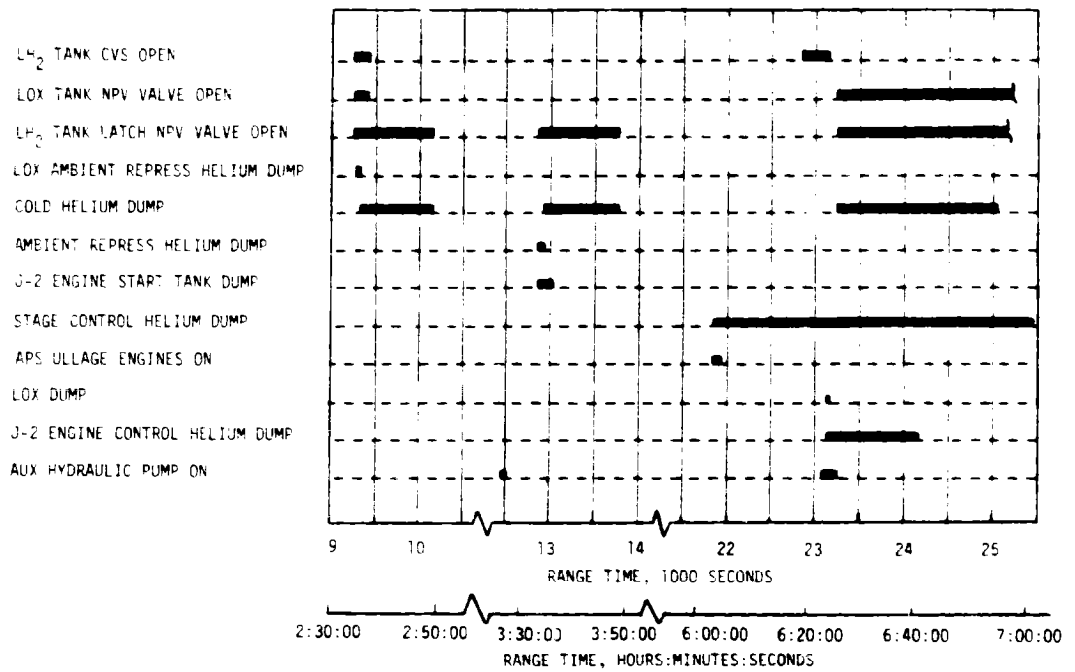

Figure 7-17. S-IVB LOX Dump and Orbital Safing Sequence

that 2542 lbm of LOX was dumped. During dump, the ullage pressure decreased from 24.2 to 23.6 psia. LOX dump ended at 23,168.5 seconds (06:26:08.5) as scheduled by closure of the Main Oxidizer Valve (MOV). A steady-state LOX dump thrust of 700 lbf was attained. The total impulse before MOV closure was 32,200 lbf-s, resulting in a calculated velocity change of 28.0 ft/s. Figure 7-19 shows the LOX dump thrust, LOX flowrate, oxidizer mass, and LOX ullage pressure during LOX dump. The predicted curves presented for the LOX flowrate and dump thrust correspond with the quantity of LOX dumped and the actual ullage pressure.

Seventy-two seconds following termination of LOX dump, the LOX NPV valve was opened and remained open for the duration of the mission. LOX tank ullage pressure decayed from 23.6 psia at 23,241 seconds (06:27:20) to zero pressure at approximately 37,000 seconds (10:16:40), as shown in Figure 7-18.

Sufficient impulse was derived from the LOX dump, LH_2 CVS operation, and APS ullage burn to achieve a successful lunar impact. For further discussion of the lunar impact refer to Section 17.

7.13.3 Cold Helium Dump

A total of approximately 156 lbm of helium was dumped during the three programed dumps, which occurred as shown in Figure 7-17.

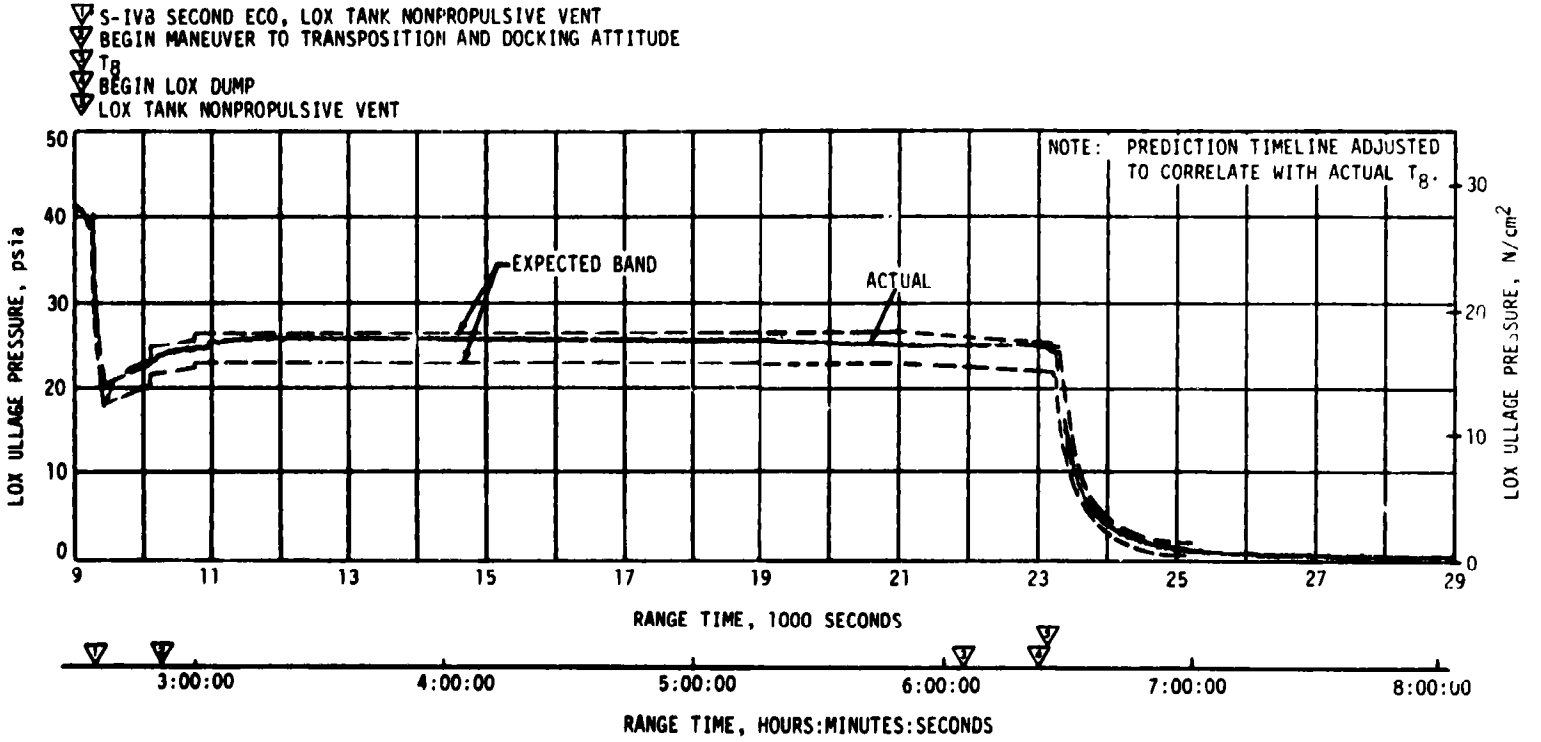

Figure 7-18. S-IVB LOX Tank Ullage Pressure - Second Burn and Translunar Coast

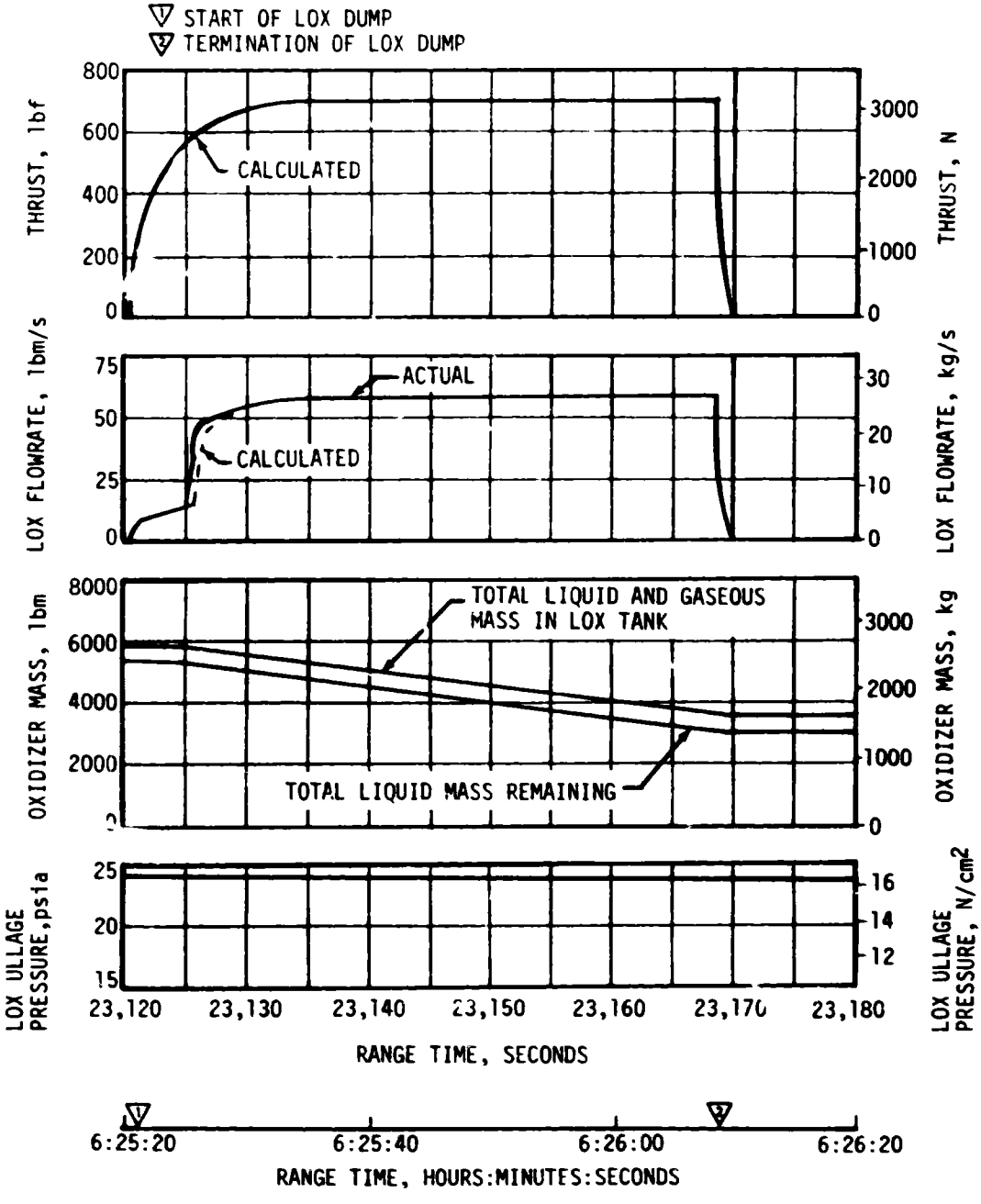

Figure 7-19. S-IVB LOX Dump Parameter Histories

7.13.4 Ambient Helium Dump

The two LOX ambient repressurization spheres were dumped through the LOX ambient repress control module into the LOX tank NPV system for 40 seconds. During this dump the pressure decayed from 2880 psia to 1230 psia.

During the LH_2 ambient repressurization helium dump approximately 42.0 lbm of helium in LOX repressurization sphere No. 1 and the LH_2 repressurization spheres was dumped via the fuel tank. The 62-second dump began at 12,864 seconds (03:34:24). The pressure decayed from 2950 psia to 320 psia.

7.13.5 Stage Pneumatic Control Sphere Safing

The stage pneumatic control sphere and LOX repressurization sphere No. 2 were safed by initiating the J-2 engine pump purge and flowing helium through the engine pump seal cavities for 3600 seconds. This activity began at 21,841 seconds (06:04:01) and satisfactorily reduced the pressure in the spheres from 2020 psia to 1150 psia.

7.13.6 Engine Start Tank Safing

The engine start tank was safed during a period of approximately 150 seconds beginning at 12,864 seconds (03:34:24). Safing was accomplished by opening the tank vent valve. Pressure was decreased from 1245 psia to 20 psia with 3.7 lbm of hydrogen being vented.

7.13.7 Engine Control Sphere Safing

The safing of the engine control sphere began at 23,120 seconds (06:25:20). The helium control solenoid was energized to vent helium through the engine purge system. The initial pressure in the sphere was approximately 3400 psia. At this time gaseous helium from the ambient repressurization spheres began flowing to the engine control sphere. Helium from the control sphere and repressurization spheres continued to vent until 24,170 seconds (06:42:50). During this time, the pressure in the repressurization spheres had decayed from about 650 to 125 psia. The control sphere pressure had decayed to 110 psia. Subsequent to the closing of the control solenoid, the control sphere repressurized to 160 psia without any noticeable decay in stage ambient repressurization sphere pressure. During the safing period, a total of 13.6 lbm of helium was vented overboard.

7.14 HYDRAULIC SYSTEM

The S-IVB hydraulic system performance was satisfactory during the entire mission (S-IC/S-II boost, first and second burns of S-IVB, and orbital coast).

SECTION 8

STRUCTURES

8.1 SUMMARY

The structural loads experienced during the S-IC boost phase were well below design values. The maximum bending moment was 116 x 10^6 lbf-in at the S-IC LOX tank (45 percent of the design value). Thrust cutoff transients experienced by AS-509 were similar to those of previous flights. The maximum longitudinal dynamic responses at the Instrument Unit (IU) were ±0.25 g and ±0.35 g at S-IC Center Engine Cutoff (CECO) and Outboard Engine Cutoff (OECO), respectively. The magnitudes of the thrust cutoff responses are considered normal.

During S-IC stage boost, 4 to 5 hertz oscillations were detected beginning at approximately 100 seconds. The maximum amplitude measured at the IU was ±0.06 g. Oscillations in the 4 to 5 hertz range have been observed on previous flights and are considered to be normal vehicle response to flight environment. POGO did not occur during S-IC boost.

The S-II stage center engine LOX feedline accumulator successfully inhibited the 14 to 16 hertz POGO oscillations experienced on previous flights. A peak response of ±0.6 g was measured on engine No. 5 gimbal pad during steady-state engine operation. As on previous flights, low amplitude 11 hertz oscillations were experienced near the end of S-II burn. Peak engine No. 1 gimbal pad response was ±0.16 g. POGO did not occur during S-II boost. The POGO limiting backup cutoff system performed satisfactorily during prelaunch and flight operations. The system did not produce any discrete outputs.

The structural loads experienced during the S-IVB stage burns were well below design values. During first burn the S-IVB experienced low amplitude, 16 to 20 hertz oscillations. The amplitudes measured on the gimbal block were comparable to previous flights and well within the expected range of values. Similarly, S-IVB second burn produced intermittent low amplitude oscillations in the 12 to 14 hertz frequency range which peaked near second burn cutoff.

8.2 TOTAL VEHICLE STRUCTURES EVALUATION

8.2.1 Longitudinal Loads

The structural loads experienced during boost were well within design values. The AS-509 vehicle liftoff occurred at a steady-state acceleration of 1.2 g. Maximum longitudinal dynamic response measured during thrust buildup and release was ±0.25 g in the IU (Figure 8-1) and ±0.50 g at the Command Module (CM). Comparable values have been seen on previous flights.

The longitudinal loads experienced at the time of maximum bending moment (76 seconds) were as expected and are shown in Figure 8-2. The steady-state longitudinal acceleration was 1.9 g as compared to 1.9 g and 2.0 g on AS-508 and AS-507, respectively.

Figure 8-2 also shows that the maximum longitudinal loads imposed on the S-IC stage thrust structure, fuel tank, and intertank area occurred at S-IC CECO (135 seconds) at a longitudinal acceleration of 3.5 g. The maximum longitudinal loads imposed on all vehicle structure above the S-IC intertank area occurred at S-IC OECO (164 seconds) at an acceleration of 3.8 g.

8.2.2 Bending Moments

Lateral response of the vehicle at liftoff was comparable to those seen on previous flights. The maximum response level seen at the CM was approximately ±0.16 g (0.111 Grms) as compared to the AS-508 maximum of ±0.17 g (0.118 Grms). The ±0.16 g was 25 percent of the predicted 3-sigma value of ±0.64 g.

The inflight winds that existed during the maximum dynamic pressure phase of the flight peaked at 102.6 knots at 43,720 feet altitude. As shown

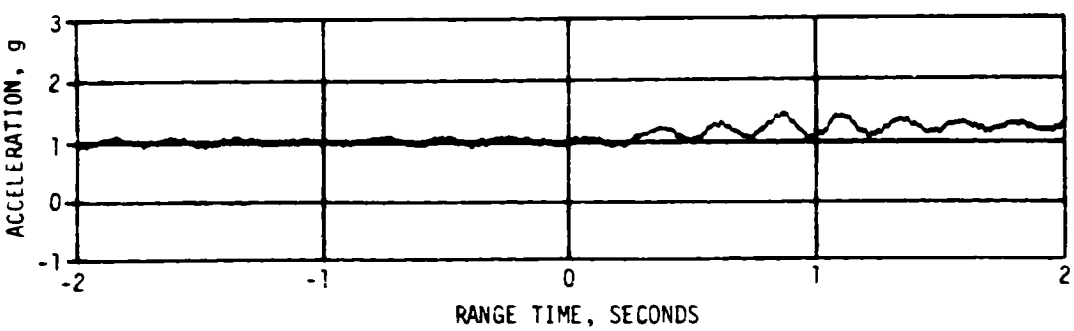

Figure 8-1. Longitudinal Acceleration at IU During Thrust Buildup and Launch

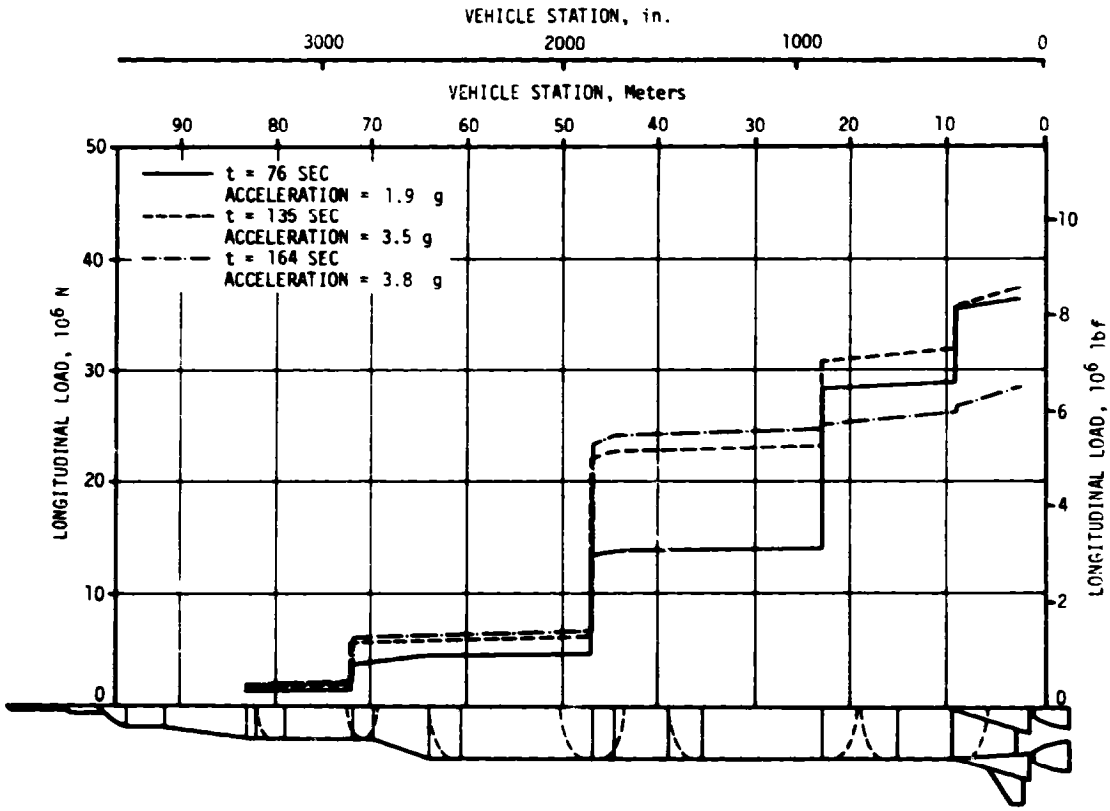

Figure 8-2. Longitudinal Load at Time of Maximum Bending Moment, CECO and OECO

in Figure 8-3, the maximum bending moment imposed on the vehicle was 116 x 10^6 lbf-in at an altitude of 33,465 feet. This moment loading is approximately 45 percent of the design value.

8.2.3 Vehicle Dynamic Characteristics

8.2.3.1 Longitudinal Dynamic Characteristics

During S-IC stage boost, the significant vehicle response was the expected 4 to 5 hertz first longitudinal mode response. The low amplitude oscillations began at approximately 100 seconds and continued until S-IC CECO. The peak amplitude measured in the IU was ±0.06 g as compared to ±0.04 g and ±0.07 g on AS-508 and AS-507, respectively. The AS-509 IU response during S-IC burn is compared with previous flight data in Figure 8-4. Spectral analysis of engine chamber pressure measurements shows no detectable buildup of structural/propulsion coupled oscillations. POGO did not occur during S-IC boost.

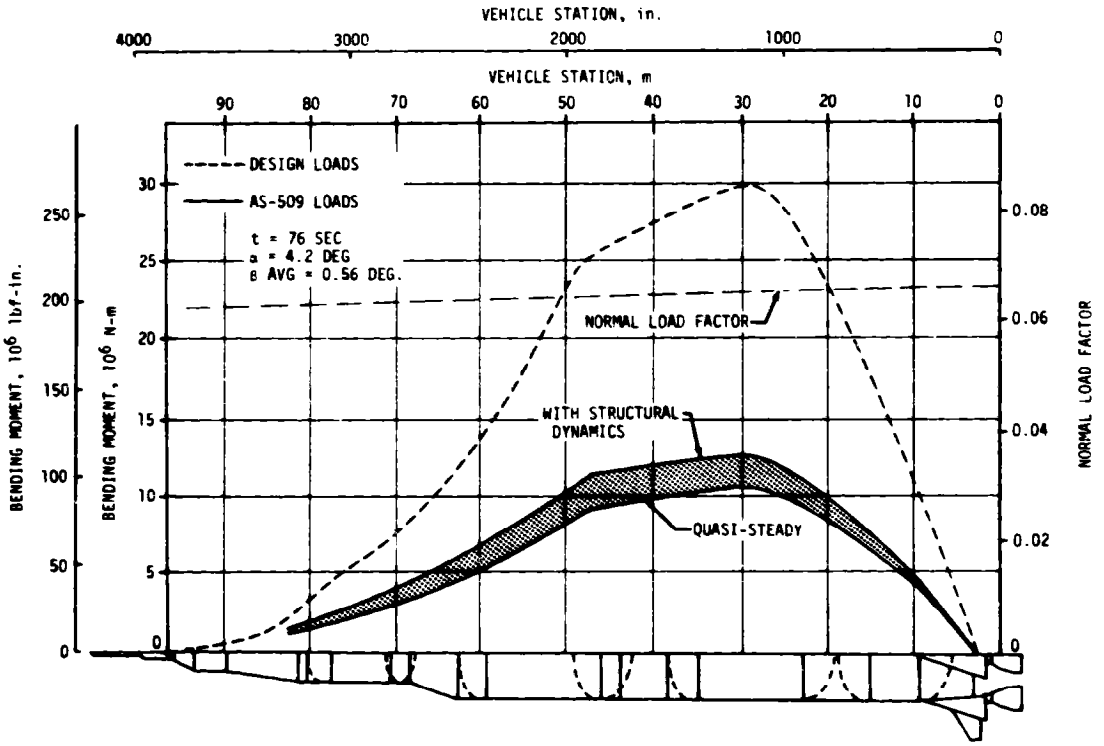

Figure 8-3. Bending Moment Distribution at Time of Maximum Bending Moment

The AS-509 S-IC CECO and OECO transient responses (Figure 8-5) were similar to those of previous flights. The maximum longitudinal dynamics at the IU resulting from S-IC CECO and OECO were ±0.25 g and ±0.35 g, respectively. Corresponding values on AS-508 were ±0.20 g at CECO and ±0.28 g at OECO.

The S-II 14 to 16 hertz POGO oscillations encountered on AS-508 were not observed on AS-509. The AS-509 vehicle incorporated a center engine accumulator in the LOX feedline of the S-II stage to inhibit such oscillations by "de-tuning" or uncoupling the structural and propulsion responses. Figure 8-6 shows a comparison between the AS-508 levels and the responses seen on AS-509. The peak gimbal pad response of approximately ±33.7 g (reconstructed value) on AS-508 compares to a peak response of ±0.6 g on AS-509. The ±0.6 g level is typical of the maximum response throughout the steady-state regime when the center engine was operational. The effectiveness of the accumulator system in suppressing the POGO oscillations generally exceeded expectations.

The purpose of the accumulator is to reduce the fundamental feedline frequency from about 26 hertz to about 3.5 to 4.0 hertz. This is to uncouple the feedline response from the fundamental crossbeam response

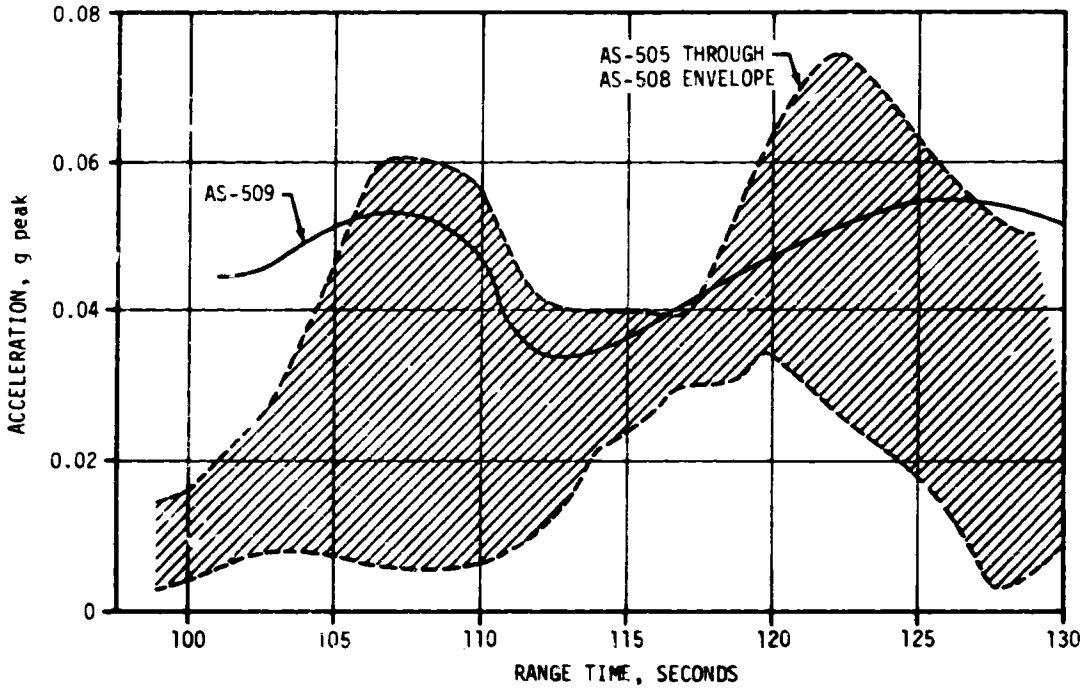

Figure 8-4. IU Accelerometer Response During S-IC Burn

at 16 hertz. Details of accumulator operation can be found in paragraph 6.9. The response of the center engine gimbal pad during accumulator fill was about ±0.8 g as shown in Figure 8-7, well within the expected value. During the fill of the accumulator, the center engine LOX inlet pressure underwent a buildup that was sustained for a short time interval. This buildup to a maximum of about 44 psi peak-to-peak with a frequency of about 65 hertz is shown in Figure 8-7. This phenomena was expected since it had been noted on several static firings. The static firing of S-II-15 displayed a similar trend with a pressure buildup of about 37 psi peak-to-peak with a frequency content of about 80 hertz. Evidence of the 65 to 80 hertz frequency can be seen in the center engine gimbal pad at a very low amplitude of less than ±0.5 g. This low level shows that there is no strong coupling between the pressure pulses at the pump and structural response; likewise, there is no evidence that these phenomena contributed to any engine performance degradation.

Near the end of S-II burn, AS-509 experienced the 11 hertz low amplitude oscillations that have occurred on all previous flights. The peak response at engine No. 1 gimbal pad was ±0.16 g for AS-509 compared to ±0.17 g on AS-508. A similar comparison of other parameters shows that the AS-509 levels were consistent with those noted on previous flights. A summary of the engine No. 1 gimbal pad responses for all flights is shown in Table 8-1.

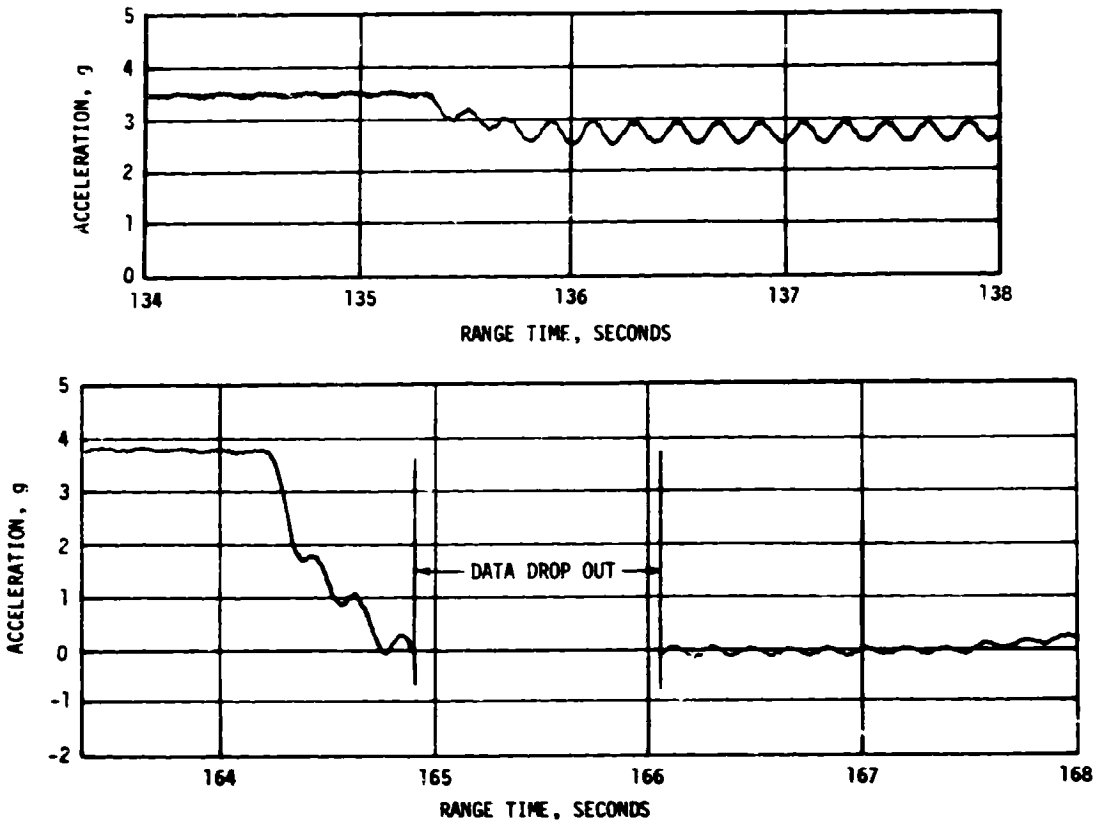

Figure 8-5. Longitudinal Acceleration at IU at S-IC CECO and OECO

A flight crew report of a low amplitude "POGO type" oscillation was made at 520 seconds. The CM longitudinal responses in the 518 to 521-second time period, when the report was made, had an amplitude of less than ±0.1 g at 9 to 9.5 hertz. During the period of maximum S-II 11 hertz oscillations (541 to 543 seconds) the CM longitudinal responses remained below ±0.1 g at 10.5 hertz. The low level CM responses are considered to be related to two different structural modes. At the time of the crew report (520 seconds), the CM was responding to a fundamental CM mode. This 9 to 9.5 hertz response is considered to be the normal forced CM response to noise content in the outboard engines. The CM response during the 11 hertz oscillation period (541 to 543 seconds) occurred in the second longitudinal vehicle mode at 10.5 to 11.5 hertz.

Since there were no S-II POGO oscillations present on AS-509 to mask other responses, it has been possible to identify certain modal trends in the data which had been unclear in previous flights. One such trend

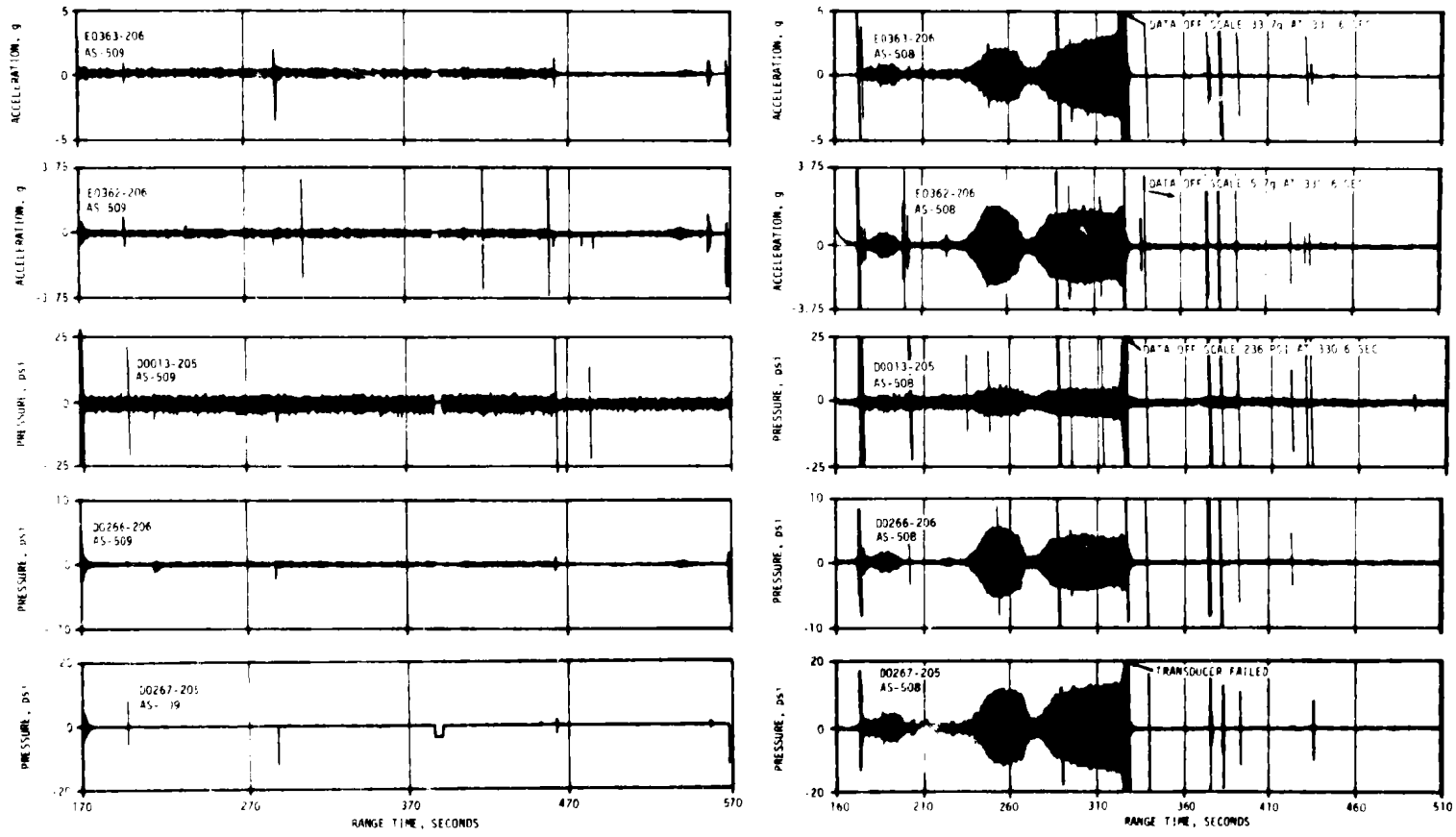

Figure 8-6. AS-509/AS-508 Acceleration and Pressure Oscillations During S-II Burn (8 to 20 Hz Filter)

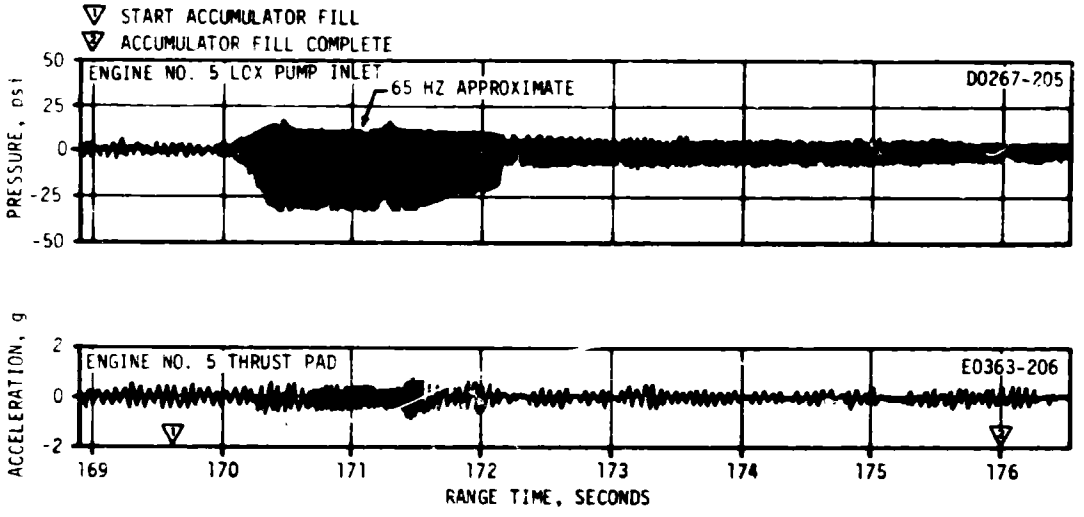

Figure 8-7. AS-509 Pump Inlet Pressure and Thrust Pad Acceleration Oscillations during Accumulator Fill Transient (0 to 110 Hz Filter)

Table 8-1. S-II Engine No. 1 Peak Response Summary for Post CECO 11 Hertz Oscillations (8 to 14 Hertz Bandpass Filter)

FLIGHT	RANGE TIME AT PEAK AMPLITUDE (SECONDS)	ACCELERATION		LOX LEVEL AT PEAK AMPLITUDE (INCHES OF LOX)	LOX LEVELS AT 1/3 AMPLITUDE (INCHES OF LOX)	
		PEAK AMPLITUDE (G)	FREQUENCY (HZ)		START	STOP
501	NO MEASUREMENT OF ACCELERATION					
502	547	0.07	10.4	30	32	28
503	512	1.12	10.9	23	36	15
504	535	0.18	11.6	8	14	6
505	545	0.22	11.0	16	23	14
506	NO LOW FREQUENCY OSCILLATION INSTRUMENTATION					
507	545	0.09	11.4	15	27	12
508	582	0.17	11.1	19	27	9
509	542	0.16	11.0	26	32	18

DATA QUESTIONABLE
AS-502 - 2 ENGINES OUT
AS-502 & AS-503 - LARGE ATTENUATION AT 11 HZ ON E_1 ACCELERATION

which is considered significant is the probable definition of the fundamental mode of the outboard LOX feedline. Figure 8-8 shows a contourgram of the amplitude/frequency density of the engine No. 1 LOX pump inlet pressure. The solid line has been sketched on top of the contour to indicate the frequency time history trend of the outboard LOX line. Sensitivity of the line frequency to NPSP and EMR can be inferred by comparing the trends of NPSP with the suggested fundamental feedline frequency (Figure 8-8).

During S-IVB first burn, low frequency (16 to 20 hertz) longitudinal oscillations similar to those observed on previous flights were again evident on AS-509. The AS-509 amplitudes (±0.06 g at gimbal block) were well below the maximum measured on AS-505 (±0.3 g) and within the expected range of values.

The S-IVB second burn produced intermittent, low level, 10 to 14 hertz oscillations similar to those experienced on all previous flights. The oscillations, corresponding to the first longitudinal mode, began approximately 100 seconds prior to second cutoff. The oscillations peaked 10 to 40 seconds prior to cutoff with approximately ±0.06 g seen at the gimbal pad. This compares to a ±0.07 g level measured on AS-508.

There was no significant change in vibration levels at around 2 minutes into second burn when the flight crew reported a "buzzing" which continued until engine cutoff. Engine mixture ratio shift occurred about 2.5 minutes

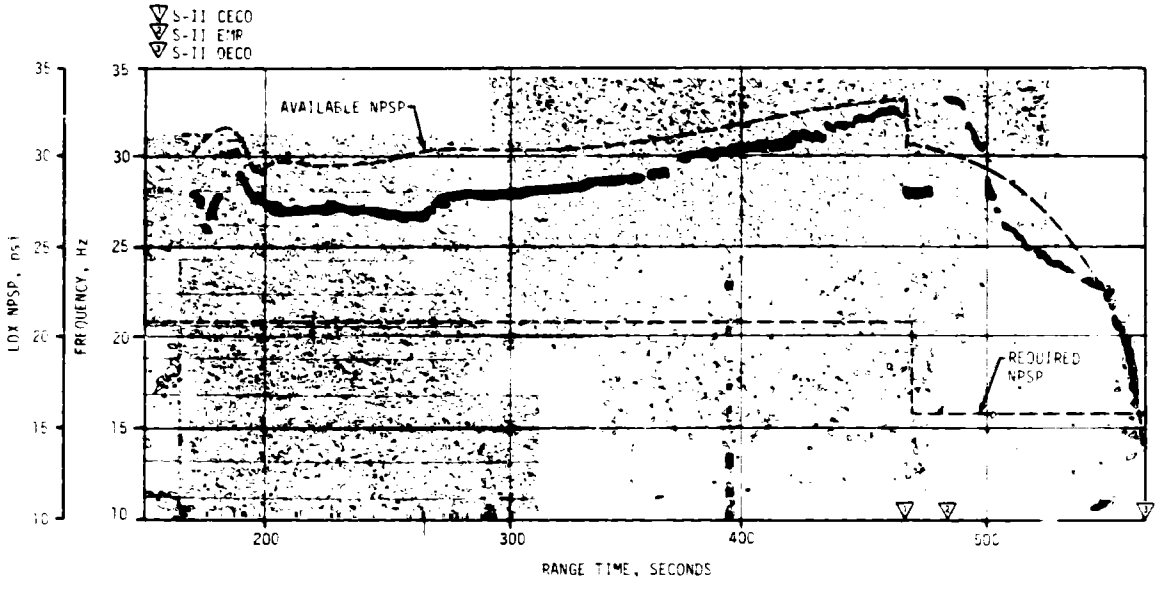

Figure 8-8. S-II Engine No. 1 LOX Pump Inlet Pressure Contourgram/NPSP Comparison

into second burn and resulted in increased acceleration but no significant change in vibration. This is not the nonpropulsive venting problem experienced on AS-505.

8.3 POGO LIMITING BACKUP CUTOFF SYSTEM

AS-509 incorporated a vibration limit monitor system which would provide for automatic engine shutdown if response levels exceeded predetermined levels.

The backup cutoff system consists of three sensors, a two-out-of-three voting logic, and an engine cutoff arming function. Each sensor consists of an accelerometer, filter, noise rejector, limit detector and solid-state output switch. Each sensor provides three outputs: an analog signal proportional to the filtered acceleration oscillation; a discrete 40 millisecond pulse which is current limited, and a discrete 40 millisecond pulse that is not current limited. The analog signal and current limited pulse are used as inputs to the telemetry system. The unlimited pulse is used to energize a relay in the voting logic. The voting circuit prevents a single circuit malfunction from providing an inadvertent engine cutoff. The arming function prevents engine cutoff until normal structural dynamic vibrations due to separation and engine start have been attenuated.

The backup cutoff system did not produce discrete outputs during prelaunch or flight operations. The analog outputs from each sensor were ± 2.8 g peak during S-II engine start with the sinusoidal phase angle difference between the three units being less than ± 12 degrees. The coincidence between discrete outputs would have been within ± 2 milliseconds if the beam vibration had exceeded the preset limit of 13.6 ± 1 g peak.

The G switch performance is depicted in Figure 8-9. This is an overlay of the response of the three G switches following engine start. The amplitude and phase correlation between the three measurements was less than 0.1 g in amplitude and 12 degrees in phase.

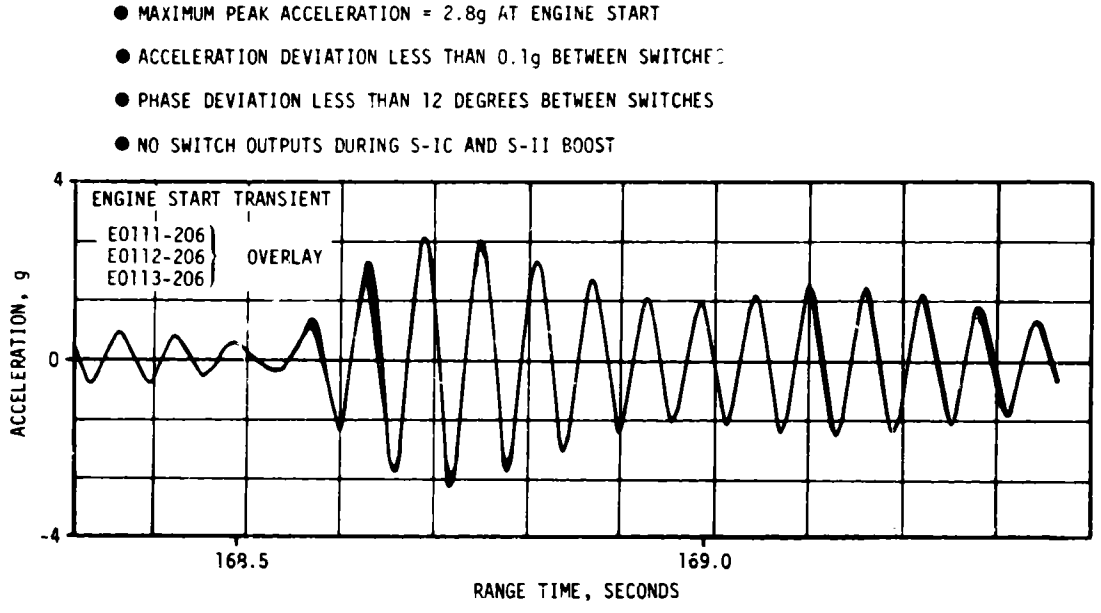

Figure 8-9. G-Switch Performance

SECTION 9

GUIDANCE AND NAVIGATION

9.1 SUMMARY

9.1.1 Performance of the Guidance and Navigation System as Implemented in the Flight Program

The guidance and navigation system performed satisfactorily in the accomplishment of all mission objectives.

9.1.2 Guidance and Navigation System Components

The ST-124M-3 inertial platform, the Launch Vehicle Data Adapter (LVDA), and the Launch Vehicle Digital Computer (LVDC) performance was satisfactory. LVDA telemetry, however, indicated one hardware measurement failure. The LVDA internal hardware monitor of the switch selector register driver status did not indicate the correct state of the bit 5 driver. This is a measurement for telemetry only; performance of the driver and all associated switch selector functions was unaffected and satisfactory.

9.2 GUIDANCE COMPARISONS

The postflight guidance error analysis was based on comparisons of the ST-124M-3 platform system measured velocities with the final postflight trajectory established from external tracking data (see paragraph 4.2). Velocity differences for boost-to-Earth Parking Orbit (EPO) are shown in Figure 9-1. A positive difference indicates trajectory data greater than the platform system measurement. The velocity differences at first S-IVB Engine Cutoff (ECO) were 0.30 m/s (0.98 ft/s), -2.09 m/s (-6.86 ft/s), and -0.82 m/s (-2.69 ft/s) for vertical, crossrange, and downrange velocities, respectively. These differences are relatively small and well within the accuracy of the data compared and the expected hardware errors. Telemetry indicated no velocity shift as seen on AS-508 during the AS-509 thrust buildup and liftoff.

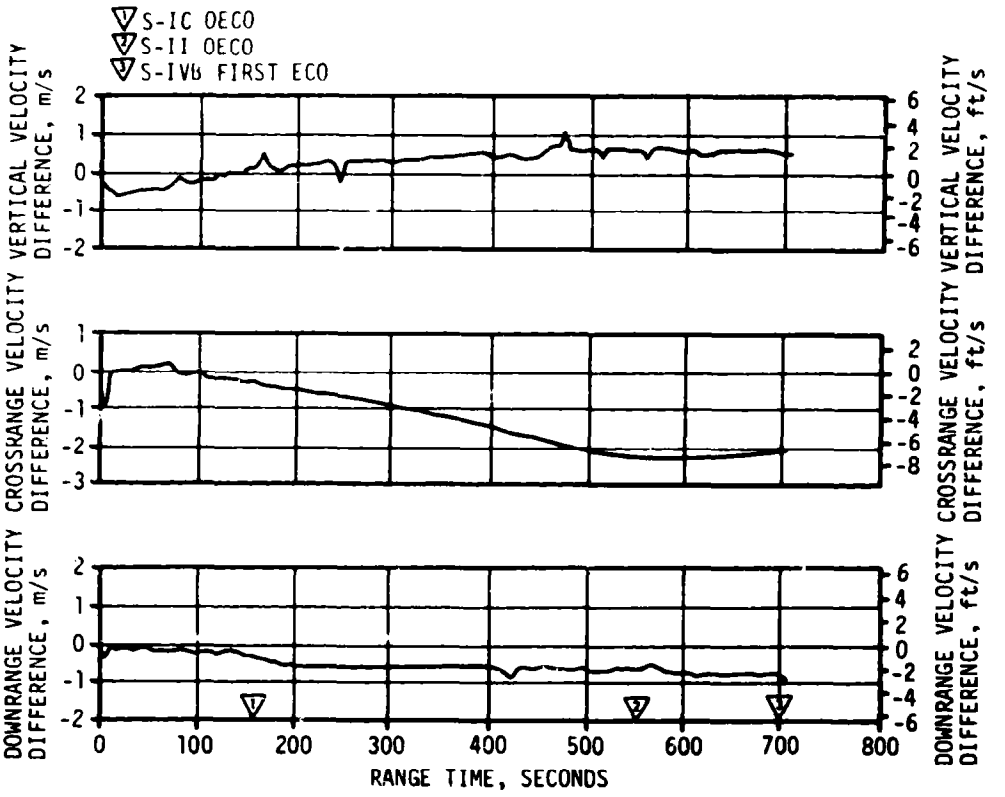

Figure 9-1. Trajectory and ST-124M-3 Platform Velocity Comparison Boost-to-EPO (Trajectory Minus Guidance)

The platform velocity comparisons for the second S-IVB burn mode are shown in Figure 9-2. The curves represent the differences in velocity accumulated from Time Base 6 (T_6) initiation. The crossrange velocity differences are consistent with the boost-to-parking orbit data. The vertical and downrange velocity differences are not compatible with the boost-to-parking orbit data and/or hardware errors. The second burn trajectory was constructed by constraining the telemetered platform velocity measurements to parking orbit and translunar orbit solutions. The in-plane velocity differences indicate some inconsistency between the two orbit solutions. Since both the vertical and downrange differences have built up to about 1 m/s (3 ft/s) at ignition, the trajectory state vector at ignition for the Translunar Injection (TLI) solution appears more accurate than the EPO solution.

Platform velocity measurements at significant event times are shown in Table 9-1 along with corresponding values from both the postflight and Operational Trajectories (OT). The differences between the telemetered and postflight trajectory data reflect some combination of small guidance hardware errors and tracking errors. The differences between the telemetered and OT values reflect off-nominal performance and environmental conditions. The values shown for the second S-IVB burn mode represent component velocity changes from T_6. The characteristic velocity

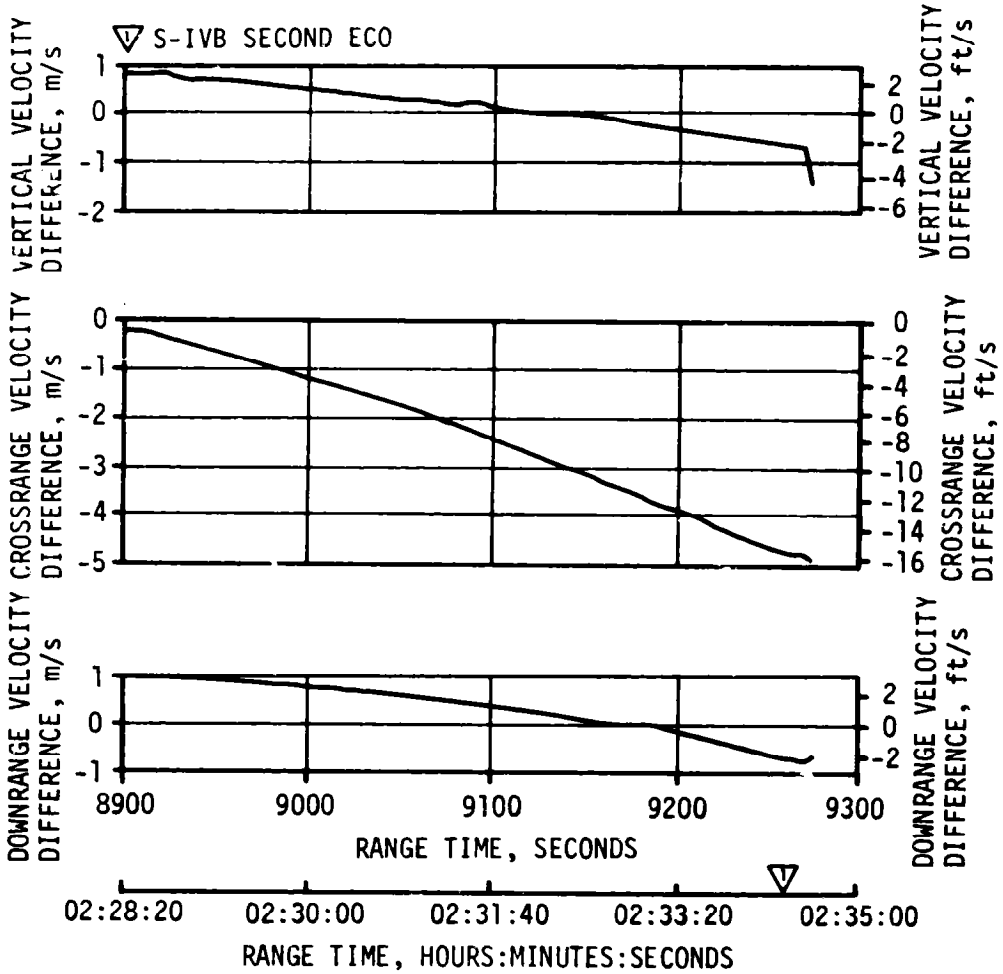

Figure 9-2. Trajectory and ST-124M-3 Platform Velocity Comparison at S-IVB Second Burn (Trajectory Minus Guidance)

determined from the platform measured velocities during second burn was close to nominal. At TLI, the guidance characteristic velocity was 0.05 m/s (0.16 ft/s) higher than the postflight trajectory and 0.17 m/s (0.56 ft/s) lower than the OT. However, the measured velocity increase between cutoff signal and TLI was 0.44 m/s (1.44 ft/s) higher than the OT. The velocity increase after first S-IVB cutoff was also higher than the OT by 0.16 m/s (0.52 ft/s).

Comparisons of navigation (PACSS 13 Coordinate System) positions, velocities, and flight path angle are shown for significant flight event times in Table 9-2. Position and velocity component differences between LVDC and OT values reflect off-nominal flight environment and vehicle performance. Velocity cutoff was given with only -0.02 m/s (-0.07 ft/s) deviation. At first guidance cutoff signal, the LVDC

Table 9-1. Inertial Platform Velocity Comparisons (PACSS 12 Coordinate System)

EVENT	DATA SOURCE	VELOCITY - M/S (FT/S)		
		VERTICAL ($\dot{X}$)	CROSSRANGE ($\dot{Y}$)	DOWN RANGE ($\dot{Z}$)
S-IC OECO	Guidance (LVDC)	2617.80 (8588.58)	2.75 (9.02)	2216.20 (7271.00)
	Postflight Trajectory	2617.98 (8589.17)	2.34 (7.68)	2215.63 (7269.13)
	Operational Trajectory	2622.71 (8604.27)	-1.44 (-4.73)	2212.61 (7258.09)
S-II OECO	Guidance (LVDC)	3466.65 (11,373.52)	-6.40 (-21.00)	6825.15 (22,392.22)
	Postflight Trajectory	3467.20 (11,375.33)	-8.59 (-28.18)	6824.57 (22,390.32)
	Operational Trajectory	3475.09 (11,401.21)	-4.33 (-14.21)	6818.74 (22,371.19)
S-IVB FIRST ECO	Guidance (LVDC)	3229.02 (10,593.90)	-1.90 (-6.23)	7603.04 (24,944.36)
	Postflight Trajectory	3229.32 (10,594.88)	-3.99 (-13.09)	7602.22 (24,941.67)
	Operational Trajectory	3234.54 (10,612.01)	-2.32 (-7.61)	7602.36 (24,942.13)
PARKING ORBIT INSERTION	Guidance (LVDC)	3228.25 (10,591.37)	-1.90 (-6.23)	7604.65 (24,949.64)
	Postflight Trajectory	3328.73 (10,592.95)	-3.94 (-12.93)	7603.94 (24,947.31)
	Operational Trajectory	3233.91 (10,609.94)	-2.31 (-7.58)	7603.85 (24,947.01)
S-IVB SECOND ECO*	Guidance (LVDC)	2662.07 (8733.83)	77.70 (254.92)	-1670.41 (-5480.35)
	Postflight Trajectory	2661.31 (8731.33)	72.90 (239.17)	-1671.23 (-5483.04)
	Operational Trajectory	2659.77 (8726.27)	77.69 (254.88)	-1675.30 (-5496.40)
TRANSLUNAR INJECTION *	Guidance (LVDC)	2665.55 (8745.24)	77.90 (255.58)	-1671.90 (-5485.24)
	Postflight Trajectory	2664.02 (8740.22)	73.01 (239.53)	-1672.59 (-5487.50)
	Operational Trajectory	2662.81 (8736.25)	77.85 (255.40)	-1676.60 (-5500.67)

*Values represent velocity change from Time Base 6.

Table 9-2. Guidance Comparisons (PACSS 13)

EVENT	DATA SOURCE	POSITIONS METERS (FT)				VELOCITIES M/S (FT/S)				FLIGHT PATH ANGLE (DEG)
		X_s	Y_s	Z_s	R	$\dot{X}_s$	$\dot{Y}_s$	$\dot{Z}_s$	V_s	γ
S-IC OECO	Guidance (LVDC)	6,438,364.6 (21,123,243.4)	35,900.5 (117,783.8)	163,667.3 (536,966.2)	6,440,545.1 (21,130,397.3)	850.17 (2789.27)	99.55 (313.48)	2597.91 (8523.33)	2735.29 (8974.05)	19.575
	Postflight Trajectory	6,438,311.2 (21,123,068.2)	35,899.2 (117,779.5)	163,614.6 (536,793.3)	6,440,489.9 (21,130,216.2)	850.42 (2790.09)	99.21 (312.37)	2597.32 (8521.39)	2734.51 (8972.47)	19.564
	Operational Trajectory	6,437,910.7 (21,121,754.2)	35,621.2 (116,867.3)	164,033.7 (538,168.1)	6,440,098.6 (21,128,932.3)	845.18 (2773.03)	95.42 (313.04)	2593.86 (8511.16)	2729.75 (8956.39)	19.50
S-II OECO	Guidance (LVDC)	6,278,525.2 (20,598,836.0)	67,951.5 (222,938.0)	1,901,747.2 (6,239,328.1)	6,560,574.6 (21,524,194.9)	-1952.14 (-6404.66)	65.28 (214.17)	6703.51 (21,993.47)	6962.36 (22,908.01)	0.621
	Postflight Trajectory	6,278,632.6 (20,599,188.3)	67,467.3 (221,349.4)	1,901,501.5 (6,238,522.0)	6,560,601.1 (21,524,281.8)	-1951.60 (-6402.89)	63.19 (207.32)	6703.09 (21,991.77)	6961.72 (22,905.84)	0.621
	Operational Trajectory	6,282,761.6 (20,612,734.7)	67,618.1 (221,844.0)	1,884,926.3 (6,184,141.5)	6,559,772.2 (21,521,562.3)	-1927.04 (-6322.66)	67.93 (222.85)	6704.47 (21,996.73)	6976.24 (22,888.46)	0.67
S-IVB First ECO	Guidance (LVDC)	5,901,671.6 (19,362,439.6)	76,585.4 (251,264.4)	2,870,880.3 (9,418,898.6)	6,563,348.7 (21,533,296.3)	-3408.85 (-11,183.89)	57.06 (187.20)	7005.91 (22,985.27)	7791.42 (25,562.41)	-0.00046
	Postflight Trajectory	5,901,855.5 (19,363,043.0)	75,818.9 (248,749.7)	2,870,560.8 (9,417,850.4)	6,563,365.5 (21,533,351.4)	-3408.58 (-11,183.01)	55.25 (181.27)	7005.19 (22,982.91)	7790.65 (25,559.88)	-0.00437
	Operational Trajectory	5,896,982.2 (19,347,054.2)	76,650.8 (251,479.1)	2,880,434.8 (9,450,245.2)	6,563,320.6 (21,533,204.0)	-3420.31 (-11,221.48)	56.94 (186.82)	7000.34 (22,967.00)	7791.44 (25,562.46)	0.00
Parking Orbit Insertion	Guidance (LVDC)	5,867,147.9 (19,249,172.9)	77,151.4 (253,121.4)	2,940,772.3 (9,648,203.1)	6,563,346.6 (21,533,289.4)	-3492.65 (-11,458.83)	56.15 (184.22)	6966.50 (22,855.97)	7793.19 (25,568.21)	-0.00075
	Postflight Trajectory	5,867,349.8 (19,249,835.3)	76,367.4 (250,549.2)	2,940,424.6 (9,647,062.3)	6,563,362.6 (21,533,341.9)	-3492.16 (-11,457.22)	54.35 (178.31)	6965.95 (22,854.17)	7792.47 (25,565.85)	-0.00304
	Operational Trajectory	5,862,358.1 (19,233,458.2)	77,215.5 (253,331.8)	2,950,247.7 (9,679,290.1)	6,563,319.8 (21,533,201.0)	-3503.86 (-11,495.60)	55.99 (183.69)	6960.72 (22,837.00)	7793.06 (25,567.78)	0.00
Time Base 6	Guidance (LVDC)	-6,539,546.9 (-21,455,206.4)	-41,900.3 (-137,468.2)	-591,473.9 (-1,940,531.2)	6,566,374.2 (21,543,222.4)	701.30 (2300.85)	-129.30 (-424.21)	-7762.95 (-25,469.00)	7795.64 (25,576.25)	0.0121
	Postflight Trajectory	-6,534,469.5 (-21,438,548.2)	-42,353.0 (-138,953.4)	-615,946.3 (-2,020,821.2)	6,563,571.9 (21,534,028.5)	733.02 (2404.92)	-127.23 (-417.42)	-7761.75 (-25,465.06)	7797.33 (25,581.79)	-0.0041
	Operational Trajectory	-6,538,938.7 (-21,453,211.0)	-41,899.8 (-137,466.5)	-590,964.8 (-1,938,860.9)	6,565,722.6 (21,541,084.6)	700.49 (2298.20)	-129.31 (-424.25)	-7763.67 (-25,471.36)	7796.28 (25,578.35)	0.01
S-IVB Second ECO	Guidance (LVDC)	-2,050,021.8 (-6,725,793.3)	-114,186.9 (-374,628.9)	-6,373,565.0 (-20,910,646.3)	6,696,115.2 (21,968,881.9)	9831.26 (32,254.79)	53.84 (176.64)	-4544.83 (-14,910.86)	10,831.07 (35,535.01)	6.9742
	Postflight Trajectory	-2,020,042.1 (-6,627,434.7)	-114,630.4 (-376,084.0)	-6,380,841.7 (-20,934,520.0)	6,693,941.3 (21,961,749.7)	9847.95 (32,309.55)	51.43 (168.73)	-4512.87 (-14,806.00)	10,832.86 (35,540.88)	7.0473
	Operational Trajectory	-2,004,243.7 (-6,575,602.7)	-114,043.8 (-374,159.4)	-6,394,262.2 (-20,978,550.5)	6,701,983.9 (21,988,136.2)	9844.02 (32,296.65)	54.56 (179.00)	-4505.27 (-14,781.07)	10,826.13 (35,518.80)	7.18
Translunar Injection	Guidance (LVDC)	-1,951,544.0 (-6,402,703.4)	-113,639.8 (-372,834.0)	-6,418,605.2 (-21,058,416.0)	6,709,689.3 (22,013,416.3)	9861.28 (32,353.28)	55.46 (181.96)	-4461.58 (-14,637.73)	10,823.75 (35,510.99)	7.4258
	Postflight Trajectory	-1,923,461.7 (-6,310,569.9)	-115,343.0 (-378,421.9)	-6,424,840.9 (-21,078,874.3)	6,707,577.0 (22,006,486.2)	9876.83 (32,404.30)	52.98 (173.82)	-4429.32 (-14,531.89)	10,824.67 (35,514.01)	7.4814
	Operational Trajectory	-1,905,643.1 (-6,252,109.9)	-113,489.5 (-372,340,9)	-6,438,903.8 (-21,125,012.5)	6,715,939.0 (22,033,920.6)	9872.93 (32,391.50)	56.15 (184.22)	-4421.79 (-14,507.19)	10,818.05 (35,492.29)	7.63

radius vector was 28 meters (92 ft) greater than the OT prediction. The LVDC and postflight trajectory data are in good agreement for the boost-to-parking orbit burn mode. The differences are well within the accuracies of the hardware measurements and/or trajectory data. Vent thrust was lower than the LVDC programed thrust from orbital navigation (ECO +100 seconds) to approximately 2500 seconds (00:41:40). Figure 9-3 presents the continuous vent thrust profiles used in the LVDC along with a postflight reconstruction and updated nominal. The low initial vent thrust also has been observed on both AS-507 and AS-508 flights. The low initial vent thrust together with the state vector differences at EPO caused oscillatory buildup in velocity component differences between the LVDC and postflight trajectory during parking orbit. Table 9-3 presents a breakdown of the factors contributing to the position and velocity errors at T_6. At T_6, the differences in geocentric radius and total velocity were -2802 meters (-9194 ft) and 1.69 m/s (5.54 ft/s), respectively. Table 9-4 presents the state vector differences at TLI between the LVDC and both the postflight trajectory and OT. The LVDC

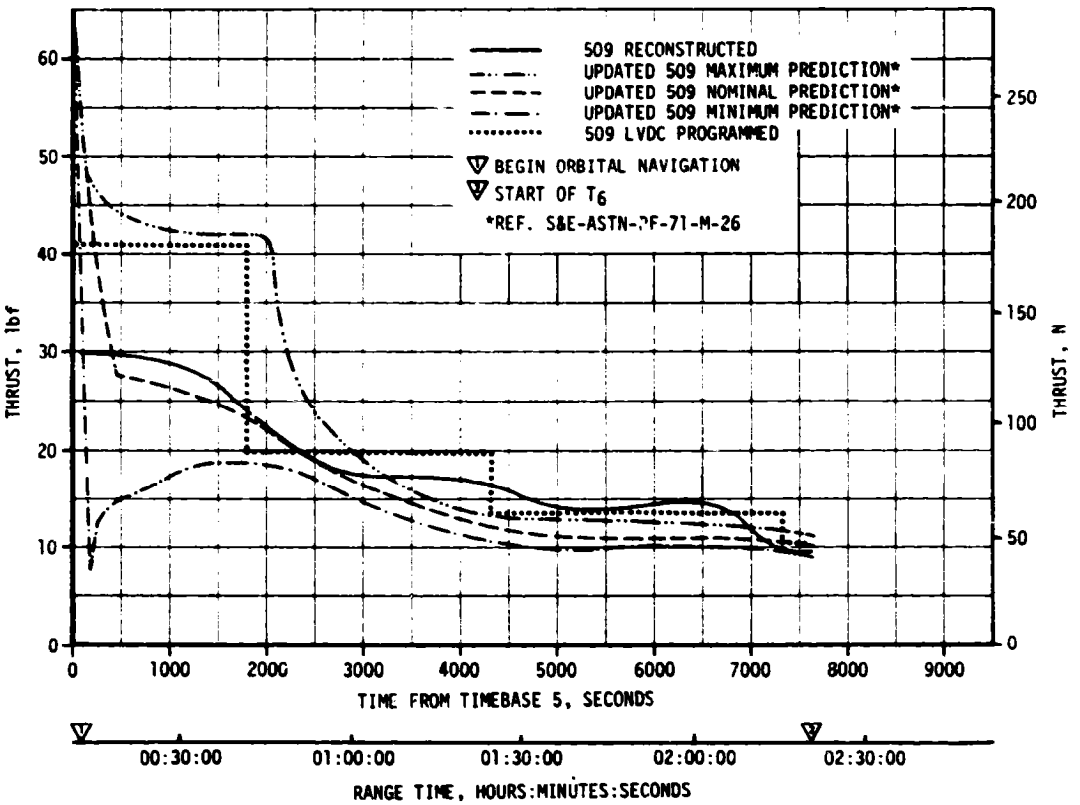

Figure 9-3. LH_2 Continuous Vent Thrust During Parking Orbit

Table 9-3. Contributing Factors To Space Fixed Component Differences (OMPT-LVDC)

DIFFERENCE SOURCE	POSITION, KM (10^3 FT)			VELOCITY, M/S (FT/S)		
	XS	YS	ZS	XDS	YDS	ZDS
Parking Orbit Insertion Differences Caused By:						
1. ST-124M-3 Error*	0.20 (0.66)	-0.83 (-2.72)	-0.35 (-1.15)	0.54 (1.77)	-2.12 (-6.96)	-0.88 (-2.89)
2. Gravity Difference	-0.01 (-0.03)	0.04 (0.13)	0.03 (0.10)	-0.02 (-0.07)	0.25 (0.82)	0.14 (0.46)
3. Tracking	0.16 (0.52)	0.01 (0.03)	-0.32 (-1.05)	0.31 (1.02)	0.08 (0.26)	0.37 (1.21)
Total Difference Parking Orbit Insertion (OMPT-LVDC)	0.35 (1.15)	-0.78 (-2.56)	-0.64 (-2.10)	0.833 (2.73)	-1.79 (-5.87)	-0.37 (-1.21)
Resulting Vector Difference at T_6	2.87 (9.42)	-0.13 (-0.43)	-11.48 (-37.66)	14.09 (46.23)	1.97 (6.46)	-0.34 (-1.12)
Venting	2.09 (6.86)	-0.21 (-0.69)	-12.18 (-39.96)	16.07 (52.72)	0.03 (0.10)	1.01 (3.31)
Tracking	0.01 (0.03)	-0.37 (-1.21)	-0.84 (-2.76)	1.60 (5.25)	0.06 (0.20)	0.38 (1.25)
Total Difference (T_6) (OMPT-LVDC)	4.97 (16.31)	-0.45 (-1.48)	-24.50 (-80.38)	31.76 (104.20)	2.06 (6.76)	1.05 (3.44)

NOTE: Hundredths position is for reference only and does not reflect accuracy to that place.

*Computed from Recovered Error Coefficients.

telemetry indicated a radius vector 6250 meters (20,504 ft) lower than the OT and 2112 meters (6930 ft) higher than the postflight trajectory. Total velocity was 5.70 m/s (18.70 ft/s) higher than the OT and 0.92 m/s (3.02 ft/s) lower than the postflight trajectory. Table 9.5 shows the guidance system accuracy of achieving targeted end conditions. The performance of the guidance system was satisfactory.

9.3 NAVIGATION AND GUIDANCE SCHEME EVALUATION

The available data indicate that the events scheduled at preset times occurred within acceptable tolerances. All flight program routines, including variable launch azimuth, time tilt, iterative guidance, navigation, and minor loop functions were accomplished properly.

Table 9-4. State Vector Differences at Translunar Injection

PARAMETER	OPERATIONAL TRAJECTORY MINUS LVDC	POSTFLIGHT TRAJECTORY MINUS LVDC
ΔX_s, meters (ft)	45,901 (150,594)	28,082 (92,133)
ΔY_s, meters (ft)	150 (493)	-1,703 (-5,588)
ΔZ_s, meters (ft)	-20,299 (-66,596)	-6,236 (-20,458)
ΔR, meters (ft)	6,250 (20,504)	-2,112 (-6,930)
$\Delta \dot{X}_s$, m/s (ft/s)	11.65 (38.22)	15.55 (51.02)
$\Delta \dot{Y}_s$, m/s (ft/s)	0.69 (2.26)	-2.48 (-8.14)
$\Delta \dot{Z}_s$, m/s (ft/s)	39.79 (130.54)	32.26 (105.84)
ΔV_s, m/s (ft/s)	-5.70 (-18.70)	0.92 (3.02)

9.3.1 Variable Launch Azimuth

Due to the unscheduled hold in the countdown at approximately -482 seconds, the variable launch azimuth function of the flight program was required to perform over a time variation greater than for any previous vehicle. The shift of range zero time from the nominal value of 20:23:00 Universal Time (UT) to 21:03:02 UT resulted in a change of the flight azimuth from 72.067 degrees nominal to 75.5579 degrees. The performance of the flight program in achieving the targeted parameters was more accurate than any previous Saturn/Apollo launch.

The time delta between true UT and UT received by the LVDC was approximately 250 milliseconds. The flight program sensed a UT which yielded an elapsed time from window opening (TD) of 2440.9414 seconds, while the correct TD was approximately 2440.6914 seconds. A comparison of the

Table 9-5. AS-509 Guidance System Accuracy

EVENT	PARAMETER	TARGETED	GUIDANCE ACHIEVED	GUIDANCE ACHIEVED MINUS TARGETED
Parking Orbit Insertion Terminal Point	Inclination, deg	31.114279	31.114285	0.000006
	Descending Node, deg	117.43194	117.43231	0.00037
	Radius, m	6,563,366.0	6,563,354.6	-11.4
	Velocity, m/s	7793.0429	7793.0449	0.0020
	Path Angle, deg	0.0	-0.000511	0.000511
Translunar Injection Terminal Point	Inclination, deg	30.812924	30.813160	0.000236
	Descending Node, deg	117.40299	117.40258	-0.00041
	Twice Specific Orbital Energy, m^2/s^2	-1,665,728.0	-1,665,685.3	42.7
	Eccentricity	0.97243580	0.97243651	0.00000071
	Argument of Perigee, deg	-124.19118	-124.19213	-0.00095

results of both TD's is shown for targeting parameters below:

	ACTUAL	CORRECTED	DIFFERENCE (ACTUAL-CORRECTED)
TD	2440.9414	2440.6914	0.2500
A_Z (pirads)	0.4197662	0.4197642	0.0000020
A_Z (deg)	75.5579	75.5575	0.0004
i	31.114276	31.114407	-0.000131
λ	117.43191	117.43252	-0.00061
C_{3_a}	-1,665,727	-1,665,728	-1
cos σ_a	0.9957228	0.9957228	0
n_a	-0.6353672	-0.6353672	0
σ_a	-0.1480349	-0.1480349	0
e_a	0.9724502	0.9724502	0

The differences are not enough to affect parking orbit noticeably and the effect was negligible-to-nonexistent at TLI.

9.3.2 First Boost Period

All first stage maneuvers were performed within predicted tolerances. The 1.25 degree yaw maneuver was initiated at T_1 +1.388 seconds and terminated at T_1 +9.326 seconds. Pitch and roll guidance was initiated at T_1 +12.244 seconds and the roll maneuver was completed at T_1 +27.430 seconds. The pitch time tilt polynomial was arrested at T_1 +163.518 seconds.

Iterative Guidance Mode (IGM) performance for first boost was nominal. The pitch and yaw rate-limited steering commands are illustrated in Figure 9-4. Phase I IGM began properly at T_3 +40.6 seconds and was implemented at T_3 +41.802 seconds. Implementation of IGM was accompanied by a +6.877 degree change in pitch command and a -0.452 degree change in yaw command. The time to go in Phase I IGM (TII) reached zero at approximately T_3 +307.4 seconds. The first S-II engine mixture ratio shift switch selector command was issued at T_3 +308.749 seconds followed by Phase II IGM implementation in the artificial Tau mode at T_3 +309.926 seconds. Real Tau 2 computation was implemented at T_3 +320.960 seconds with a change in Tau 2 of 18.50 seconds.

The Chi freeze was initiated at the start of T_4 and released at T_4 +9.195 seconds with the implementation of Phase III IGM. The commanded pitch change at Phase III IGM start was -0.036 degree and the commanded yaw change was +0.042 degree. The real Tau 3 computation was implemented at T_4 +20.37 seconds with a -21.98 second change in Tau 3.

Terminal guidance was initiated at T_4 +108.017 seconds and the high speed cutoff loop was entered at T_4 +134.106 seconds. Ten passes through the high speed loop were made before S-IVB cutoff. The velocity at the time of the S-IVB velocity cutoff command was 7791.42 m/s (25,562.40 ft/s). Table 9-6 shows the parking orbit insertion parameters.

9.3.3 Earth Parking Orbit

At the start of T_5 a Chi freeze was initiated using the gimbal angle readings on the first pass to establish the commanded angles (Chi's) for the freeze. The local reference maneuver scheduled for T_5 +20 seconds was initiated within the one computation cycle tolerance at T_5 +21.302 seconds.

The initiation of orbital navigation occurred at T_5 +101.533 seconds which was within the one computation cycle tolerance from the scheduled start at T_5 +100 seconds. Orbital navigation was terminated and boost navigation resumed at approximately T_6 -9 seconds. The exact time of boost navigation resumption could not be determined because of missing telemetry data, but entry to boost navigation before T_6 start was confirmed.

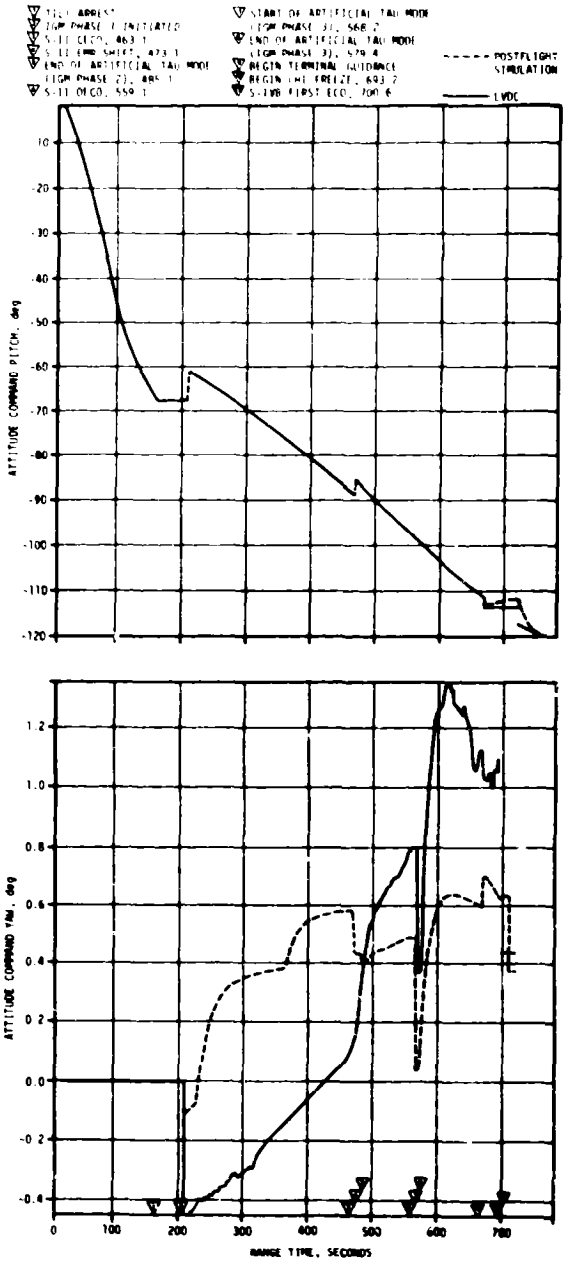

Figure 9-4. Attitude Commands During Boost-to-EPO

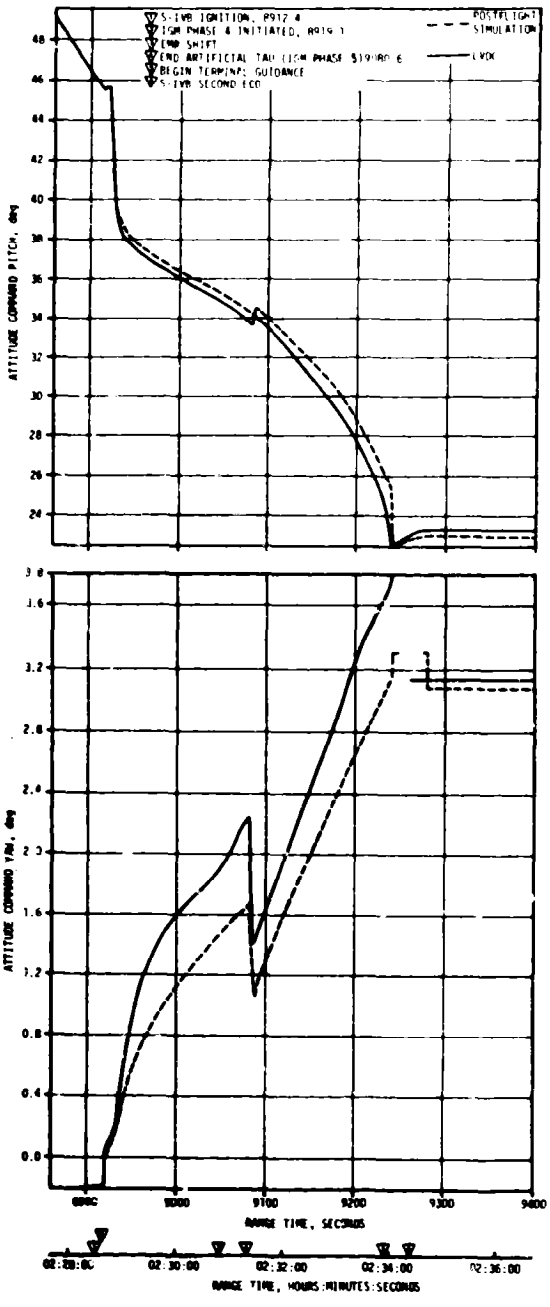

Figure 9-5. Attitude Commands During S-IVB Second Burn

Table 9-6. Parking Orbit Insertion Parameters

PARAMETER	OPERATIONAL TRAJECTORY (OT)	POSTFLIGHT TRAJECTORY (OMPT)	GUIDANCE (LVDC)	OMPT MINUS OT	LVDC MINUS OT
Space-Fixed Velocity, m/s (ft/s)	7793.058 (25,567.7)	7792.470 (25,565.8)	7793.190 (25,568.2)	-0.587 (-1.9)	0.133 (0.4)
Geocentric Radius, meters (ft)	6,563,320 (21,533,158)	6,563,362 (21,533,297)	6,563,345 (21,533,242)	42 (139)	25 (84)
Flight Path Angle, deg	-0.000787	-0.003050	-0.000746	-0.002264	0.000041
Descending Node, deg	117.429981	117.455978	117.429870	0.025996	-0.000111
Inclination, deg	31.114436	31.120518	31.114338	0.006082	-0.000098
Eccentricity	0.000014	0.000157	0.000037	0.000143	0.000023

9.3.4 Second Boost Period

Sequencing of restart preparations by the flight program was accomplished as predicted. Transfer ellipse targeting was computed and telemetered just prior to initiation of second burn IGM.

IGM for the S-IVB second burn was implemented at T_6 +584.941 seconds with a change of -5.637 degrees in pitch attitude command and a change of 0.244 degree in yaw attitude command. The pitch and yaw Chi values are illustrated in Figure 9-5. The post mixture ratio shift IGM phase was implemented at T_6 +717.020 seconds following the engine mixture ratio shift. Real Tau 3 computations were implemented at T_6 +746.418 seconds with a -63.51-second change in Tau 3.

Terminal guidance steering was initiated at T_6 +901.893 seconds and the high speed loop was entered at T_6 +926.731 seconds. Three passes through the high speed loop were made with the velocity cutoff command occurring at the start of the fourth pass. The velocity at the time of S-IVB cutoff command was 10,231.021 m/s (35,534.85 ft/s). Table 9-7 shows the TLI parameters.

9.3.5 Post TLI Period

The local horizontal maneuver was initiated at T_7 +151.594 seconds. The Transposition Docking and Ejection (TD&E) maneuver was initiated at T_7 +900.869 seconds. The minor loop Chi's had all reached commanded values by T_7 +1129.7 seconds. The vehicle had reached the commanded

Table 9-7. Translunar Injection Parameters

PARAMETER	OPERATIONAL TRAJECTORY (OT)	POSTFLIGHT TRAJECTORY (OMPT)	GUIDANCE (LVDC)	OMPT MINUS OT	LVDC MINUS OT
Space-Fixed Velocity, m/s, (ft/s)	10,818.044 (35,492.2)	10,824.669 (35,513.9)	10,823.753 (35,510.9)	6.625 (21.7)	5.709 (18.7)
Geocentric Radius, meters (ft)	6,715,938 (22,033,874)	6,707 7 (22,006,442)	6,709,688 (22,013,367)	-8361 (-27 432)	-6250 (-20,507)
Descending Node, deg	117.400850	117.359111	117.402217	-0.041739	0.001367
Inclination, deg	30.812696	30.813569	30.813378	0.000873	0.000682
Eccentricity	0.972307	0.972246	0.972521	-0.000061	0.000214
C_3, m^2/s^2 (ft^2/s^2)	-1,673,578 (-18,014,244)	-1,678,167 (-18,063,639)	-1,660,602 (-17,874,571)	-4589 (-49,395)	12,976 (139,673)

attitude by T_7 +1259.9 seconds. The implementation of post-TLI orbital navigation occurred at T_7 +151.371 seconds.

At 10,955.861 seconds (03:02:35.861) (T_7 +1692.389 seconds), telemetry from the H0060-603 measurement (LVDC/LVDA telemetry) ceased as discussed in paragraph 15.3.3. No further details of flight program performance are available beyond that time. Certain key events can be monitored by discrete telemetry but no navigation or guidance information is available.

9.4 GUIDANCE SYSTEM COMPONENT EVALUATION

9.4.1 LVDC and LVDA Performance

The LVDC and LVDA and all constituent circuits and modules performed nominally with the exception of one hardware monitor measurement. The telemetered status of the monitor did not reflect the true state of the associated hardware, switch selector register bit 5.

The LVDC flight program steps in commanding a switch selector function include the following:

a. Execute a switch selector stage select and address command for a given switch selector function to set the LVDA switch selector register.

b. Effect a time delay to ensure that at least one of the four LVDA Data Output Multiplexer (DOM) storage channels will accept data.

c. Execute a Process Input/Output (PIO) command to read the status of the LVDA Switch Selector Register and Discrete Output Register driver outputs (SSDO word) which are stored in DOM for telemetry via measurement H0060-603.

For each switch selector function command that required a logical one output from switch selector register bit 5, the SSDO word indicated that bit 5 was a logical zero. For each case, the switch selector function and switch selector feedback outputs were correct. Therefore, the failure mechanism did not affect the SS5 driver output function.

A review of system test data indicates that the failure was present at liftoff and occurred prior to or during IU-509 systems test. Further investigation revealed that the LVDA component level tests as presently configured will not detect the observed failure. Recommendation of changes to the LVDA component level tests and to systems test data evaluation are in progress.

The multiplexer latch and multiplexer serializer logic circuits and the telemetry storage select and delay line logic circuits through which the SS5 driver output status signal flows are common with other data signal flow. The only circuits which are unique to the SS5 driver output monitor are Discrete Input, Type A (DIA) circuit, AND circuit, and interconnecting networks from the SS5 driver to the multiplexer latch input (DM7A). The failure mechanism, therefore, is constrained to these circuits.

For the observed indications, any mechanism which could produce the equivalent effect of a voltage, $\leq$ 2.5 vdc, at point A of the circuit in Figure 9-6 is a possible cause of the failure which existed between points B and C.

9.4.2 ST-124M-3 Stabilized Platform Subsystem

The ST-124M-3 Stabilized Platform Subsystem (ST-124M-3 SPS) operated within desired limits through the first 13,900 seconds (03:51:40) of flight as depicted in available data. Although the vibration levels at liftoff were slightly higher than those on IU-508, no accelerometer anomalies were in evidence.

Proper servo loop response was evident at liftoff. Pickoff deflections at Command and Service Module (CSM) separation were lower than on IU-508. Pickoff deflections were:

	AS-509	AS-508
X gyro	0.67°P-P	1.6°P
Y gyro	0.17°P-P	0.32°P-P
Z gyro	0.41°P-P	1.36°P-P

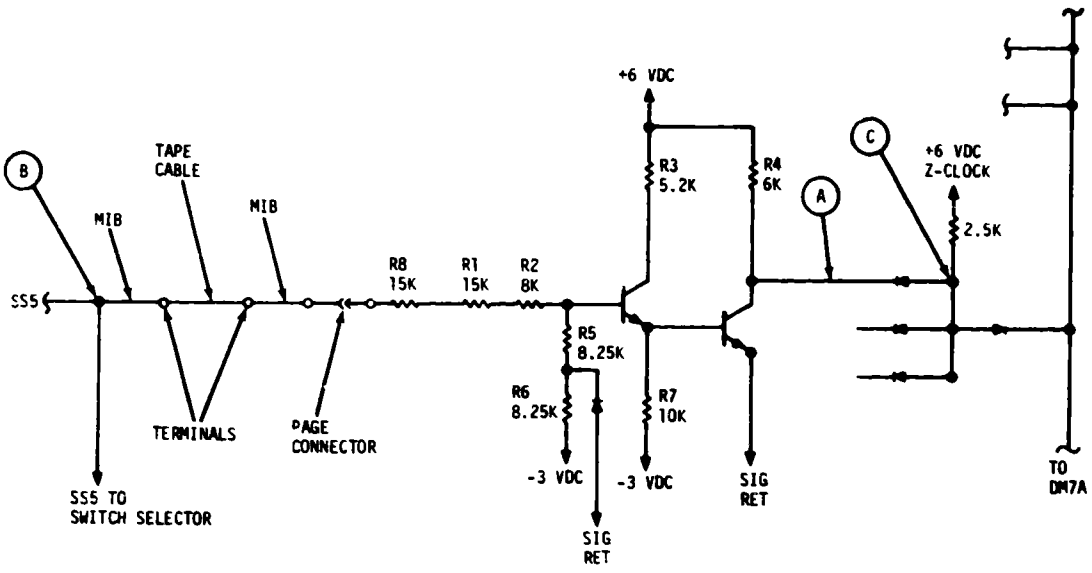

Figure 9-6. Switch Selector Bit 5 Driver Monitor Circuit

As on previous vehicles, oscillations of 0.25°P-P at approximately 5 hertz were in evidence on the Z* gyro pickoff before and after S-IC CECO. Also, spurts of 2.5 hertz at 0.1°P-P were noted on the Z** gyro pickoff just prior to S-II CECO.

The accelerometer servo loops operated properly even though the vibration levels at liftoff were slightly higher than those on IU-508 where a velocity anomaly occurred. As on previous vehicles, the E0009-603 measurement showed a slightly higher burst of vibration at 3.3 seconds. This is the time period where the velocity anomalies occurred on IU-506 and IU-508. As can be seen on Figure 9-7, the Y (crossrange) accelerometer pickoff perturbation was small in this time period.

At CSM separation the accelerometer gyro pickoff deflections were comparable to that of IU-508:

	AS-509	AS-508
X	0.95°P-P	1.0°P-P
Y	2.5°P-P	2.9°P-P
Z	2.5°P-P	2.2°P-P

* On AS-508, this was erroneously reported as being on the X gyro pickoff.
**On AS-508, this was erroneously reported as being on the Y gyro pickoff.

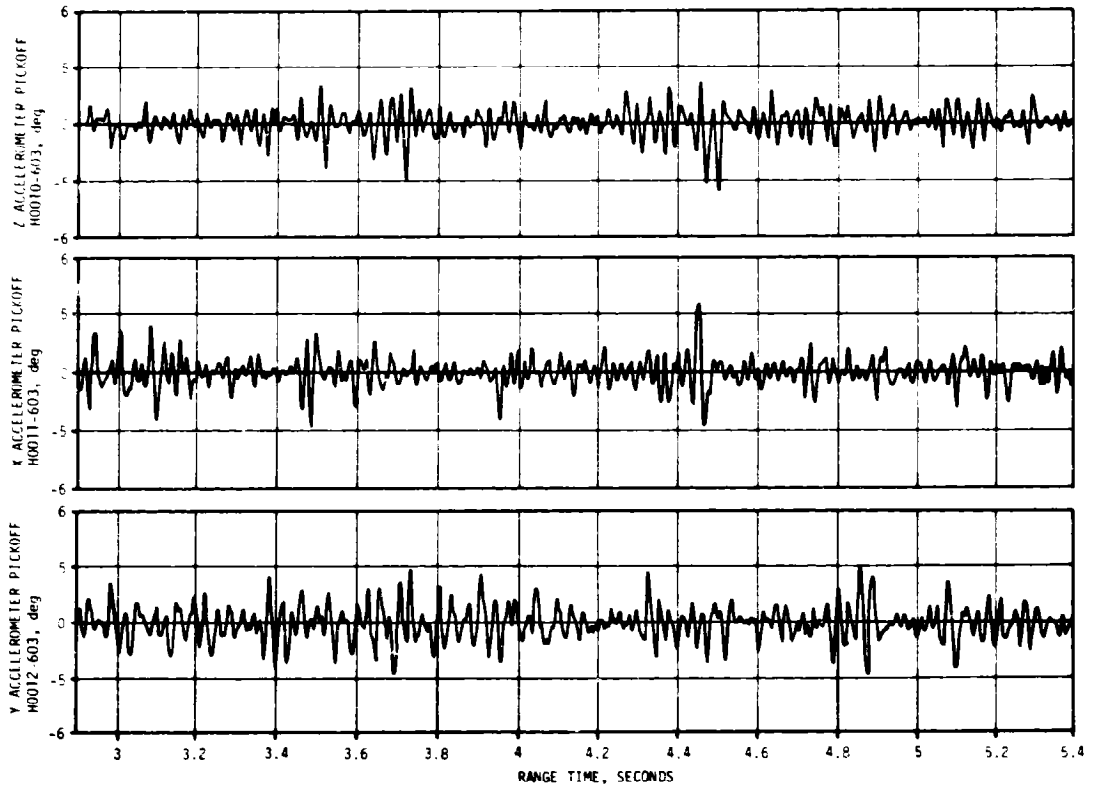

Figure 9-7. Accelerometer Head Deflections

SECTION 10

CONTROL AND SEPARATION

10.1 SUMMARY

The AS-509 control system, which was essentially the same as the AS-508, performed satisfactorily. The Flight Control Computer (FCC), Thrust Vector Control (TVC) System, and Auxiliary Propulsion System (APS) satisfied all requirements for vehicle attitude control during the flight. Bending and slosh dynamics were adequately stabilized. The prelaunch programed yaw, roll, and pitch maneuvers were properly executed during S-IC boost.

During the maximum dynamic pressure region of flight, the launch vehicle experienced winds that were less than 95-percentile January winds. The maximum average pitch and yaw engine deflections were in the maximum dynamic pressure region.

S-IC/S-II first and second plane separations were accomplished with no significant attitude deviations. Related data indicate that the S-IC retromotors performed as expected. At Iterative Guidance Mode (IGM) initiation, a pitchup transient occurred similar to that seen on previous flights. The S-II retromotors and S-IVB ullage motors performed as expected and provided a normal S-II/S-IVB separation.

Satisfactory control of the vehicle was maintained during first and second S-IVB burns and during coast in Earth Parking Orbit (EPO). During the Command and Service Module (CSM) separation from the S-IVB/Instrument Unit (IU) and during the Transposition, Docking, and Ejection (TD&E) maneuver, the control system maintained the vehicle in a fixed inertial attitude to provide a stable docking platform. Following TD&E, S-IVB/IU attitude control was maintained during the evasive maneuver, the maneuver to lunar impact attitude, and the LOX dump and APS burn.

10.2 S-IC CONTROL SYSTEM EVALUATION

The AS-509 control system performed satisfactorily during S-IC powered flight. The vehicle flew through winds which were less than 95 percentile for January in the maximum dynamic pressure region of flight. Less than 10 percent of the available engine deflection was used throughout the flight (based on average engine gimbal angle). The S-IC outboard engines canted as planned.

All dynamics were within vehicle capability. In the region of high dynamic pressure, the maximum angles of attack were approximately 2.6 degrees in pitch and 3.9 degrees in yaw. The maximum average pitch and yaw engine deflections were -0.4 degree and 0.5 degree, respectively, in the maximum dynamic pressure region. Both deflections were due to wind shears. The absence of any divergent bending or slosh dynamics showed that these modes were adequately stabilized.

Vehicle attitude errors required to trim out the effects of thrust unbalance, thrust misalignment, and control system misalignments were within predicted envelopes. Vehicle dynamics prior to S-IC/S-II first plane separation were within staging requirements.

Maximum control parameters during S-IC burn are listed in Table 10-1. Pitch and yaw attitude error time histories are shown in Figure 10-1. Dynamics in the region between liftoff and 40 seconds resulted primarily from guidance commands. In the region between 40 and 110 seconds, maximum dynamics were caused by the pitch tilt program, wind magnitude, and wind shears. Dynamics from 110 seconds to separation were caused by high altitude winds, separated air flow aerodynamics, center engine shutdown, and tilt arrest. The transient at Center Engine Cutoff (CECO) indicates that the center engine cant was 0.23 degree in pitch and 0.15 degree in yaw.

The attitude errors between liftoff and 20 seconds indicate that the equivalent thrust vector misalignments prior to outboard engine cant were -0.02, 0.0, and -0.02 degree in pitch, yaw, and roll, respectively.

Table 10-1. Maximum Control Parameters During S-IC Flight

PARAMETER	PITCH PLANE		YAW PLANE		ROLL PLANE	
	AMPLITUDE	RANGE TIME (SEC)	AMPLITUDE	RANGE TIME (SEC)	AMPLITUDE	RANGE TIME (SEC)
Attitude Error, deg	0.91	95.0	-1.26	4.0	-0.80	14.0
Angular Rate, deg/s	-1.0	83.5	-0.52	80.0	1.2	15.0
Average Gimbal Angle, deg	-0.39	84.5	0.51	76.5		
Angle-of-Attack, deg	2.57	76.8	3.90	76.8		
Angle-of-Attack Dynamic Pressure Product, deg-N/cm^2 (deg-lbf/ft^2)	7.97 (1660)	77.0	12.1 (2530)	77.0		
Normal Acceleration, m/s^2 (ft/s^2)	-0.34 (-1.12)	90.0	0.69 (2.26)	75.5		

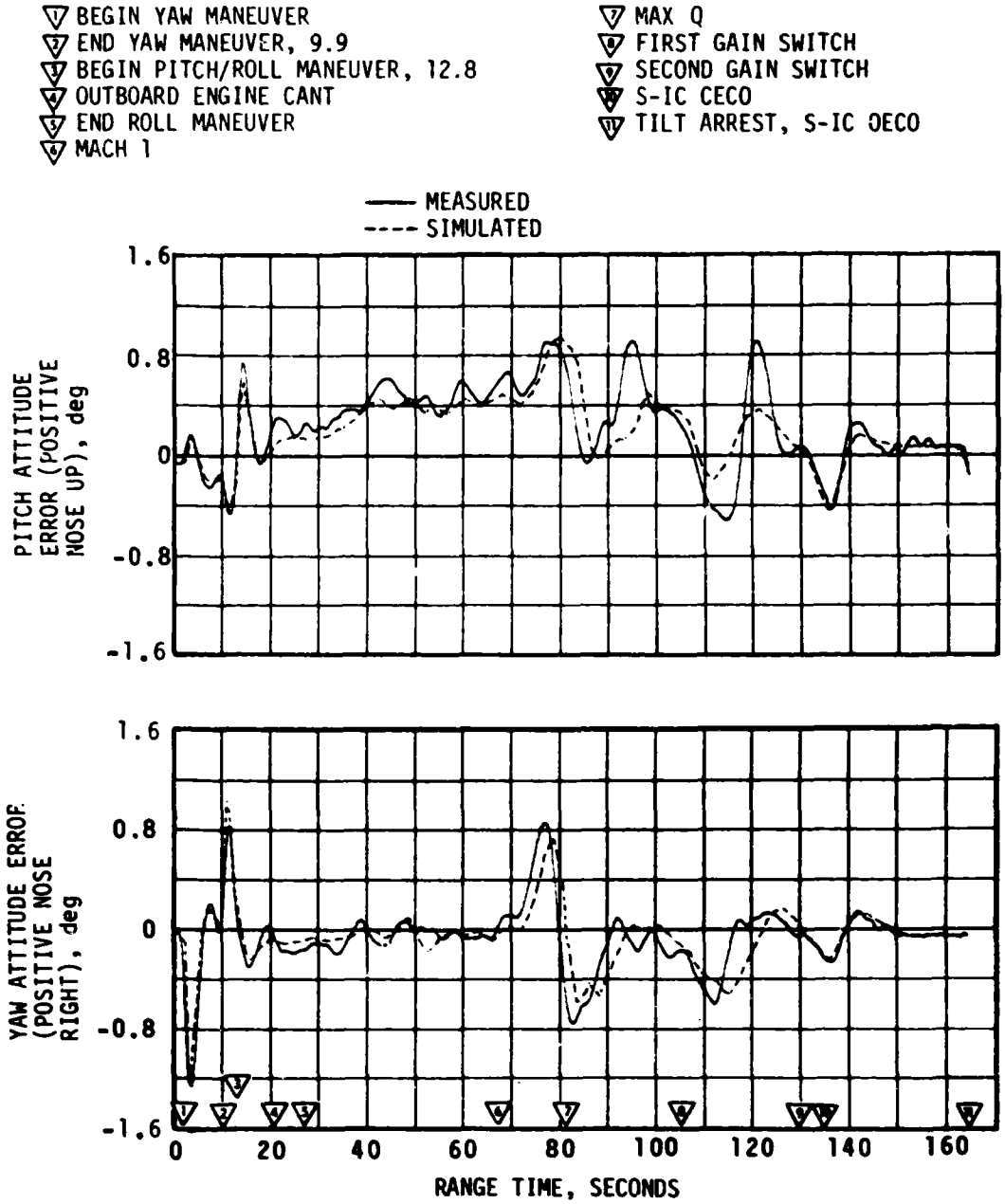

Figure 10-1. Pitch and Yaw Plane Dynamics During S-IC Burn

These errors are required to trim out the effects of thrust unbalance, offset Center-of-Gravity (CG), thrust vector misalignment, and control system misalignments. The equivalent thrust vector misalignments after outboard engine cant were 0.03, 0.01, and 0.01 degree in pitch, yaw, and roll, respectively.

The predicted and measured misalignments, slow release forces, winds, and thrust-to-weight ratio are shown in Table 10-2.

Table 10-2. AS-509 Liftoff Misalignment Summary

PARAMETER	PREFLIGHT PREDICTED			LAUNCH		
	PITCH	YAW	ROLL	PITCH	YAW	ROLL
Thrust Misalignment, deg*	±0.34	±0.34	±0.34	-0.02	0.0	-0.02
Center Engine Cant, deg	-	-	-	0.23	0.15	-
Servo Amp Offset, deg/eng	±0.1	±0.1	±0.1	-	-	-
Vehicle Stacking & Pad Misalignment, deg	±0.29	±0.29	0.0	-0.05	0.05	-0.02
Attitude Error at Holddown Arm Release, deg	-	-		-0.11	0.01	0.01
Peak Soft Release Force Per Rod, N(lbf)	415,900 (93,500)			Data Not Available		
Wind	19.55 m/s (38 knots) at 161.5 meters (530 feet)			8.5 m/s**(16.5 knots) at 161.5 meters (530 feet)		
Thrust to Weight Ratio	1.177			1.213†		

*Thrust misalignment of 0.34 degree encompasses the center engine cant. A positive polarity was used to determine minimum fin tip/umbilical tower clearance. A negative polarity was used to determine vehicle/GSE clearances.
**One minute average about T-0.
†Determined by simulating vehicle rise history recorded by camera during launch.

Because of the DP1-A0 multiplexer data loss reported in paragraph 15.3.2, pitch and yaw angle-of-attack measurements are not available. Figure 10-2 shows the simulated pitch, yaw, and total angles of attack compared to those calculated from postflight trajectory parameters. A total angle-of-attack measurement was available from spacecraft telemetry. This measurement is shown in Figure 10-3. The peak angle-of-attack measured at the Q-Ball during the high dynamic pressure region of flight was 4.76 degrees.

10.3 S-II CONTROL SYSTEM EVALUATION

The S-II stage attitude control system performance was satisfactory. The maximum values of pitch and yaw control parameters occurred in response to IGM Phase 1 initiation. The maximum values of roll control parameters occurred in response to S-IC/S-II separation disturbances. The response at other times was within expectations. The maximum control parameter values for the period of S-II burn are shown in Table 10-3.

Between the events of S-IC Outboard Engine Cutoff (OECO) and initiation of IGM, the attitude commands were held constant. Significant events occurring during that interval were S-IC/S-II separation, S-II stage J-2 engine start, second plane separation, and Launch Escape Tower (LET) jettison. The attitude control dynamics throughout this interval indicated stable operation as shown in Figure 10-4. Steady state attitudes were achieved within 20 seconds of S-IC/S-II separation.

At IGM initiation the FCC received TVC commands to pitch the vehicle up and then down. The transient magnitudes experienced were similar to previous flights.

At S-II CECO the guidance routines reacted properly to the decrease in total thrust. The attitude commands that resulted were similar to nominal CECO conditions except that the magnitudes were somewhat higher (See Figure 10-4). Differences between the two can be accounted for largely by engine location misalignments, thrust vector misalignments, and uncertainties in engine thrust buildup characteristics.

10.4 S-IVB CONTROL SYSTEM EVALUATION

The S-IVB TVC system provided satisfactory pitch and yaw control during powered flight. The APS provided satisfactory roll control during first and second burns.

During S-IVB first and second burns, control system transients were experienced at S-II/S-IVB separation, guidance initiation, Engine Mixture Ratio (EMR) shift, terminal guidance mode, and S-IVB Engine Cutoff (ECO). These transients were expected and were well within the capabilities of the control system.

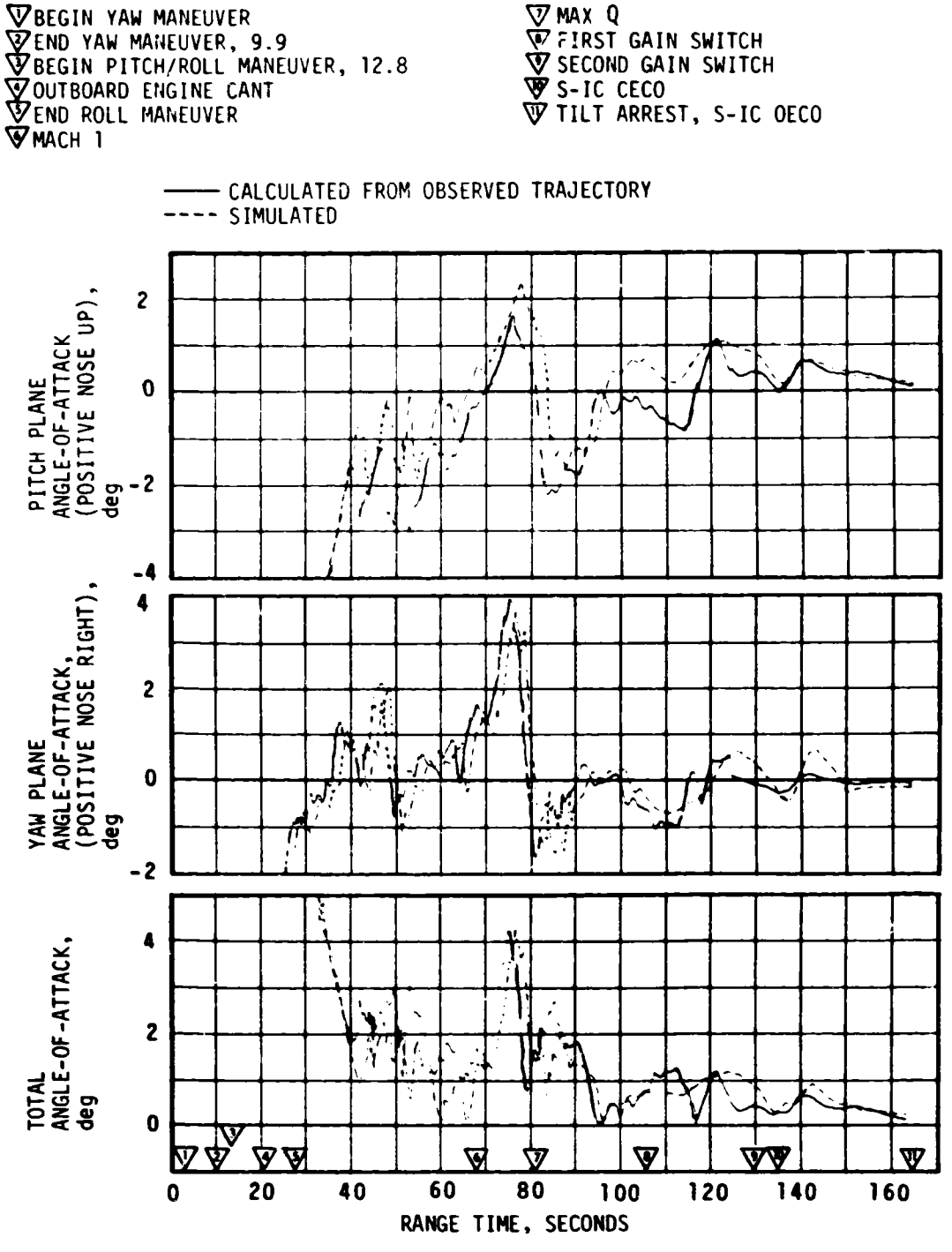

Figure 10-2 Angle-of-Attack During S-IC Burn

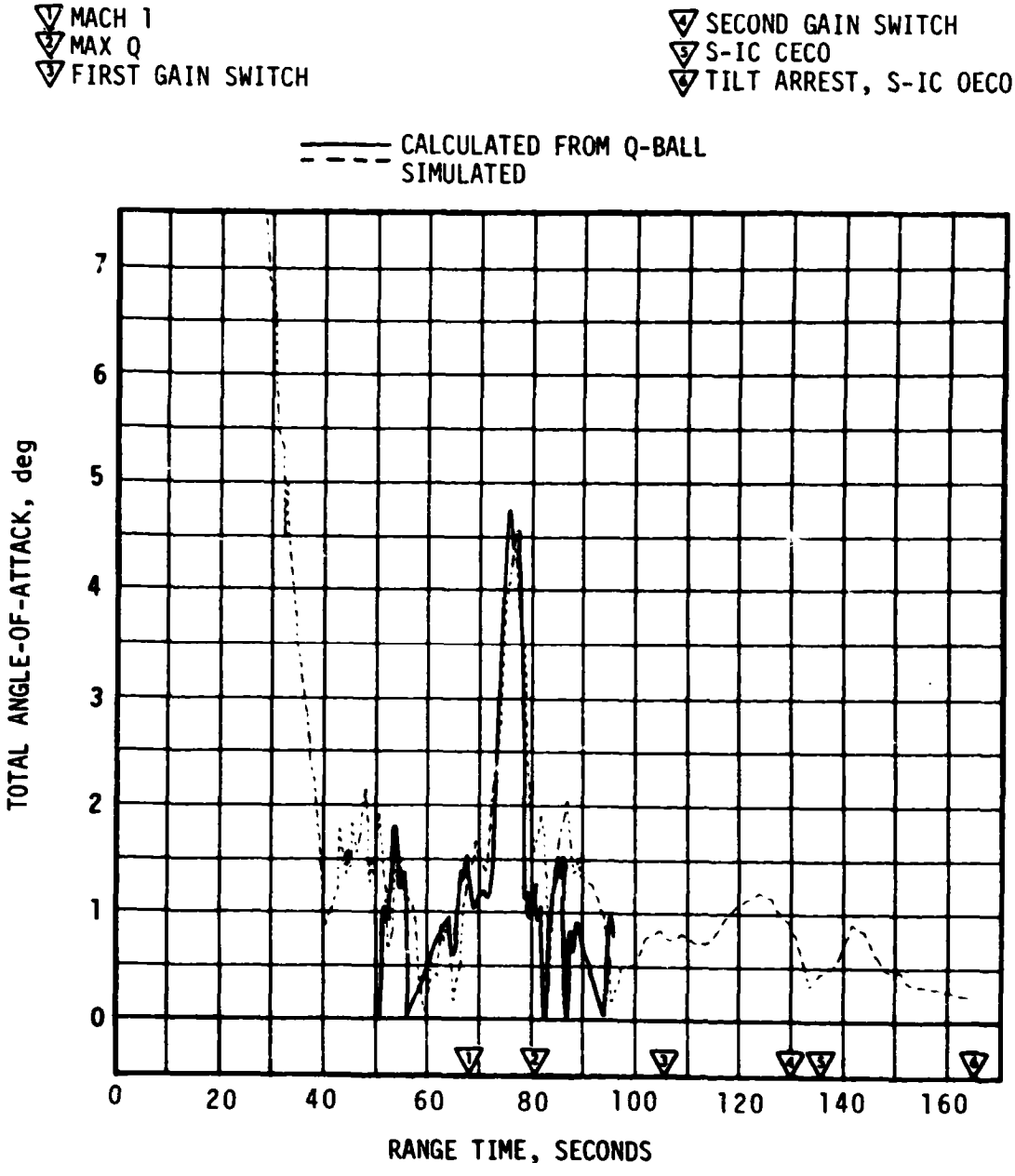

Figure 10-3. Total Angle-of-Attack at Q-Ball

Table 10-3. Maximum Control Parameters During S-II Burn

PARAMETER	PITCH PLANE		YAW PLANE		ROLL PLANE	
	AMPLITUDE	RANGE TIME (SEC)	AMPLITUDE	RANGE TIME (SEC)	AMPLITUDE	RANGE TIME (SEC)
Attitude Error, deg	-2.0	209.0	0.5	207.5	-2.0	168.0
Angular Rate, deg/s	1.1	211.0	-0.2	209.0	2.0	168.7
Average Gimbal Angle. deg	-0.9	207.5	0.3	207.5	-0.6	167.5

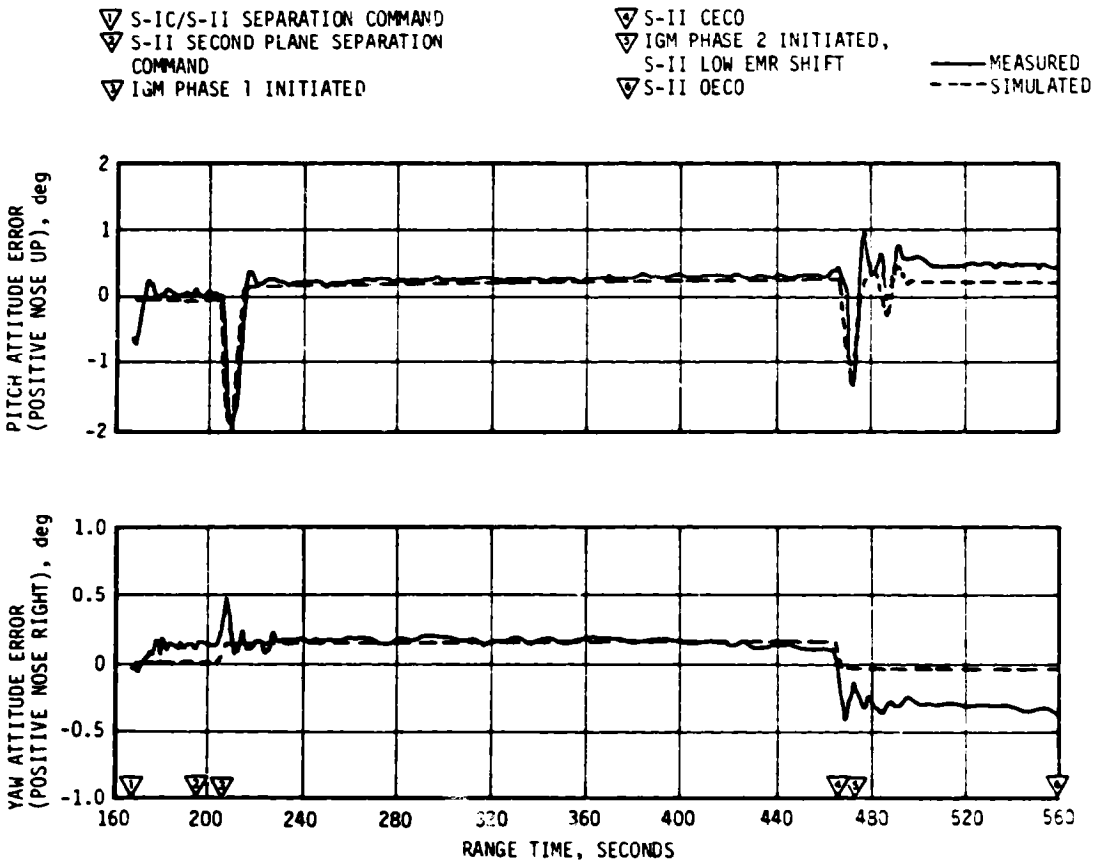

Figure 10-4. Pitch and Yaw Plane Attitude Errors During S-II Burn

10.4.1 Control System Evaluation During First Burn

The S-IVB first burn pitch and yaw attitude errors are presented in Figure 10-5. The maximum attitude errors and rates occurred at IGM initiation. A summary of the first burn maximum values of critical flight control parameters is presented in Table 10-4.

The pitch and yaw effective thrust vector misalignments during first burn were 0.30 and -0.27 degree, respectively. As experienced on previous flights, a steady-state roll torque of 36.8 N-m (27.2 lbf-ft), counterclockwise looking forward, required roll APS firings during first burn. The steady-state roll torque experienced on previous flights has ranged between 61.4 N-m (45.3 lbf-ft) counterclockwise and 54.2 N-m (40.0 lbf-ft) clockwise.

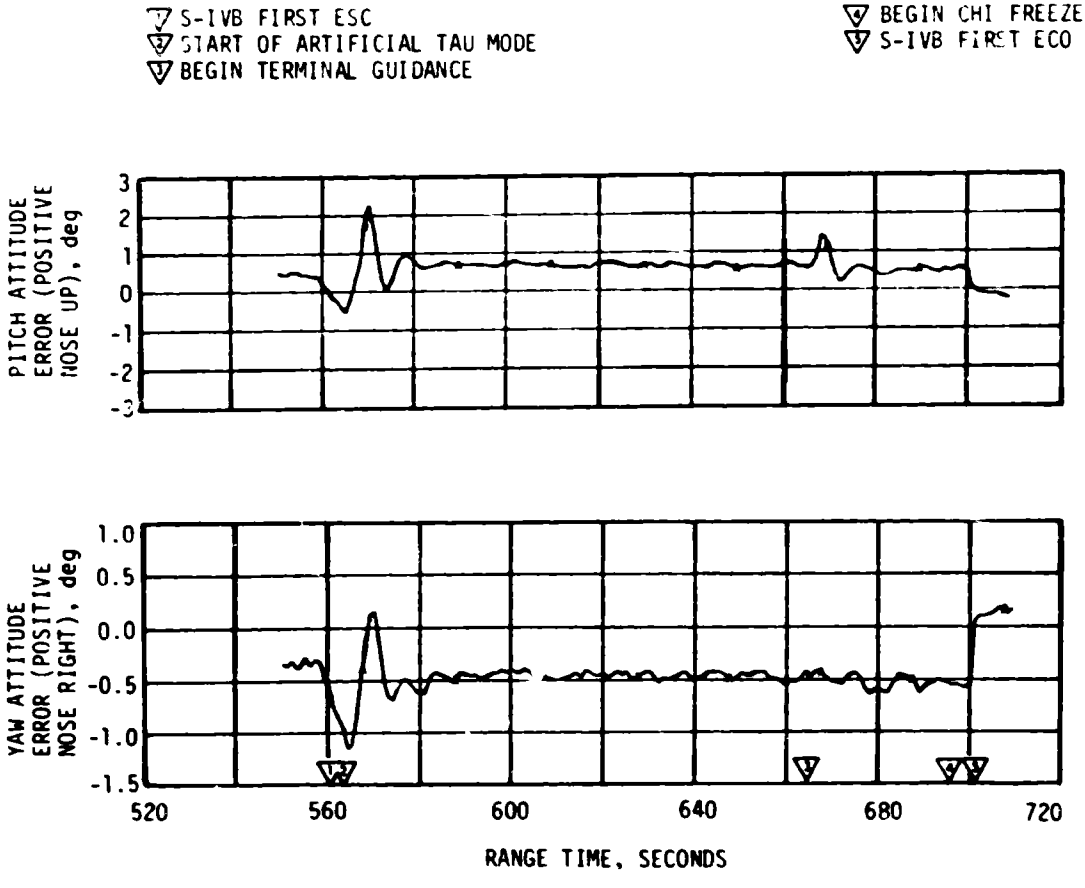

Figure 10-5. Pitch and Yaw Attitude Errors During S-IVB First Burn

Table 10-4. Maximum Control Parameters During S-IVB First Burn

PARAMETER	PITCH PLANE		YAW PLANE		ROLL PLANE	
	AMPLITUDE	RANGE TIME (SEC)	AMPLITUDE	RANGE TIME (SEC)	AMPLITUDE	RANGE TIME (SEC)
Attitude Error, deg	2.34	570.1	-1.22	564.4	-0.77	568.8
Angular Rate, deg/s	-1.05	571.3	0.47	567.0	0.45	560.2
Maximum Gimbal Angle, deg	1.36	569.7	-1.2	564.3	-	-

Propellant sloshing during first burn was observed on data obtained from the Propellant Utilization (PU) mass probe sensors. The propellant slosh did not have any noticeable effect on the operation of the attitude control system.

10.4.2 Control System Evaluation During Parking Orbit

The APS provided satisfactory orientation and stabilization during parking orbit. Following S-IVB first ECO, the vehicle was maneuvered to the inplane local horizontal and the orbital pitch rate was established. The pitch attitude error for parking orbit is shown in Figure 10-6.

10.4.3 Control System Evaluation During Second Burn

The S-IVB second burn pitch and yaw attitude errors are presented in Figure 10-7. The maximum attitude errors and rates occurred at IGM initiation. A summary of the second burn maximum values of critical flight control parameters is presented in Table 10-5. Control system attitude error transients resulted from pitch and yaw attitude commands at the termination of the artificial Tau guidance mode (EMR shift plus 30 seconds).

The pitch and yaw effective thrust vector misalignments during second burn were approximately 0.43 and -0.29 degree, respectively. The steady-state roll torque during second burn ranged from 36.6 N-m (27.0 lbf-ft), counterclockwise looking forward, at the low EMR to 29.6 N-m (21.8 lbf-ft) at the 5.0:1.0 EMR.

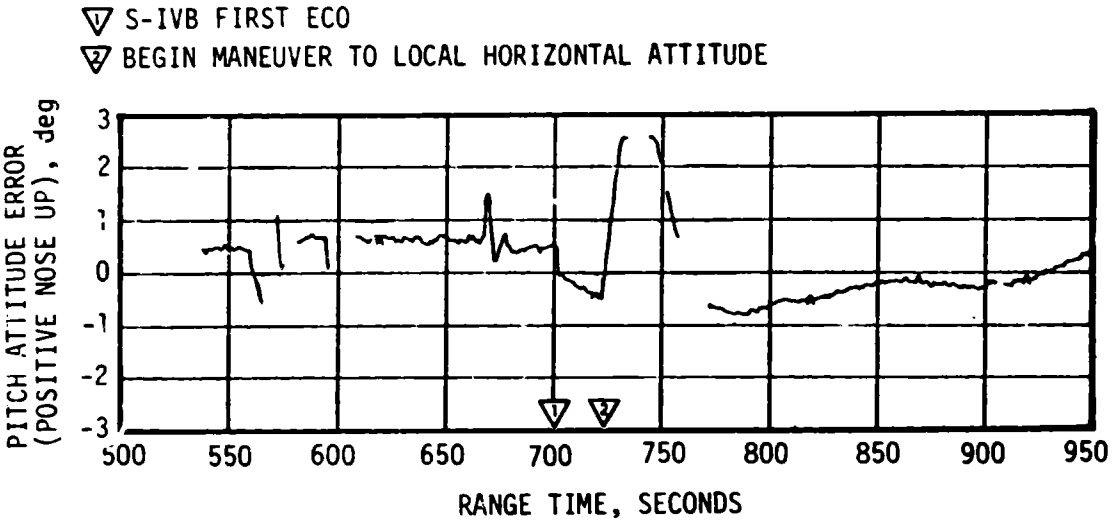

Figure 10-6. Pitch Attitude Error During Parking Orbit

Propellant sloshing during second burn was observed on data obtained from the PU mass probe sensors. The propellant slosh did not have any noticeable effect on the operation of the attitude control system.

10.4.4 Control System Evaluation After S-IVB Second Burn

The APS provided satisfactory orientation and stabilization from Translunar Injection (TLI) through the S-IVB/IU Passive Thermal Control Maneuver ("Barbecue Maneuver"). Each of the planned maneuvers was performed satisfactorily although the maneuvers after spacecraft separation were delayed due to the delay in spacecraft docking. Effects of the delay in docking on attitude control is discussed below. Effects of telemetry data loss on evaluation of attitude control is also discussed below.

Significant periods of interest related to translunar coast attitude control were the maneuver to the inplane local horizontal following second ECO, the maneuver to the TD&E attitude, spacecraft separation, spacecraft docking, Lunar Module (LM) ejection, the maneuver to the evasive ullage burn attitude, the maneuver to the LOX dump attitude, the maneuver to the lunar impact ullage burn attitude, and the "Barbecue Maneuver." The pitch attitude error for events during which telemetry data were available is shown in Figure 10-8.

Following S-IVB second ECO, control response to the maneuver to the inplane local horizontal and the maneuver to the separation TD&E attitude was nominal.

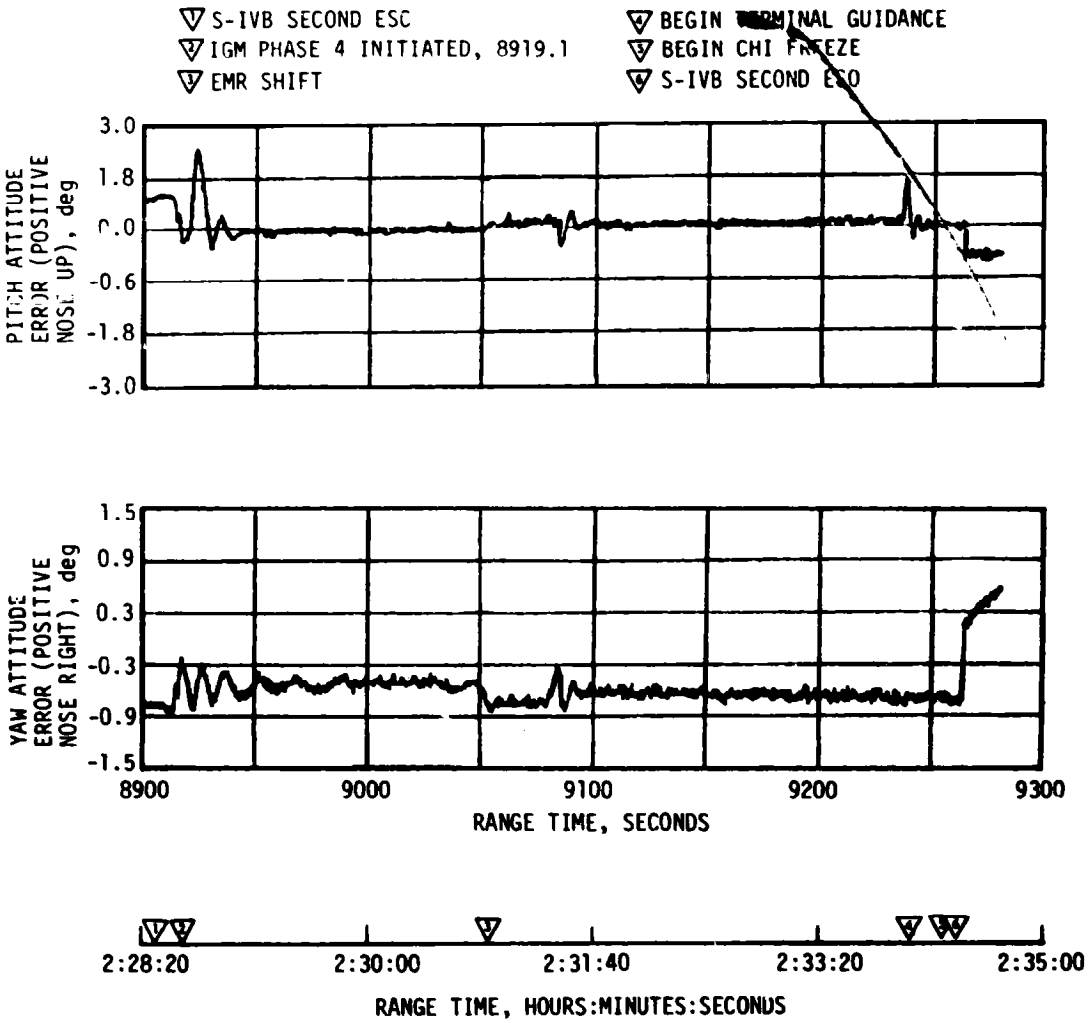

Figure 10-7. Pitch and Yaw Attitude Errors During S-IVB Second Burn

Spacecraft separation, which occurred at 10,949.4 seconds (03:02:29.4), appeared normal, as indicated by the relatively small disturbances induced on the S-IVB.

At 10,955.9 seconds (03:02:35.9) the loss of H0060-603 data (as discussed in paragraph 15.3.3) prevented the further monitoring of vehicle attitude angles and guidance commands. Vehicle orientation and stabilization was monitored by vehicle attitude errors, vehicle angular rates, and spacecraft observation.

Table 10-5. Maximum Control Parameters During S-IVB Second Burn

PARAMETER	PITCH PLANE		YAW PLANE		ROLL PLANE	
	AMPLITUDE	RANGE TIME (SEC)	AMPLITUDE	RANGE TIME (SEC)	AMPLITUDE	RANGE TIME (SEC)
Attitude Error, deg	2.4	8923.7	-0.85	8911.3	0.75	8989.5
Angular Rate, deg/s	-1.4	8926.0	0.35	8924.0	0.16	8990.0
Maximum Gimbal Angle, deg	1.34	8923.2	-0.76	8913.2	-	-

Nominal APS engine firings were noted during three docking attempts; 11,690 seconds (03:14:50), 12,220 seconds (03:23:40), and 16,340 seconds (04:32:20).

S-IVB VHF telemetry data were available to 13,655 seconds (03:47:35). The lack of available data after this time resulted in the loss of attitude error data, angular rate data, and APS chamber pressure data. The APS control relay operation continued to be telemetered via the DP1-B0 multiplexer.

The reaction to spacecraft docking, which occurred at 17,816 seconds (04:56:56), appeared to be normal. Yaw-roll disturbances were slightly larger than those experienced on previous flights. LM ejection occurred at 20,834.4 seconds (05:47:14.4) with nominal disturbances.

At 21,330 seconds (05:55:30), a maneuver was initiated to attain the desired attitude for the evasive ullage burn. This involved maneuvering from the TD&E yaw attitude of -40.9 degrees to +40.0 degrees. At 21,842 seconds (06:04:02), the APS ullage engines were commanded on for 80 seconds to provide the necessary separation distance between the S-IVB/IU and the spacecraft.

The maneuver to the LOX dump attitude was performed at 22,423 seconds (06:13:43) and appeared to be nominal. LOX dump occurred at 23,120 seconds (06:25:20) and lasted for 48 seconds.

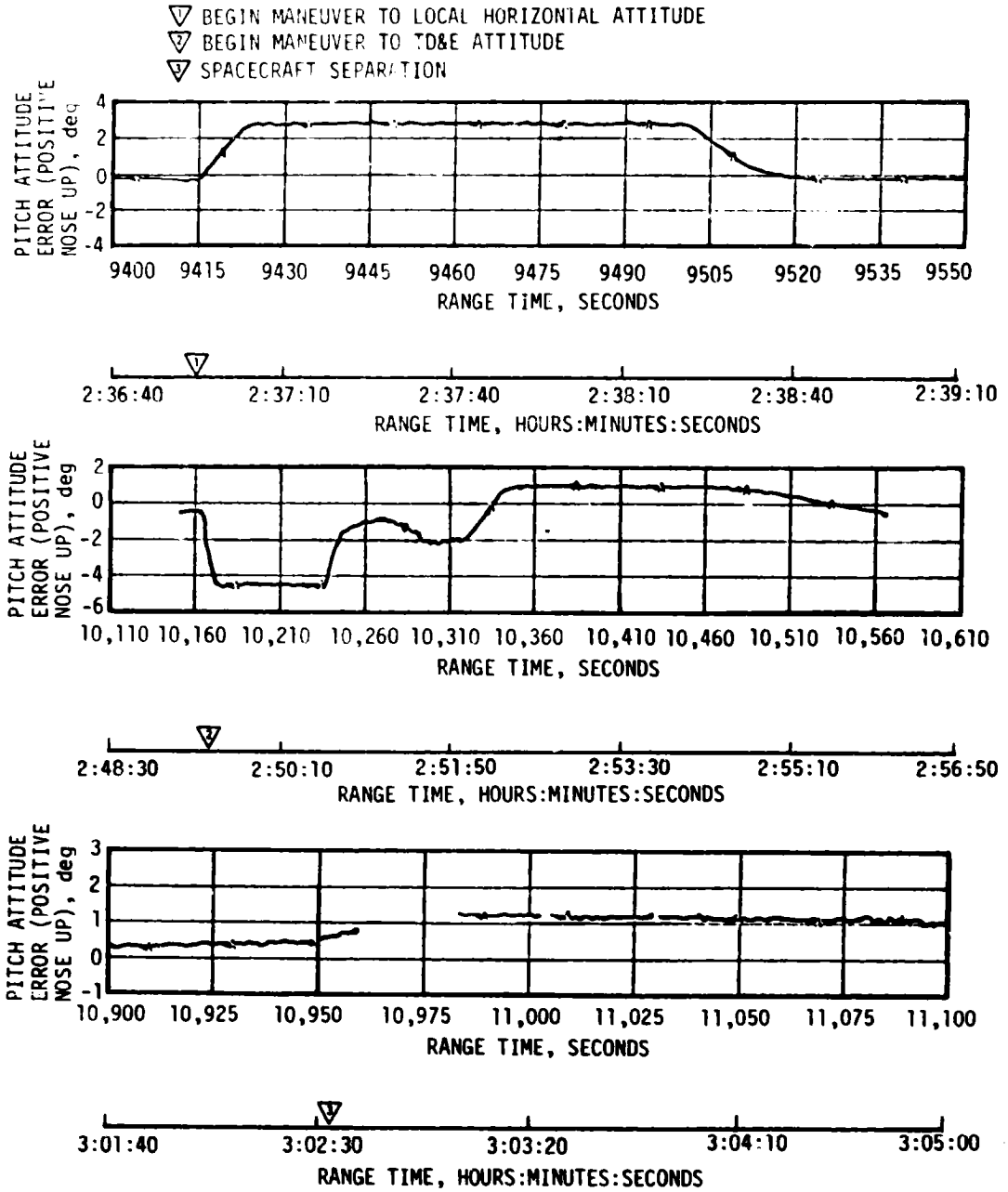

Figure 10-8. Pitch Attitude Error During Translunar Coast

At 31,421 seconds (08:43:41), a ground command was sent to perform a maneuver to the desired attitude for the APS ullage burn for lunar target impact. This was a two-axis maneuver and resulted in a pitch maneuver of -3.0 degrees and a yaw attitude maneuver of -4.0 degrees. At 32,399 seconds (08:59:59), the APS ullage engines were commanded on for 252 seconds to provide ΔV for lunar target impact.

At 42,082 seconds (11:41:22), the S-IVB was commanded via Digital Command System (DCS) to maneuver in the negative pitch and positive yaw directions and establish corresponding rates of 0.3 deg/s. Following initiation of the maneuver, a DCS command was issued at 42,116 seconds (11:41:56) to inhibit the FCC leaving the S-IVB/IU in a "Barbecue" or tumble mode until lunar impact.

APS propellant consumption for attitude control and propellant settling prior to the APS burn for lunar target impact was slightly higher than the mean predicted requirements. The total propellant (fuel and oxidizer) used prior to the ullage burn for lunar impact ΔV was 59.8 kilograms (131.9 lbm) and 59.1 kilograms (130.0 lbm) for Modules 1 and 2, respectively. This was 40.0 and 39.5 percent of the total available in each module (approximately 150.0 kilogram [330.1 lbm]). APS propellant consumption is tabulated in Section 7, Table 7-4.

10.5 INSTRUMENT UNIT CONTROL COMPONENTS EVALUATION

The Flight Program Minor Loop implemented all guidance commands, providing satisfactory attitude error outputs through the Launch Vehicle Data Adapter (LVDA) to the FCC. No Minor Loop Error Telemetry occurred during the mission. The FCC and control rate gyros functioned predictably and satisfactorily throughout the mission.

10.6 SEPARATION

S-IC/S-II separation and associated sequencing was accomplished as planned. S-IC end conditions at separation fell within estimated limits, and well within the staging limits. The AS-509 measured longitudinal acceleration of the S-IC dropped stage was similar to previous vehicles. Pitch and yaw rate measurements showed no disturbances, indicating normal staging.

Second plane separation occurred as predicted. There were no vehicle attitude disturbances attributed to the second plane separation. Calculations indicate that the separation dynamics were similar to previous flights.

S-II/S-IVB separation was normal with nominal S-II retromotor and S-IVB ullage motor performance. Vehicle dynamics were well within staging limits.

Vehicle dynamics were normal during CSM separation and the TD&E maneuver. The vehicle maintained a stable docking platform during the several docking attempts.

SECTION 11

ELECTRICAL NETWORKS AND EMERGENCY DETECTION SYSTEM

11.1 SUMMARY

The AS-509 launch vehicle electrical systems and Emergency Detection System (EDS) performed satisfactorily throughout all phases of flight. Operation of the batteries, power supplies, inverters, Exploding Bridge Wire (EBW) firing units and switch selectors was normal.

11.2 S-IC STAGE ELECTRICAL SYSTEM

The S-IC stage electrical system performance was satisfactory. Battery voltages were within performance limits of 26.5 to 32.0 vdc during powered flight. The battery currents were near predicted and below the maximum limits of 50 amperes for each battery. Battery power consumption was within the rated capacity of each battery, as shown in Table 11-1.

The two measuring power supplies were within the 5 ±0.05 vdc limit during powered flight.

Table 11-1. S-IC Stage Battery Power Consumption

BATTERY	BUS DESIGNATION	RATED CAPACITY (AMP-MIN)	POWER CONSUMPTION*	
			AMP-MIN	PERCENT OF CAPACITY
Operational	1D10	500	28.5	5.7
Instrumentation	1D20	500	84.5	16.9

* Battery power consumptions were calculated from power transfer until S-IC/S-II separation.

All switch selector channels functioned as commanded by the Instrument Unit (IU) and were within required time limits.

The separation and retromotor EBW firing units were armed and triggered as programed. Charging time and voltage characteristics were within performance limits.

The range safety command system EBW firing units were in the required state-of-readiness if vehicle destruct had been necessary.

11.3 S-II STAGE ELECTRICAL SYSTEM

The S-II stage electrical system performed satisfactorily. Battery voltages remained within specified limits through the prelaunch and flight periods. Bus currents also remained within required and predicted limits. Main bus current averaged 37 amperes during S-IC boost and varied from 48 to 53 amperes during S-II boost. Instrumentation bus current averaged 21 amperes during S-IC and S-II boost. Recirculation bus current averaged 90 amperes during S-IC boost. Ignition bus current averaged 30 amperes during the S-II ignition sequence. Battery power consumption was within the rated capacity of each battery, as shown in Table 11-2.

The five temperature bridge power supplies, the three instrumentation power supplies, and the five LH_2 inverters all performed within acceptable limits.

All switch selector channels functioned as commanded by the IU and were within required time limits.

Table 11-2. S-II Stage Battery Power Consumption

BATTERY	BUS DESIGNATION	RATED CAPACITY (AMP-HR)	POWER CONSUMPTION*		TEMPERATURE(°F)	
			AMP-HR	PERCENT OF CAPACITY	MAX	MIN
Main	2D11	35	14.58	41.7	94.0	87.0
Instrumentation	2D21	35	9.86	28.2	86.0	82.0
Recirculation No. 1	2D51	30	12.23	40.8	87.0	81.0
Recirculation No. 2	2D51 and 2D61	30	12.27	40.9	84.0	78.0

*Battery power consumptions were calculated from activation until S-II/S-IVB separation and include 6.1 AMP-HR consumed during the battery activation procedure.

Performance of the EBW circuitry for the separation systems was satisfactory. Firing units charge and discharge responses were within predicted time and voltage limits. The range safety command system EBW firing units were in the required state-of-readiness if vehicle destruct had been necessary.

11.4 S-IVB STAGE ELECTRICAL SYSTEM

The S-IVB stage electrical system performance was satisfactory. The battery voltages, currents, and temperatures remained within the normal range beyond the required battery lifetime. Forward No. 2 battery depleted at 30,560 seconds (08:29:20) after supplying 111.2 percent of the rated capacity. Battery voltage and currents are shown in Figures 11-1 through 11-4. Battery power consumption and capacity for each battery are shown in Table 11-3.

The three 5-vdc and seven 20-vdc excitation modules all performed within acceptable limits. The LOX and LH_2 chilldown inverters performed satisfactorily.

All switch selector channels functioned as commanded by the IU and were within required time limits.

Performance of the EBW circuitry for the separation system was satisfactory. Firing units charge and discharge responses were within predicted time and voltage limits. The range safety command system EBW firing units were in the required state-of-readiness if vehicle destruct had been necessary.

11.5 INSTRUMENT UNIT ELECTRICAL SYSTEM

The evaluation of the IU electrical system on AS-509 was accomplished using CP-1 telemetry data, since the normally used DP1-A0 data were lost as discussed in paragraph 15.3.2. Analysis of these data indicates that the electrical system functioned normally. Available data extend through 13,655 seconds (03:47:35) of the flight. All battery voltages increased gradually from liftoff, but remained within the required limits. Battery currents remained within the predicted range. Loss of the DP1-A0 data precluded evaluation of the 6D10, 6D30 and 6D40 battery temperatures. However, the 6D20 battery temperature measurement indicated a stable temperature condition. Available battery voltage, current, and temperature plots are shown in Figures 11-5 through 11-8. Battery power consumption and capacity for each battery are shown in Table 11-4.

Based on analysis of CP-1 data, all indications are that the 56-vdc power supply functioned within predicted limits.

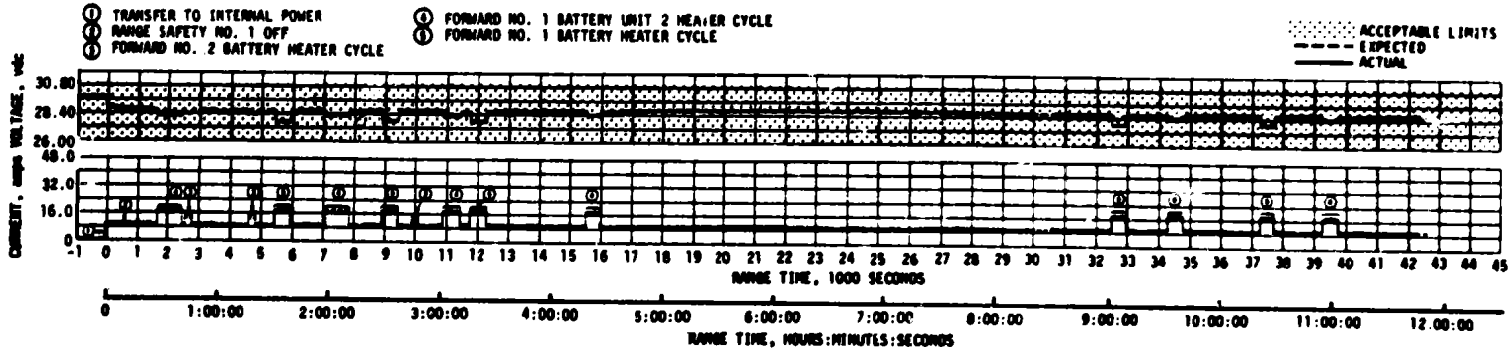
① TRANSFER TO INTERNAL POWER
② RANGE SAFETY NO. 1 OFF
③ FORWARD NO. 2 BATTERY HEATER CYCLE
④ FORWARD NO. 1 BATTERY UNIT 2 HEATER CYCLE
⑤ FORWARD NO. 1 BATTERY HEATER CYCLE
ACCEPTABLE LIMITS
EXPECTED
ACTUAL
CURRENT, amps VOLTAGE, vdc
30.80
28.40
26.00
48.0
32.0
16.0
0
-1 0 1 2 3 4 5 6 7 8 9 10 11 12 13 14 15 16 17 18 19 20 21 22 23 24 25 26 27 28 29 30 31 32 33 34 35 36 37 38 39 40 41 42 43 44 45
RANGE TIME, 1000 SECONDS
0 1:00:00 2:00:00 3:00:00 4:00:00 5:00:00 6:00:00 7:00:00 8:00:00 9:00:00 10:00:00 11:00:00 12:00:00
RANGE TIME, HOURS:MINUTES:SECONDS

Figure 11-1. S-IVB Stage Forward No. 1 Battery Voltage and Current

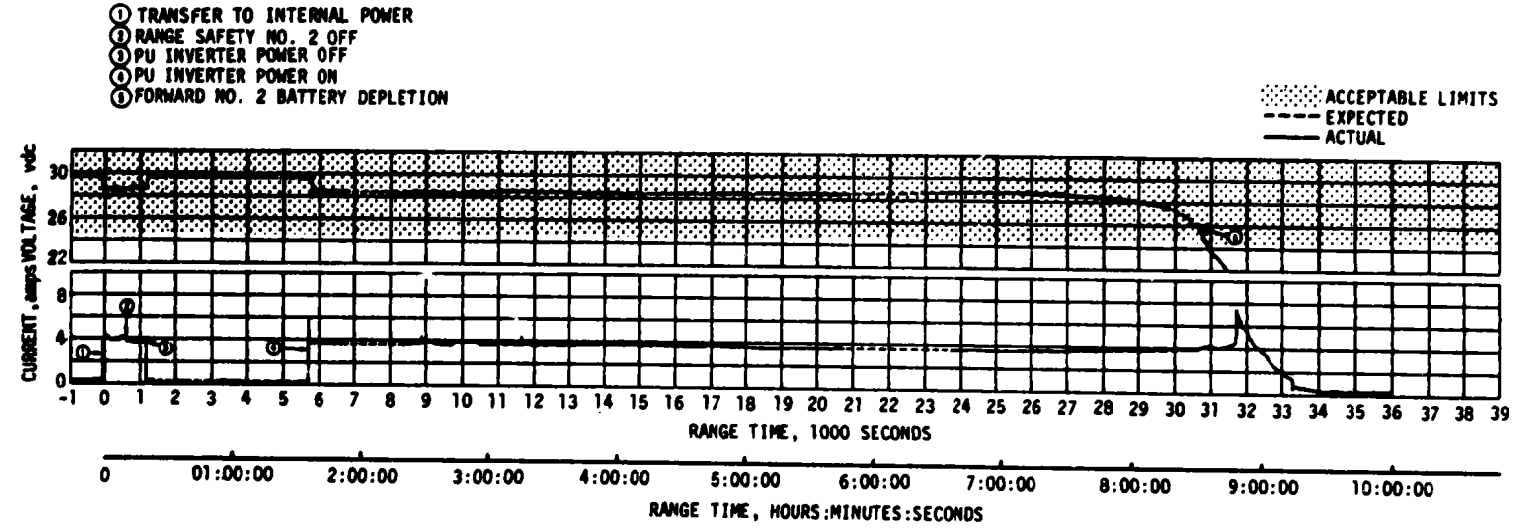
① TRANSFER TO INTERNAL POWER
② RANGE SAFETY NO. 2 OFF
③ PU INVERTER POWER OFF
④ PU INVERTER POWER ON
⑤ FORWARD NO. 2 BATTERY DEPLETION
ACCEPTABLE LIMITS
EXPECTED
ACTUAL
CURRENT, amps VOLTAGE, vdc
30
26
22
8
4
0
-1 0 1 2 3 4 5 6 7 8 9 10 11 12 13 14 15 16 17 18 19 20 21 22 23 24 25 26 27 28 29 30 31 32 33 34 35 36 37 38 39
RANGE TIME, 1000 SECONDS
0 01:00:00 2:00:00 3:00:00 4:00:00 5:00:00 6:00:00 7:00:00 8:00:00 9:00:00 10:00:00
RANGE TIME, HOURS:MINUTES:SECONDS

Figure 11-2. S-IVB Stage Forward No. 2 Battery Voltage and Current

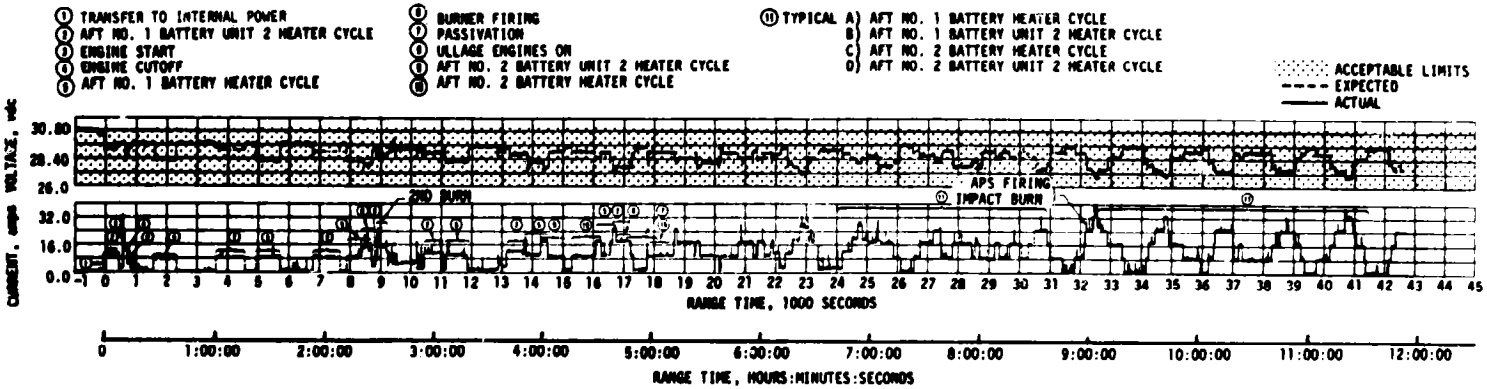

Figure 11-3. S-IVB Stage Aft No. 1 Battery Voltage and Current

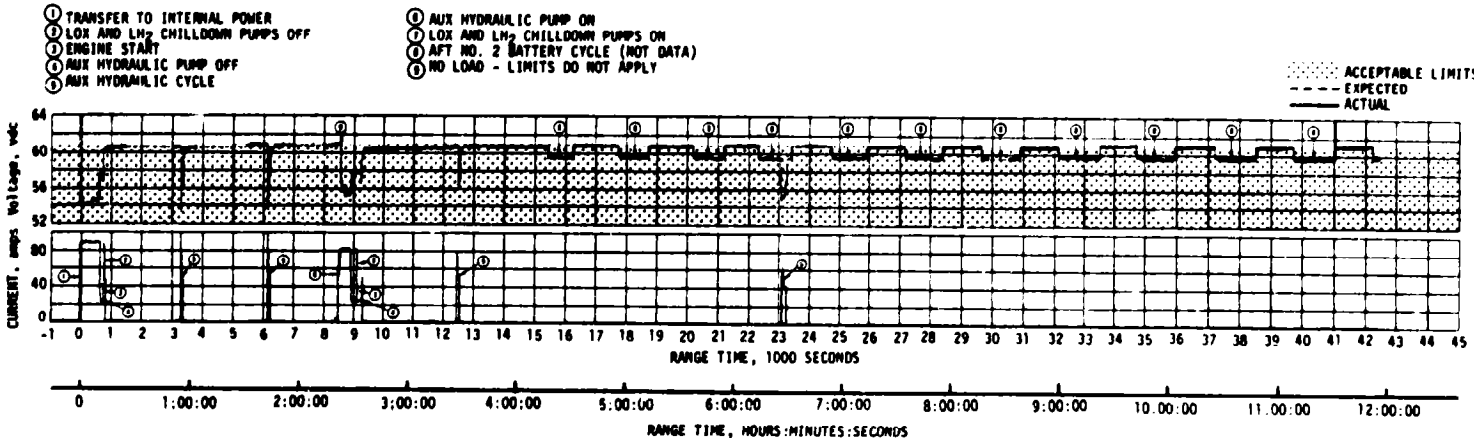

Figure 11-4. S-IVB Stage Aft No. 2 Battery Voltage and Current

Table 11-3. S-IVB Stage Battery Power Consumption

BATTERY	RATED CAPACITY (AMP-HR)	POWER CONSUMPTION	
		AMP-HR*	PERCENT OF CAPACITY
Forward No. 1	300.0	150.26	50.1
Forward No. 2	24.75	27.53**	111.2
Aft No. 1	300.0	147.02	49.0
Aft No. 2	75.0	40.12	53.5

*Actual usage to 43,000 seconds (11:56:40) is based on flight data.
**The battery voltage fell below the defined depletion level of 26.0 volts at 30,560 seconds (08:29:20). Calculations of actual power consumption was terminated at this time.

The 5-vdc measuring power supply appeared to function properly based on the CP-1 data available for analysis. A pertubation of the 5-volt bus at liftoff was noted during the DP-1 link investigation, but it is not presently believed that a problem exists in the 5-vdc measuring power supply.

Available data indicate that all switch selector channels functioned as commanded by the Launch Vehicle Digital Computer (LVDC) and were within required time limits.

11.6 SATURN V EMERGENCY DETECTION SYSTEM (EDS)

The performance of the AS-509 EDS was normal and no abort limits were exceeded. All switch selector events associated with EDS for which data are available were issued at the nominal times. The discrete indications for EDS events also functioned normally. The performance of all thrust OK pressure switches and associated voting logic, which monitors engine status, was nominal insofar as EDS operation was concerned. S-II and S-IVB tank ullage pressures remained within the abort limits and displays to the crew were normal.

The maximum angle-of-attack dynamic pressure sensed by the Q-ball was 1.28 psid at 75.6 seconds. This pressure was only 40 percent of the EDS abort limit of 3.2 psid.

As noted in Section 10, none of the rate gyros gave any indication of angular overrate in the pitch, yaw or roll axis. The maximum angular rates were well below the abort limits.

Table 11-4. IU Battery Power Consumption

BATTERY	RATED CAPACITY (AMP-HR)	POWER CONSUMPTION	
		AMP-HR*	PERCENT OF CAPACITY
6D10	350	69.2	19.8
6D20	350	338.8**	96.8**
6D30	350	80.6	23.0
6D40	350	121.6	34.7

*Actual usage to 13,655 seconds (03:47:35) is based on flight data.
**The CCS transponder which was powered by the 6D20 battery was operating at S-IVB/IU lunar impact which occurred at 297,473.4 seconds (82:37:53.4). Power consumption until S-IVB/IU lunar impact was calculated based on nominal operation.

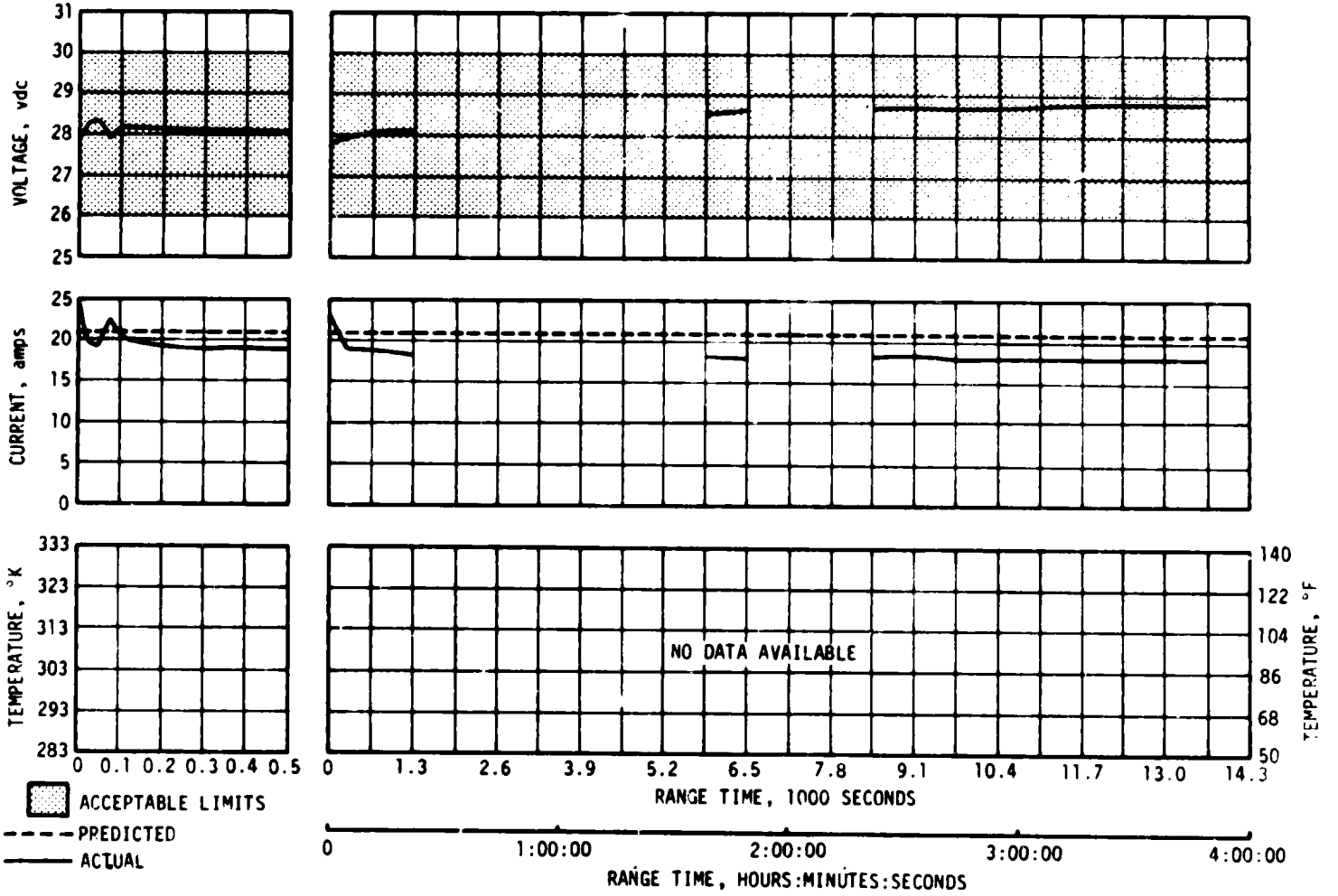

Figure 11-5. IU Battery 6D10 Voltage, Current, and Temperature

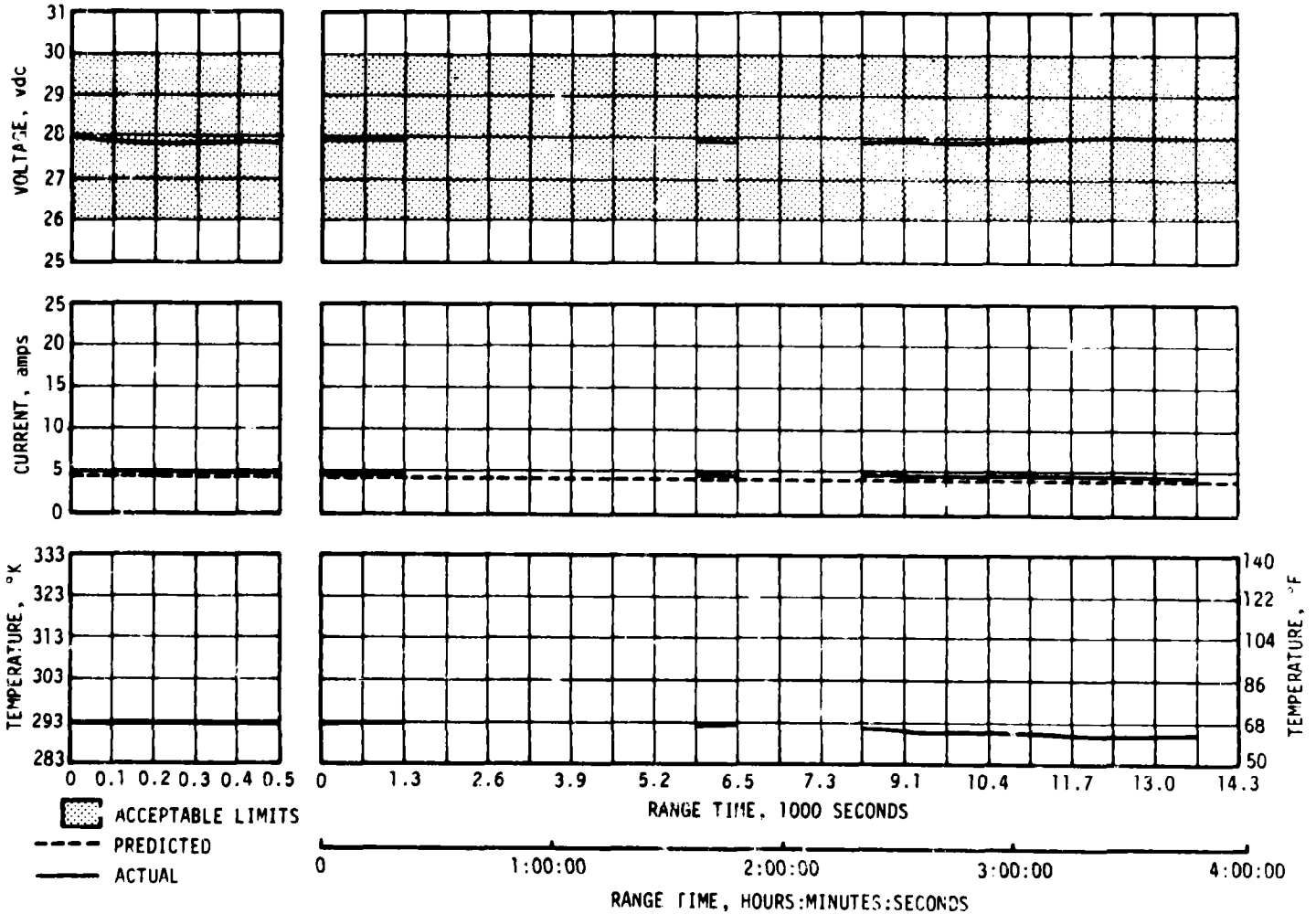

Figure 11-6. IU Battery 6D20 Voltage, Current, and Temperature

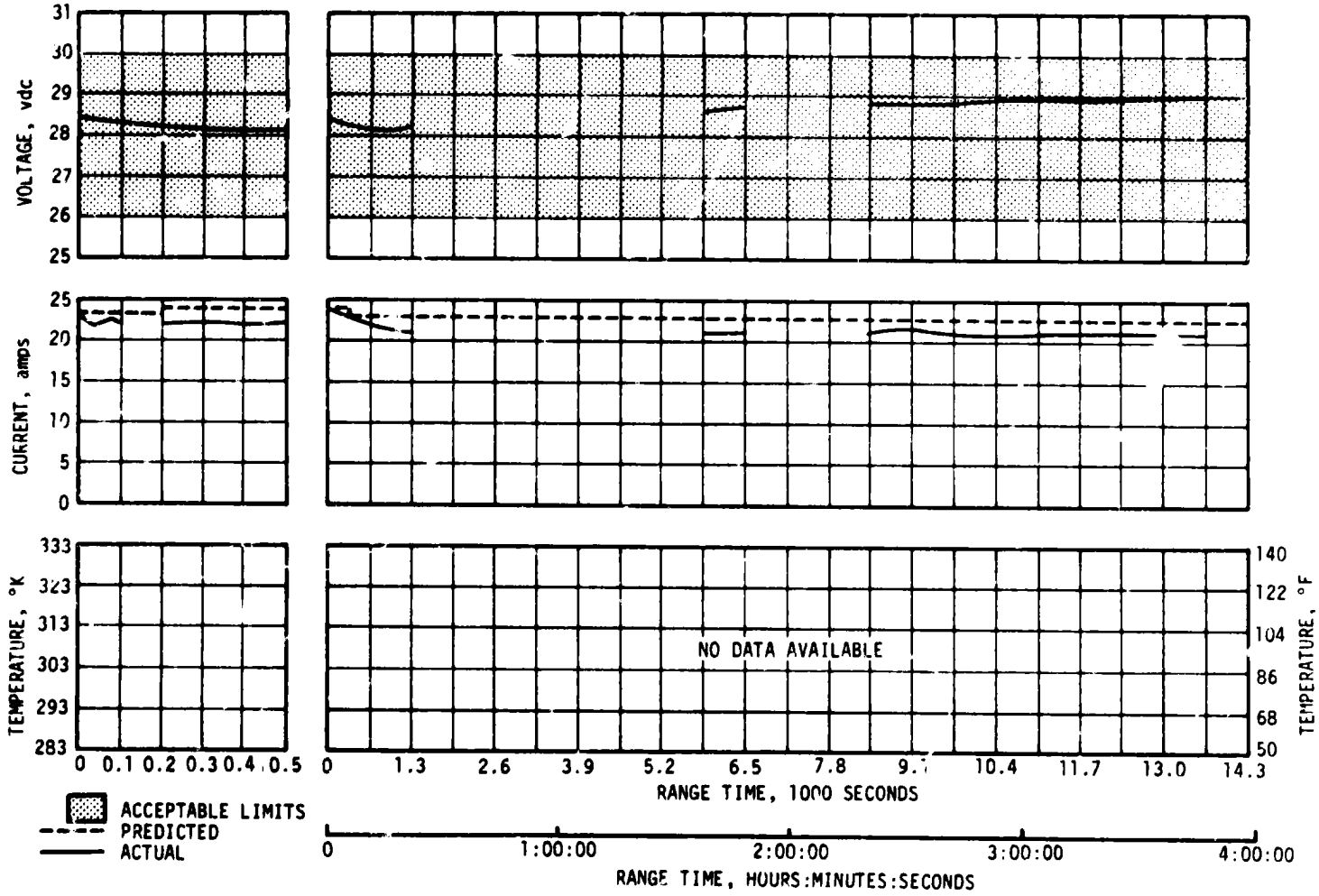

Figure 11-7. IU Battery 6D30 Voltage, Current, and Temperature

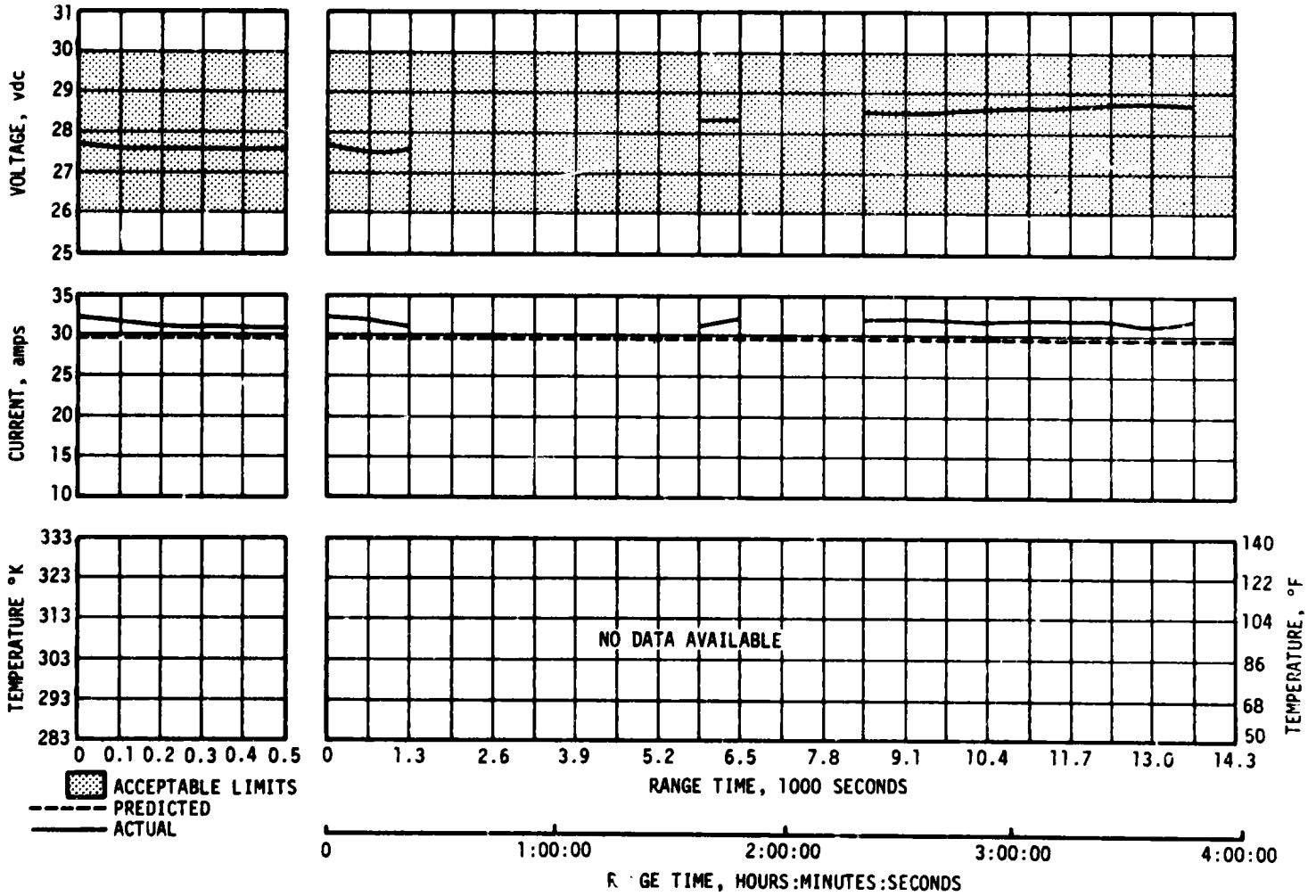

Figure 11-8. IU Battery 6D40 Voltage, Current, and Temperature

SECTION 12

VEHICLE PRESSURE ENVIRONMENT

12.1 SUMMARY

The S-IC base heat shield was instrumented with two differential pressure measurements. The AS-509 flight data have trends and magnitudes similar to those seen on previous flights.

The AS-509 S-II base pressure environments are consistent with the trends and magnitudes seen on previous flights.

12.2 BASE PRESSURES

12.2.1 S-IC Base Pressures

The S-IC base heat shield was instrumented with two differential (internal minus external) pressure measurements. The AS-509 flight data, Figure 12-1, show good agreement with previous flight data with similar trends and magnitudes. The maximum differential pressure of approximately 0.17 psid occurred at an altitude of approximately 5.4 n mi.

12.2.2 S-II Base Pressures

The S-II stage base heat shield forward face pressures are presented in Figure 12-2 together with the postflight analytical values and the data band from previous flights. The AS-509 data compare favorably with previous flight data prior to interstage separation, but were slightly lower following separation than on previous flights.

The AS-509 thrust cone static pressure data presented in Figure 12-3 appear to be biased by approximately 0.15 psia, based on the pressure prior to J-2 ignition when compared to transducers D0150-206 (Figure 12-2) and D0158-206 (Figure 12-4). After interstage separation, the transducer records a constant negative value which again indicates that the transducer is biased. Under the assumption that the data is biased by 0.15 psia, good agreement is obtained between flight data, postflight analysis, and previous flight data prior to interstage separation. Following separation the AS-509 pressures would be slightly higher than on previous flights.

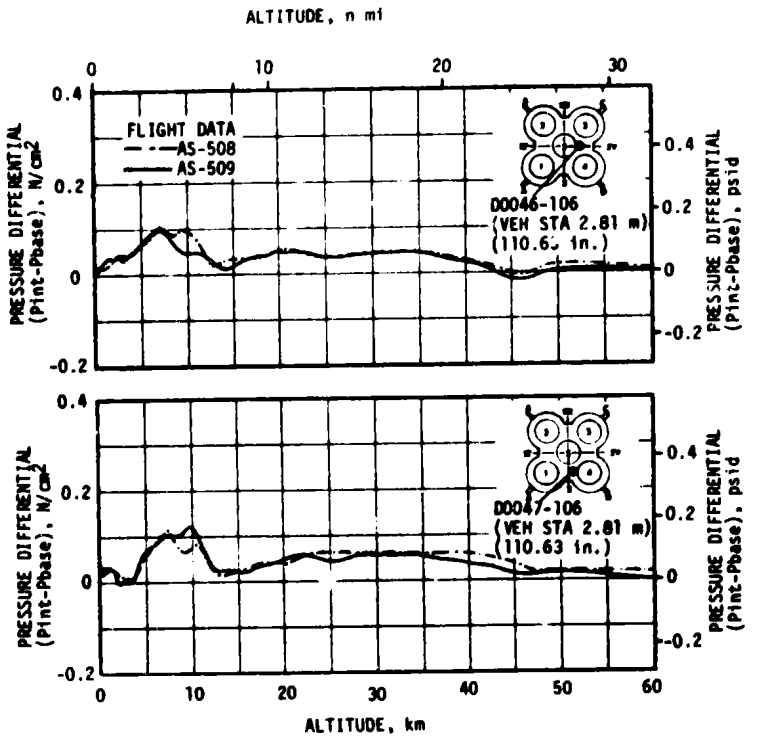

Figure 12-1. S-IC Base Heat Shield Differential Pressure

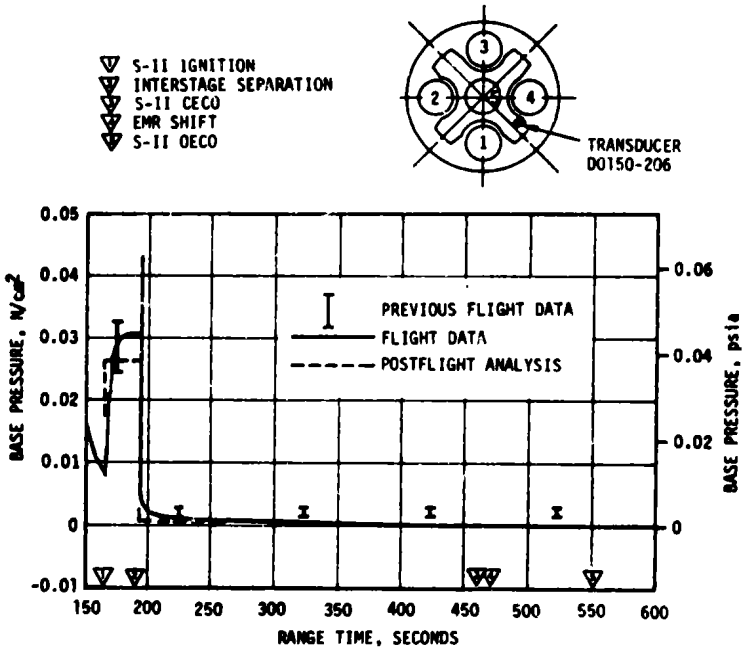

Figure 12-2. S-II Heat Shield Forward Face Pressure

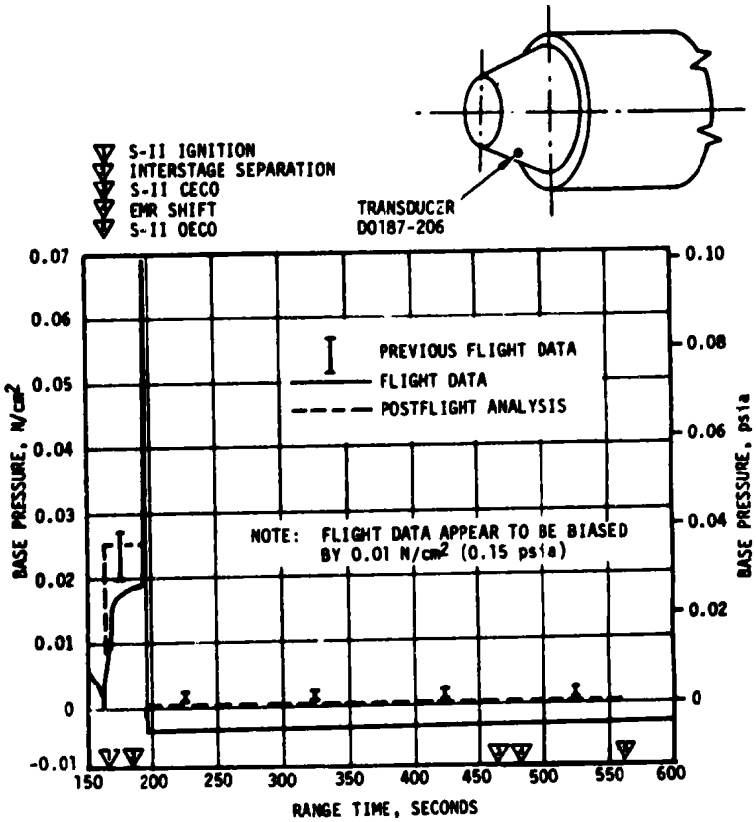

Figure 12-3. S-II Thrust Cone Pressure

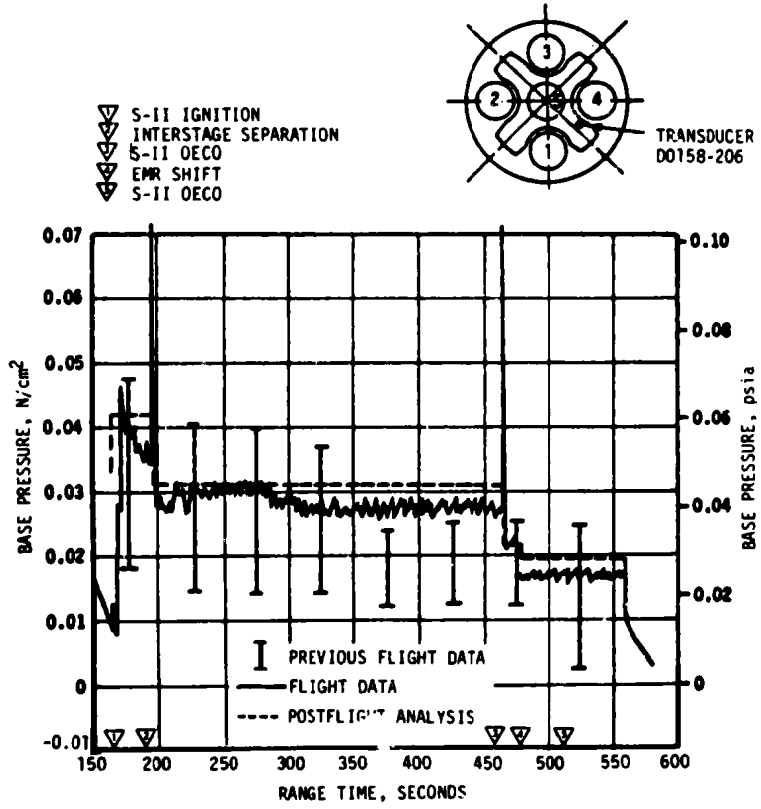

Figure 12-4. S-II Heat Shield Aft Face Pressure

The heat shield aft face pressures observed on AS-509 were comparable to those measured on previous flights except during the period 100 seconds prior to Center Engine Cutoff (CECO). During this period the AS-509 pressures were slightly higher than on previous flights. The flight data trends are consistent with those observed during previous flights and the steady-state engine control positions for the AS-509 flight.

SECTION 13

VEHICLE THERMAL ENVIRONMENT

13.1 SUMMARY

The AS-509 S-IC base region thermal environments exhibited trends and magnitudes similar to those seen on previous flights.

The base thermal environments on the S-II stage were similar to those measured on previous flights and were well below design limits. The total heating rate measurement indicated higher magnitudes prior to Center Engine Cutoff (CECO) than on previous flights, which was consistent with the closer inboard gimbaled position of the engines on AS-509.

Aerodynamic heating environments and S-IVB base thermal environments were not measured on AS-509.

13.2 S-IC BASE HEATING

Thermal environments in the base region of the AS-509 S-IC stage were recorded by two total calorimeters and two gas temperature probes which were located on the base heat shield. The sensing surfaces of the total calorimeters were mounted flush with the heat shield surface. The base gas temperature sensing surfaces were mounted at distances aft of the heat shield surface of 0.25 inch (C0050-106) and 2.50 inches (C0052-106). Data from these instruments are compared with AS-508 flight data and are presented in Figures 13-1 and 13-2. The AS-509 data exhibit similar trends and magnitudes as previous flights. The maximum recorded total heating rate was approximately 26 watt/cm^2 and occurred at 19 kilometers. The maximum gas temperature was approximately 1150°K, recorded 2.5 inches aft of the heat shield at an altitude of 25 kilometers. In general, CECO on AS-509 produced a spike in the thermal environment data with a magnitude and duration similar to previous flight data.

Ambient gas temperatures under the engine cocoons (measurements C0242-101 through C0242-105) were within the band of previous flight data and within the predicted band. These temperatures are shown in Figure 13-3.

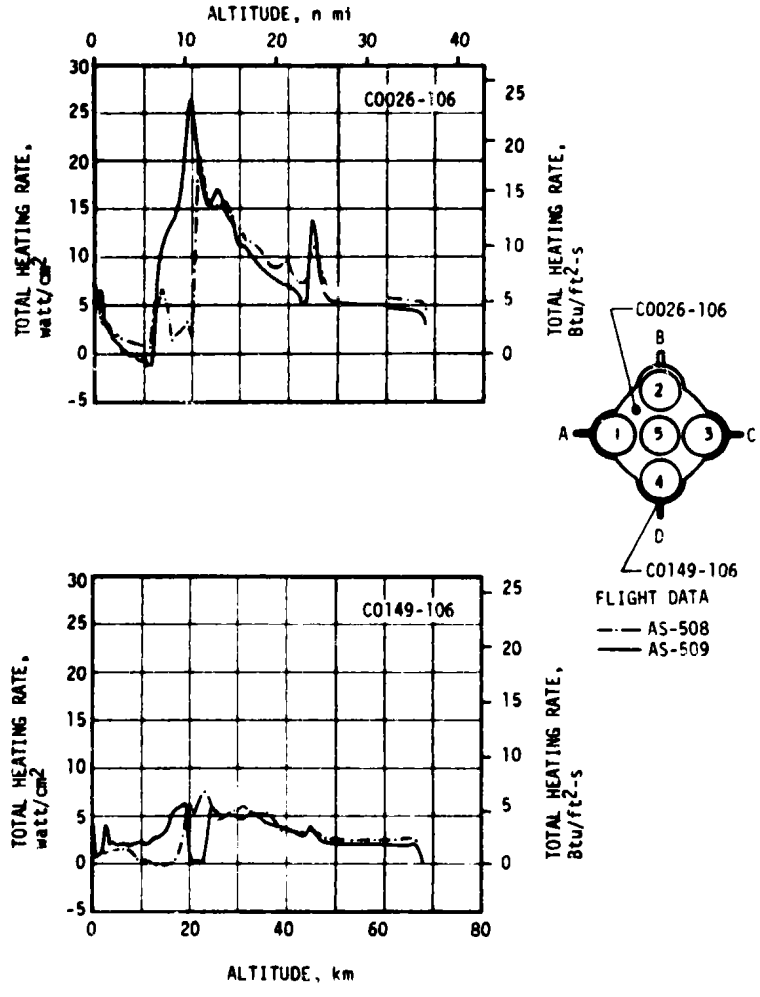

Figure 13-1. S-IC Base Region Total Heating Rate

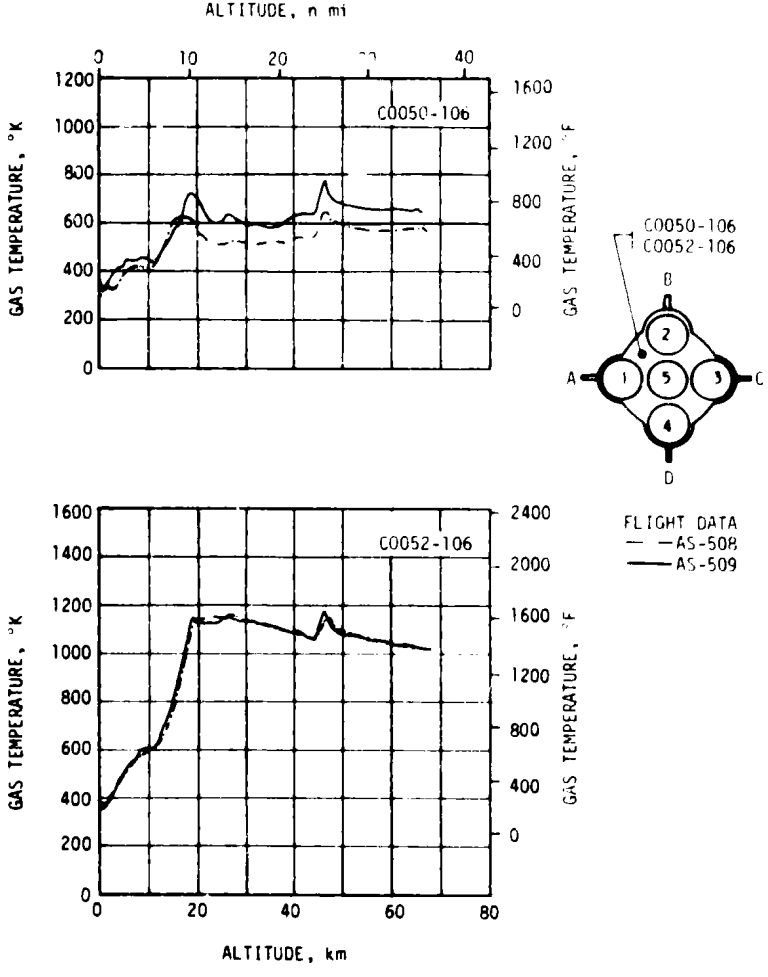

Figure 13-2. S-IC Base Region Gas Temperature

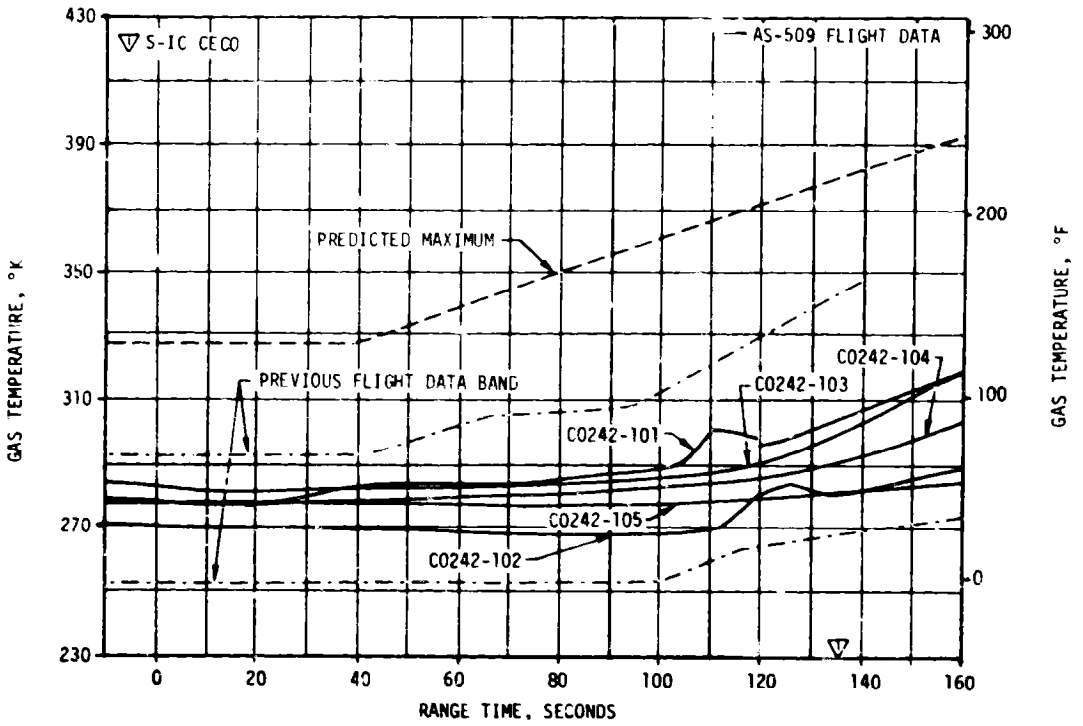

Figure 13-3. S-IC Ambient Gas Temperature Under Engine Cocoon

13.3 S-II BASE HEATING

Figure 13-4 presents the AS-509 total heating rate throughout S-II burn, as recorded by transducer C0722-206 on the aft face of the base heat shield. The postflight analytical curve for this transducer and the previous flight data band are also shown for comparison. The analytical heat rate represents the theoretical response of the transducer to the total thermal environment reflected by thermal math models. Key flight parameters relating to engine performance, engine position and reference temperatures are used in the postflight analysis. The math models are based on both theoretical and empirical postulates. The AS-509 flight data prior to CECO was higher than that recorded during all previous flights. This is consistent with the steady-state J-2 engine control positions which were determined to be closer inboard prior to CECO than on previous flights. The postflight analysis heating rates are presented in the form of a band to account for the uncertainty in engine position due to structural compliance and engine misalignment. The flight measured heating rates are well within the maximum design allowable values.

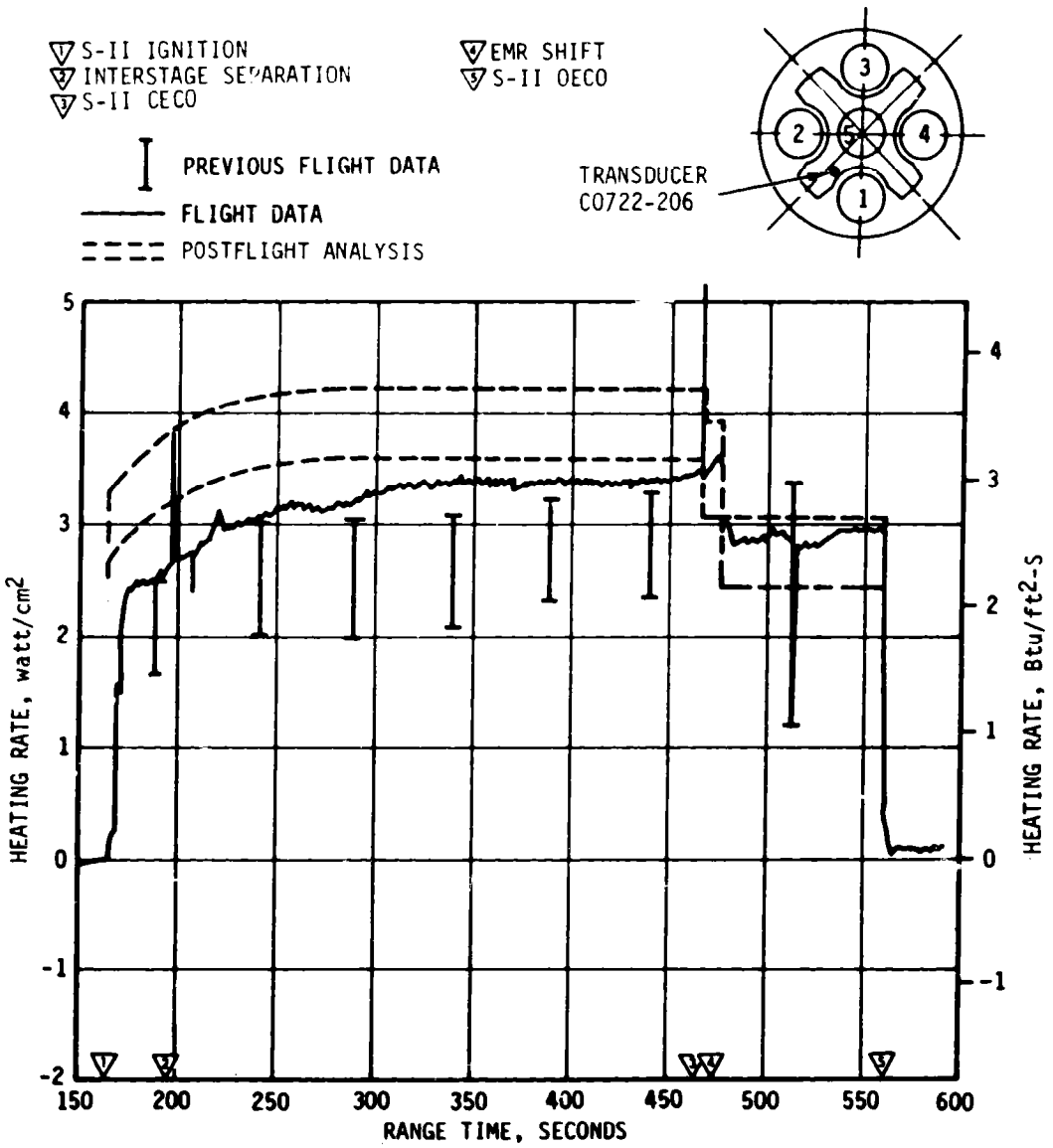

Figure 13-4. S-II Heat Shield Aft Heat Rate

Figure 13-5 shows the AS-509 flight data and postflight analysis of the heat shield recovery temperature transducer C0731-206. The analytical temperature curve represents a calculated transducer reading based on math models using key flight parameters. The gas recovery temperature is an analytically derived value computed from the flight measurement data. Note that the flight values are the probe temperatures and not the

gas recovery temperatures. As shown in Figure 13-5, the AS-509 flight gas recovery temperature values were on the low side of the previous flight data envelope. This is contrary to the expected trend, since the steady-state engine deflection pattern indicates that the engines were gimbaled closer inboard prior to CECO than on previous flights. However, as indicated by the previous flights data envelope, a considerable probe temperature variation exists between different flights which cannot be explained by the variation of the parameters considered in the

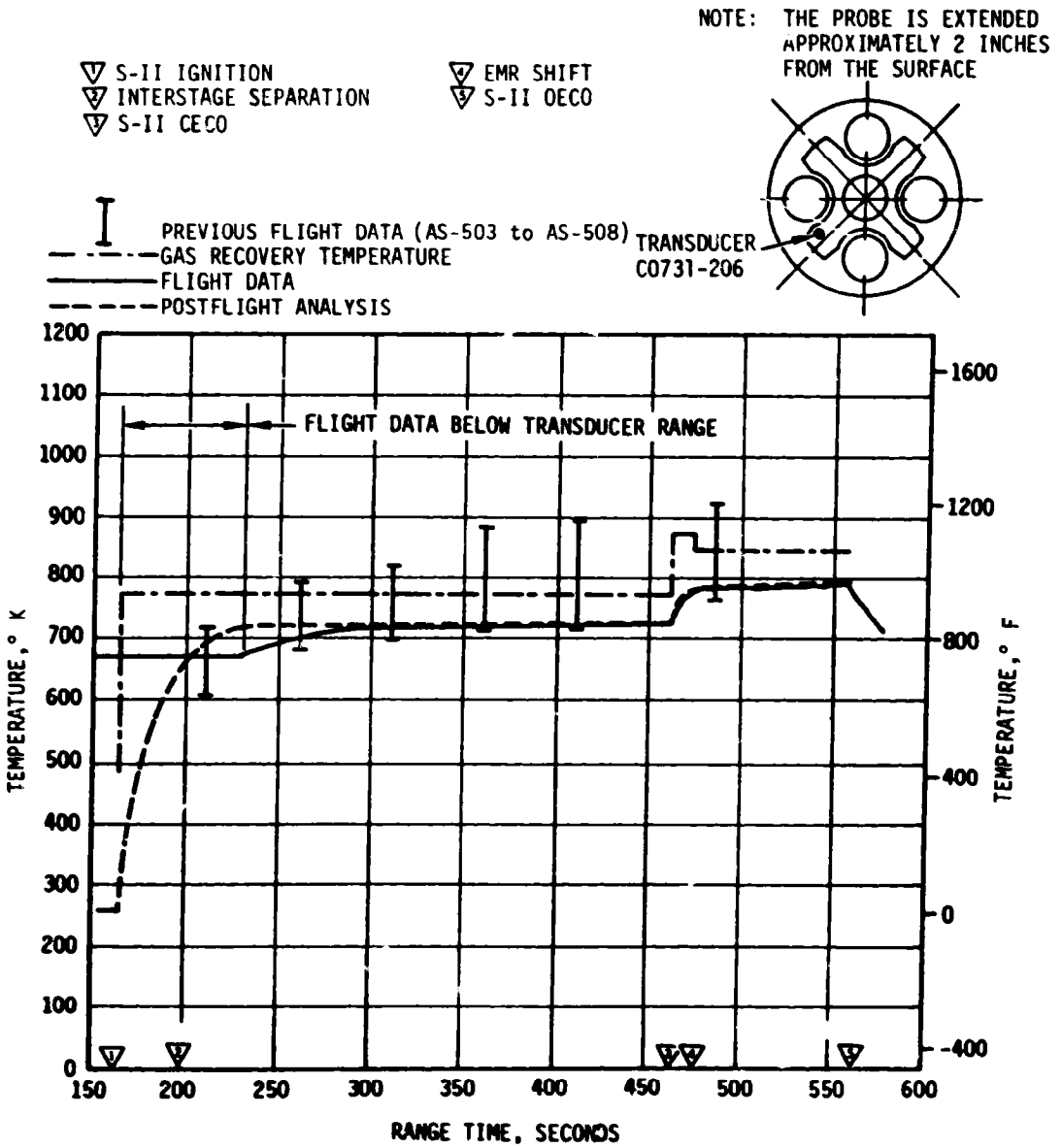

Figure 13-5. S-II Heat Shield Recovery Temperature

analysis alone. Also, since the initial temperature is below the probe range, it is not possible to determine if the probe temperature is biased, which might possibly account for the apparent discrepancy between the measured high total heat flux and low gas recovery temperature.

Figure 13-6 shows the AS-509 flight data and postflight analysis of the heat shield aft radiation heat rate. The analytical radiation heat rate represents the heat rate at the transducer location and is derived from a math model. Good agreement is obtained between flight and the postflight analytical values which do not include engine position effects. Comparison with the previous flight data envelope shows that the AS-509 data

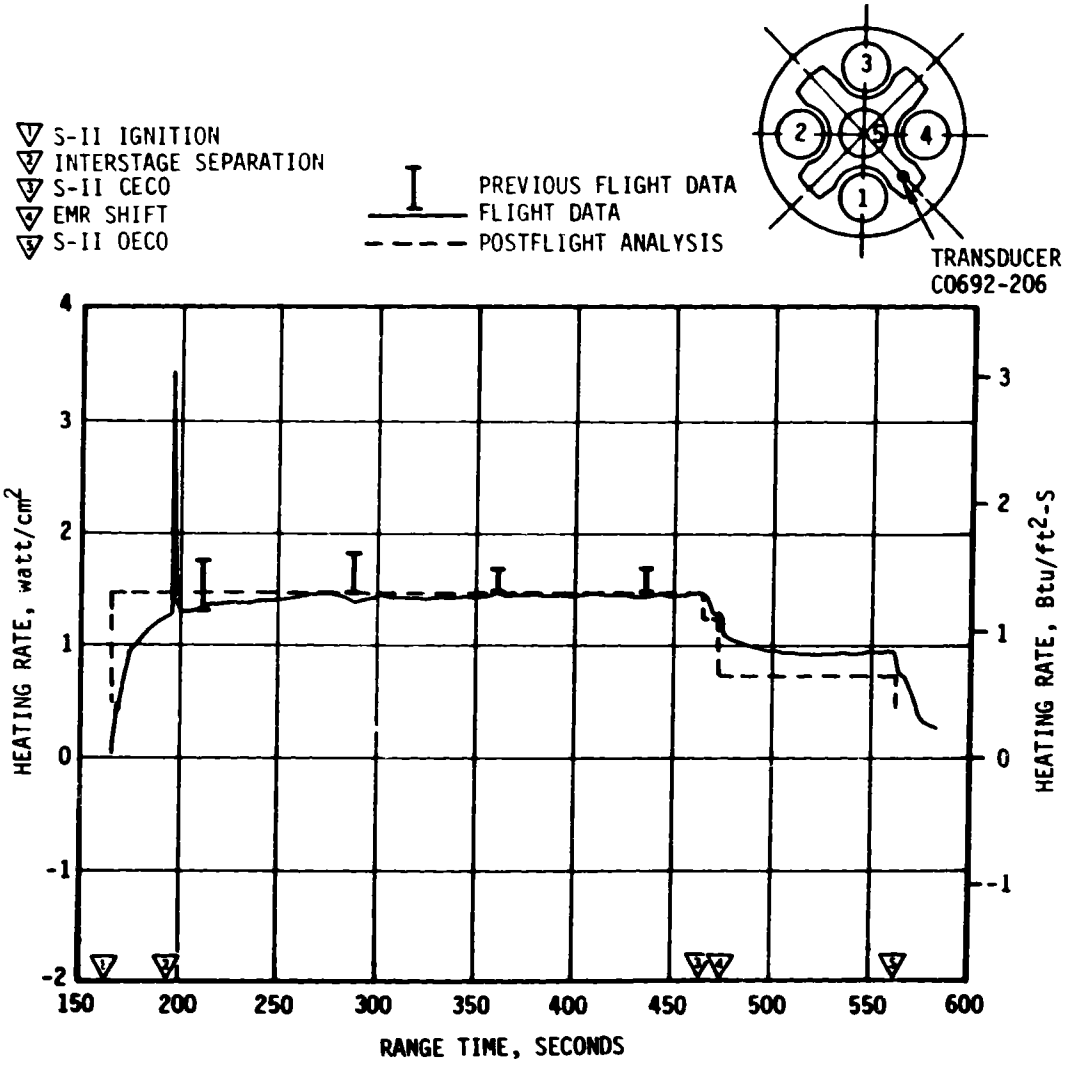

Figure 13-6. S-II Heat Shield Aft Radiation Heat Rate

were on the low side which is contrary to the expected trend based on the AS-509 closer inboard steady-state engine control positions.

There were no structural temperature measurements on the base heat shield and only three thrust cone forward surface temperature measurements in the base region. To evaluate the structural temperatures on the aft surface of the heat shield, a postflight analysis was performed using maximum AS-509 postflight analysis base heating rates. The maximum postflight analysis temperature was 743°K which compares favorably with previous flights, and was well below the maximum design temperatures of 1066°K (no engine out) and 1116°K (one control engine out). The effectiveness of the heat shield and flexible curtains was evidenced by the relatively low temperatures recorded on the thrust cone forward surface. The maximum measured temperature on the thrust cone forward surface was 269°K. The measured temperatures were well below design values.

13.4 VEHICLE AEROHEATING THERMAL ENVIRONMENT

Aerodynamic heating environments were not measured on the AS-509 S-IC stage. Due to the similarity in the trajectory, the aerodynamic heating environments are believed to be approximately the same as previous flight environments. Flow separation on the AS-509 vehicle was observed from ground optical data (Melbourne Beach) to occur at approximately 110 seconds. The forward point of flow separation versus flight time is presented in Figure 13-7. The effects of CECO during the AS-509 flight were similar to previous flights. At higher altitudes the measured location of the forward point of flow separation is questionable due to loss of resolution in the ground optical data.

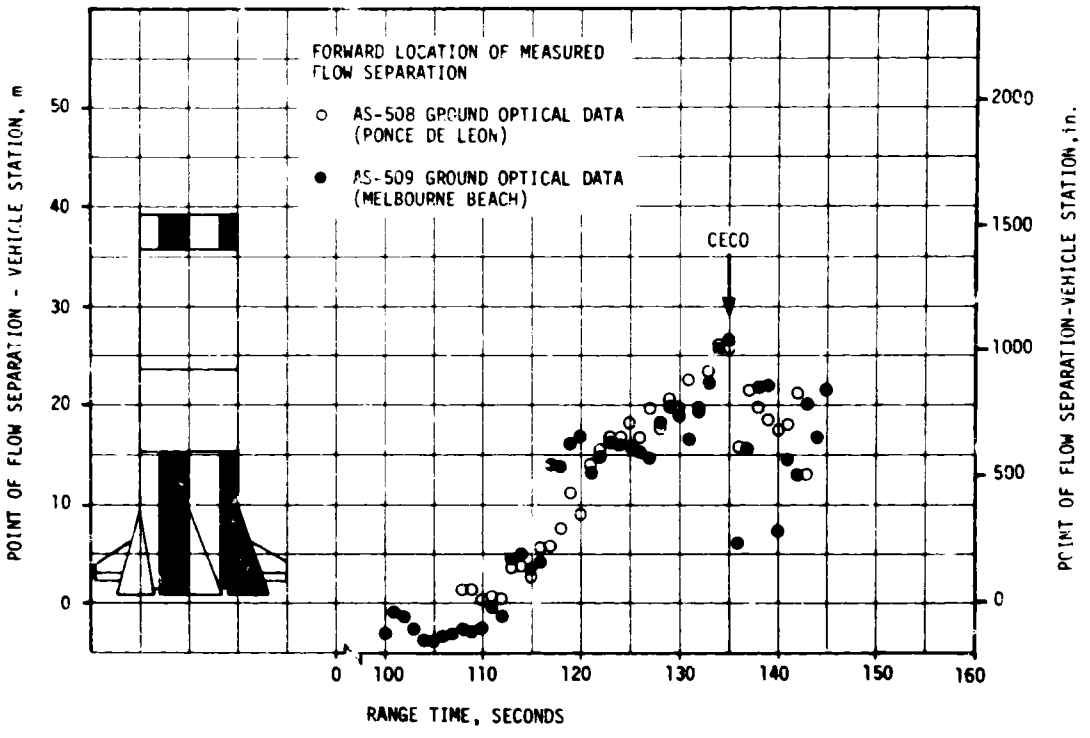

Figure 13-7. Forward Location of Separated Flow on S-IC Stage

SECTION 14

ENVIRONMENTAL CONTROL SYSTEMS

14.1 SUMMARY

The S-IC stage forward compartment ambient temperatures were maintained above the minimum performance limit during AS-509 countdown. The S-IC stage aft compartment environmental conditioning system performed satisfactorily.

The S-II thermal control and compartment conditioning system apparently performed satisfactorily since the ambient temperatures external to the containers were normal, and there were no problems with the equipment in the containers.

The Instrument Unit (IU) Environmental Control System (ECS) performed satisfactorily for the duration of its mission. Coolant temperatures, pressures, and flowrates were maintained within the required limits.

14.2 S-IC ENVIRONMENTAL CONTROL

The S-IC stage forward skirt ECS has three phases of operation during prelaunch operations. When onboard electrical systems are energized, but prior to cryogenic loading, conditioned air is used to maintain the desired environment. When cryogenic loading begins, warmed GN_2 is substituted for the conditioned air. The third phase uses a warmer GN_2 flow to offset the cooling effects caused by S-II stage J-2 engine thrust chamber chilldown. All three phases functioned satisfactorily as evidenced by ambient temperature readings.

The most severe prelaunch forward compartment thermal environment (-63.2°F at C0206-120) occurred during J-2 engine chilldown and was above the minimum performance limit of -90°F. During AS-509 flight the lowest forward compartment temperature measured was -133.2°F at instrument location C0206-120.

After the initiation of LOX loading, the temperature in the vicinity of the battery (12K10) decreased to 59°F which is within the new battery qualification limits of 35 to 95°F per ECP 578. The temperature increased to 68°F at liftoff. Just prior to liftoff, the other ambient temperatures

ranged from 66.7°F at instrument location C0203-115 to 81.1°F at instrument location C0205-115. During flight the lowest aft compartment temperature recorded was 53.6°F at instrument location C0203-115.

14.3 S-II ENVIRONMENTAL CONTROL

The engine compartment conditioning system mairtained the ambient temperature and thrust cone surface temperatures within design ranges throughout the launch countdown. The system also maintained an inert atmosphere within the compartment as evidenced by the absence of H_2 or O_2 indications on the hazardous gas monitor.

No equipment container temperature measurements were taken. However, since the ambient measurements external to the containers were satisfactory and there were no problems with the equipment in the containers, it is assumed that the thermal control system performed adequately.

14.4 IU ENVIRONMENTAL CONTROL

14.4.1 Thermal Conditioning System

Performance of the IU Thermal Conditioning System (TCS) was satisfactory throughout flight. The temperature of the coolant supplied to the coldplates and internally cooled components was continuously maintained within the required 45 to 68°F temperature band. The TCS with the new coolant Dronite Flo-Cool 100 performed as predicted.

Figure 14-1 shows the TCS coolant control temperature (C0015-601) out to 14,000 seconds (03:53:20). The range of measurement C0015-601 does not allow reading the minimum coolant temperature; however, extrapolation of the data indicates that the coolant temperature did not drop below the specification limit.

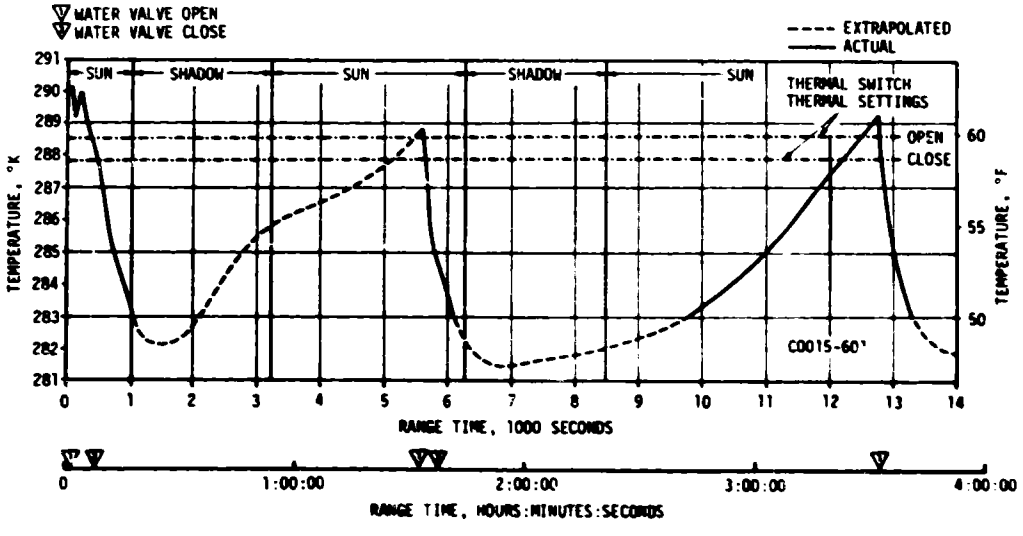

Figure 14-1. IU TCS Coolant Control Temperature

The water valve opened initially at 183 seconds allowing water to flow to the sublimator. Significant cooling was evident at approximately 240 seconds when the coolant temperature, monitored at the temperature control point, began to decrease rapidly. At the first thermal switch sampling of 483 seconds, the coolant temperature was above the switch activation point. The switch activated at 493 seconds, just 10 seconds late for the water valve to close, causing the valve to remain open until the second sampling at 781 seconds. The coolant control temperature and sublimator heat rejection rate for the initial startup is shown in Figure 14-2. Switch selector event times revealed that thermal cycling of the water valve was still taking place at 27,180 seconds (07:33:00), indicating normal system performance at that time.

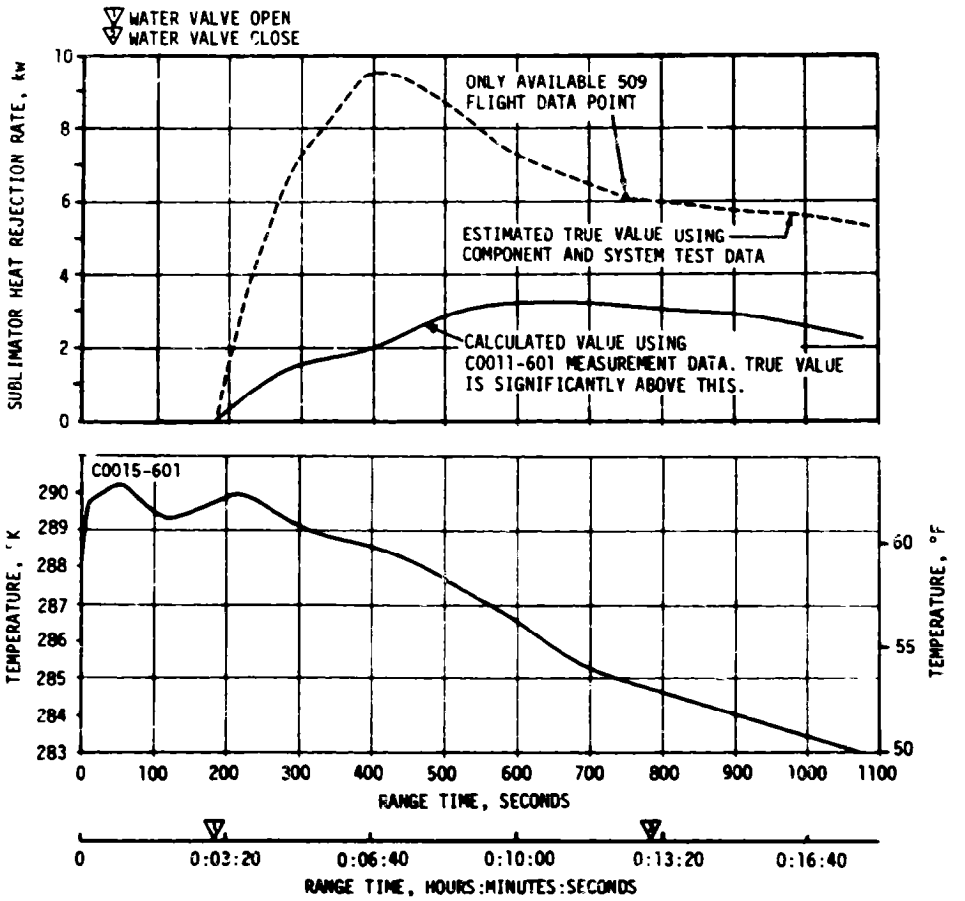

Figure 14-2. IU Sublimator Performance During Ascent

Hydraulic performance of the TCS with the new coolant was as expected. Available flowrates and pressures are presented in Figure 14-3. The TCS GN_2 sphere pressure decay which is indicative of the GN_2 usage rate was nominal as shown in Figure 14-4.

Available component temperatures remained within the expected temperature ranges as shown in Figure 14-5. As expected, the component temperatures averaged slightly higher on AS-509 than on previous Saturn V flights due to the lower heat dissipation ability of the new coolant (Oronite Flo-Cool 100).

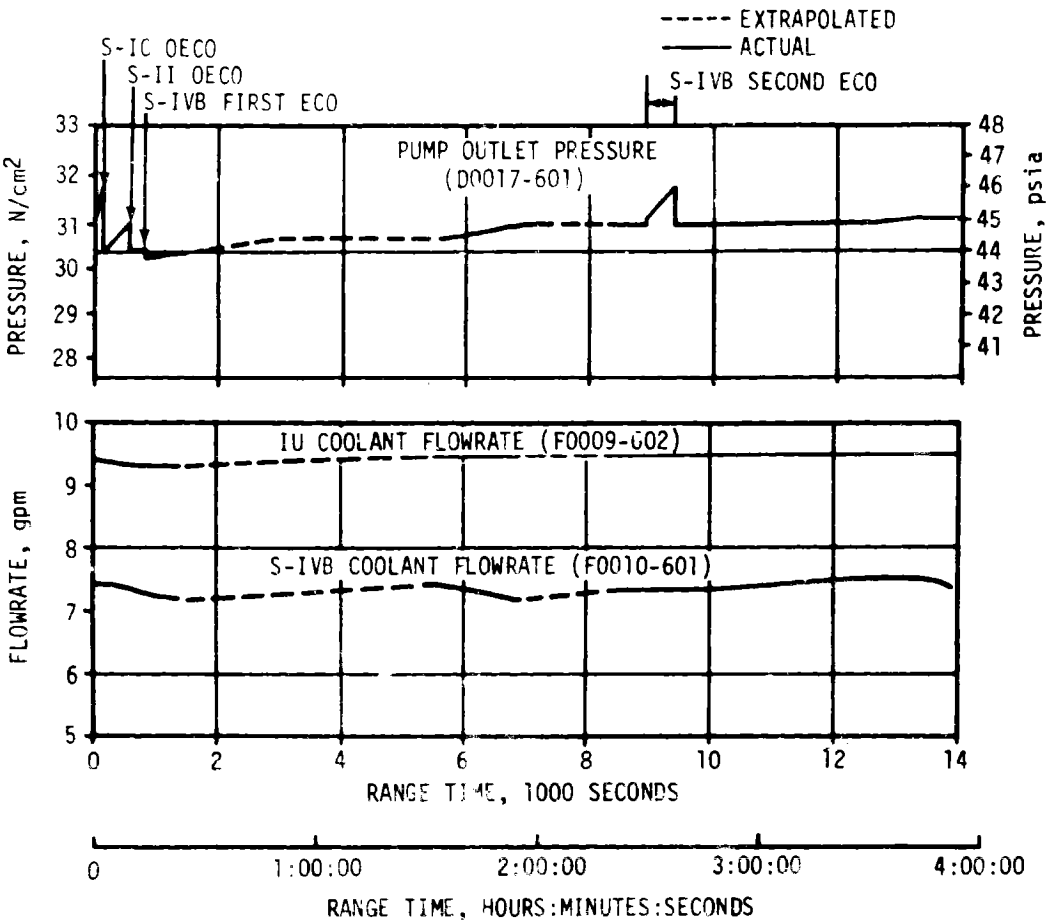

Figure 14-3. IU TCS Hydraulic Performance

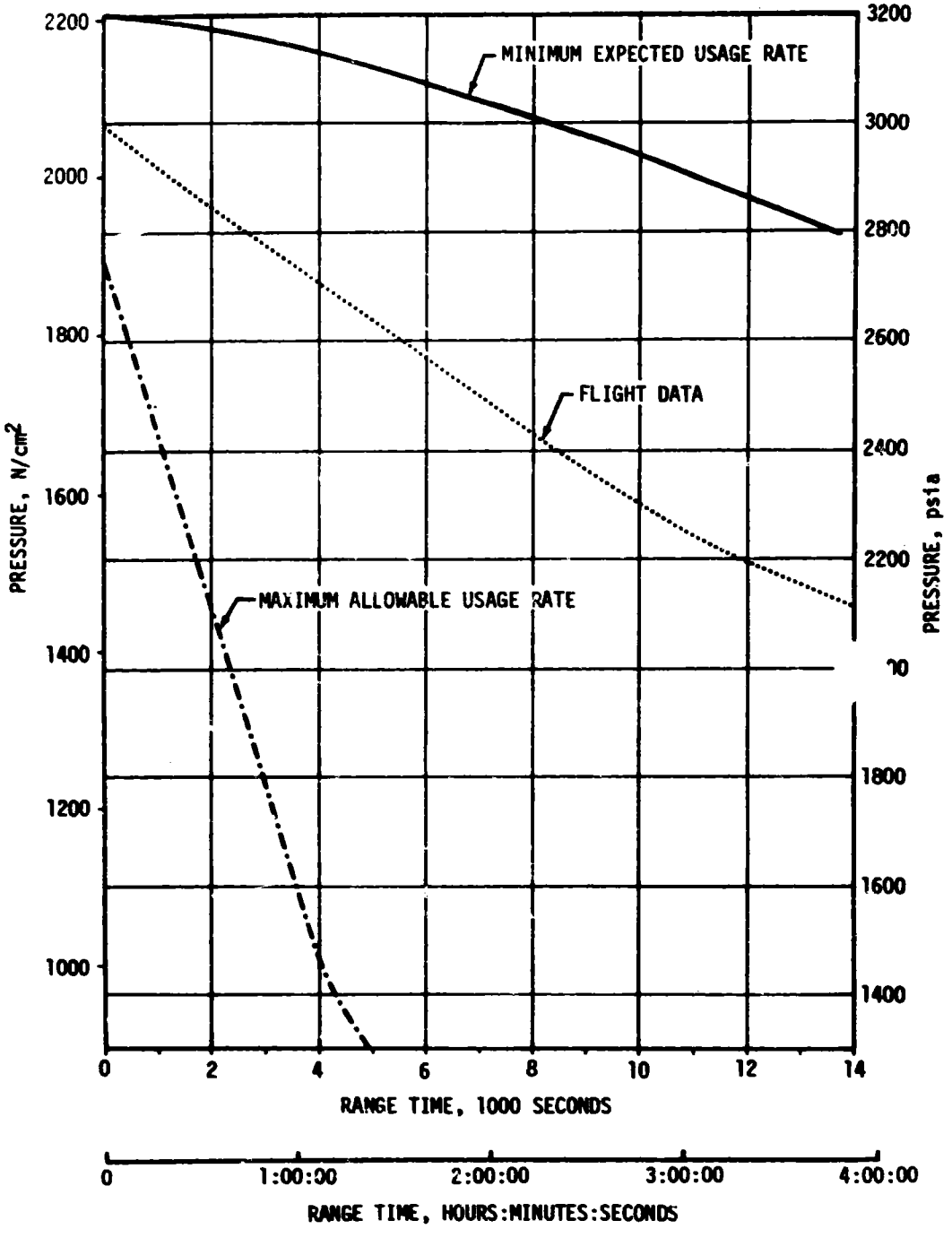

Figure 14-4. IU TCS GN_2 Sphere Pressure

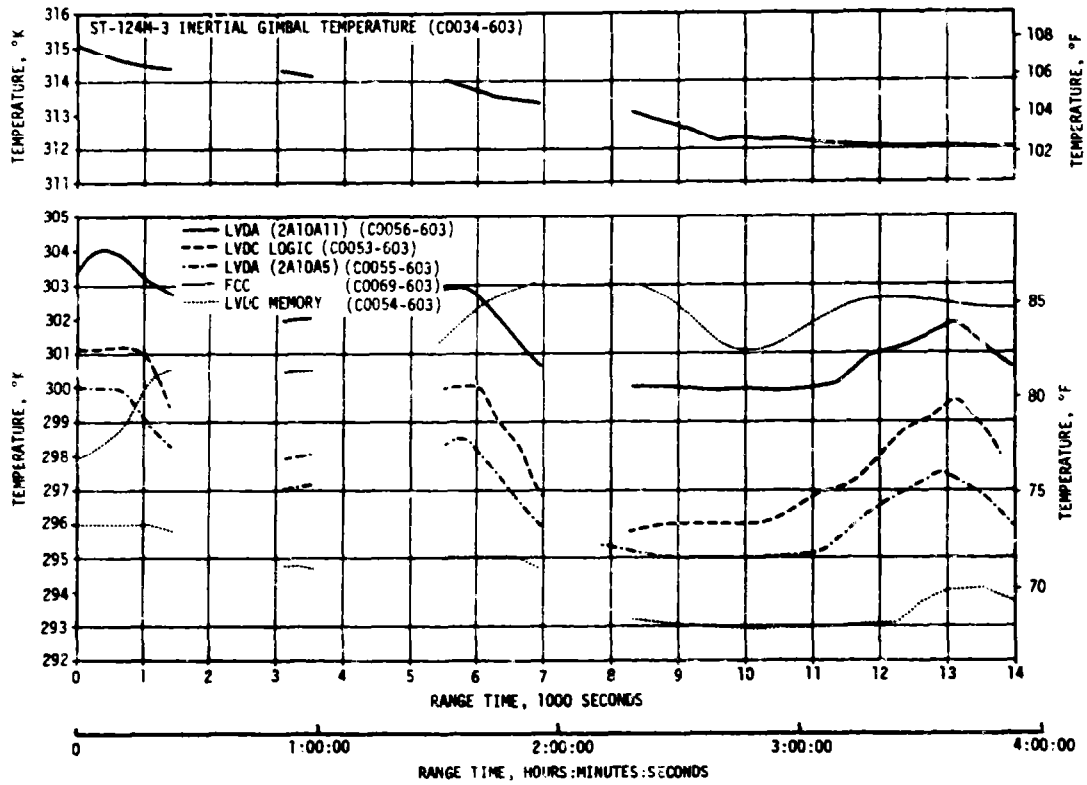

Figure 14-5. Selected IU Component Temperatures

14.4.2 ST-124M-3 Gas Bearing System (GBS)

The GBS performance was nominal. The ST-124M-3 internal ambient pressure (D0012-603) and gas bearing inlet pressure (D0011-603) are shown in Figure 14-6.

The GBS GN_2 supply sphere pressure decay was as expected for the nominal case as shown in Figure 14-7.

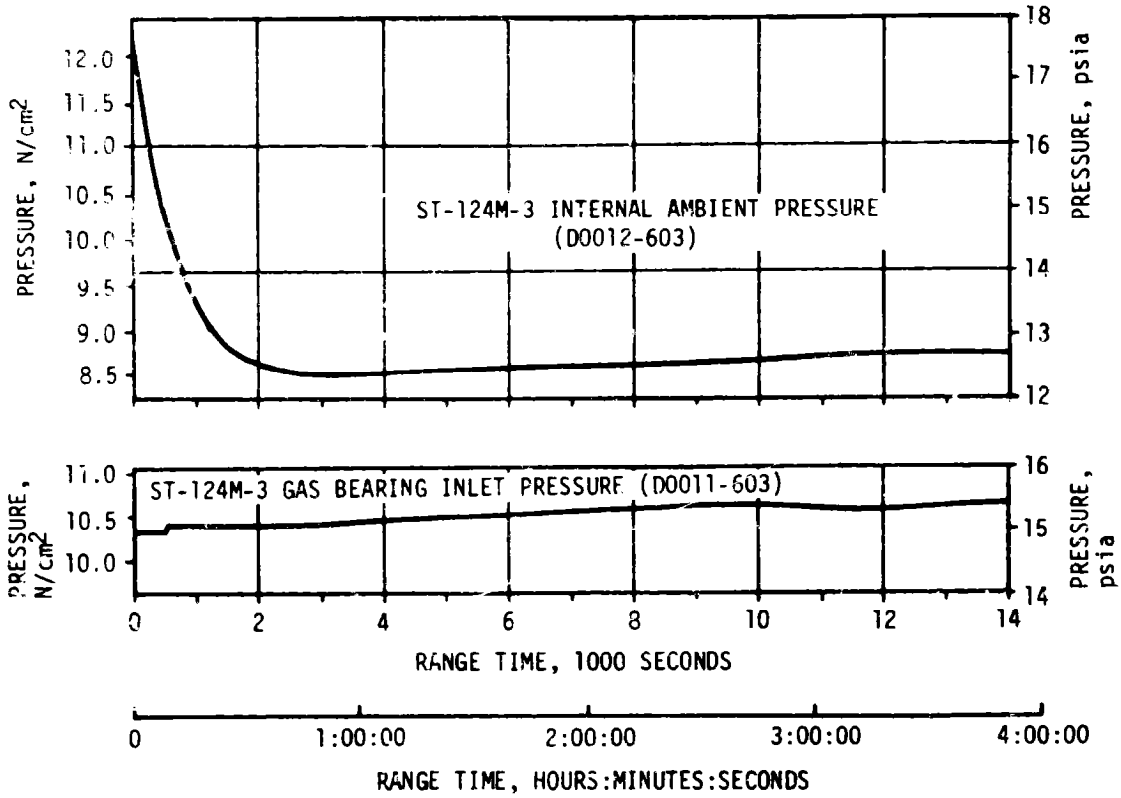

Figure 14-6. IU Inertial Platform GN_2 Pressures

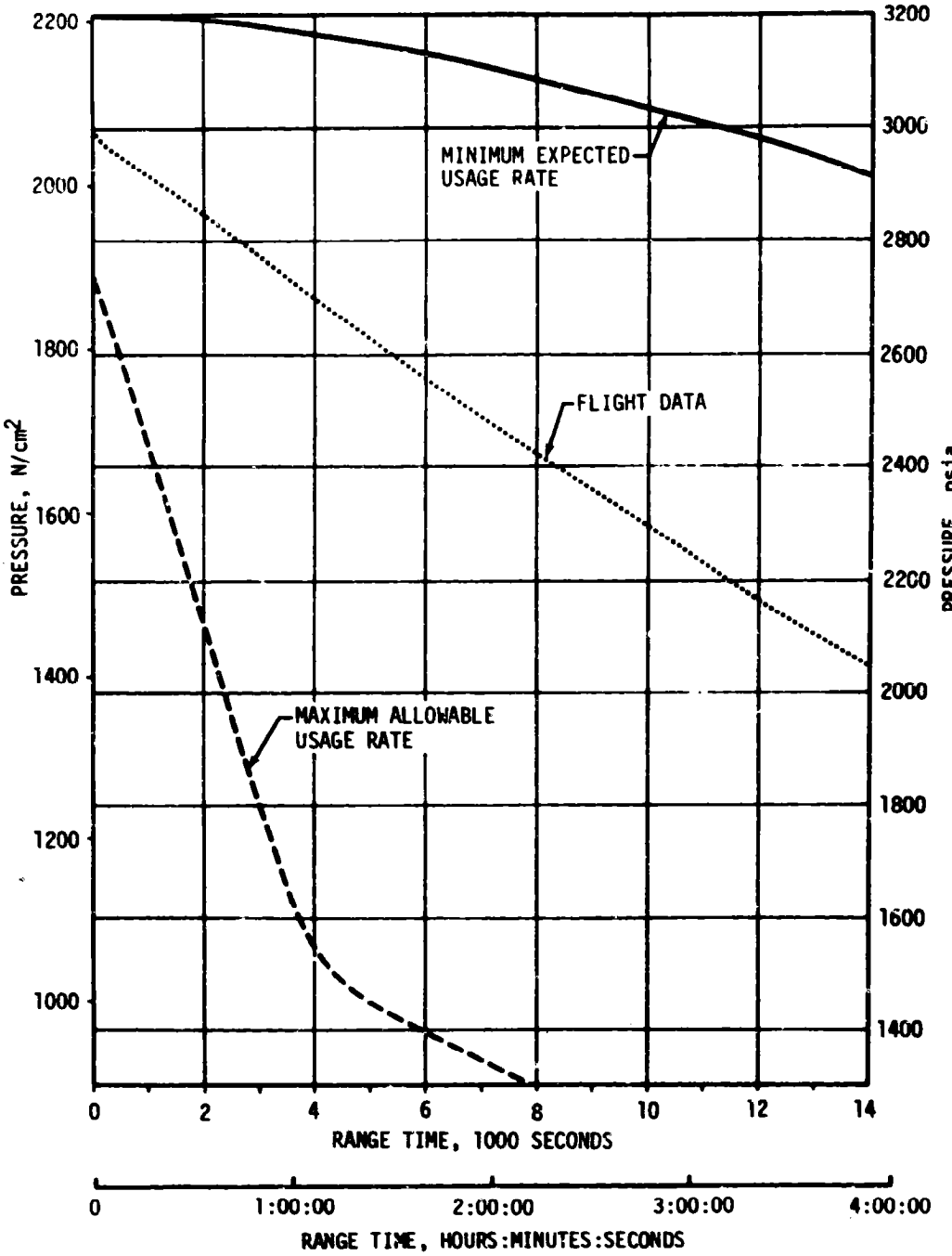

Figure 14-7. IU GBS GN_2 Sphere Pressure

SECTION 15

DATA SYSTEMS

15.1 SUMMARY

All elements of the data system performed satisfactorily throughout flight except the Instrument Unit (IU) telemetry system. The DP1-A0 270 multiplexer data and the 410K multiplexer data were lost at 0.409 second and at 10,955.861 seconds (03:02:35.861), respectively. In addition, the DP-1 telemetry RF output measurement changed abruptly several times during the flight.

The vehicle measurement reliability was 95.5 percent. Telemetry performance was normal except for the noted problems. Radiofrequency (RF) propagation was generally good, though the usual problems due to flame effects and staging were experienced. Usable VHF data were received until 18,360 seconds (05:06:00). The Secure Range Safety Command Systems (SRSCS) on the S-IC, S-II and S-IVB stages were ready to perform their functions properly, on command, if flight conditions during the launch phase had required destruct. The system properly safed the S-IVB on a command transmitted from Bermuda (BDA) at 710.2 seconds. The performance of the Command and Communication System (CCS) was excellent. Usable CCS telemetry data were received to 53,039 seconds (14:43:59) at which time the telemetry subcarrier was inhibited. Carnarvon (CRO), Goldstone (GDS), Hawaii (HAW), Honeysuckle (HSK), and Merritt Island Launch Area (MILA) were receiving CCS carrier signal at S-IVB/IU lunar impact at 297,473.4 seconds (82:37:53.4). Good tracking data were received from the S-Band radar, with BDA indicating final Loss of Signal (LOS) at 28,950 seconds (08:02:30).

The 65 ground engineering cameras provided good data during the launch.

15.2 VEHICLE MEASUREMENTS EVALUATION

The AS-509 launch vehicle had 1382 measurements scheduled for flight; three measurements were waived prior to start of the automatic countdown sequence leaving 1379 measurements active for flight. Of the waived measurements, one provided some valid data during the flight. Sixty-two measurements failed during flight resulting in an overall measurement system reliability of 95.5 percent. Fifty-nine of these failed measurements and one of the ten partially failed measurements were caused by

IU telemetry system problems discussed in paragraphs 15.3.2 and 15.3.3. These measurement failures affected the postflight evaluation of the applicable vehicle systems.

A summary of measurement reliability is presented in Table 15-1 for the total vehicle and for each stage. The waived measurements, totally failed measurements, partially failed measurements, and questionable measurements are listed by stage in Tables 15-2, 15-3 and 15-4.

15.3 AIRBORNE VHF TELEMETRY SYSTEMS EVALUATION

15.3.1 Performance Summary

Performance of the eight VHF telemetry links was generally satisfactory, as indicated in Table 15-5. However, three significant problems occurred in the IU telemetry system. First, all analog data routed through the DP1-A0 270 multiplexer was lost at 0.409 second. Second, the H0060-603 computer word routed through the 410K multiplexer locked in an all zero state at 10,955.861 seconds (03:02:35.861). Finally, the DP-1 telemetry RF output measurement, J0029-602, changed abruptly several times during the flight. These problems are discussed in paragraphs 15.3.2, 15.3.3 and 15.3.4.

The S-IC, S-II and S-IVB telemetry systems and the balance of the IU telemetry system operation were normal throughout flight. All inflight calibrations occurred as programed and were within specifications. Data

Table 15-1. AS-509 Measurement Summary

MEASUREMENT CATEGORY	S-IC STAGE	S-II STAGE	S-IVB STAGE	INSTRUMENT UNIT	TOTAL VEHICLE
Scheduled	287	598	271	226	1382
Waived	1	1	1	0	3
Failures	0	1	2	59	62
Partial Failures	5	1	3	1	10
Questionable	0	1	0	0	1
Reliability Percent	100.0	99.8	99.3	73.4	95.5

Table 15-2. AS-509 Flight Measurements Waived Prior to Flight

MEASUREMENT NUMBER	MEASUREMENT TITLE	NATURE OF FAILURE	REMARKS
		S-IC STAGE	
D0119-103	Engine Gimbal System Filter Manifold Differential Pressure	Out-of-tolerance during performance of V-27153 (MTO1)	Probable cause: Silicon oil leakage in transducer. Invalid data throughout flight.
		S-II STAGE	
C0001-202	E2 LOX Pump Discharge Temperature	Measurement indicated approximately 4°F warmer than other equivalent measurements	At 81 seconds the measurement returned to agreement with other measurements.
		S-IVB STAGE	
C0059-406	Temperature, LOX Tank Ullage Gas, 100 Percent	Indicated higher than nominal temperature	First observed during CDDT LOX loading. Indicated trend information. Malfunction probably caused by excessive contact resistance of an in-line electrical connector.

degradation and dropouts were experienced at various times during boost, as on previous flights, due to the attenuation of RF signals. Signal attenuation was caused by main engine flame effects, S-IC/S-II staging, S-II ignition and S-II second plane separation. The magnitude of these effects was comparable to that experienced on previous flights. Loss of these data, however, posed no problem since losses were of such short duration as to have little or no impact on flight analysis. Usable VHF telemetry data were received to 18,360 seconds (05:06:00). A summary of available VHF telemetry coverage showing Acquisition of Signal (AOS) and LOS for each station is shown in Figure 15-1.

15.3.2 Loss of DP1-A0 Analog Data

All analog data routed through the DP1-A0 270 multiplexer (S/N 461) were lost at 0.409 second and for the remainder of the flight. This resulted in the loss of 59 out of 101 IU DP1-A0 PCM measurements. The remaining 42 measurements were redundantly routed through the CP1-A0 telemetry link.

All data channels showed an abrupt change followed by a transient, as shown in Figure 15-2. The data tended to level out at 14.3 percent of full scale until 4.63 seconds when it decayed to 11.6 percent of full scale within 250 milliseconds.

Table 15-3. AS-509 Measurement Malfunctions

MEASUREMENT NUMBER	MEASUREMENT TITLE	NATURE OF FAILURE	TIME OF FAILURE (RANGE TIME)	DURATION SATISFACTORY OPERATION	REMARKS
TOTAL MEASUREMENT FAILURES, S-II STAGE					
C0003-202	E2 Fuel Turbine Inlet Temperature	Measurement went to top or range	168 seconds	168 seconds	Measurement failed at 168 seconds but did not provide useful data prior to failure since it monitors S-II engine No. 2 performance. Probably caused by open circuit in sensor.
TOTAL MEASUREMENT FAILURES, S-IVB STAGE					
C0199-401	Temperature - Thrust Chamber Jacket	Indicated higher than nominal temperature	8904 seconds	Throughout flight except during S-IVB second burn	Probably the result of inadequate sensor-to-jacket thermal contact.
D0050-403	Pressure - Engine Pump Purge Regulator	Data suppression	587 seconds	0 to 587 seconds; 701 seconds to end of data	Malfunction was apparently caused by an electrical short circuit of the 5 volt supply between the bus isolation module and the transducer potentiometer.
TOTAL MEASUREMENT FAILURES, IU					
C0006-601	Temp, Sublimator Water Inlet	Signal level went to 14.3 percent	0.4 second	0 to 0.4 second	Possible 270 multiplexer failure.
C0057-900	Temp, Q-Ball Int.				
C0062-603	Temp, Accel Sig Cond				
C0063-603	Temp, ST-124M Electronic Box				
C0064-601	Temp, Battery No. 1 Internal (6D10)				
C0066-601	Temp, Battery No. 3 Internal (6D30)				
C0067-603	Temp, 250 VA Inverter				
C0068-601	Temp, Battery No. 4 Internal (6D40)				
D0001-900	EDS - Delta P Pitch, Q-Ball				
D0003-900	EDS - Delta P Yaw, Q-Ball				
D0024-601	Inlet Pressure Coolant Pump				
D0035-900	Vector Sum, Q-Ball Redundant				
D0043-601	Press, Sublimator Water Inlet				
D0068-603	Press, RTG Cook Diffuser Inlet No. 1 Press Gauge				
FC 102-601	Flow Rate Sublimator Bypass Coolant				
G0003-601	Position Coolant Control Valve				
H0001-102	Valve Current, Pitch Actuator	Signal level went to 14.3 percent	0.4 second	0 to 0.4 second	Possible 270 multiplexer failure.

Table 15-3. AS-509 Measurement Malfunctions (Continued)

MEASUREMENT NUMBER	MEASUREMENT TITLE	NATURE OF FAILURE	TIME OF FAILURE (RANGE TIME)	DURATION SATISFACTORY OPERATION	REMARKS
TOTAL MEASUREMENT FAILURES, IU (CONTINUED)					
M0001-103	Valve Current, Pitch Actuator	Signal level went to 14.3 percent	0.4 second	0 to 0.4 second	Possible 270 multiplexer failure.
M0001-104	Valve Current, Pitch Actuator				
M0001-202	Valve Current, Pitch Actuator				
M0001-203	Valve Current, Pitch Actuator				
M0001-204	Valve Current, Pitch Actuator				
M0002-101	Valve Current, Yaw Actuator				
M0002-102	Valve Current, Yaw Actuator				
M0002-103	Valve Current, Yaw Actuator				
M0002-104	Valve Current, Yaw Actuator				
M0002-201	Valve Current, Yaw Actuator				
M0002-202	Valve Current, Yaw Actuator				
M0002-203	Valve Current, Yaw Actuator				
M0002-204	Valve Current, Yaw Actuator				
M0002-403	Valve Current, Yaw Actuator				
M0035-403	Voltage, 4.8 KHZ Platform Excitation				
M0035-403	Voltage, 4.8 KHZ Servo Amp Supply				
M0040-403	Output Z Gyro Servo				
M0045-403	Output X Gyro Servo				
M0045-403	Output Y Gyro Servo				
[illegible]	C-Band Receiver Input Signal (0038535)				
[illegible]	C-Band Interrogation PRF (0038535)				
[illegible]	C-Band Receiver Input Signal (0038536)				
[illegible]	C-Band Interrogation PRF (0038536)				
[illegible]	Static Phase Error				
[illegible]	CCS ABC				
[illegible]	CCS Amp Helix Current				
[illegible]	Summation Gyro Currents (ST-128A-3)				
[illegible]	Summation Accel Currents (ST-128A-3)				
[illegible]	Voltage, 56 VCC Supply				
[illegible]	Voltage, 210 VA Inverter Phase BC	Signal level went to 14.3 percent	0.4 second	0 to 0.4 second	Possible 270 multiplexer failure.

Table 15-3. AS-509 Measurement Malfunctions (Continued)

MEASUREMENT NUMBER	MEASUREMENT TITLE	NATURE OF FAILURE	TIME OF FAILURE (RANGE TIME)	DURATION SATISFACTORY OPERATION	REMARKS
TOTAL MEASUREMENT FAILURES, IU (CONTINUED)					
M0024-603	Data Adapter +20 Volt Supply	Signal level went to 14.3 percent	0.4 second	0 to 0.4 second	Possible 270 multiplexer failure.
M0025-603	Data Adapter +12 Volt Supply				
M0026-603	Data Adapter +6 Volt Supply (LVDC)				
M0027-603	Data Adapter -3 Volt Supply				
M0028-603	Data Adapter -20 Volt Supply				
M0029-603	Data Adapter +6 Volt Supply (LVDC)				
R0008-602	Ang Vel, Yaw EDS Group 1 (Ref)				
R0012-602	Ang Vel, Roll EDS Group 2 (Ref)				
R0013-602	Ang Vel, Pitch EDS Group 3 (Ref)				
R0033-602	EDS Monitor Ang Vel Roll Group 1				
R0034-602	EDS Monitor Ang Vel Roll Group 2				
R0035-602	EDS Monitor Ang Vel Roll Group 3	Signal level went to 14.3 percent	0.4 second	0 to 0.4 second	Possible 270 multiplexer failure.
PARTIAL MEASUREMENT FAILURES, S-IC STAGE					
Au001-116	Acceleration, Long.	Rectification error at liftoff	-3 to 13 seconds	152 seconds	Same phenomenon seen on previous flights.
C0003-104	Temperature, Turbine Manifold, Engine No. 4	Failed off scale high	108 seconds	108 seconds	Probable transducer failure (Rocketdyne).
C0003-105	Temperature, Turbine Manifold, Engine No. 5	Failed off scale high	120 to 136 seconds	149 seconds	Probable transducer failure (Rocketdyne).
F0044-102	Flow Rate, LOX Heat Exchanger Inlet, DC	Dropped to zero	112 seconds	112 seconds	Probable signal conditioner failure.
K0013-118	LOX Level Cutoff Number 3	Indicated dry for one sample	99.5 seconds	165 seconds	Probable transducer false trigger.
PARTIAL MEASUREMENT FAILURES, S-II STAGE					
C0649-206	O_2 Pressure Regulator Outlet Temperature	Measurement went to bottom of range	364 seconds	364 seconds	Measurement provided good data until 364 seconds. Probably caused by open circuit in sensor.

Table 15-3. AS-509 Measurement Malfunctions (Continued)

MEASUREMENT NUMBER	MEASUREMENT TITLE	NATURE OF FAILURE	TIME OF FAILURE (RANGE TIME)	DURATION SATISFACTORY OPERATION	REMARKS
PARTIAL MEASUREMENT FAILURES, S-IVB STAGE					
D0236-403	Press-Ambient He Pneu Sphere	Indicated 200 psia lower than backup measurement	13,300 seconds	0 to 13,300 seconds	Probable mechanical degradation of the transducer pressure sensing element.
M0012-411	Freq-PU Inv/Conv	Frequency indication decreased abruptly to off-scale-low	19,930 seconds	0 to 19,930 seconds	Probable failure of the signal conditioning circuitry.
M0055-411	Misc-T/M RF Syst Refl Pwr	Higher than normal data level	Preliftoff	Data usable during entire flight	Possible system calibration shift.
PARTIAL MEASUREMENT FAILURES, IU					
M0060-603	Guidance Computer Operation	All bits went to zero	10,955 seconds	0 to 10,956 seconds	Possible 410 multiplexer failure.

Table 15-4. AS-509 Questionable Flight Measurements

MEASUREMENT NUMBER	MEASUREMENT TITLE	REASON QUESTIONED	REMARKS
S-II STAGE			
D0258-206	LOX Tank Ullage Pressure	Measurement was 2 psia higher than redundant system (D0257-206) prior to tank pressurization. It was 2 psia lower than redundant measurement after pressurization.	CDDT data looked O.K, but there appeared to be an equivalent trend with a delta pressure of 0.5 psia.

Table 15-5. AS-509 Launch Vehicle Telemetry Links

LINK	FREQUENCY MHZ	MODULATION	STAGE	FLIGHT PERIOD (RANGE TIME, SEC)	PERFORMANCE SUMMARY
AF-1	256.2	FM/FM	S-IC	0 to 200	SATISFACTORY
AP-1	244.3	PCM/FM	S-IC	0 to 200	DATA DROPOUTS Range Time (sec) — Duration (sec) 136.8 (intermittent) — 2.9 164.9 — 1.1 168.0 — 2.3
BF-1	241.5	FM/FM	S-II	0 to 784	SATISFACTORY
BF-2	234.0	FM/FM	S-II	0 to 784	DATA DROPOUTS Range Time (sec) — Duration (sec) 101.5 — 1.0 164.9 — 1.1 196.0 — 0.6 205.0 — 1.5
BP-1	248.6	PCM/FM	S-II	0 to 784	
CP-1	258.5	PCM/FM	S-IVB	Flight Duration	SATISFACTORY DATA DROPOUTS Range Time (sec) — Duration (sec) 164.9 — 1.1
DF-1	250.7	FM/FM	IU	Flight Duration	SATISFACTORY DATA DROPOUTS Range Time (sec) — Duration (sec) 164.9 — 1.1
DP-1	245.3	PCM/FM	IU	Flight Duration	UNSATISFACTORY
DP-1B (CCS)	2282.5	PCM/FM	IU	Flight Duration	DATA DROPOUTS Range Time (sec) — Duration (sec) 0.4 (DP-1, DP-1B: AO 270 Multiplexer) — See paragraph 15.3.2 164.9 (DP-1) — 1.1 165.0 (DP-1B) — 5.0 196.0 (DP-1B) — 6.0 10955.9 (DP-1, DP-1B: 410 Multiplexer) — See paragraph 15.3.3

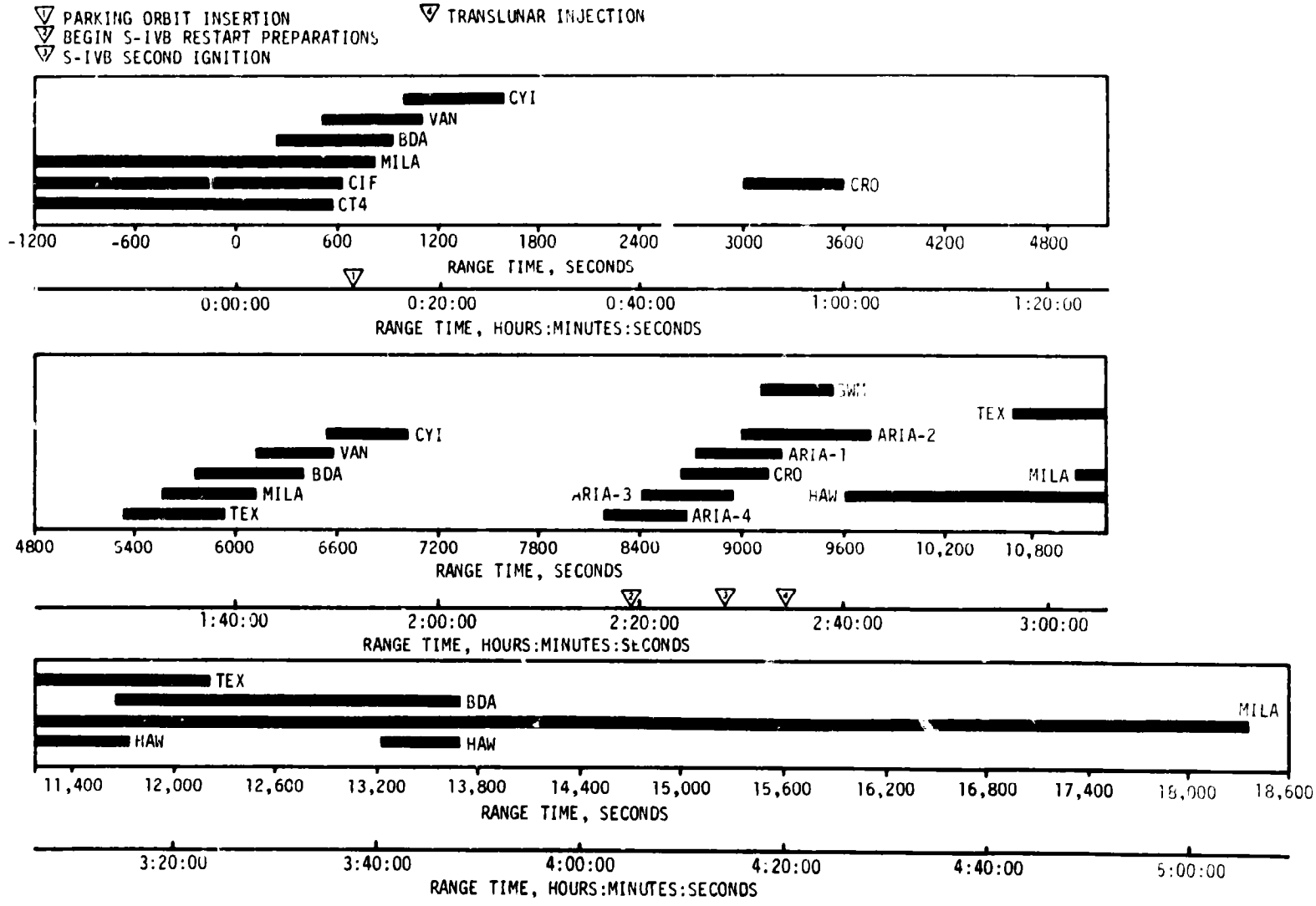

Figure 15-1. VHF Telemetry Coverage Summary

At 0.40 second CP1-A0 word 29 containing the IU 5 volt master measuring supply voltage (6D81) went to the maximum value that the PCM/DDAS assembly could code (1023 digital counts or all ones). This was a change of 120 ±5 millivolts and indicates that the voltage was probably nigher but could not be coded by the PCM/DDAS assembly. However, there was only a slight change in measurement M0001-602 (5 counts or a 31 millivolt change in the 5 volt level) at this same time, although they are measurements of the same voltage. There was also a slight change in at least two other measurements (D0011-603 and D0012-603) that used this same 5 volt master measuring supply. A reason has not yet been established as to why these measurements did not show a more significant increase in value. This disturbance in the 5 volt level lasted 4 seconds, which corresponds to the same time frame for the transient in the DP1-A0 data. This 5 volt master measuring supply is common to both the CP1-A0 and DP1-A0 270 multiplexers. There was no noticeable change at the problem time in the 6D30 battery current or the 6D31 bus voltage which supplies power to the DP1-A0 270 multiplexer. However, the nominal 270 multiplexer current drain is only 0.1 ampere and cannot be identified in the 6D30 current measurement data.

Every time the DP1-A0 270 multiplexer was scheduled to calibrate, there was a disturbance in the bit pattern of the data stream. Engineering tests have shown that this is characteristic of trying to calibrate a "dead box" (power off).

Failure testing is continuing in an attempt to duplicate the complete failure characteristic using an engineering 270 multiplexer.

15.3.3 Loss of H0060-603 Guidance Computer Word

Data transmitted through the 410K multiplexer (S/N 442) was lost at 10,955.861 seconds (03:02:35.861), resulting in the loss of all guidance computer data (H0060-603). This failure occurred between channel 11 frame 10 and channel 23 frame 10 (between 10,955.858 and 10,955.861 seconds [03:02:35.858 and 03:02:35.861]) with the data going to all zeros. The computer word ending in channel 11 frame 10 was a valid computer word. Therefore, the problem occurred in less than 3.336 milliseconds. All computer words for at least 14 seconds prior to this problem area were valid.

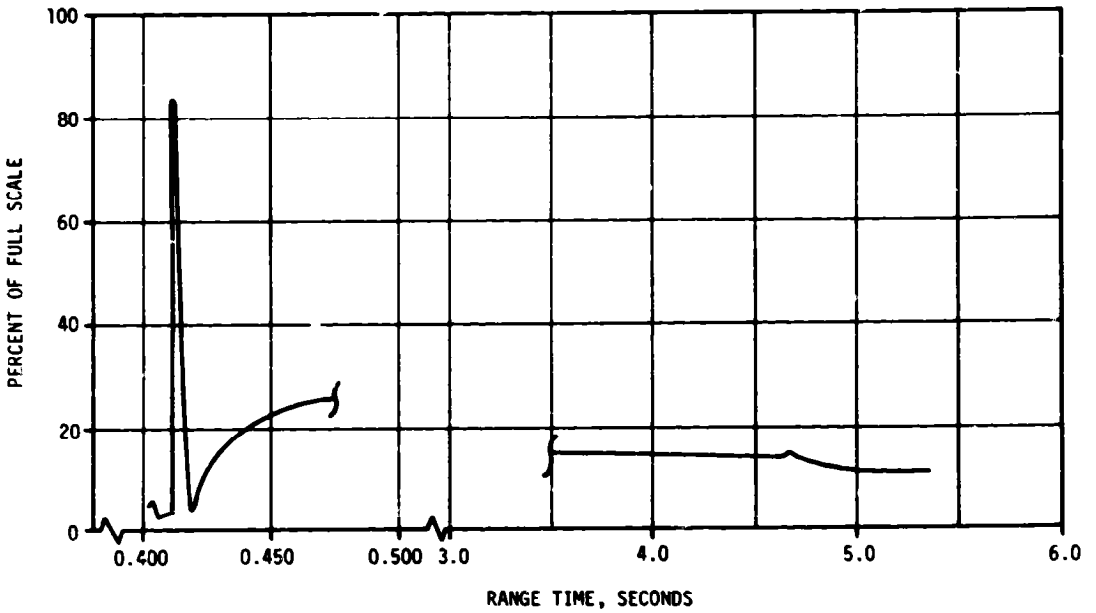

Figure 15-2. DP1-A0 270 Multiplexer Analog Data

The 410K multiplexer is supplied by the 6D30 battery. There was a discernible excursion in the 6D31 bus voltage and the 6D30 battery current at the time of the failure as can be seen in Figures 15-3 and 15-4. The voltage dropped from 28.74 to 28.65 volts while the current rose from 20.72 to 22.52 amperes. This disturbance lasted for 1.162 seconds and then the voltage abruptly increased and the current decreased. When the current decreased, it leveled out at an average of 0.2 ampere lower than the current prior to the problem. The voltage increased to an average of 0.01 volt higher than the voltage prior to the problem. The IBM acceptance test for the 410K multiplexer (S/N 442), showed a current drain of approximately 0.18 ampere. This tends to indicate that the 410K multiplexer ceased to draw current. The first effect seen in the failure sequence was the abrupt loss of data and a sudden increase in current and decrease in battery voltage. The second effect observed was an abrupt return of current to a lower value and tends to indicate involvement of the 410K multiplexer power supply. A simulation of these events using engineering hardware is being attempted.

15.3.4 DP-1 Telemetry RF Output Power Fluctuations

The DP-1 telemetry RF power output measurement, J0029-602, was slightly below the desired level of 15 watts at liftoff and exhibited abrupt changes or level shifts during the flight. These shifts were not significant enough to cause any telemetry data interruptions.

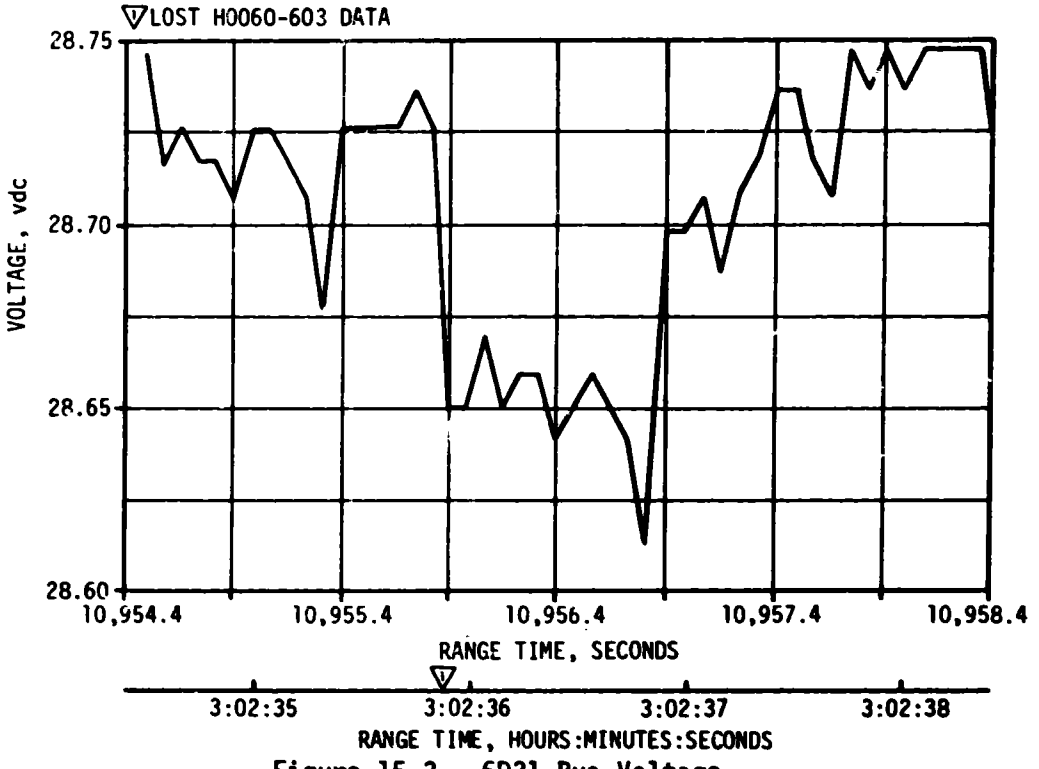

Figure 15-3. 6D31 Bus Voltage

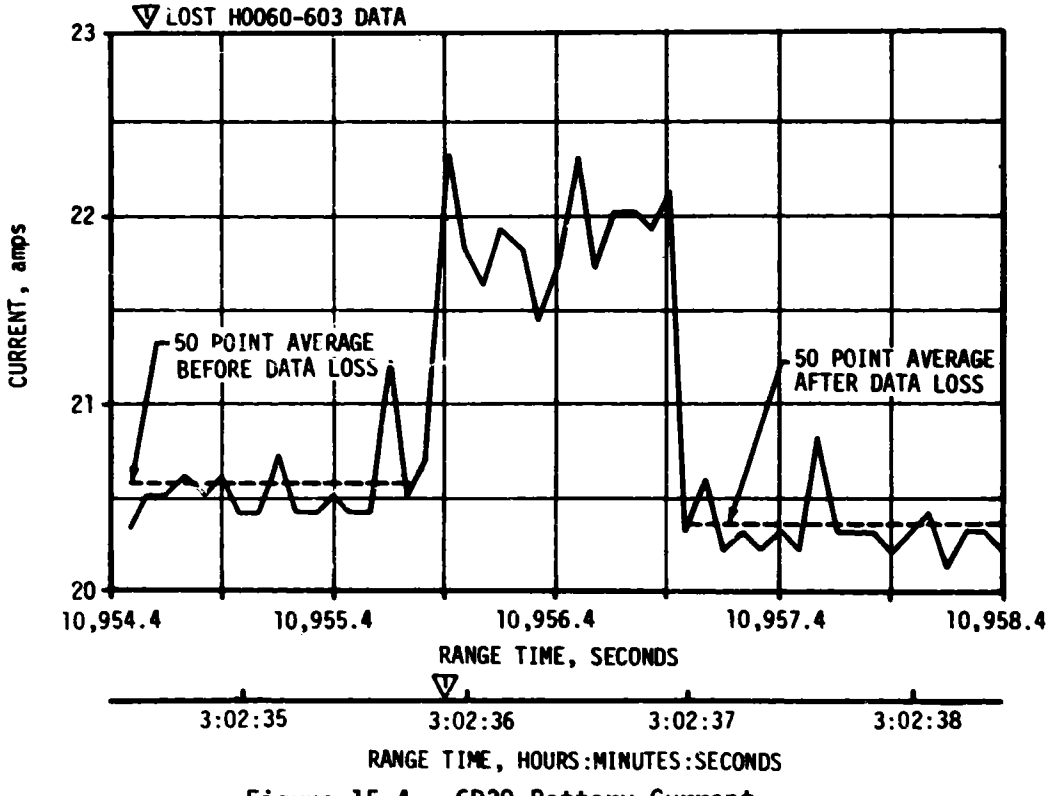

Figure 15-4. 6D30 Battery Current

Evaluation of the DP-1 and DF-1 signal strength data indicates that the problem may have been caused by an intermittent fault in the antenna system which is common to both the DP-1 and DF-1 telemetry links.

Tests are being conducted on engineering antenna subsystems in an attempt to duplicate the observed phenomena.

Prior to launch the DP-1 transmitter was replaced two different times to correct unrelated problems.

15.4 C-BAND RADAR SYSTEM EVALUATION

The C-Band radar performed satisfactorily during flight, although several of the ground stations experienced problems with their equipment which caused some loss of signal. MILA transferred to skin track from 23 to 33 seconds, then resumed beacon track. This action may have been precipitated by phase front disturbances which have been experienced on previous flights. These phase front disturbances are caused by a sudden antenna null or a distorted beacon return and result in erroneous antenna pointing information. The existence of this phenomenon could not be verified since signal strength strip charts were not available.

The BDA FPQ-6 radar experienced two dropouts of less than 60 seconds each at 13,294 seconds (03:41:34) and 13,792 seconds (03:49:52). These dropouts were caused by ground station computer problems.

The MILA/TPQ-18 radar experienced two dropouts because of transmitter overload. One dropout occurred at 19,140 seconds (05:19:00) and lasted for 60 seconds. The second dropout occurred at 23,580 seconds (06:33:00) and lasted for 3 minutes.

A 5-minute dropout was experienced by the BDA/FPQ-6 radar, beginning at 23,760 seconds (06:36:00), possibly because of unfavorable look angles. Another dropout was experienced by the BDA/FPQ-6 radar at 25,540 seconds (07:05:40) and lasted for 2 minutes. The ground station transmitter overloaded and caused this loss.

Patrick Air Force Base (PAFB) used only skin track during their contact time.

BDA indicated final LOS at 28,950 seconds (08:02:30). A summary of available C-Band radar coverage showing AOS and LOS for each station is shown in Figure 15-5.

15.5 SECURE RANGE SAFETY COMMAND SYSTEMS EVALUATION

Telemetered data indicated that the command antennas, receivers/decoders, Exploding Bridge Wire (EBW) networks, and destruct controllers on each powered stage functioned properly during flight. They were in the

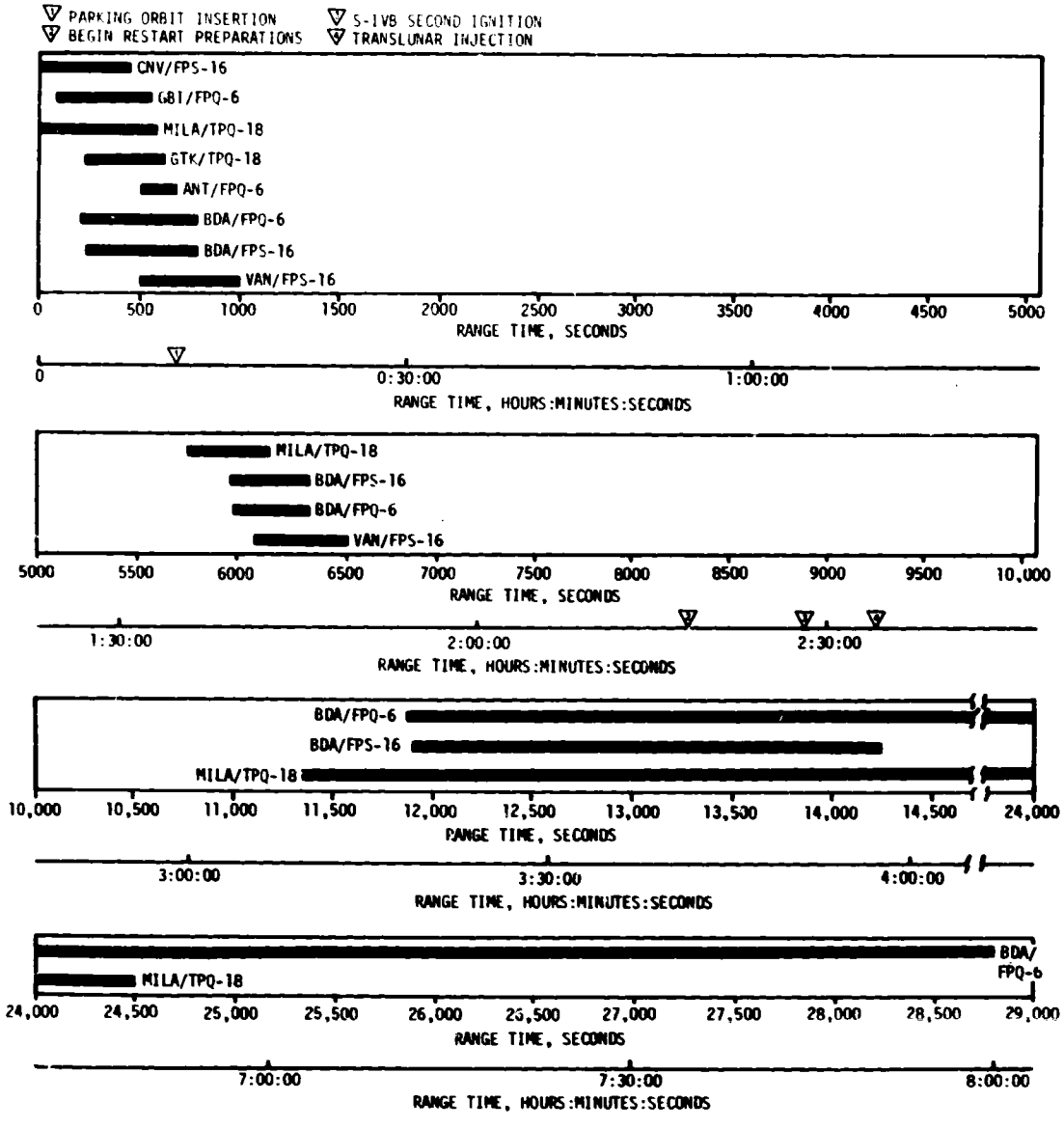

Figure 15-5. C-Band Radar Coverage Summary

required state-of-readiness if flight conditions during the launch had required vehicle destruct. Since no arm/cutoff or destruct commands were required, all data except receiver signal strength remained unchanged during the flight. Power to the S-IVB stage range safety command systems was cutoff at 710.2 seconds by ground command from BDA, thereby deactivating (safing) the systems.

15.6 COMMAND AND COMMUNICATION SYSTEM EVALUATION

The performance of the CCS was excellent. No onboard equipment malfunctions occurred. Ground stations were able to acquire and maintain two-way lock with the CCS until S-IVB/IU lunar impact.

The RF portion of the CCS performed satisfactorily during boost, earth orbit, and translunar coast, with minor exceptions. Downlink data dropouts occurred during S-IC/S-II staging and at S-II second plane separation. Other downlink dropouts were caused by vehicle antenna nulls, multipath effects and station handover. None of these dropouts caused any significant loss of data.

Uplink dropouts during the flight are unknown due to the loss of the uplink CCS AGC measurement, J0076-603, caused by the DP1-A0 telemetry system problem.

The last CCS telemetry data were received at 53,039 seconds (14:43:59) when the telemetry subcarrier was inhibited by a scheduled switch selector command. CRO, GDS, HAW, HSK and MILA indicated LOS at S-IVB/IU lunar impact at 297,473.4 seconds (82:37:53.4). A summary of CCS coverage giving AOS and LOS for each station is shown in Figure 15-6.

The performance of the command section of the CCS was satisfactory. All ground commands transmitted with valid command subcarrier lock were accepted by the onboard equipment on the first transmission. One command was attempted when the subcarrier was not in-lock and was, therefore, not accepted. Seven commands were retransmitted. However, the repetition of these commands were caused by ground station problems. The most significant ground station problem occurred at HSK beginning at 40,961 seconds (11:22:41). Five HSK commands were repeated because the Message Acceptance Pulse (MAP) waiting period of 750 milliseconds was too short for the transmission range at that time. On future flights a change in the MAP waiting period to 1 second after TLI +6 hours should resolve this problem. The CCS command history is shown in Table 15-6.

15.7 GROUND ENGINEERING CAMERAS

In general, ground camera coverage was good. Sixty-five items were received from KSC and evaluated. Two cameras jammed before acquiring requested data. Three cameras had bad timing, one camera was out of

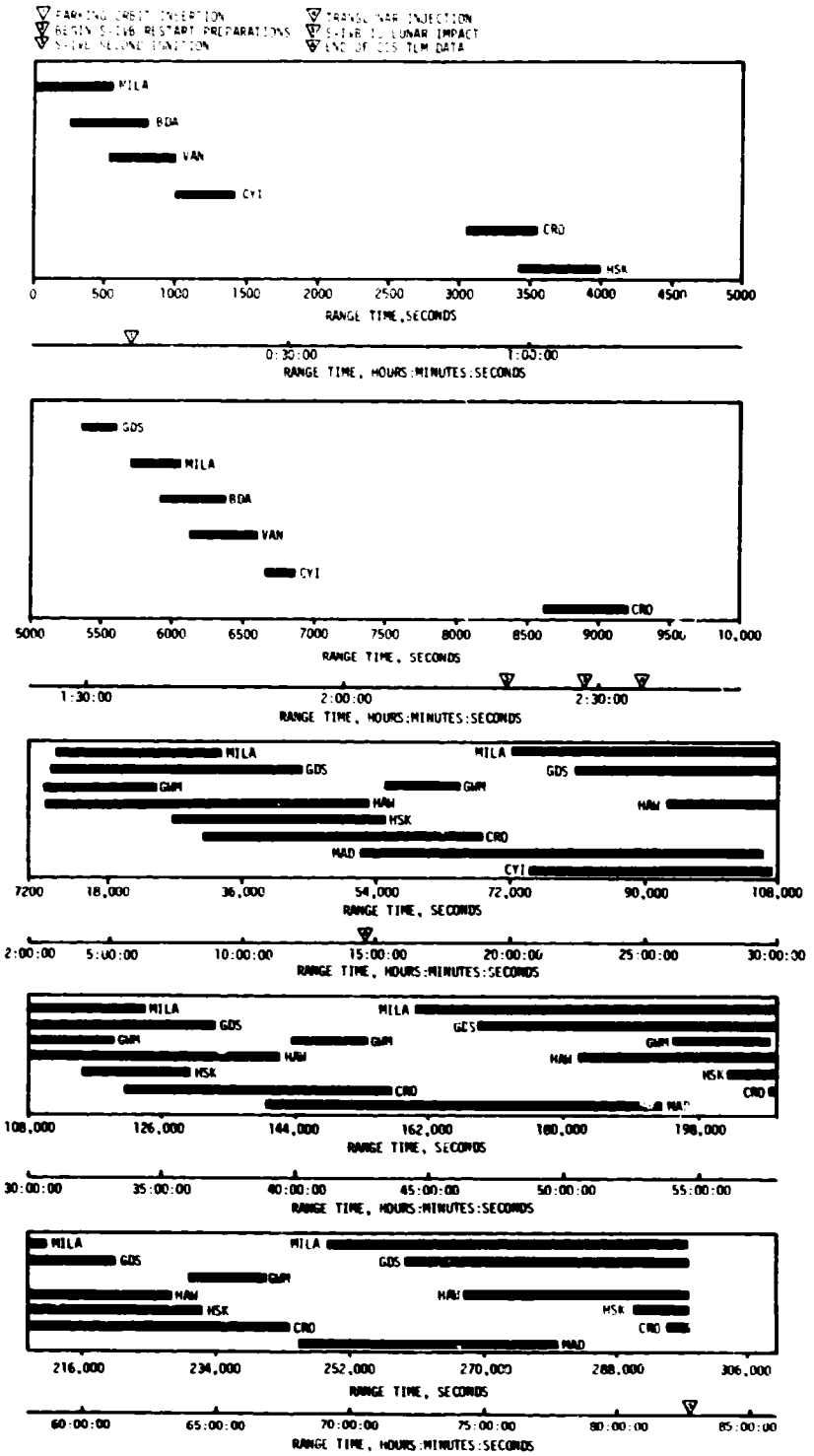

Figure 15-6. CCS Coverage Summary

Table 15-6. Command and Communication System Command History, AS-509

RANGE TIME		TRANSMITTING STATION	COMMAND	NUMBER OF WORDS TRANSMITTED	REMARKS
SECONDS	HRS:MINS:SEC				
21,277	05:54:37	GDS	Terminate	1	Accepted
21,330	05:55:30	GDS	Execute Maneuver B	1	Accepted
21,839	06:03:59	GDS	Initiate Timebase 8	1	Accepted
23,443	06:30:43	GDS	Switch to Low Gain	2	Accepted*
31,421	08:43:41	GDS	Lunar Impact Attitude Correction	7	Accepted
40,961	11:22:41	HSK	Switch to Omni	4	Accepted***
41,114	11:25:14	HSK	Switch to Low Gain	4	Accepted***
41,796	11:36:36	HSK	LV Spin Up	4	Accepted***
41,855	11:37:35	HSK	Terminate	4	Not Accepted**
41,902	11:38:22	HSK	Terminate	4	Accepted***
41,966	11:39:26	HSK	Terminate	4	Accepted***
42,082	11:41:22	HSK	LV Spin Up	7	Accepted****
42,100	11:41:40	HSK	FCC Power Off A	3	Accepted****
42,114	11:41:54	HSK	FCC Power Off B	3	Accepted****
42,151	11:42:31	HSK	Switch to Omni	1	Accepted****

*Command was transmitted twice because the ground station failed to capture the Computer Reset Pulse (CRP).

**Command was retransmitted due to lack of verification pulses after first transmission. Command was not accepted since the command subcarrier was not in lock at this time.

***Commands were accepted by the IU on the first transmission. However, all these commands were retransmitted because the Message Acceptance Pulse (MAP) waiting period was too short.

****Commands were sent in the MAP override mode (command words are sequentially transmitted without waiting for a MAP). This was done to get around the short MAP waiting period problem.

focus, one camera had fogged film, and one camera had a short run. As a result of these eight failures, system efficiency was 88 percent. Only one tracking item (Melbourne Beach) was included in the 65 items because of low cloud coverage.

SECTION 16

MASS CHARACTERISTICS

16.1 SUMMARY

Total vehicle mass, determined from postflight analysis, was within 0.80 percent of prediction from ground ignition through S-IVB stage final shutdown. This small variation indicates that hardware weights, propellant loads, and propellant utilization were close to predicted values during flight.

16.2 MASS EVALUATION

Postflight mass characteristics are compared with final predicted mass characteristics (MSFC Memorandum S&E-ASTN-SAE-70-83) and the operational trajectory (MSFC Memorandum S&E-AERO-MFT-26-71).

The postflight mass characteristics were determined from an analysis of all available actual and reconstructed data from S-IC ignition through S-IVB second burn cutoff. Dry weights of the launch vehicle are based on actual stage weighings and evaluation of the weight and balance log books (MSFC Form 998). Propellant loading and utilization was evaluated from propulsion system performance reconstructions. Spacecraft data were obtained from the Manned Spacecraft Center (MSC).

Differences in dry weights of the inert stages and the loaded spacecraft were all within 0.47 percent of predicted, which was well within acceptable limits.

During S-IC burn phase, the total vehicle mass was less than predicted by 1313.6 kilograms (2896 lbm) (0.03 percent) at ignition, and greater than predicted by 574.2 kilograms (1266 lbm) (0.07 percent) at S-IC/S-II separation. These differences are attributed to: (1) less than predicted S-IC dry weight and propellant loading at ignition; (2) greater than predicted upper stage mass; (3) shorter than predicted S-IC burn resulting in higher residuals. S-IC burn phase total vehicle mass is shown in Tables 16-1 and 16-2.

During S-II burn phase, the total vehicle mass was greater than predicted by 214.5 kilograms (473 lbm) (0.03 percent) at ignition, and less than predicted by 208.2 kilograms (459 lbm) (0.09 percent) at S-II/S-IVB separation. These differences are due primarily to a greater than

predicted upper stage mass and a longer than expected S-II burn. Total vehicle mass for the S-II burn phase is shown in Tables 16-3 and 16-4.

Total vehicle mass during both S-IVB burn phases, as shown in Tables 16-5 through 16-8, was within 0.8 percent of the predicted values. A difference of 244 kilograms (538 lbm) (0.15 percent) from predicted at first burn ignition was due largely to a greater than predicted propellant loading. The difference at completion of second burn was 509 kilograms (1122 lbm) (0.80 percent) resulting from a shorter than expected burn.

A summary of mass utilization and loss, both actual and predicted, from S-IC stage ignition through spacecraft separation is presented in Table 16-9. A comparison of actual and predicted mass, center of gravity, and moment of inertia is shown in Table 16-10.

Table 16-1. Total Vehicle Mass--S IC Burn Phase--Kilograms

EVENTS	GROUND IGNITION		HOLDDOWN ARM RELEASE		CENTER ENGINE CUTOFF		OUTBOARD ENGINE CUTOFF		S-IC/S-II SEPARATION	
	PRED	ACT	PRED	ACT	PRED	ACT	PRED	ACT	PRED	ACT
RANGE TIME--SEC	-6.60	-6.50	0.20	0.20	135.26	135.14	165.04	164.10	165.80	164.80
DRY STAGE	130407.	130321.	130407.	130321.	130407.	130321.	130407.	130321.	130407.	130321.
LOX IN TANK	1476533.	1481490.	1447777.	1449604.	216173.	211300.	1162.	79.	1041.	840.
LOX BELOW TANK	21096.	21156.	21855.	21916.	21840.	21839.	18004.	18329.	15905.	16171.
LOX ULLAGE GAS	189.	191.	216.	244.	2748.	2937.	3318.	3520.	3323.	3547.
FUEL IN TANK	648038.	643667.	637909.	633288.	102618.	100081.	8388.	8696.	7316.	7584.
FUEL BELOW TANK	4313.	4317.	5996.	6000.	5996.	6000.	5958.	5962.	5958.	5962.
FUEL ULLAGE GAS	32.	72.	32.	77.	208.	263.	241.	302.	242.	302.
N2 PURGE GAS	36.	36.	36.	36.	19.	19.	19.	19.	19.	19.
HELIUM IN BOTTLE	288.	288.	288.	284.	112.	98.	79.	59.	78.	58.
FROST	635.	635.	635.	635.	340.	340.	340.	340.	340.	340.
RETROROCKET PROP	1026.	1026.	1026.	1026.	1026.	1026.	1026.	1026.	1026.	1026.
OTHER	239.	104.	239.	104.	239.	104.	239.	104.	239.	104.
TOTAL STAGE	2284837.	2283509.	2246422.	2243539.	484732.	474332.	169188.	169660.	165901.	166261.
TOTAL S-IC/S-II IS	5189.	5170.	5189.	5170.	5189.	5170.	5189.	5170.	5156.	5137.
TOTAL S-II STAGE	488017.	488014.	488027.	488014.	487806.	487793.	487806.	487793.	487806.	487794.
TOT S-II/S-IVB IS	3656.	3655.	3656.	3655.	3656.	3655.	3656.	3655.	3655.	3655.
TOTAL S-IVB STAGE	117991.	118268.	117991.	118268.	117900.	118178.	117900.	118178.	117900.	118178.
TOTAL INSTRU UNIT	2037.	2043.	2037.	2043.	2037.	2043.	2037.	2043.	2037.	2043.
TOTAL SPACECRAFT	50440.	50404.	50440.	50404.	50440.	50404.	50440.	50404.	50440.	50404.
TOTAL UPPERSTAGE	667343.	667558.	667343.	667558.	667031.	667246.	667031.	667246.	666998.	667213.
TOTAL VEHICLE	2952180.	2950866.	2913765.	2911097.	1148763.	1141578.	836219.	836906.	832900.	833474.

Table 16-2. Total Vehicle Mass--S-IC Burn Phase--Pounds Mass

EVENTS	GROUND IGNITION		HOLDDOWN ARM RELEASE		CENTER ENGINE CUTOFF		OUTBOARD ENGINE CUTOFF		S-IC/S-II SEPARATION	
	PRED	ACT	PRED	ACT	PRED	ACT	PRED	ACT	PRED	ACT
RANGE TIME--SEC	-6.60	-6.50	0.20	0.20	135.26	135.14	165.04	164.10	165.80	164.80
DRY STAGE	287500.	287310.	287500.	287310.	287500.	287310.	287500.	287310.	287500.	287310.
LOX IN TANK	3259607.	3266126.	3191802.	3195831.	476581.	465837.	2563.	2160.	2297.	1854.
LOX BELOW TANK	46509.	46643.	48184.	48318.	48149.	48147.	39694.	40410.	35065.	35653.
LOX ULLAGE GAS	418.	423.	477.	538.	6060.	6475.	7315.	7761.	7328.	7778.
FUEL IN TANK	1428679.	1419043.	1406350.	1396161.	226234.	220642.	18494.	19167.	16130.	16722.
FUEL BELOW TANK	9509.	9518.	13219.	13228.	13219.	13228.	13136.	13145.	13136.	13145.
FUEL ULLAGE GAS	71.	160.	71.	170.	459.	580.	532.	666.	534.	668.
N2 PURGE GAS	80.	80.	80.	80.	43.	43.	43.	43.	43.	43.
HELIUM IN BOTTLE	636.	637.	636.	627.	248.	217.	175.	131.	174.	129.
FROST	1400.	1400.	1400.	1400.	750.	750.	750.	750.	750.	750.
RETROROCKET PROP	2264.	2264.	2264.	2264.	2264.	2264.	2264.	2264.	2264.	2264.
OTHER	528.	230.	528.	230.	528.	230.	528.	230.	528.	230.
TOTAL STAGE	5037204.	5033835.	4952514.	4946158.	1068038.	1045773.	372997.	374037.	365751.	366544.
TOTAL S-IC/S-II IS	11441.	11400.	11441.	11400.	11441.	11400.	11441.	11400.	11368.	11327.
TOTAL S-II STAGE	1075917.	1075889.	1075917.	1075889.	1075429.	1075401.	1075429.	1075401.	1075429.	1075401.
TOT S-II/S-IVB IS	8061.	8060.	8061.	8060.	8061.	8060.	8061.	8060.	8061.	8060.
TOTAL S-IVB STAGE	260126.	260738.	260126.	260738.	259926.	260538.	259926.	260538.	259926.	260538.
TOTAL INSTRU UNIT	4492.	4505.	4492.	4505.	4492.	4505.	4492.	4505.	4492.	4505.
TOTAL SPACECRAFT	111203.	111122.	111203.	111122.	111203.	111122.	111203.	111122.	111203.	111122.
TOTAL UPPERSTAGE	1471240.	1471714.	1471240.	1471714.	1470552.	1471026.	1470552.	1471026.	1470479.	1470953.
TOTAL VEHICLE	6508444.	6505548.	6423 54.	6417871.	2532590.	2516749.	1843549.	1845063.	1836230.	1837497.

Table 16-3. Total Vehicle Mass--S-II Burn Phase--Kilograms

EVENTS	S-IC IGNITION		S-II IGNITION		S-II MAINSTAGE		S-II ENGINE CUTOFF		S-II/S-IVB SEPARATION	
	PRED	ACT	PRED	ACT	PRED	ACT	PRED	ACT	PRED	ACT
RANGE TIME--SEC	-6.60	-6.50	167.50	166.50	169.50	168.50	556.90	559.05	557.90	560.00
S-IC/S-II SMALL IS	615.	614.	0.	0.	0.	0.				
S-IC/S-II LARGE S	3957.	3945.	3957.	3945.	3957.	3945.				
S-IC/S-II PROPELLANT	616.	610.	312.	309.	0.	0.				
TOTAL S-IC/S-II IS	5189.	5170.	4270.	4255.	3957.	3945.				
DRY STAGE	35402.	35434.	35402.	35434.	35402.	35434.	35402.	35434.	35402.	35434.
LOX IN TANK	378990.	379139.	378990.	379139.	378534.	378683.	817.	550.	679.	415.
LOX BELOW TANK	737.	737.	736.	737.	800.	800.	787.	787.	787.	787.
LOX ULLAGE GAS	149.	149.	149.	149.	151.	151.	2247.	2247.	2254.	2254.
FUEL IN TANK	72314.	72121.	72308.	72115.	72094.	71900.	1960.	1342.	1505.	1486.
FUEL BELOW TANK	104.	104.	110.	111.	127.	127.	123.	123.	123.	123.
FUEL ULLAGE GAS	58.	58.	58.	58.	58.	59.	595.	595.	599.	599.
INSULATION PURGE GAS	17.	17.	0.	0.	0.	0.				
FROST	204.	204.	0.	0.	0.	0.				
START TANK	13.	13.	13.	13.	2.	2.	2.	2.	2.	2.
OTHER	34.	34.	34.	34.	34.	34.	34.	34.	34.	34.
TOTAL S-II STAGE	488027.	488014.	487806.	487793.	487206.	487193.	41572.	41118.	41389.	40936.
TOT S-II/S-IVB IS	3656.	3655.	3656.	3655.	3656.	3655.	3656.	3655.	3656.	3655.
TOTAL S-IVB STAGE	117991.	118268.	117900.	118178.	117900.	118178.	117900.	118178.	117898.	118175.
TOTAL IU	2037.	2043.	2037.	2043.	2037.	2043.	2037.	2043.	2037.	2043.
TOTAL SPACECRAFT	50440.	50404.	50440.	50404.	50440.	50404.	46347.	46309.	46347.	46309.
TOTAL UPPER STAGE	174125.	174372.	174035.	174281.	174035.	174281.	169941.	170186.	169939.	170184.
TOTAL VEHICLE	667343.	667558.	666111.	666330.	665199.	665421.	211513.	211305.	211329.	211121.

Table 16-4. Total Vehicle Mass--S-II Burn Phase--Pounds Mass

EVENTS	S-IC IGNITION		S-II IGNITION		S-II MAINSTAGE		S-II ENGINE CUTOFF		S-II/S-IVB SEPARATION	
	PRED	ACT	PRED	ACT	PRED	ACT	PRED	ACT	PRED	ACT
RANGE TIME--SEC	-6.60	-6.50	167.50	166.50	169.50	168.50	556.90	559.05	557.90	560.00
S-IC/S-II SMALL IS	1356.	1354.	0.	0.	0.	0.				
S-IC/S-II LARGE IS	8725.	8699.	8725.	8699.	8725.	8699.				
S-IC/S-II PROPELLANT	1360.	1347.	689.	683.	0.	0.				
TOTAL S-IC/S-II IS	11441.	11400.	9414.	9382.	8725.	8699.				
DRY STAGE	78050.	78120.	78050.	78120.	78050.	78120.	78050.	78120.	78050.	78120.
LOX IN TANK	835531.	835859.	835531.	835859.	834525.	834853.	1802.	1213.	1499.	911.
LOX BELOW TANK	1625.	1625.	1624.	1624.	1764.	1764.	1736.	1736.	1736.	1736.
LOX ULLAGE GAS	329.	329.	329.	329.	333.	333.	4955.	4955.	4971.	4971.
FUEL IN TANK	159427.	159001.	159413.	158986.	158941.	158514.	3441.	2960.	3318.	2837.
FUEL BELOW TANK	231.	231.	244.	245.	282.	282.	272.	272.	272.	272.
FUEL ULLAGE GAS	128.	128.	129.	129.	130.	130.	1313.	1313.	1321.	1321.
INSULATION PURGE GAS	38.	38.	0.	0.	0.	0.				
FROST	450.	450.	0.	0.	0.	0.				
START TANK	30.	30.	30.	30.	5.	5.	5.	5.	5.	5.
OTHER	76.	76.	76.	76.	76.	76.	76.	76.	76.	76.
TOTAL S-II STAGE	1075917.	1075889.	1075429.	1075401.	1074107.	1074078.	91651.	90650.	91249.	90249.
TOT S-II/S-IVB IS	8061.	8060.	8061.	8060.	8061.	8060.	8061.	8060.	8061.	8060.
TOTAL S-IVB STAGE	260126.	260738.	259926.	260538.	259926.	260538.	259926.	260538.	259921.	260533.
TOTAL IU	4492.	4505.	4492.	4505.	4492.	4505.	4492.	4505.	4492.	4505.
TOTAL SPACECRAFT	111203.	111122.	111203.	111122.	111203.	111122.	102178.	102095.	102178.	102095.
TOTAL UPPER STAGE	383882.	384425.	383682.	384225.	383682.	384225.	374657.	375198.	374652.	375193.
TOTAL VEHICLE	1471240.	1471714.	1468525.	1469008.	1466514.	1467002.	466308.	465848.	465902.	465442.

Table 16-5. Total Vehicle Mass--S-IVB First Burn Phase--Kilograms

EVENTS	S-IC IGNITION		S-IVB IGNITION		S-IVB MAINSTAGE		S-IVB ENGINE CUTOFF		S-IVB END DECAY	
	PRED	ACT	PRED	ACT	PRED	ACT	PRED	ACT	PRED	ACT
RANGE TIME--SEC	-6.60	-6.50	561.00	563.40	563.50	565.90	702.29	700.56	702.50	700.80
DRY STAGE	11407.	11353.	11384.	11330.	11384.	11330.	11323.	11269.	11323.	11269.
LOX IN TANK	85942.	86230.	85939.	86230.	85814.	86101.	61319.	61476.	61292.	61650.
LOX BELOW TANK	166.	166.	166.	166.	180.	180.	180.	180.	180.	180.
LOX ULLAGE GAS	17.	23.	20.	23.	23.	24.	104.	77.	105.	77.
FUEL IN TANK	19709.	19730.	19704.	19724.	19657.	19674.	14675.	14763.	14665.	14753.
FUEL BELOW TANK	21.	21.	26.	26.	26.	26.	26.	26.	26.	26.
FUEL ULLAGE GAS	20.	19.	20.	19.	20.	20.	63.	61.	64.	61.
ULLAGE ROCKET PROP	53.	53.	9.	8.						
APS PROPELLANT	285.	299.	285.	299.	285.	299.	283.	298.	283.	298.
HELIUM IN BOTTLES	201.	206.	201.	206.	200.	205.	180.	182.	179.	182.
FROST	136.	136.	45.	45.	45.	45.	45.	45.	45.	45.
START TANK GAS	2.	2.	2.	2.	0.	0.	3.	2.	3.	2.
OTHER	25.	24.	25.	24.	25.	24.	25.	24.	25.	24.
TOTAL S-IVB STAGE	117991.	118267.	117933.	118109.	117666.	117933.	88233.	88808.	88195.	88770.
TOTAL IU	2037.	2043.	2037.	2043.	2037.	2043.	2037.	2043.	2037.	2043.
TOTAL SPACECRAFT	46347.	46309.	46347.	46309.	46347.	46309.	46347.	46309.	46347.	46309.
TOTAL UPPERSTAGE	48384.	48352.	48384.	48352.	48384.	48352.	48384.	48352.	48384.	48352.
TOTAL VEHICLE	166375.	166620.	166218.	166462.	166051.	166286.	136617.	137161.	136580.	137123.

Table 16-6. Total Vehicle Mass--S-IVB First Burn Phase--Pounds Mass

EVENTS	S-IC IGNITION		S-IVB IGNITION		S-IVB MAINSTAGE		S-IVB ENGINE CUTOFF		S-IVB END DECAY	
	PRED	ACT	PRED	ACT	PRED	ACT	PRED	ACT	PRED	ACT
RANGE TIME--SEC	-6.60	-6.50	561.00	563.40	563.50	565.90	702.29	700.56	702.50	700.80
DRY STAGE	25155.	25030.	25099.	24979.	25099.	24979.	24964.	24844.	24964.	24844.
LOX IN TANK	189470.	190106.	189466.	190106.	189189.	189821.	135186.	136418.	135126.	136357.
LOX BELOW TANK	367.	367.	367.	367.	397.	397.	397.	397.	397.	397.
LOX ULLAGE GAS	39.	51.	46.	51.	52.	53.	231.	170.	232.	170.
FUEL IN TANK	43452.	43498.	43441.	43486.	43337.	43375.	32355.	32547.	32332.	32525.
FUEL BELOW TANK	48.	48.	58.	58.	58.	58.	58.	58.	58.	58.
FUEL ULLAGE GAS	45.	42.	45.	44.	44.	44.	141.	135.	143.	135.
ULLAGE ROCKET PROP	118.	118.	22.	19.						
APS PROPELLANT	630.	661.	630.	661.	630.	661.	626.	657.	626.	657.
HELIUM IN BOTTLES	445.	455.	444.	455.	443.	453.	397.	403.	396.	401.
FROST	300.	300.	100.	100.	100.	100.	100.	100.	100.	100.
START TANK GAS	5.	5.	5.	5.	1.	1.	7.	5.	7.	5.
OTHER	56.	55.	56.	55.	56.	55.	56.	55.	56.	55.
TOTAL S-IVB STAGE	260126.	260736.	259778.	260386.	259410.	259999.	194521.	195789.	194438.	195706.
TOTAL IU	4492.	4505.	4492.	4505.	4492.	4505.	4492.	4505.	4492.	4505.
TOTAL SPACECRAFT	102178.	102095.	102178.	102095.	102178.	102095.	102178.	102095.	102178.	102095.
TOTAL UPPERSTAGE	106670.	106600.	106670.	106600.	106670.	106600.	106670.	106600.	106670.	106600.
TOTAL VEHICLE	366796.	367336.	366448.	366986.	366080.	366599.	301191.	302389.	301108.	302306.

Table 16-7. Total Vehicle Mass--S-IVB Second Burn Phase--Kilograms

EVENTS	S-IVB IGNITION		S-IVB MAINSTAGE		S-IVB ENGINE CUTOFF		S-IVB END DECAY		SPACECRAFT SEPARATION	
	PRED	ACT	PRED	ACT	PRED	ACT	PRED	ACT	PRED	ACT
RANGE TIME--SEC	8911.90	8912.40	8914.40	8914.90	9268.24	9263.24	9268.40	9263.50	14068.40	20850.00
DRY STAGE	11323.	11269.	11323.	11269.	11323.	11269.	11323.	11269.	11323.	11269.
LOX IN TANK	61225.	61772.	61103.	61650.	1993.	2456.	1965.	2429.	1876.	2340.
LOX BELOW TANK	166.	166.	180.	180.	180.	180.	180.	180.	166.	166.
LOX ULLAGE GAS	172.	120.	172.	120.	261.	204.	261.	205.	261.	205.
FUEL IN TANK	13627.	13775.	13579.	13730.	1060.	1185.	1031.	1174.	991.	1135.
FUEL BELOW TANK	26.	26.	26.	26.	26.	26.	26.	26.	21.	21.
FUEL ULLAGE GAS	159.	149.	160.	150.	279.	283.	279.	283.	279.	283.
APS PROPELLANT	236.	246.	236.	246.	234.	241.	234.	241.	219.	227.
HELIUM IN BOTTLES	143.	170.	143.	170.	79.	114.	79.	113.	79.	113.
FROST	45.	45.	45.	45.	45.	45.	45.	45.	45.	45.
START TANK GAS	2.	2.	0.	0.	3.	2.	3.	2.	3.	2.
OTHER	25.	24.	25.	24.	25.	24.	25.	24.	25.	24.
TOTAL S-IVB STAGE	87154.	87768.	86997.	87614.	15493.	16034.	15456.	15997.	15294.	15835.
TOTAL IU	2037.	2043.	2037.	2043.	2037.	2043.	2037.	2043.	2037.	2043.
TOTAL SPACECRAFT	46347.	46309.	46347.	46309.	46347.	46309.	46347.	46309.	625.	625.
TOTAL UPPERSTAGE	48384.	48352.	48384.	48352.	48384.	48352.	48384.	48352.	2663.	2669.
TOTAL VHICLE	135539.	136121.	135381.	135967.	63878.	64387.	63841.	64350.	17958.	18505.

Table 16-8. Total Vehicle Mass--S-IVB Second Burn Phase--Pounds Mass

EVENTS	S-IVB IGNITION		S-IVB MAINSTAGE		S-IVB ENGINE CUTOFF		S-IVB END DECAY		SPACECRAFT SEPARATION	
	PRED	ACT	PRED	ACT	PRED	ACT	PRED	ACT	PRED	ACT
RANGE TIME--SEC	8911.90	8912.40	8914.40	8914.90	9268.24	9263.24	9268.40	9263.50	14068.40	20850.00
DRY STAGE	24964.	24844.	24964.	24844.	24964.	24844.	24964.	24844.	24964.	24844.
LOX IN TANK	134979.	136134.	134710.	135916.	4394.	5415.	4334.	5357.	4138.	5159.
LOX BELOW TANK	367.	367.	397.	397.	397.	397.	397.	397.	367.	367.
LOX ULLAGE GAS	380.	265.	381.	266.	576.	451.	576.	452.	576.	452.
FUEL IN TANK	30043.	30370.	29937.	30270.	2295.	2614.	2274.	2590.	2185.	2504.
FUEL BELOW TANK	58.	58.	58.	58.	58.	58.	58.	58.	48.	48.
FUEL ULLAGE GAS	352.	330.	353.	332.	616.	626.	616.	626.	616.	626.
APS PROPELLANT	521.	543.	521.	543.	517.	533.	517.	533.	485.	501.
HELIUM IN BOTTLES	316.	376.	316.	375.	176.	252.	176.	251.	176.	251.
FROST	100.	100.	100.	100.	100.	100.	100.	100.	100.	100.
START TANK GAS	5.	5.	1.	1.	7.	5.	7.	5.	7.	5.
OTHER	56.	55.	56.	55.	56.	55.	56.	55.	56.	55.
TOTAL S-IVB STAGE	192143.	193497.	191796.	193157.	34157.	35350.	34076.	35268.	33719.	34912.
TOTAL IU	4492.	4505.	4492.	4505.	4492.	4505.	4492.	4505.	4492.	4505.
TOTAL SPACECRAFT	102178.	102095.	102178.	102095.	102178.	102095.	102178.	102095.	1380.	1 80.
TOTAL UPPERSTAGE	106670.	106600.	106670.	106600.	106670.	106600.	106670.	106600.	5872.	5885.
TOTAL VHICLE	298813.	300097.	298466.	299757.	140827.	141950.	140746.	141868.	39591.	40797.

Table 16-9. Flight Sequence Mass Summary

MASS HISTORY	PREDICTED KG	PREDICTED LBM	ACTUAL KG	ACTUAL LBM
S-IC STAGE, TOTAL	2284836.	5037204.	2283308.	5033835.
S-IC/S-II IS, TOTAL	5189.	11441.	5170.	11400.
S-II STAGE, TOTAL	488027.	1075917.	488014.	1075889.
S-II/S-IVB IS, TOTAL	3656.	8061.	3655.	8060.
S-IVB STAGE, TOTAL	117991.	260126.	118268.	260738.
INSTRUMENT UNIT	2037.	4492.	2043.	4505.
SPACECRAFT, TOTAL	50440.	111203.	50404.	111122.
1ST FLT STG AT IGN	2952179.	6508444.	2950866.	6505548.
THRUST BUILDUP	-38414.	-84690.	-39769.	-87677.
1ST FLT STG AT HDAR	2913765.	6423754.	2911096.	6417871.
FROST	-294.	-650.	-294.	-650.
MAINSTAGE	-2075910.	-4576601.	-2072527.	-4569142.
N2 PURGE GAS	-16.	-37.	-16.	-37.
THRUST DECAY-IE	-821.	-1811.	-849.	-1873.
ENG EXPENDED PROP	-189.	-418.	-189.	-418.
S-II INSUL PURGE	-17.	-38.	-17.	-38.
S-II FROST	-204.	-450.	-204.	-450.
S-IVB FROST	-90.	-200.	-90.	-200.
THRUST DECAY-OE	0.	0.	0.	0.
1ST FLT STG AT OECO	836219.	1843549.	836906.	1845063.
THRUST DECAY-OE	-3286.	-7245.	-3398.	-7493.
S-IC/S-II ULL RKT	-33.	-73.	-33.	-73.
1ST FLT STG AT SEP	832899.	1836230.	833474.	1837497.
STG AT SEPARATION	-165901.	-365751.	-166261.	-366644.
S-IC/S-II SMALL IS	-615.	-1356.	-614.	-1354.
S-IC/S-II ULL RKT	-83.	-184.	-83.	-184.
2ND FLT STG AT SSC	666299.	1468939.	666515.	1469415.
FUEL LEAD	0.	0.	0.	0.
S-IC/S-II ULL RKT	-187.	-414.	-184.	-407.
2ND FLT STG AT IGN	666111.	1468525.	666330.	1469008.
THRUST BUILDUP	-587.	-1296.	-588.	-1297.
START TANK	-11.	-25.	-11.	-25.
S-IC/S-II ULL RKT	-312.	-689.	-309.	-683.
2ND FLT STG AT MS	665199.	1466514.	665420.	1467002.
MAINSTAGE	-445571.	-982317.	-446012.	-983289.
LES	-4093.	-9025.	-4094.	-9027.
S-IC/S-II LARGE IS	-3957.	-8725.	-3945.	-8699.
TD & ENG PROP	-62.	-138.	-62.	-138.
2ND FLT STG AT COS	211513.	466308.	211305.	465848.
THRUST DECAY	-181.	-401.	-181.	-401.
S-IVB ULL RKT PROP	-2.	-5.	-2.	-5.
2ND FLT STG AT SEP	211329.	465902.	211121.	465442.
STG AT SEPARATION	-41389.	-91249.	-40936.	-90249.
S-II/S-IVB IS DRY	-3175.	-7001.	-3172.	-6995.
S-II/S-IVB PROP	-480.	-1060.	-483.	-1065.
S-IVB AFT FRAME	-21.	-48.	-21.	-48.
S-IVB ULL RKT PROP	-1.	-3.	-1.	-3.
S-IVB DET PKG	-1.	-3.	-1.	-3.
3RD FLT STG AT SSC	166258.	366537.	166504.	367079.

Table 16-9. Flight Sequence Mass Summary (Continued)

MASS HISTORY	PREDICTED KG	PREDICTED LBM	ACTUAL KG	ACTUAL LBM
3RD FLT STG 1ST SSC	166258.	366537.	166504.	367079.
ULLAGE ROCKET PROP	-39.	-88.	-42.	-93.
FUEL LEAD	0.	0.	0.	0.
3RD FLT STG 1ST IGN	166218.	366448.	166462.	366986.
ULLAGE ROCKET PROP	-9.	-22.	-8.	-19.
START TANK	-1.	-4.	-1.	-4.
THRUST BUILDUP	-155.	-342.	-165.	-364.
3RD FLT STG 1ST MS	166051.	366080.	166286.	366599.
ULLAGE ROCKET CASE	-61.	-135.	-61.	-135.
MAINSTAGE	-29370.	-64750.	-29062.	-64071.
APS	-1.	-4.	-1.	-4.
3RD FLT STG 1ST COS	136617.	301191.	137161.	302389.
THRUST DECAY	-37.	-82.	-37.	-83.
3RD FLT STG 1ST ETD	136580.	301108.	137123.	302306.
ENGINE PROP	-18.	-40.	-18.	-40.
FUEL TANK LOSS	-942.	-2078.	-877.	-1935.
LOX TANK LOSS	-14.	-31.	-37.	-83.
APS	-47.	-105.	-51.	-114.
START TANK	-0.	-2.	0.	0.
O2/H2 BURNER	-7.	-16.	-7.	-16.
3RD FLT STG 2ND SSC	135549.	298835.	136130.	300117.
FUEL LEAD	-9.	-22.	-9.	-20.
3RD FLT STG 2ND IGN	135539.	298813.	136121.	300097.
START TANK	-1.	-4.	-1.	-4.
THRUST BUILDUP	-155.	-343.	-152.	-336.
3D FLT STG 2ND MS	135381.	298466.	135967.	299757.
MAINSTAGE	-71501.	-157634.	-71575.	-157797.
APS	-1.	-4.	-4.	-10.
3RD FLT STG 2ND COS	63878.	140827.	64387.	141950.
THRUST DECAY	-36.	-81.	-37.	-82.
3RD FLT STG 2ND ETD	63841.	140746.	64350.	141868.
JETTISON SLA	-1171.	-2583.	-1171.	-2582.
CSM	-29290.	-64575.	-29233.	-64448.
S-IVB STAGE LOSS	-97.	-214.	-97.	-214.
STRT TRANS/DOCK	33281.	73374.	33848.	74624.
CSM	29290.	64575.	29233.	64448.
END TRANS/DOCK	62572.	137949.	63081.	139072.
CSM	-29290.	-64575.	-29233.	-64448.
LM	-15258.	-33640.	-15279.	-33685.
S-IVB STAGE LOSS	-64.	-142.	-64.	-142.
LAU VEH AT S/C SEP	17958.	39591.	18505.	40797.
S/C NOT SEPARATED	-625.	-1380.	-625.	-1380.
IU	-2037.	-4492.	-2043.	-4505.
S-IVB STAGE	-15294.	-33719.	-15835.	-34912.

Table 16-10. Mass Characteristics Comparison

EVENT		MASS		LONGITUDINAL C.G. (X STA.)		RADIAL C.G.		ROLL MOMENT OF INERTIA		PITCH MOMENT OF INERTIA		YAW MOMENT OF INERTIA	
		KILO POUNDS	O/O DEV.	METERS INCHES	DELTA	METERS INCHES	DELTA	KG-M2 X10-6	O/O DEV.	KG-M2 X10-6	O/O DEV.	KG-M2 X10-6	O/O DEV.
S-IC STAGE DRY	PRED	130408. 287500.		9.326 367.2		0.0594 2.3409		2.506		16.508		16.434	
	ACTUAL	130322. 287310.	-0.06	9.326 367.2	0.000 0.00	0.0594 2.3409	0.0000 0.0000	2.504	-0.06	16.498	-0.06	16.423	-0.06
S-IC/S-II INTERSTAGE, TOTAL	PRED	5190. 11441.		41.628 1638.9		0.1508 5.9396		0.132		0.079		0.079	
	ACTUAL	5171. 11400.	-0.35	41.628 1638.9	0.000 0.00	0.1508 5.9396	0.0000 0.0000	0.131	-0.35	0.078	-0.35	0.079	-0.35
S-II STAGE, DRY	PRED	35403. 78050.		47.894 1885.6		0.1772 6.9778		0.577		1.944		1.956	
	ACTUAL	35435. 78120.	0.09	47.894 1885.6	0.000 0.00	0.1772 6.9778	0.0000 0.0000	0.577	0.09	1.946	0.09	1.958	0.09
S-II/S-IVB INTERSTAGE, TOTAL	PRED	3656. 8061.		66.471 2617.0		0.0647 2.5495		0.065		0.044		0.044	
	ACTUAL	3656. 8060.	-0.00	66.471 2617.0	0.000 0.00	0.0647 2.5495	0.0000 0.0000	0.065	-0.00	0.044	-0.00	0.044	-0.00
S-IVB STAGE, DRY	PRED	11408. 25150.		72.534 2855.7		0.2265 8.9196		0.082		0.301		0.299	
	ACTUAL	11353. 25030.	-0.47	72.534 2855.7	0.000 0.00	0.2265 8.9196	0.0000 0.0000	0.082	-0.47	0.299	-0.47	0.298	-0.47
VEHICLE INSTRUMENT UNIT	PRED	2038. 4492.		82.407 3244.4		0.4721 18.5884		0.019		0.010		0.009	
	ACTUAL	2043. 4505.	0.29	82.407 3244.4	0.000 0.0018.5884	0.4721	0.0000 0.0000	0.019	0.29	0.010	0.29	0.000	-99.86
SPACECRAFT, TOTAL	PRED	50441. 111203.		91.544 3604.1		0.1093 4.3046		0.092		1.603		1.606	
	ACTUAL	50404. 111122.	-0.06	91.541 3604.0	-0.002 -0.09	0.1106 4.3566	0.0013 0.0519	0.092	-0.44	1.605	0.11	1.608	0.11

Table 16-10. Mass Characteristics Comparison (Continued)

EVENT		MASS		LONGITUDINAL C.G. (X STA.)		RADIAL C.G.		ROLL MOMENT OF INERTIA		PITCH MOMENT OF INERTIA		YAW MOMENT OF INERTIA	
		KILO POUNDS	D/D DEV.	METERS INCHES	DELTA	METERS INCHES	DELTA	KG-M2 X10-6	D/D DEV.	KG-M2 X10-6	D/D DEV.	KG-M2 X10-6	D/D DEV.
		2952181.		30.347		0.0039							
	PRED	6508444.		1194.7		0.1565		3.582		880.489		880.489	
1ST FLIGHT STAGE AT IGNITION													
		2950868.		30.372	0.025	0.0042	0.0002						
	ACTUAL	6505550.	-0.03	1195.7	0.98	0.1655	0.0090	3.581	-0.000	877.577	-0.009	877.478	-0.009
		2913766.		30.294		0.0042							
	PRED	6423754.		1192.6		0.1655		3.617		881.471		881.392	
1ST FLIGHT STAGE AT HOLDDOWN ARM RELEASE													
		2911098.		30.318	0.024	0.0042	0.0000						
	ACTUAL	6417873.	-0.08	1193.6	0.95	0.1655	0.0000	3.617	-0.000	880.910	-0.010	880.830	-0.010
		836220.		46.425		0.0144							
	PRED	1843548.		1827.7		0.5700		3.603		443.741		443.665	
1ST FLIGHT STAGE AT OUTBOARD ENGINE CUTOFF SIGNAL													
		836907.		46.410	-0.015	0.0141	-0.0003						
	ACTUAL	1845063.	0.08	1827.1	-0.59	0.5571	-0.0129	3.602	-0.001	444.295	0.12	444.219	0.12
		832900.		46.569		0.0144							
	PRED	1836229.		1833.4		0.5700		3.601		439.345		439.269	
1ST FLIGHT STAGE AT SEPARATION													
		833475.		46.558	-0.011	0.0143	-0.0000						
	ACTUAL	1837497.	0.07	1833.0	-0.43	0.5664	-0.0035	3.600	-0.001	439.761	0.09	439.685	0.09
		666300.		55.792		0.0170							
	PRED	1468939.		2196.5		0.6700		0.968		136.508		136.525	
2ND FLIGHT STAGE AT START SEQUENCE COMMAND													
		666516.		55.793	0.001	0.0177	0.0007						
	ACTUAL	1469415.	0.03	2196.5	0.03	0.7000	0.0299	0.968	-0.000	136.524	0.01	136.539	0.02
		665200.		55.804		0.0172							
	PRED	1466514.		2197.0		0.6800		0.957		136.369		136.395	
2ND FLIGHT STAGE AT MAINSTAGE													
		665421.		55.805	0.000	0.0177	0.0005						
	ACTUAL	1467002.	0.03	2197.0	0.03	0.7000	0.0199	0.956	-0.003	136.407	0.01	136.421	0.02
		211514.		71.244		0.0518							
	PRED	466308.		2804.9		2.0406		0.859		44.492		44.498	
2ND FLIGHT STAGE AT CUTOFF SIGNAL													
		211305.		71.295	0.050	0.0538	0.0020						
	ACTUAL	465848.	-0.09	2806.8	1.98	2.1203	0.0797	0.855	-0.000	44.475	-0.07	44.489	-0.06

Table 16-10. Mass Characteristics Comparison (Continued)

EVENT		MASS		LONGITUDINAL C.G. (X STA.)		RADIAL C.G.		ROLL MOMENT OF INERTIA		PITCH MOMENT OF INERTIA		YAW MOMENT OF INERTIA	
		KILO POUNDS	O/O DEV.	METERS INCHES	DELTA	METERS INCHES	DELTA	KG-M2 X10-6	O/O DEV.	KG-M2 X10-6	O/O DEV.	KG-M2 X10-6	O/O DEV.
		211330.		71.266		0.0518							
	PRED	465901.		2805.7		2.0406		0.855		44.366		44.372	
2ND FLIGHT STAGE AT SEPARATION													
		211121.		71.318	0.051	0.0541	0.0022						
	ACTUAL	465442.	-0.09	2807.8	2.01	2.1303	0.0897	0.855	-0.00	44.049	-0.70	44.062	-0.69
		166259.		77.212		0.0361							
3RD FLIGHT STAGE AT 1ST START SEQUENCE COMMAND	PRED	366537.		3039.8		1.4239		0.201		13.545		13.544	
		166504.		77.201	-0.011	0.0360	-0.0001						
	ACTUAL	367079.	0.15	3039.4	-0.44	1.4182	-0.0056	0.200	-0.21	13.540	-0.03	13.538	-0.03
		166218.		77.212		0.0361							
3RD FLIGHT STAGE AT 1ST IGNITION	PRED	366448.		3039.8		1.4239		0.201		13.546		13.545	
		166462.		77.201	-0.011	0.0360	-0.0001						
	ACTUAL	366986.	0.15	3039.4	-0.44	1.4182	-0.0056	0.200	-0.21	13.541	-0.03	13.539	-0.03
		166091.		77.214		0.0361							
3RD FLIGHT STAGE AT 1ST MAINSTAGE	PRED	366079.		3039.9		1.4239		0.201		13.544		13.543	
		166287.		77.203	-0.010	0.0360	-0.0001						
	ACTUAL	366599.	0.14	3039.5	-0.41	1.4182	-0.0056	0.200	-0.21	13.539	-0.03	13.537	-0.03
		136618.		78.095		0.0436							
3RD FLIGHT STAGE AT 1ST CUTOFF SIGNAL	PRED	301190.		3074.6		1.7203		0.200		12.743		12.741	
		137161.		78.066	-0.029	0.0434	-0.0002						
	ACTUAL	302389.	0.40	3073.9	-1.14	1.7095	-0.0108	0.199	-0.22	12.735	0.09	12.733	0.09
		136580.		78.097		0.0436							
3RD FLIGHT STAGE AT 1ST END THRUST DECAY. START COAST	PRED	301108.		3074.6		1.7203		0.200		12.742		12.740	
		137124.		78.068	-0.029	0.0434	-0.0002						
	ACTUAL	302306.	0.40	3073.9	-1.14	1.7095	-0.0108	0.199	-0.22	12.733	0.09	12.731	0.09
		135549.		78.102		0.0437							
3RD FLIGHT STAGE AT 2ND START SEQUENCE COMMAND	PRED	298835.		3074.9		1.7218		0.199		12.740		12.739	
		136131.		78.074	-0.027	0.0435	-0.0001						
	ACTUAL	300117.	0.43	3073.8	-1.09	1.7143	-0.0075	0.199	-0.16	12.730	0.08	12.728	0.07

Table 16-10. Mass Characteristics Comparison (Continued)

EVENT		MASS		LONGITUDINAL C.G. (X STA.)		RADIAL C.G.		ROLL MOMENT OF INERTIA		PITCH MOMENT OF INERTIA		YAW MOMENT OF INERTIA	
		KILO POUNDS	O/O DEV.	METERS INCHES	DELTA	METERS INCHES	DELTA	KG-M2 X10-6	O/O DEV.	KG-M2 X10-6	O/O DEV.	KG-M2 X10-6	O/O DEV.
		135539.		78.101		0.0437							
	PRED	298812.		3074.8		1.7218		0.199		12.741		12.740	
3RD FLIGHT STAGE AT 2ND IGNITION		136122.		78.074	-0.027	0.0435	-0.0001						
	ACTUAL	300097.	0.43	3073.7	-1.09	1.7143	-0.0075	0.199	-0.16	12.751	0.08	12.750	0.08
		135382.		78.107		0.0437							
	PRED	298465.		3075.0		1.7218		0.199		12.736		12.737	
3RD FLIGHT STAGE AT 2ND MAINSTAGE		139968.		78.079	-0.027	0.0435	-0.0001						
	ACTUAL	299757.	0.43	3073.9	-1.09	1.7143	-0.0075	0.199	-0.16	12.747	0.08	12.746	0.07
		63878.		85.787		0.0907							
3RD FLIGHT STAGE AT 2ND CUTOFF SIGNAL	PRED	140827.		3377.4		3.5711		0.198		5.335		5.334	
		64387.		85.649	-0.138	0.0904	-0.0002						
	ACTUAL	141950.	0.80	3372.0	-5.43	3.5623	-0.0087	0.198	-0.15	5.469	2.51	5.468	2.51
		63841.		85.796		0.0907							
3RD FLIGHT STAGE AT 2ND END THRUST DECAY	PRED	140746.		3377.8		3.5711		0.198		5.326		5.324	
		64350.		85.658	-0.138	0.0904	-0.0002						
	ACTUAL	141868.	0.80	3372.3	-5.43	3.5623	-0.0087	0.198	-0.15	5.460	2.52	5.458	2.52
		33217.		78.806		0.0798							
	PRED	73231.		3102.6		3.1437		0.142		1.691		1.688	
CSM SEPARATED		33784.		78.669	-0.137	0.0794	-0.0003						
	ACTUAL	74482.	1.71	3097.2	-5.40	3.1284	-0.0153	0.142	0.00	1.736	2.62	1.732	2.60
		62508.		85.256		0.1252							
	PRED	137806.		3356.5		4.9309		0.189		4.747		4.742	
CSM DOCKED		63018.		85.115	-0.140	0.1241	-0.0010						
	ACTUAL	138930.	0.82	3350.9	-5.53	4.8892	-0.0416	0.189	-0.13	4.869	2.57	4.863	2.56
		17958.		73.697		0.1511							
	PRED	39591.		2899.8		5.9526		0.111		0.621		0.617	
SPACECRAFT SEP-ARATED		18505.		73.555	-0.102	0.1504	-0.0007						
	ACTUAL	40797.	3.05	2895.8	-4.03	5.9222	-0.0303	0.111	-0.03	0.632	1.69	0.627	1.65

SECTION 17

LUNAR IMPACT

17.1 SUMMARY

All aspects of the S-IVB/Instrument Unit (IU) Lunar Impact objective were accomplished successfully except the precise determination of the impact point. The final impact solution is expected to satisfy the mission objective. At 297,472.17 seconds (82:37:52.17) (actual time of occurrence at the moon), the S-IVB/IU impacted the lunar surface at approximately 8.07 degrees south latitude and 26.04 degrees west longitude, which is approximately 294 kilometers (159 n mi) from the target of 1.596 degrees south latitude and 33.25 degrees west longitude. Impact velocity was 2543 m/s (8343 ft/s). The mission objectives were to maneuver the S-IVB/IU such that it would have at least a 50 percent probability of impacting the lunar surface within 350 kilometers (189 n mi) of the target, and to determine the actual impact point within 5 kilometers (2.7 n mi), and the time of impact within 1 second.

17.2 TIME BASE 8 MANEUVERS

Following Command and Service Module (CSM)/Lunar Module (LM) ejection, the S-IVB/IU was maneuvered to an inertially fixed attitude as required for the evasive burn. Time base 8 (T_8) was initiated 6392 seconds later than nominal at 21,840 seconds (06:04:00) vehicle time. The delay in initiating T_8 was directly due to the problems experienced with the CSM/LM docking. The Auxiliary Propulsion System (APS) ullage engines were then burned for 80 seconds to provide a near nominal spacecraft/launch vehicle separation velocity. At 22,423 seconds (06:13:43) vehicle time, the stage maneuvered to the Continuous Vent System (CVS)/LOX dump attitude. The initial lunar targeting velocity change was then accomplished by means of a 300-second duration CVS vent and a 48-second duration LOX dump. The velocity change resulting from the CVS vent was larger than nominal due to the increased pressure resulting from the delay in the T_8 event. The velocity change resulting from the LOX dump was near nominal.

The final lunar impact targeting maneuver was accomplished by a commanded 252-second APS burn at a commanded local horizontal attitude of 222 degrees pitch and -14 degrees yaw. This APS burn, premission planned for

23,374.2 seconds (06:29:34.2), was initiated late at 32,399 seconds (08:59:59) vehicle time as a result of the delay in T_8 initiation and to allow time for adequate ground tracking. The burn provided an actual velocity change which was near the required value that was determined in real time. The attitude and duration for this final APS burn were determined in real time by the Lunar Impact Team at the Huntsville Operations Support Center (HOSC) based on the APS vector provided by the Mission Control Center (MCC). Loss of the IU DP1-A0 data and IU guidance computer data (See paragraph 15.3) created uncertainties as to actual IU systems status and prevented real time use of telemetered attitude and delta velocity data. However the remaining telemetered data available plus crew observations were sufficient for conduct of the lunar impact operations in an effective manner.

Table 17-1 shows the actual and nominal maneuver duration times, velocity increments along the S-IVB/IU longitudinal body axis, and maneuver attitudes for the various lunar targeting events during T_8. Figure 17-1 shows the velocity change profile during T_8.

Due to the late initiation of T_8 the lunar impact commands were given at a point further from earth than ever before. The communications aspect of the late commands is discussed in paragraph 15.6.

17.3 TRAJECTORY EVALUATION

Figure 17-2 shows the radius and space-fixed velocity (earth centered) profiles from the APS lunar impact burn to lunar impact. Table 17-2 shows the actual and nominal geocentric orbit parameters following the final impact maneuver. The orbit parameters are based on two-body calculations.

17.4 LUNAR IMPACT CONDITION

Figure 17-3 shows various impact points relative to the target and seismometer locations. The impact parameters and miss distances are presented in Table 17-3. The distance from the impact point to the target is 294 kilometers (159 n mi) which is within the 350-kilometer (189 n mi) mission objective. The distance from the impact point to the seismometer is 175 kilometers (94 n mi).

A summary of impact times recorded by the various tracking sites is shown in Table 17-4. The average of the recorded times was used as the best available time of impact, and is considered accurate to within 0.05 second.

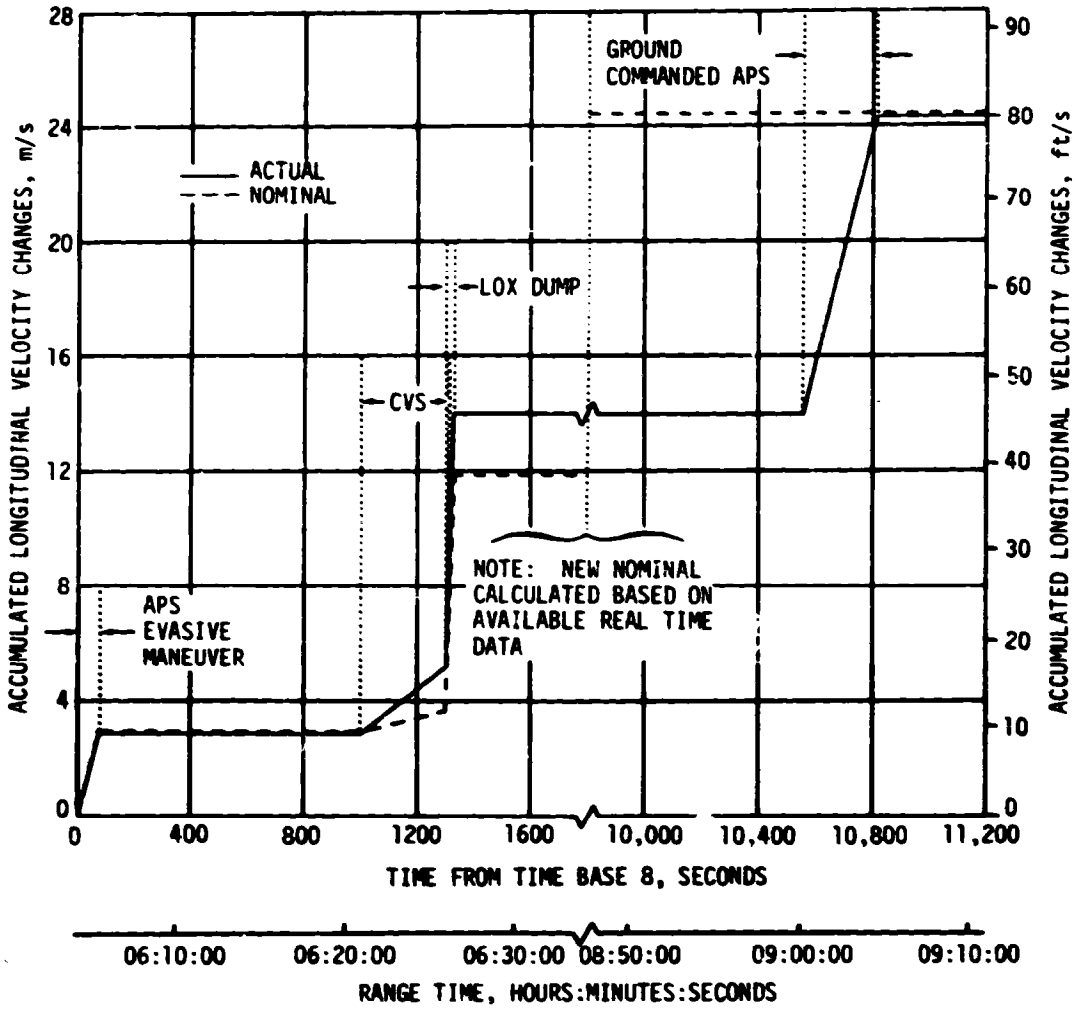

Figure 17-1. Accumulated Longitudinal Velocity Change During Time Base 8

17.5 TRACKING

Approximately 80 hours of S-IVB/IU tracking data, from Translunar Injection (TLI) to lunar impact, were obtained. Figure 17-4 shows the data considered by Goddard Space Flight Center (GSFC) in the orbit and impact location determinations. Table 17-5 lists the tracking sites, their configuration sizes, and abbreviations used.

An S-IVB/IU tumble rate of approximately 10 revolutions per hour caused the range-rate data to have relatively high non-Gaussian noise. This noise has hindered an accurate determination of the impact point to date.

The final solution of the actual impact point is expected to be accurate to within 0.10 degree in latitude and 0.05 degree in longitude which is within a region having dimensions of approximately 3.4 kilometers (1.8 n mi).

Table 17-1. Lunar Targeting Maneuvers

PARAMETER	ACTUAL	NOMINAL	ACT-NOM
START OF TIME BASE 8			
Range Time hr:min:sec (sec)	06:04:00 (21,840)	04:17:28 (15,448)	01:46:32 (6,392)
APS EVASIVE BURN			
Initiation, sec from T_8	1	1	0
Duration, sec	80	80	0
Velocity Increment, m/s (ft/s)	2.90 (9.51)	2.98 (9.78)	-0.08 (-0.27)
Local Horizontal Attitude			
pitch, deg	189	176	13
yaw, deg	40	40	0
CVS VENT			
Initiation, sec from T_8	1,000	1,000	0
Duration, sec	300	300	0
Velocity Increment, m/s (ft/s)	2.30 (7.55)	0.44 (1.44)	1.86 (6.11)
Local Horizontal Attitude			
pitch, deg	225	225	0
yaw, deg	-10	-10	0
LOX DUMP			
Initiation, sec from T_8	1,280	1,280	0
Duration, sec	48	48	0
Velocity Increment, m/s (ft/s)	8.82 (28.94)	8.30 (27.23)	0.52 (1.71)
Local Horizontal Attitude			
pitch, deg	225	225	0
yaw, deg	-10	-10	0
APS LUNAR IMPACT BURN*			
Initiation, sec from T_8	10,558	10,560	-2
Duration, sec	252	252	0
Velocity Increment, m/s (ft/s)	10.27 (33.69)	10.42 (34.19)	-0.15 (-0.50)
Local Horizontal Attitude			
pitch, deg	222	222	0
yaw, deg	-14	-14	0

NOTE: Range times used are times of occurrence at the vehicle, reference Figure 2-1.

*Nominals for APS LUNAR IMPACT BURN calculated in real time

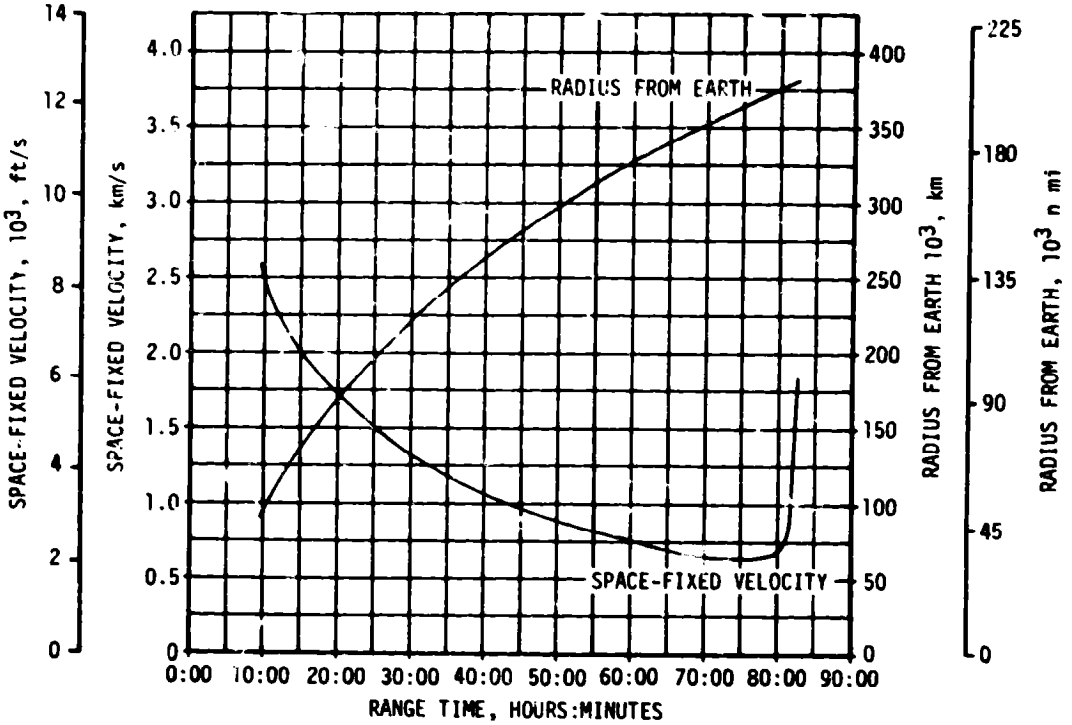
SPACE-FIXED VELOCITY, 10³, ft/s
SPACE-FIXED VELOCITY, km/s
RADIUS FROM EARTH 10³, km
RADIUS FROM EARTH, 10³ n mi
RADIUS FROM EARTH
SPACE-FIXED VELOCITY
RANGE TIME, HOURS:MINUTES
0:00 10:00 20:00 30:00 40:00 50:00 60:00 70:00 80:00 90:00

Figure 17-2. Lunar Impact Trajectory Radius and Space-Fixed Velocity Profiles

Table 17-2. Geocentric Orbit Parameters Following APS Lunar Impact Burn

PARAMETER	ACTUAL	NOMINAL	ACT-NOM
Semimajor Axis, km (n mi)	216,820 (117,073)	217,729 (117,564)	-909 (-491)
Eccentricity	0.970	0.970	0.000
C_3* km^2/s^2 ($n\ mi^2/s^2$)	-1.838 (-0.536)	-1.831 (-0.534)	-0.007 (-0.002)
Perigee Radius, km (n mi)	6484 (3501)	6455 (3485)	29 (16)

* Twice the specific energy

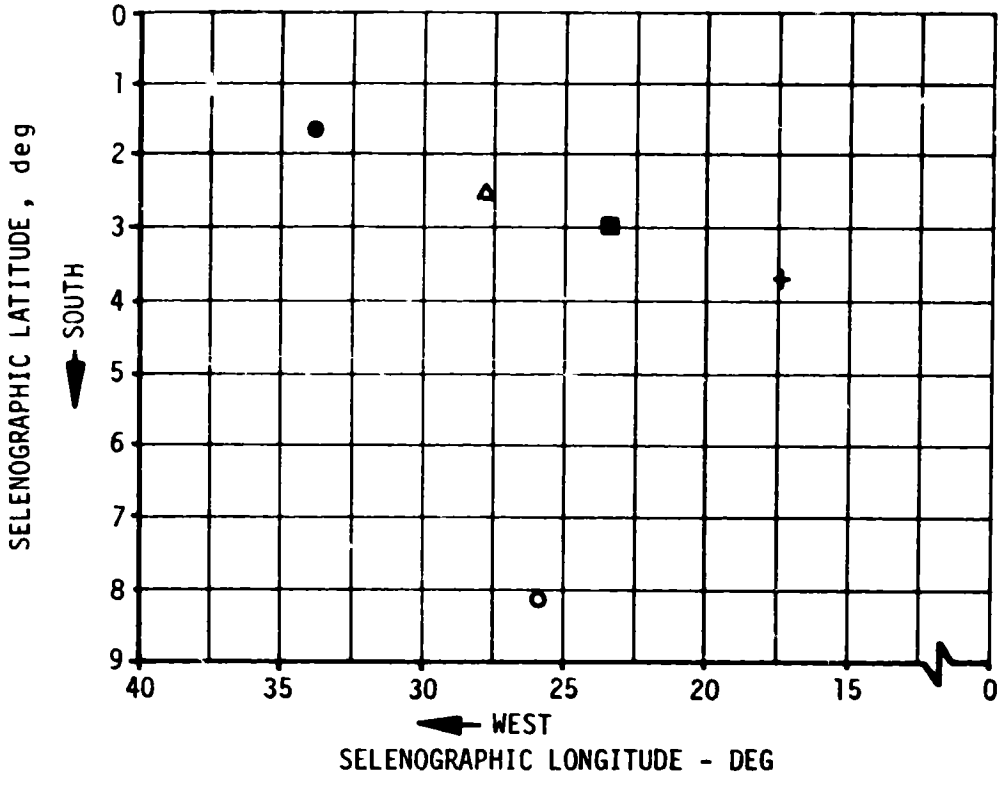

LEGEND:

- O APOLLO 14 LUNAR IMPACT ACTUAL
  AS-509 (8.07 DEG SOUTH - 26.04 DEG WEST)
- \+ APOLLO 14 LANDING SITE
  AS-509 (3.67 DEG SOUTH - 17.49 DEG WEST)
- ■ APOLLO 12 SEISMOMETER
  AS-507 (2.99 DEG SOUTH - 23.34 DEG WEST)
- △ APOLLO 13 LUNAR IMPACT ACTUAL
  AS-508 (2.5 DEG SOUTH - 27.9 DEG WEST)
- ● APOLLO 14 LUNAR IMPACT TARGET
  AS-509 (1.596 DEG SOUTH - 33.250 DEG WEST)

Figure 17-3. Comparison of Lunar Impact Points

Table 17-3. S-IVB/IU Lunar Impact Parameters

PARAMETER AT IMPACT	ACTUAL	NOMINAL	ACT-NOM
Stage Mass, kg (lbm)	~13,987 (~30,836)	13,987 (30,836)	0 (0)
Moon Centered Space-Fixed Velocity, m/s (ft/s)	2543 (8343)	2544 (8346)	-1 (-3)
Impact Angle Measured from Vertical, deg	21.8	14.7	7.1
Incoming Heading Angle Measured From North to West, deg	75.7	85.8	-10.1
Tumble Rate, deg/s	~1.00	~0.35	0.65
Selenographic West Longitude, deg	26.04	33.25	-7.21
Selenographic South Latitude, deg	8.07	1.60	6.47
Impact Time, HR:MIN:SEC*	82:37:52.17	82:24:14.61	00:13:37.6
Distance to Target, km (n mi)	294 (159)	0 (0)	294 (159)
Distance to Seismometer, km (n mi)	175 (94)	304 (164)	-129 (-70)

* Actual Time (Signal Delay Time = 1.270 seconds)

Table 17-4. Summary of Lunar Impact Times

TRACKING STATION	RECORDED IMPACT TIME, HR:MIN:SEC	
	GREENWICH MEAN TIME FEBRUARY 4, 1971	RANGE TIME
Hawaii	7:40:55.43	82:37:53.43
Goldstone	7:40:55.43	82:37:53.43
Merritt Island	7:40:55.44	82:37:53.44
Carnarvon	7:40:55.44	82:37:53.44
Honeysuckle	7:40:55.44	82:37:53.44
Average	7:40:55.436	82:37:53.436

NOTE: Signal Delay Time = 1.270 seconds
Actual Impact Time = 82:37:52.17

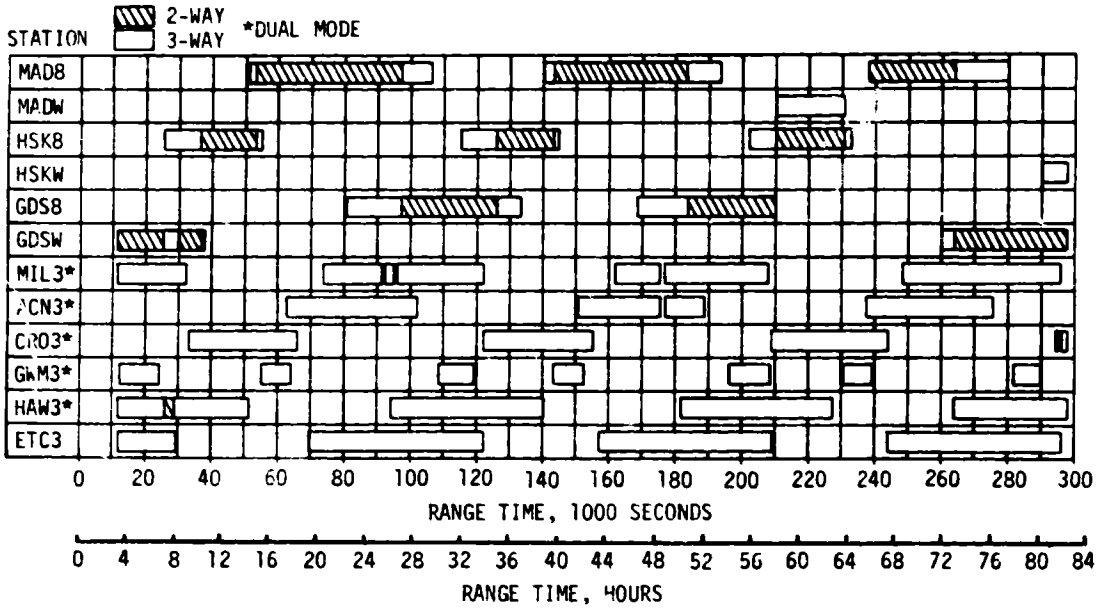

Figure 17-4. Summary of CCS Tracking Data Used for Post TLI Orbit

Table 17-5. S-IVB/IU CCS Tracking Network

STATION LOCATION	CONFIGURATION	ABBREVIATION
Madrid, Spain	Main Site - 85 Ft. Dish	MAD8
Madrid, Spain	Wing Site - 85 Ft. Dish	MADW
Canberra, Australia	Main Site - 85 Ft. Dish	HSK8
Tidbinbilla, Australia	Wing Site - 85 Ft. Dish	HSKW
Goldstone, California	Main Site - 85 Ft. Dish	GDS8
Goldstone, California	Wing Site - 85 Ft. Dish	GDSW
Merritt Island, Florida	30 Ft. Dish	MIL3
Ascension Island	30 Ft. Dish	ACN3
Carnarvon, Australia	30 Ft. Dish	CRO3
Kauai, Hawaii	30 Ft. Dish	HAW3
Goddard Experimental Test Center Greenbelt, Maryland	30 Ft. Dish	ETC3

SECTION 18

SPACECRAFT SUMMARY

The highly successful Apollo 14 mission, manned by Alan B. Shepard, Jr., Mission Commander; Stuart A. Roosa, Command Module (CM) Pilot; and Edgar D. Mitchell, Lunar Module (LM) Pilot; was launched from Kennedy Space Center, Florida, at 16:03:02 Eastern Standard Time (21:03:02 Universal Time) on January 31, 1971. The launch was delayed about 40 minutes because of restrictive weather conditions in the launch area. Activities during earth orbit checkout and translunar injection were similar to those of previous lunar landing missions. During transposition and docking, following translunar injection, six attempts were required to achieve a docking. Television was used during translunar coast to observe the probe and drogue inspection, and all operations indicated a normal functioning system. Except for a special check of ascent battery No. 5 in the lunar module, the remainder of the translunar coast period proceeded in accordance with the flight plan. Two midcourse corrections were performed at about 30.5 hours and at about 77 hours. These corrections achieved the non-free-return trajectory, the desired closest approach distance to the lunar surface, and placed the spacecraft operations back on the nominal flight plan time before lunar orbit insertion.

The spacecraft was inserted into lunar orbit at 82 hours, with the descent orbit insertion maneuver performed two revolutions later. The descent orbit insertion maneuver placed the combined spacecraft in a 58.8 by 9.6 mile orbit. The lunar module was entered at approximately 101.25 hours for activation and checkout in preparation for descent to the lunar surface.

The two spacecraft were undocked at 103.75 hours. Prior to powered descent an abort signal was set in the computer as the result of a malfunction, but a routine was manually loaded in the computer that inhibited the recognition of an abort discrete. The powered descent maneuver was initiated at 108 hours. A ranging scale problem, which would have prevented acquisition by the landing radar, was corrected by reinitializing the landing radar system. Landing in the Fra Mauro highlands occurred at 108:15:11. The landing coordinates were 3 degrees 39 minutes 56 seconds south latitude, and 17 degrees 28 minutes 42 seconds west longitude.

Preparations were begun for the first extravehicular activity 2 hours after landing. A lunar module communications problem delayed cabin depressurization about 40 minutes. The Commander began his egress and descent to the lunar surface at about 113.5 hours. As the Commander descended to the surface, he deployed the modularized equipment stowage assembly for transmission of color television pictures. The LM Pilot egressed at about 113.75 hours. The S-band antenna was erected and activated, the American flag was displayed, the Apollo lunar surface experiments package was deployed and various documented rock samples were taken during the 4.75-hour extravehicular period. The mobile equipment transporter was used during this period for carrying equipment and rock samples.

Preparations for the second extravehicular activity were begun following a 6.5-hour rest period. The goal of the second extravehicular period was to traverse to the top of Cone Crater. Time constraints prevented reaching the top, but the objectives associated with reaching the crater and gaining the desired samples were achieved. On the return traverse from the Cone Crater area, the antenna on the Apollo lunar surface experiment package central station was realigned and various documented rock and soil samples were collected. The second extravehicular period lasted almost 4.5 hours for a total extravehicular time of about 9.5 hours. During the extravehicular periods, at least 103 pounds of lunar rocks and soil were collected.

The ascent stage lifted off at about 141.75 hours and the vehicle was placed in 52.1 by 9.2-mile orbit. Rendezvous and docking operations were normal. However, during the final braking phase, the abort guidance system failed. The ascent stage was jettisoned and guided to impact approximately 36 miles west of the descent stage.

Transearth injection occurred during the 34th lunar orbit revolution at about 148.5 hours. During transearth coast, one midcourse correction was made with the reaction control system, and a special oxygen flow-rate test was performed. Good quality television coverage was provided while the four inflight demonstrations were being performed.

The entry sequence was normal and the command module landed in the Pacific Ocean at 216:01:57. The landing coordinates, as determined from the onboard computer, were 27 degrees 2 minutes 24 seconds south latitude, and 172 degrees 41 minutes 24 seconds west longitude.

SECTION 19

APOLLO 14 INFLIGHT DEMONSTRATIONS

19.1 SUMMARY

Three inflight demonstrations designed to demonstrate the effects of a zero g environment were proposed by Marshall Space Flight Center (MSFC) and flown on Apollo 14. These were an Electrophoretic Separation Demonstration, a Composites Casting Demonstration and a Heat Flow and Convection Demonstration. Preliminary assessment of the data indicate that all three demonstrations were successful. The degree of success will be determined when final data are received and evaluated.

19.2 ELECTROPHORETIC SEPARATION DEMONSTRATION

The Electrophoretic Separation Demonstration, a chemical separation process based on the motion of particles in a fluid due to the force of an electric field, was flown on Apollo 14 to show the advantages of the almost weightless environment. On earth, electrophoresis has to contend with sedimentation and thermal convective mixing which limits its usefulness for high molecular weight materials and large volume samples. This demonstration is expected to show that electrophoresis in space will not be limited by molecular weight and volume.

The instrument is a 4 by 5 by 6-inch box, weighing 5 pounds and requiring 27 watts of 115 volt, 400 cycle power for one hour. A viewing window is provided so that the action in the test tubes can be photographed employing a series of twelve 70mm Haselblad shots spaced 5 to 10 minutes apart. The electrical system includes white and ultraviolet fluorescent lights, pump motor, and 320 vdc rectified power for the electrophoresis electrodes in the ends of the tubes. The fluid system includes a peristaltic pump, filter, gas phase separator and tubing to flush the electrodes. The flowing fluid is separated from the passive fluid in the test tubes by dialysis membranes, although a dilute boric acid solution is used throughout.

The samples include: (1) a red and blue mixed dye which is easy to see and measure; (2) hemoglobin, a component of red blood cells with a molecular weight of 64,500; and (3) Deoxyribonucleic Acid (DNA), the carrier of genetic information in chromosomes, with a molecular weight several hundred times that of hemoglobin. The latter two samples are of current interest in biological research.

The objectives of the demonstration are to prove the gas phase purge system, the reduction in settling of high molecular weight material, and the sharper resolution of boundaries due to the lack of convective mixing. The unit was shown on the televised broadcast from space with the power and white light on. It was not activated at that time because it could be used only once, but it was operated later as planned. Detailed measurements will be made from the photographs. The primary assessment of the above experiment so far indicates the following:

a. The red-blue dye separation on Apollo 14 was better than that seen on earth. Development of the high-red contrast film will quantify the results. There were good measurements of mobility and resolution, and an indication of the lack of convective mixing.

b. The apparatus worked well, and the MSFC contributed phase separator scheme to keep the bubbles off the electrode did well.

c. So far, no conclusions can be drawn regarding sedimentation or other action of the high molecular weight materials, hemoglobin, and DNA. The reprint photos will help answer this, and when the apparatus is returned, analysis of the residues will give the final answer.

In conclusion, enough data have been analyzed to consider the effort worthwhile, but the final results are not yet known. Some film color adjustment techniques will have to be used to allow extracting all the data which will finally be needed.

19.3 COMPOSITES CASTING DEMONSTRATION

The objective of the Composites Casting Demonstration is to demonstrate the potential for preparing unique metal-matrix composites in a weightless environment. The absence of buoyancy and thermal convection permits processing with a liquid matrix and should result in more uniform dispersions of the reinforcing particles or fibers thus yielding a unique composite material superior to those produced on earth using solid state processes.

The demonstration was performed using a low melting point (162°F) indium-bismuth eutectic alloy, paraffin, and sodium acetate as model matrices. Dispersants included copper coated tungsten and boron carbide spheres, beryllium copper fibers, tungsten microspheres, and combinations of these with argon gas bubbles.

Composites formed by combinations of these materials do not represent practical systems, but will serve to demonstrate the effects of processing in a negligible gravity environment. The composites casting demonstration represents a variety of combinations including particle and fiber reinforced composites, liquid phase sintering of powder metal compacts, reinforced foams, immiscible mixtures, and solidification experiments.

The demonstration apparatus consists of 18 hermetically sealed capsules containing the ingredients for preparing the composite material, a heater, and a storage box, which is also used for cooling the specimens. See Table 19-1 for specimen list and abbreviated procedures.

Primary data will be obtained from postflight evaluation of the specimens. TV coverage or photography during demonstration was optional. Voice recording of specimen numbers and start and stop times for heating and cooling was required so that telemetry data from the Command Module (CM) could be evaluated postflight to determine g levels, temperatures, etc., during time of demonstration.

Specimens No. 1 through 12 with the exception of No. 3 were processed during the translunar and the transearth coasting phases of the mission. The remaining seven specimens were not processed because there was insufficient time. There were no problems with the equipment or the procedures.

Evaluation of the flight specimens will commence after they have been released from quarantine. Meanwhile evaluation procedures are being finalized and the control samples are being prepared for evaluation.

Primary indications are that the demonstration was successful.

19.4 HEAT FLOW AND CONVECTION DEMONSTRATION

The Heat Flow and Convection Demonstration that was performed for the Space Manufacturing Program on Apollo 14 is designed to obtain data on the types and amounts of convection that occur in the near weightless environment of space flight. Although normal convection will be mostly suppressed in near weightlessness, convective fluid flows can occur in space by mechanisms other than gravity, such as by surface tension gradients, and, in some cases, the residual accelerations present during space flight cause low level fluid flow. The demonstration contains four independent cells of special design that detect convection directly or detect convective effects through measurement of heat flow-rates in the fluids. The data are recorded on the onboard 16mm data acquisition camera. The temperatures are visibly displayed (and recorded on the camera) by the use of color sensitive, liquid-crystal thermal strips.

The crew reported that the demonstration was completed and also the unit was operated during a TV transmission on February 7, 1971. The radial cell and the two zone cells were successfully illustrated during the transmission. The Flow Patt cell was operated and Benard cells (caused by surface tension gradients) were clearly visible in the thin layer. Some difficulty was encountered by the astronauts in getting the fluid (Krytox) to spread properly across the cell bottom.

The primary data (16mm film) was examined and found to be of excellent quality both in focus and color. The film shows a slight yellow tint. The two radial tests and the two zone tests were performed and the data appear excellent. The unit was jarred on occasion during these runs and these effects will have to be accounted for in analyzing gravity effects. There were 4987 frames taken (out of 5000 available) during flight. This means that about 200,000 data points were recorded.

The last flow pattern run shows Benard cells in the fillet. The cells are very clearly defined and will be analyzed. The theoretical equations will have to be approximated for a wedge geometry (fillet) rather than a flat plate geometry. The original film, which is somewhat yellow, was compared to the work prints. A work print highlighting the blue is being prepared for a comparative analysis. The first work print is being read on a Telereadex for input into a computer at MSFC.

Preliminary analysis of the data indicates that this demonstration was successful.

Table 19-1. Specimen List and Abbreviated Procedure

SPECIMEN NO.	CONTENTS	PROCEDURE
1	30% W Spheres - 70% InBi	Heat 10 minutes. Do not shake. Cool 30 minutes minimum.
2	30% B_4C - 65% InBi - 5% Argon	
3	30% B_4C - 70% InBi	
4	SiC Whiskers - InBi - Argon Gas	Heat 10 minutes. Shake 60 seconds minimum. Cool 30 minutes minimum
5	BeCu Fibers - InBi - Argon Gas	
6	50% Paraffin - 50% Sodium Acetate	
7	75% InBi - 25% Argon Gas	
8	W Spheres - InBi - Argon Gas	
9	40% Paraffin - 40% Sodium Acetate - 20% Argon	
10	W Spheres - InBi	
11	BeCu Fibers - Paraffin - Argon Gas	
12	40% Paraffin - 40% Sodium Acetate - 20% Wms	
13	BeCu Fibers - InBi	
14	BeCu Fibers - Paraffin	
15	InBi Controlled Eutectic	Heat 13 minutes minimum. Do not shake. Cool 30 minutes minimum.
16	InBi Remelt - Heat 8 minutes	
17	InBi Solidification	
18	InBi Spherical Casting	Heat 13 minutes minimum. Do not remove heater from box for 120 minutes minimum.

InBi = Indium Bismuth Eutectic Alloy
W Spheres = Copper Coated Tungsten Spheres
B_4C = Copper Coated Boron Carbide Spheres
BeCu = Beryllium Copper Wires
SiC = Copper Coated Silicon Carbide Whiskers
Wms = Tungsten Microspheres

APPENDIX A

ATMOSPHERE

A.1 SUMMARY

This appendix presents a summary of the atmospheric environment at launch time of the AS-509. The format of these data is similar to that presented on previous launches of Saturn vehicles to permit comparisons. Surface and upper levels winds, and thermodynamic data near launch time are given.

A.2 GENERAL ATMOSPHERIC CONDITIONS AT LAUNCH TIME

At launch time a cold front extended through northern Florida. See Figure A-1. Scattered rain shower activity existed to the south of this front throughout the morning of launch, but the showers did not reach the launch area until just before the scheduled launch time. A band of cumulus congestus clouds with showers developed about 30 minutes before scheduled launch time along a line extending from Orlando toward northern Merritt Island Launch Area (MILA). This necessitated a 40 minute hold until the showers had moved a sufficient distance from the launch pad. Although it was raining prior to launch, there was no rain at the pad at the time of launch. The vehicle did travel through the cloud decks.

Surface winds in the Cape Kennedy area were fairly light and westerly, as shown in Table A-1.

Wind flow aloft is shown in Figure A-2 (500 millibar level). The maximum wind belt was located north of Florida giving less intense westerly wind flow over the Cape Kennedy, Florida area.

A.3 SURFACE OBSERVATIONS AT LAUNCH TIME

At launch time total sky cover was 8/10 with 7/10 cumulus at 1.2 kilometers (4000 ft), and 2/10 altocumulus at 2.4 kilometers (8000 ft). Aircraft observations indicated the depths of the layers in the vicinity of the pad to be about 0.6 to 1.2 kilometers (2000 to 4000 ft) thick. All surface observations at launch time are summarized in Table A-1. Solar radiation data are given in Table A-2.

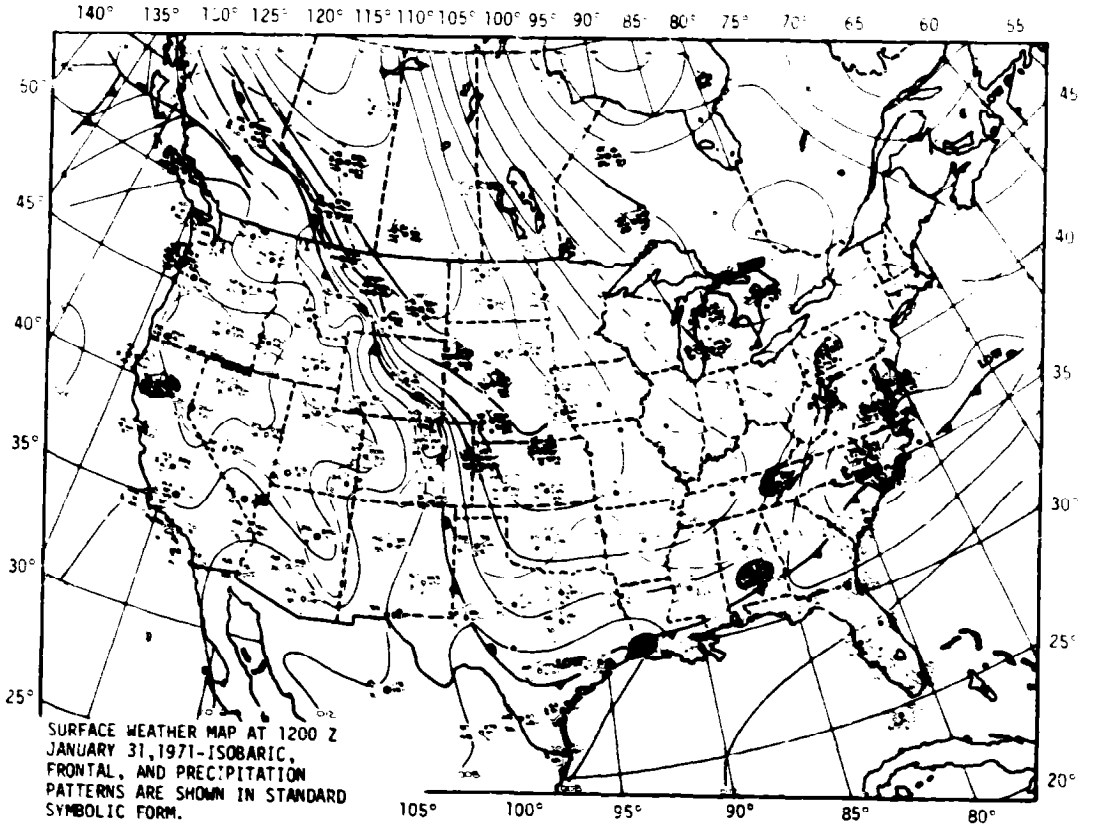
140° 135° 130° 125° 120° 115° 110° 105° 100° 95° 90° 85° 80° 75° 70° 65° 60° 55°
50° 45° 40° 35° 30° 25°
45° 40° 35° 30° 25° 20°
105° 100° 95° 90° 85° 80°
SURFACE WEATHER MAP AT 1200 Z JANUARY 31,1971-ISOBARIC, FRONTAL, AND PRECIPITATION PATTERNS ARE SHOWN IN STANDARD SYMBOLIC FORM.

Figure A-1. Surface Weather Map Approximately 9 Hours Before Launch of AS-509

Table A-1. Surface Observations at AS-509 Launch Time

LOCATION	TIME AFTER T-0 (MIN)	PRESSURE N/CM² (PSIA)	TEMPERATURE °K (°F)	DEW POINT °K (°F)	VISIBILITY KM (STAT MI)	AMOUNT (TENTHS)	SKY COVER TYPE	HEIGHT OF BASE METERS (FEET)	WIND SPEED M/S (KNOTS)	WIND DIR (DEG)
MILA (SSB) Kennedy Space Center, Florida	0	10.102 (14.65)	294.8 (71.0)	292.6 (67.0)	16 (10)	7	Cumulus	1219** (4,000)**	2.6 (5.0)	260
						2	Alto-Cumulus	2438 (8,000)		
Cape Kennedy Rawinsonde Measurements	11	10.095 (14.64)	298.7 (77.9)	284.0 (51.6)	--	--	--	--	7.0 (13.6)	240
Pad 39A Lightpole NW 18.3 m (60.0 ft)*	0	--	--	--	--	--	--	--	5.0*** (9.7)***	255***
LUT Pad 39A 161.5m (530 ft)*	0	--	--	--	--	--	--		8.5*** (16.5)***	275***

* Above natural grade.
** Estimated.
*** 1 minute average about T-0.

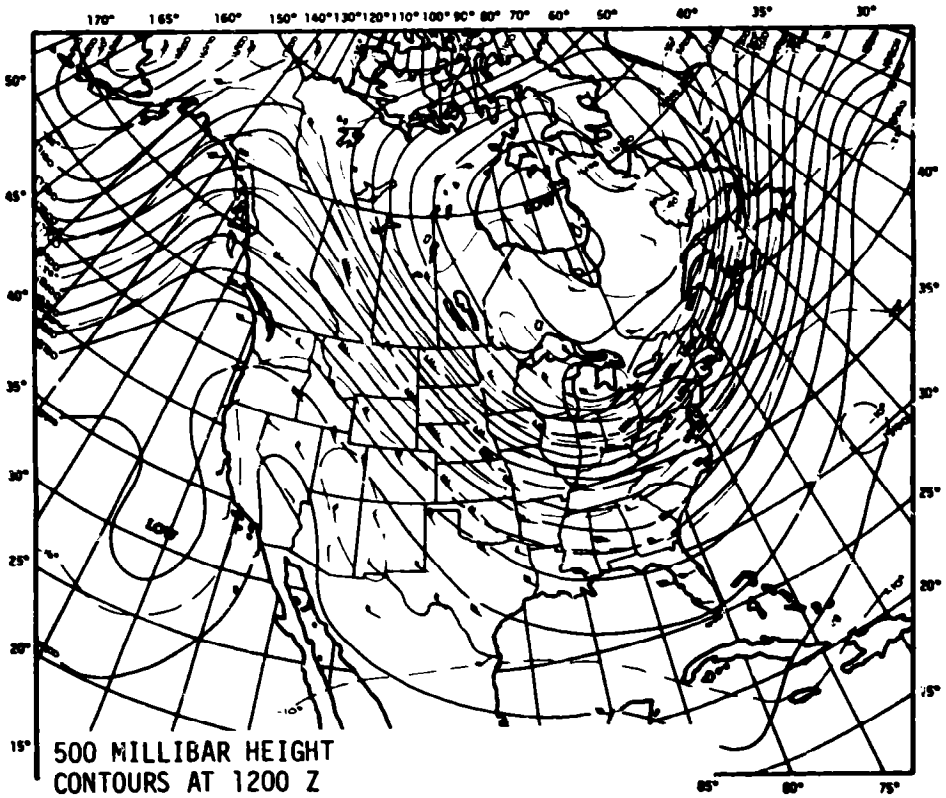
500 MILLIBAR HEIGHT
CONTOURS AT 1200 Z
JANUARY 31, 1971
CONTINUOUS LINES INDICATE HEIGHT CONTOURS IN
FEET ABOVE SEA LEVEL. DASHED LINES ARE ISO-
THERMS IN DEGREES CENTIGRADE. ARROWS SHOW
WIND DIRECTION AND SPEED AT THE 500mb LEVEL.
(ARROWS SAME AS ON SURFACE MAP).

Figure A-2. 500 Millibar Map Approximately 9 Hours Before Launch of AS-509

A.4 UPPER AIR MEASUREMENTS

Data were used from three of the upper air wind systems to compile the final meteorological tape. Table A-3 summarizes the wind data systems used. Only the Rawinsonde and the Loki Dart meteorological rocket data were used in the upper level atmospheric thermodynamic analyses.

Table A-2. Solar Radiation at AS-509 Launch Time, Launch Pad 39A

DATE	HOUR ENDING EST	TOTAL HORIZONTAL G-CAL/CM^2 MIN	NORMAL INCIDENT G-CAL/CM^2 MIN	DIFFUSE SKY G-CAL/CM^2 MIN
January 31, 1971	07.00	0.00	0.00	0.00
	08.00	0.05	0.03	0.05
	09.00	0.19	0.11	0.15
	10.00	0.31	0.08	0.27
	11.00	0.64	0.35	0.42
	12.00	0.76	0.85	0.18
	13.00	0.73	0.64	0.29
	14.00	0.86	1.06	0.19
	15.00	0.57	0.41	0.35
	16.00	0.10	0.01	0.10
	17.00	0.08	0.00	0.08
	18.00	0.04	0.00	0.04
	19.00	0.00	0.00	0.00

Table A-3. Systems Used to Measure Upper Air Wind Data for AS-509

TYPE OF DATA	RELEASE TIME		PORTION OF DATA USED			
			START		END	
	TIME (UT)	TIME AFTER T-0 (MIN)	ALTITUDE M (FT)	TIME AFTER T-0 (MIN)	ALTITUDE M (FT)	TIME AFTER T-0 (MIN)
FPS-16 Jimsphere	2121	18	175 (574)	18	15,000 (49,213)	69
Rawinsonde	2114	11	15,250 (50,033)	61	24,000 (78,740)	90
Loki Dart	2309	126	59,000 (193,569)	126	25,000 (82,021)	150

A.4.1 Wind Speed

The wind speed was 5.0 m/s (9.7 knots) at the surface, and increased to a peak of 52.77 m/s (102.6 knots) at 13.33 kilometers (43,720 ft). The winds began decreasing above this altitude, reaching a minimum of 7.0 m/s (13.6 knots) at 31.35 kilometers (102,850 ft) altitude. Above this altitude the wind speed continued to increase, as shown in Figure A-3.

A.4.2 Wind Direction

At launch time the surface wind direction was 255 degrees. The wind direction stayed approximately westerly with increasing altitude to 59.0 kilometers (193,570 ft). Figure A-4 shows a complete wind direction versus altitude profile.

A.4.3 Pitch Wind Component

The pitch wind velocity component (component parallel to the horizontal projection of the flight path) at the surface was a tail wind of 5.0 m/s (9.7 knots). The pitch component remained a tail wind with altitude, resulting in a maximum tail wind of 52.77 m/s (102.6 knots) observed at 13.33 kilometers (43,720 ft) altitude. See Figure A-5.

A.4.4 Yaw Wind Component

The yaw wind velocity component (component normal to the horizontal projection of the flight path) at the surface was a wind from the right of 0.05 m/s (0.1 knot). The peak yaw wind velocity in the high dynamic pressure region was a wind from the left of 24.9 m/s (48.5 knots) at 10.20 kilometers (33,460 ft). See Figure A-6.

A.4.5 Component Wind Shears

The largest component wind shear (Δh = 1000 m) in the altitude range of 8 to 16 kilometers (26,247 to 52,493 ft) was a yaw shear of 0.0251 sec^{-1} at 11.85 kilometers (38,880 ft). The largest pitch wind shear, in the lower levels, was 0.0201 sec^{-1} at 13.33 kilometers (43,720 ft). See Figure A-7.

A.4.6 Extreme Wind Data in the High Dynamic Region

A summary of the maximum wind speeds and wind components is given in Table A-4. A summary of the extreme wind shear values is given in Table A-5.

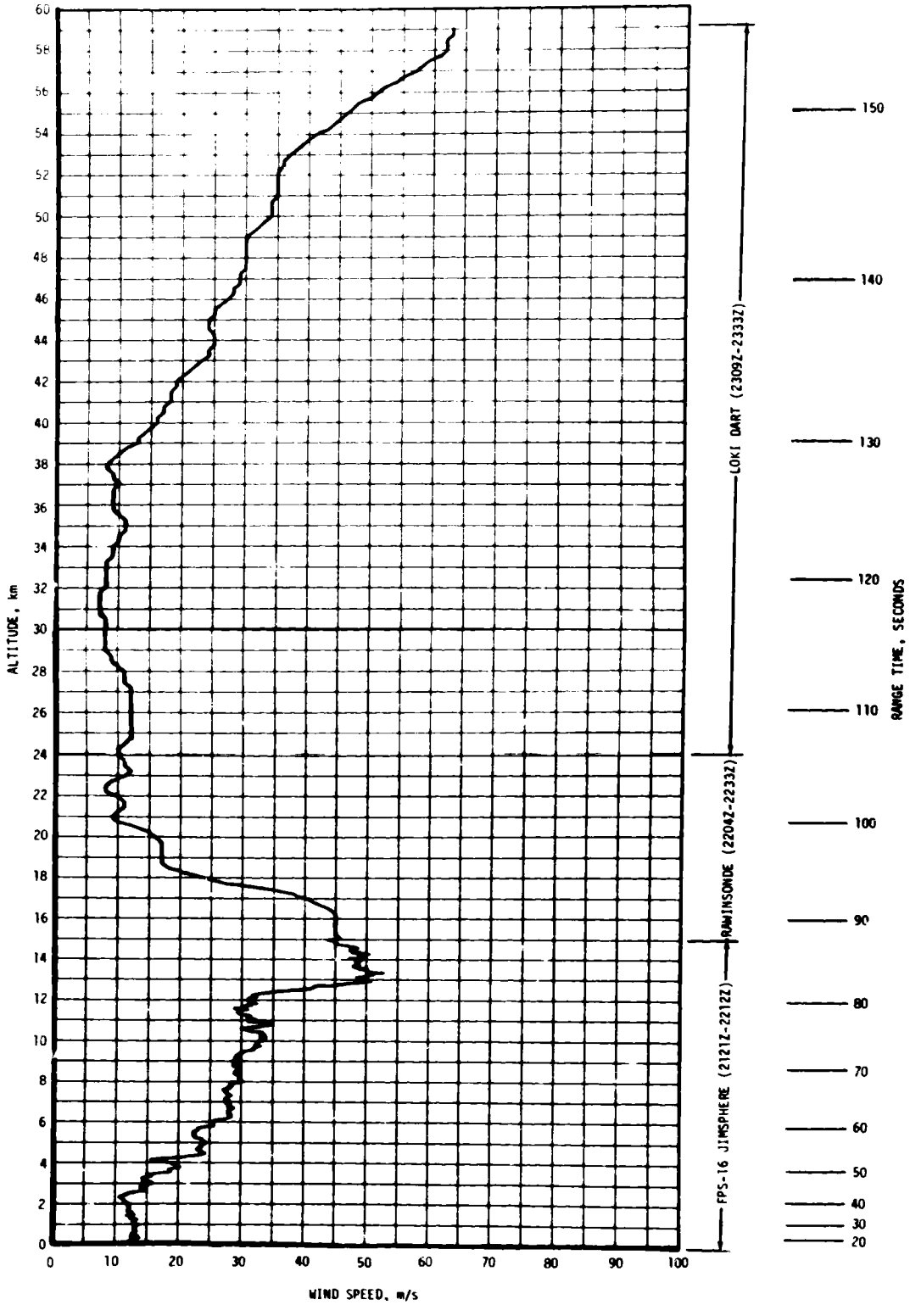

Figure A-3. Scalar Wind Speed at Launch Time of AS-509

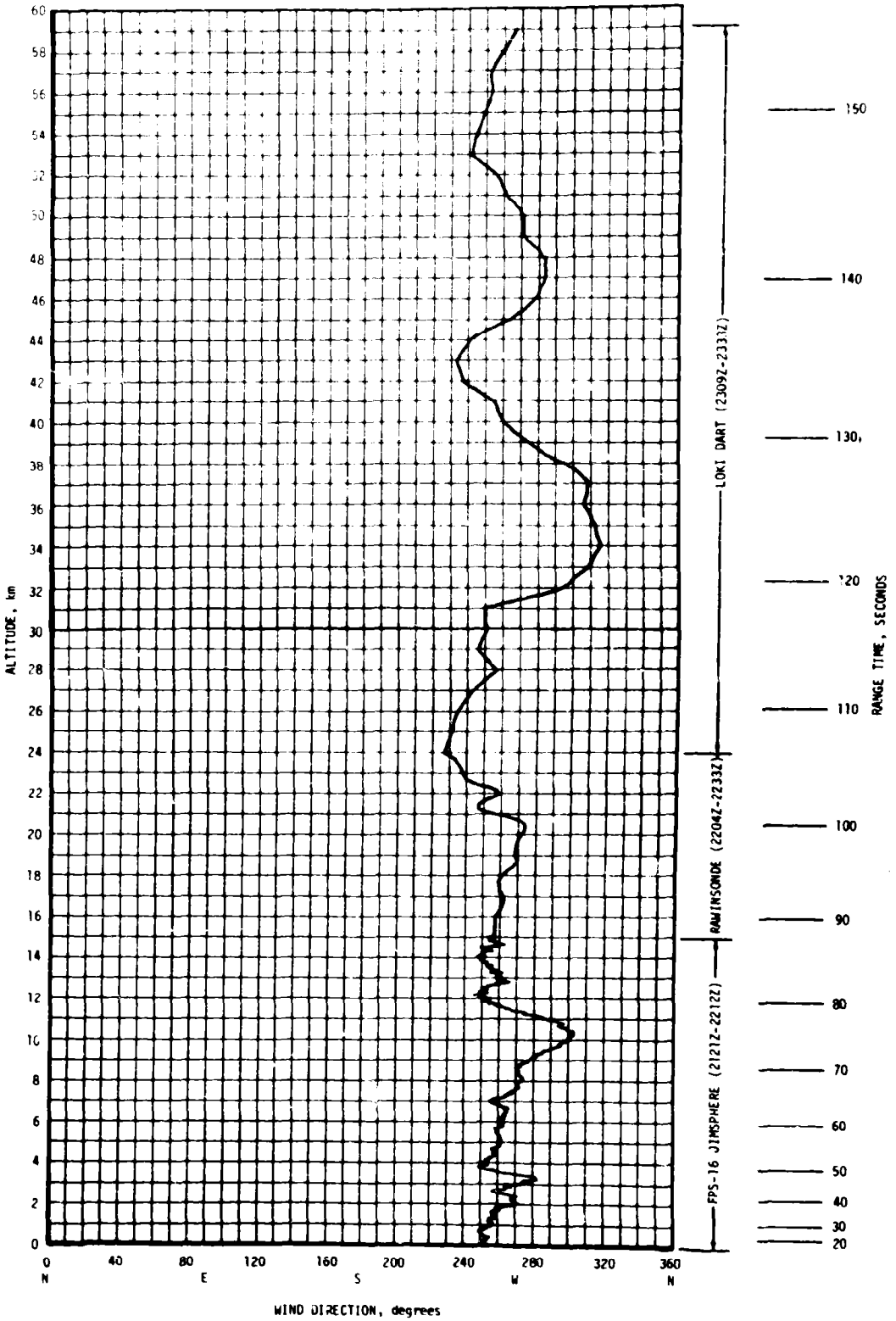

Figure A-4. Wind Direction at Launch Time of AS-509

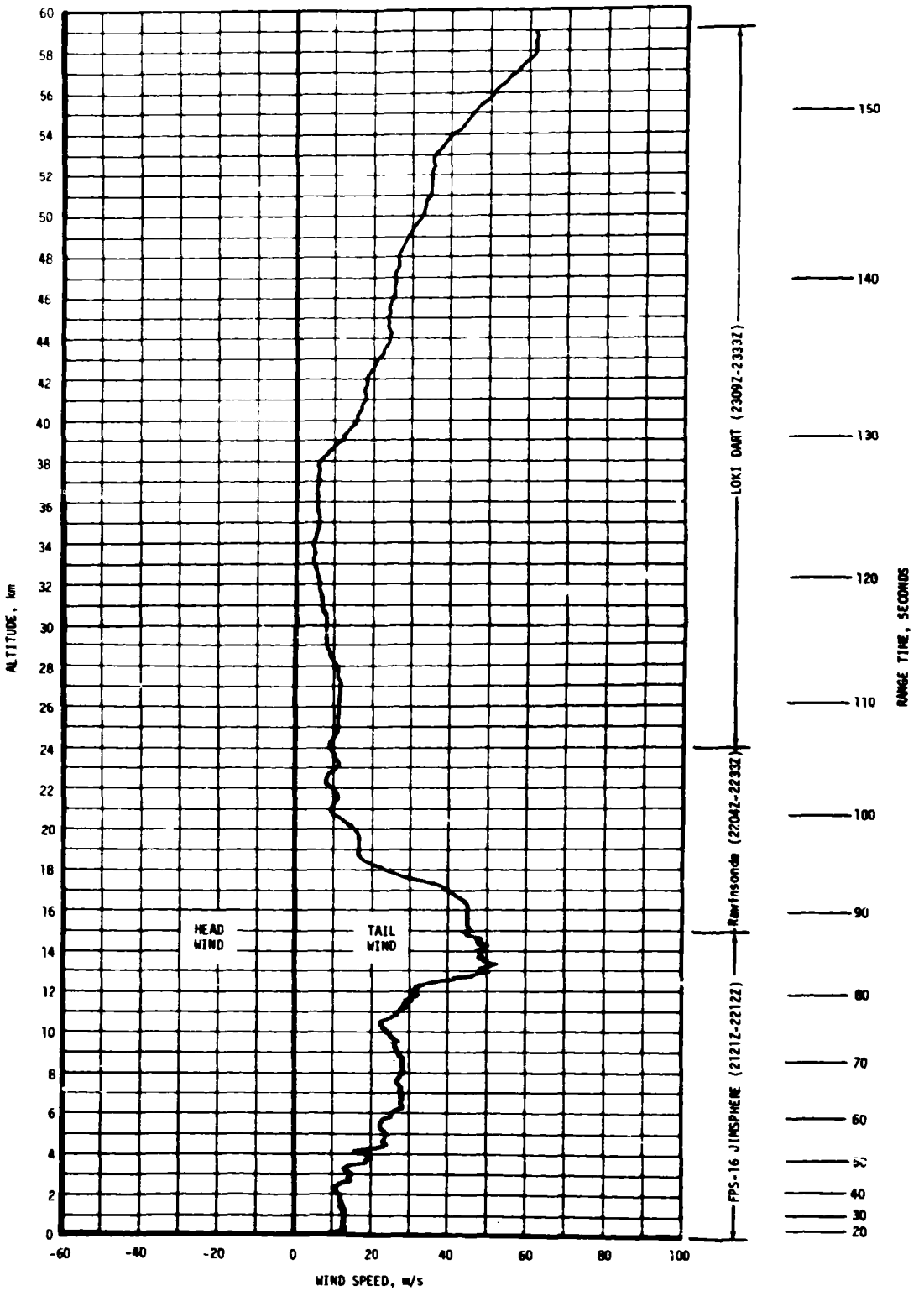

Figure A-5. Pitch Wind Velocity Component (W_X) at Launch Time of AS-509

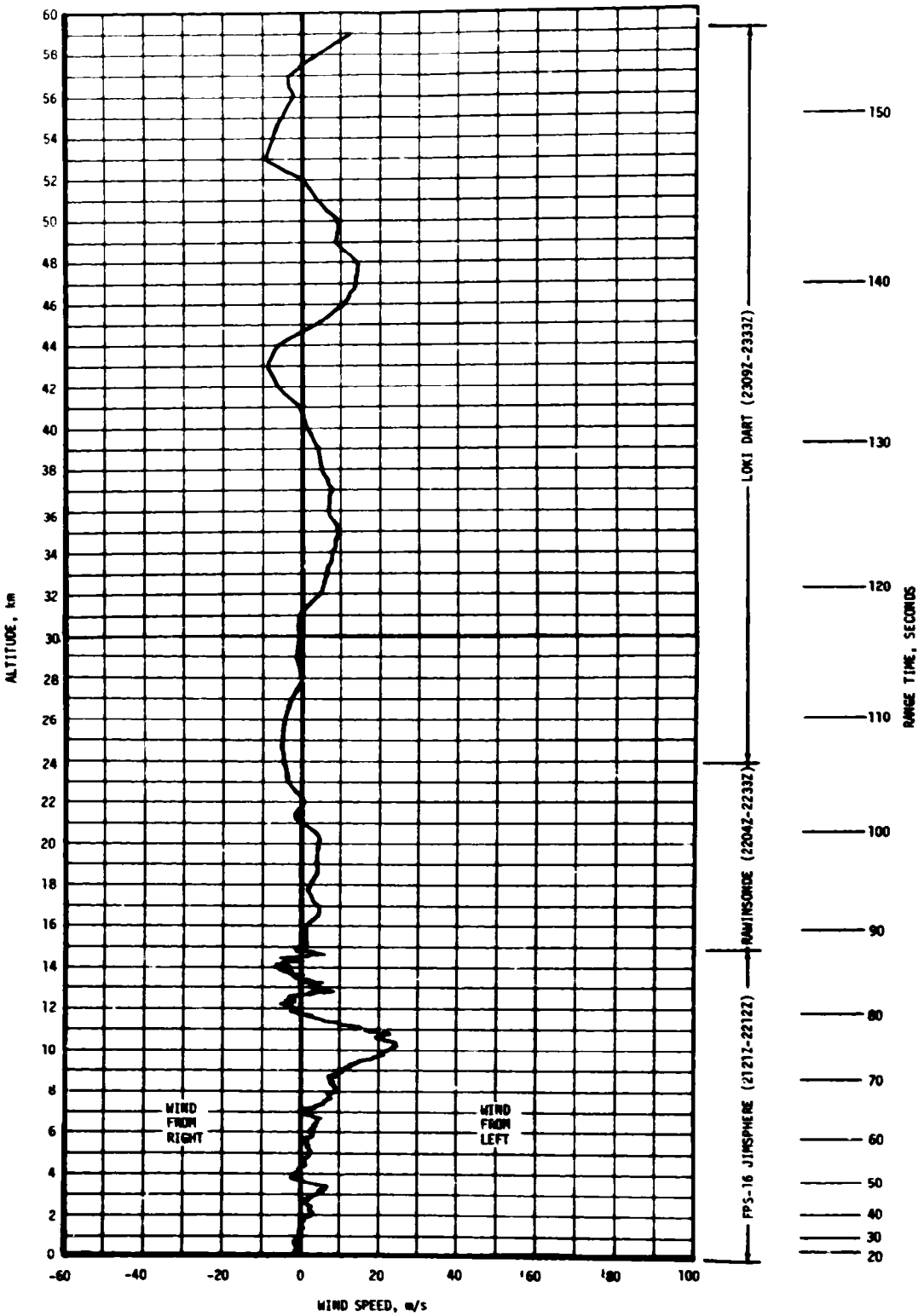

Figure A-6. Yaw Wind Velocity Component (W_Z) at Launch Time of AS-509

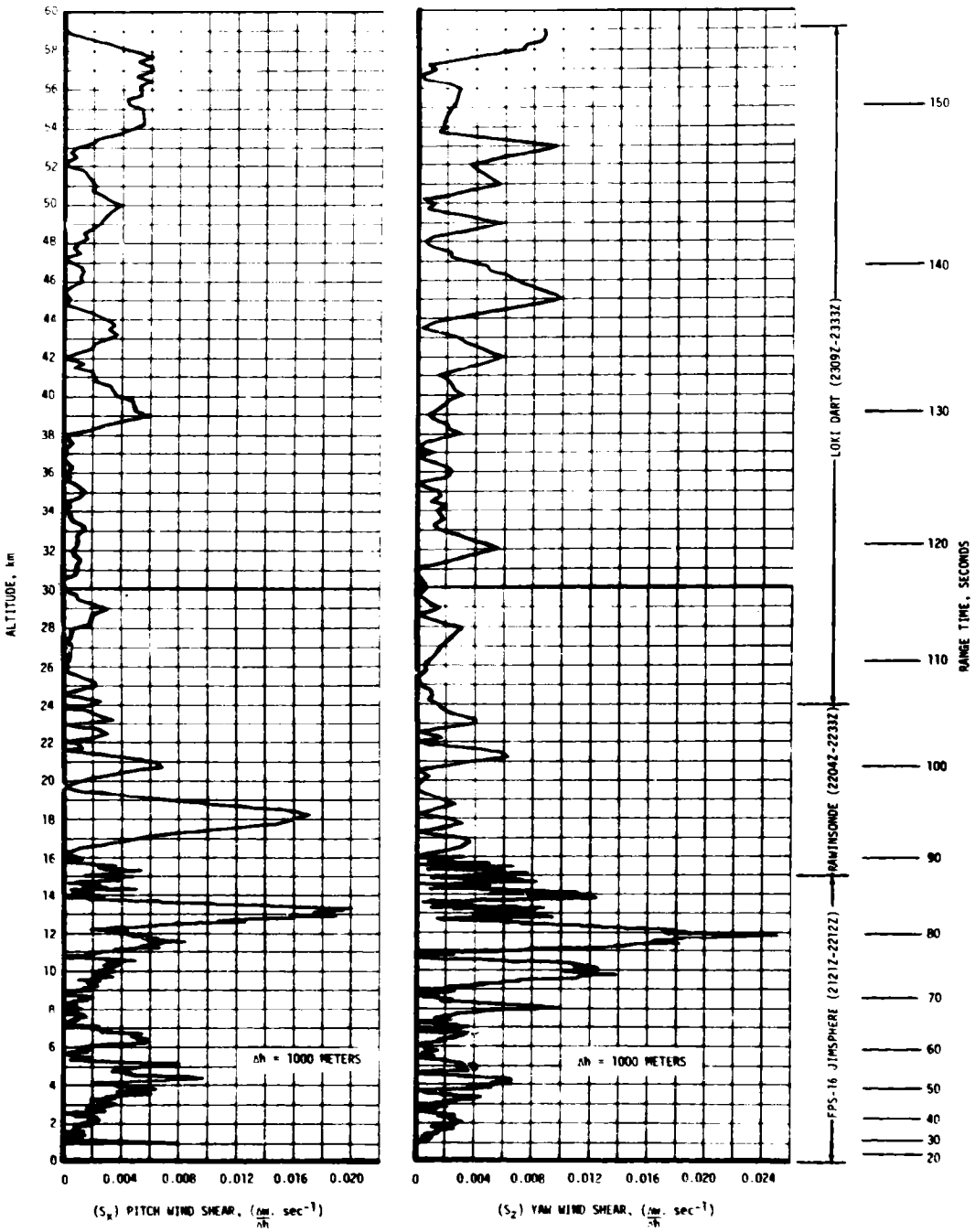

Figure A-7. Pitch (S_X) and Yaw (S_Z) Component Wind Shears at Launch Time of AS-509

Table A-4. Maximum Wind Speed in High Dynamic Pressure Region for Apollo/Saturn 501 through Apollo/Saturn 509 Vehicles

VEHICLE NUMBER	MAXIMUM WIND			MAXIMUM WIND COMPONENTS			
	SPEED M/S (KNOTS)	DIR (DEG)	ALT KM (FT)	PITCH (W_X) M/S (KNOTS)	ALT KM (FT)	YAW (W_Z) M/S (KNOTS)	ALT KM (FT)
AS-501	26.0 (50.5)	273	11.50 (37,700)	24.3 (47.2)	11.50 (37,700)	12.9 (25.1)	9.00 (29,500)
AS-502	27.1 (52.7)	255	12.00 (42,600)	27.1 (52.7)	12.00 (42,600)	12.9 (25.1)	15.75 (51,700)
AS-503	34.8 (67.6)	284	15.22 (49,900)	31.2 (60.6)	15.10 (49,500)	22.6 (43.9)	15.80 (51,800)
AS-504	76.2 (148.1)	264	11.73 (38,480)	74.5 (144.8)	11.70 (38,390)	21.7 (42.2)	11.43 (37,500)
AS-505	42.5 (92.6)	270	14.18 (46,520)	40.8 (79.3)	13.80 (45,280)	18.7 (36.3)	14.85 (48,720)
AS-506	9.6 (18.7)	297	11.40 (37,400)	7.6 (14.8)	11.18 (36,680)	7.1 (13.8)	12.05 (39,530)
AS-507	47.6 (92.5)	245	14.23 (46,670)	47.2 (91.7)	14.23 (46,670)	19.5 (37.9)	13.65 (44,780)
AS-508	55.6 (108.1)	252	13.58 (44,540)	55.6 (108.1)	13.58 (44,540)	15.0 (29.1)	12.98 (42,570)
AS-509	52.8 (102.6)	255	13.33 (43,720)	52.8 (102.6)	13.33 (43,720)	24.9 (48.5)	10.20 (33,460)

Table A-5. Extreme Wind Shear Values in the High Dynamic Pressure Region for Apollo/Saturn 501 through Apollo/Saturn 509 Vehicles

(Δh = 1000 m)				
VEHICLE NUMBER	PITCH PLANE		YAW PLANE	
	SHEAR (SEC^{-1})	ALTITUDE KM (FT)	SHEAR (SEC^{-1})	ALTITUDE KM (FT)
AS-501	0.0066	10.00 (32,800)	0.0067	10.00 (32,800)
AS-502	0.0125	14.90 (48,900)	0.0084	13.28 (43,500)
AS-503	0.0103	16.00 (52,500)	0.0157	15.78 (51,800)
AS-504	0.0248	15.15 (49,700)	0.0254	14.68 (48,160)
AS-505	0.0203	15.30 (50,200)	0.0125	15.53 (50,950)
AS-506	0.0077	14.78 (48,490)	0.0056	10.30 (33,790)
AS-507	0.0183	14.25 (46,750)	0.0178	14.58 (47,820)
AS-508	0.0166	15.43 (50,610)	0.0178	13.98 (45,850)
AS-509	0.0201	13.33 (43,720)	0.0251	11.85 (38,880)

A.5 THERMODYNAMIC DATA

Comparisons of the thermodynamic data taken at AS-509 launch time with the annual Patrick Reference Atmosphere, 1963 (PRA-63) for temperature, pressure, density, and Optical Index of Refraction are shown in Figures A-8 and A-9 and discussed in the following paragraphs.

A.5.1 Temperature

Atmospheric temperature differences were small, being less than 5 percent deviation from the PRA-63. Surface air temperature was slightly warmer than the PRA-63. Above the surface, temperature deviations oscillated about the PRA-63 values with altitude. See Figure A-8.

A.5.2 Atmospheric Pressure

Atmospheric pressure deviations were less than the PRA-63 pressure values from the surface to 59.0 kilometers (193,570 ft) altitude. All pressure values versus altitude were within 7 percent of the PRA-63 values as shown in Figure A-8.

A.5.3 Atmospheric Density

Atmospheric density deviations were small, being within 9 percent of the PRA-63 for all altitudes. See Figure A-9.

A.5.4 Optical Index of Refraction

At the surface, the Optical Index of Refraction was 7.22×10^{-6} units lower than the corresponding value of the PRA-63. The deviation became less negative with altitude, and it approximates the PRA-63 at high altitudes as is shown in Figure A-9.

A.6 COMPARISON OF SELECTED ATMOSPHERIC DATA FOR SATURN V LAUNCHES

A summary of the atmospheric data for each Saturn V launch is shown in Table A-6.

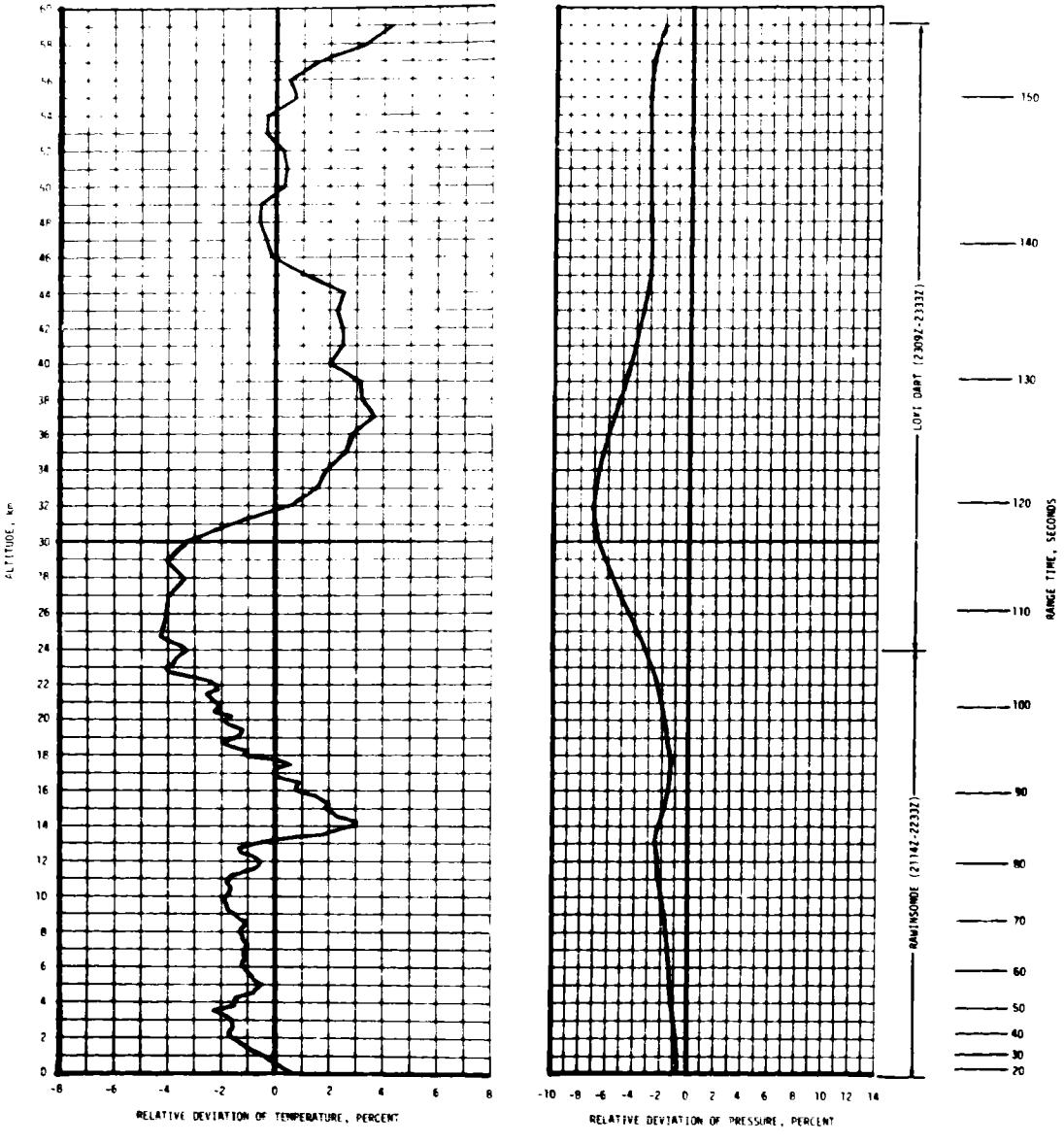

Figure A-8. Relative Deviation of Temperature and Pressure from the ?RA-63 Reference Atmosphere, AS-509

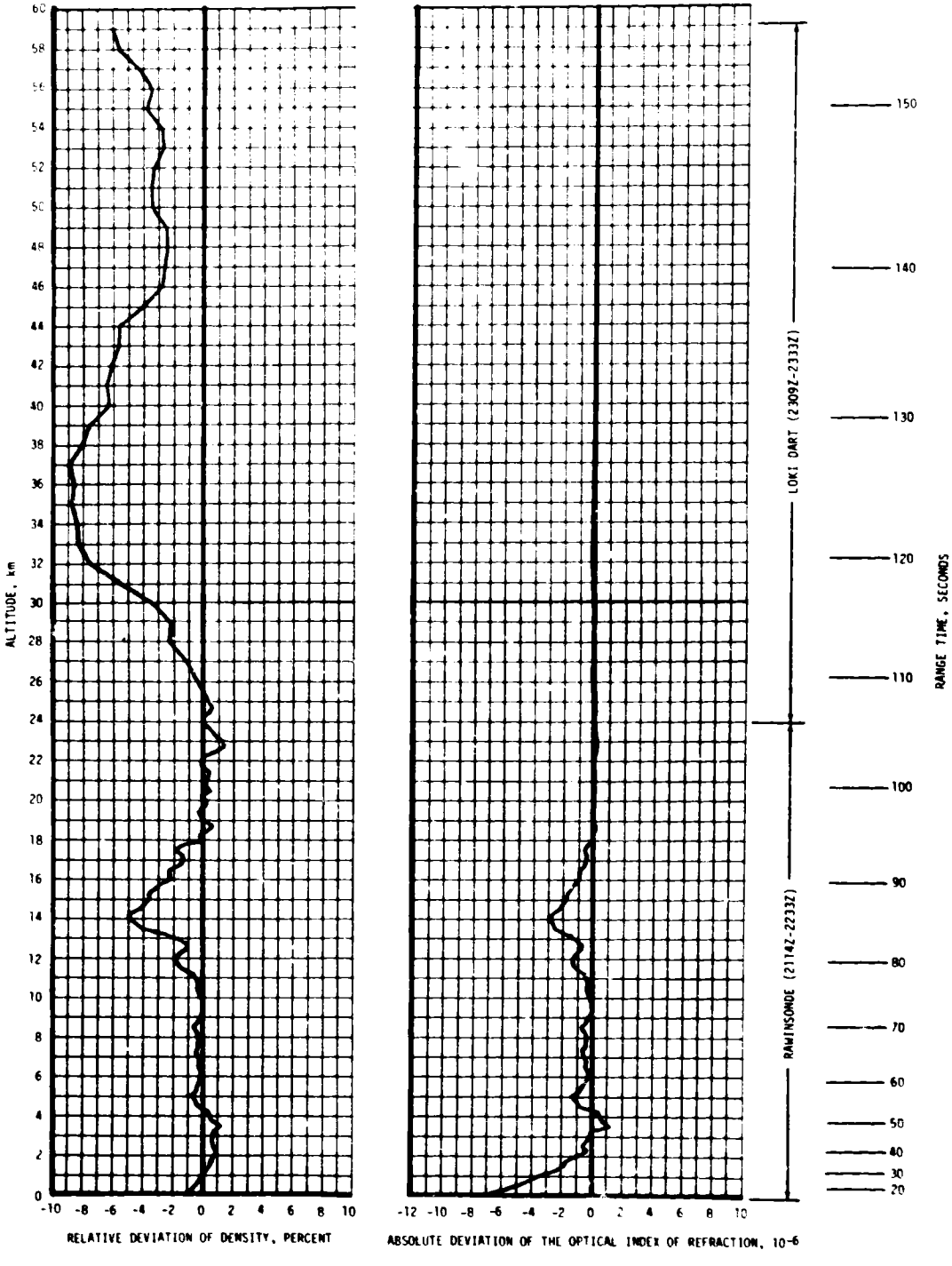
ALTITUDE, km
RELATIVE DEVIATION OF DENSITY, PERCENT
ABSOLUTE DEVIATION OF THE OPTICAL INDEX OF REFRACTION, 10-6
LOKI DART (2309Z-2333Z)
RAWINSONDE (2114Z-2233Z)
RANGE TIME, SECONDS

Figure A-9. Relative Deviation of Density and Absolute Deviation of the Index of Refraction from the PRA-63 Reference Atmosphere, AS-509

Table A-6. Selected Atmospheric Observations for Apollo/Saturn 501 through Apollo/Saturn 509 Vehicle Launches at Kennedy Space Center, Florida

VEHICLE NUMBER	VEHICLE DATA			SURFACE DATA						INFLIGHT CONDITIONS		
	DATE	TIME NEAREST MINUTE	LAUNCH COMPLEX	PRESSURE N/m²	TEMPERATURE °C	RELATIVE HUMIDITY PERCENT	WIND* SPEED m/s	WIND* DIRECTION DEG	CLOUDS	MAXIMUM WIND IN 8-16 km LAYER ALTITUDE km	SPEED m/s	DIRECTION DEG
AS-501	9 Nov 67	0700 EST	39A	10 261	17.8	55	8.0	70	1/10 cumulus	11.50	26.0	273
AS-502	4 Apr 68	0700 EST	39A	10 200	20.9	83	5.4	132	5/10 stratocumulus, 1/10 cirrus	13.00	27.1	255
AS-503	22 Dec 68	0751 EST	39A	10 207	15.0	88	1.0	360	4/10 cirrus	15.22	34.8	284
AS-504	3 Mar 69	1100 EST	39A	10 095	19.6	61	6.9	160	7/10 stratocumulus, 10/10 altostratus	11.73	76.2	264
AS-505	8 May 69	1249 EDT	39B	10 190	26.7	75	8.2	125	4/10 cumulus, 2/10 altocumulus, 10/10 cirrus	14.18	42.5	270
AS-506	3 Jul 69	0832 EDT	39A	10 203	29.4	73	3.3	175	1/10 cumulus, 2/10 altocumulus, 9/10 cirrostratus	11.80	9.6	297
AS-507	4 Nov 69	1122 EST	39A	10 081	20.0	92	6.8	280	10/10 stratocumulus with rain	14.23	47.6	245
AS-508	11 Apr 70	1413 EST	39A	10.119	24.4	57	6.3	105	4/10 altocumulus 10/10 cirrostratus	13.58	55.6	252
AS-509	31 Jan 71	1603 EST	39A	10.102	21.7	86	5.0** 8.5***	255** 275***	7/10 cumulus 2/10 altocumulus	13.33	52.8	255

*Instantaneous readings from charts at T-0 from anemometers on launch p a at 18.3 m (60.0 ft) on launch complex 39 (AGE). Heights of anemometers are above natural grade

**Not instantaneous, but one minute average about T-0.

***One minute average readings from charts at T-0 from anemometers on LUT at 161.5 m (530 ft) above natural grade.

APPENDIX B

AS-509 SIGNIFICANT CONFIGURATION CHANGES

B.1 INTRODUCTION

AS-509, ninth flight of the Saturn V series, was the seventh manned Apollo Saturn V vehicle. The AS-509 launch vehicle configuration was essentially the same as the AS-508 with significant exceptions shown in Tables B-1 through B-4.

The Apollo 14 spacecraft structure and components were essentially unchanged from the Apollo 13 configuration. However, some changes were made as a result of problems encountered on Apollo 13. A list of the most significant of these changes is shown in Table B-5.

The basic launch vehicle description is presented in Appendix B of the Saturn V Launch Vehicle Flight Evaluation Report, AS-504, Apollo 9 Mission, MPR-SAT-FE-69-4.

Table B-1. S-IC Significant Configuration Changes

SYSTEM	CHANGE	REASON
Propulsion	Orifices in [illegible] helium bubbling system [illegible] increased flowrate.	Existing flowrate marginal to prevent geysering during LOX drain.
	Two butte[illegible] in LOX fill and drain lines replaced with steel spacers.	Valves contained a seal that was not LOX compatible. Also valves are not used during launch because of possible umbilical retractor problems.
	GOX Flow Control Valve replaced with flow venturi.	Cost and weight saving. Elimination of potential problem if valve were to fail closed during flight.
Electrical	Loading system electronic units aligned so that 100 percent probe capacitance has an output of 19.4 volts instead of 20 volts.	To prevent out-of-lock signal from degrading Propellant Tanking Computer System operations.
	Two of four fuel depletion cutoff sensors relocated, voting logic circuitry added, and redundant power inputs provided to sensors and voting circuitry.	Eliminate critical single point failure modes.
Environmental Control and Electrical	Aft compartment Environmental Control System orifices returned to S-IC-7 configuration and batteries requalified to lower temperature.	Ensure aft compartment temperatures are within acceptable limits.
GSE	Pneumatic console LOX dome purge regulators and GN_2 primary regulator modified.	To eliminate regulator failures and undesirable pressure characteristics within the LOX dome purge system.

Table B-2. S-II Significant Configuration Changes

SYSTEM	CHANGE	REASON
Propulsion	Addition of a POGO suppression system consisting of a helium filled accumulator on the LOX feedline of the center engine.	To prevent the POGO oscillations that have occurred on previous flights.
	Engine servo-driven PU valve replaced with an electropneumatic-operated, two position PU valve.	To improve valve positioning reliability.
	Added 2.3 second time delay to LH_2 depletion cutoff sensor.	Reduce propellant residuals and increase payload capability.
Structure	Installation of a system (G limit switch) to monitor center engine beam vibration (POGO) levels and initiate center engine cutoff whenever dangerous levels occur.	To provide a backup to the POGO suppression system and limit the dynamic load on the center engine beam.
Insulation	Modification of insulation in the LH_2 feedline areas to minimize cork insulation debonding and wet layup blistering.	To support a 24 hour "scrub" and "turn-around" capability on insulation inspection and repair.
GSE	The LH_2 level control system in the A7-71 heat exchanger has been simplified.	To reduce the probability of a failure during launch countdown.

Table B-3. S-IVB Significant Configuration Changes

SYSTEM	CHANGE	REASON
Propellant Utilization	Variable position PU valve replaced with two position (4.5 and 5.0 EMR) valve.	Increased flight reliability by removing PU Electronics Assembly control over EMR valve.
	Elimination of the LOX depletion cutoff function.	Eliminates single point failure which could cause premature engine shutdown.
Pneumatic Control	Utilize newly designed pneumatic power control module.	Provide regulator with improved regulation characteristics.
Instrumentation	Modification of oxidizer and fuel flowmeters.	Rework flowmeter coils to insure compatability with turbines.
Electrical	Add redundant battery heater control thermostat to switch heater power "on" at 50°F, and "off" at 70°F.	Failure of heater control sensor could cause launch delay or loss of secondary mission if batteries should exceed redline requirements.
	Parallel relay modules for switch selector compatibility.	Reduce output loads of switch selector to conform to ICD requirement.
	Sequence change which positions the repressurization system mode select "on" (ambient mode) until Time Base 6 plus 5 seconds.	Eliminates single point failure which could cause the cold helium spheres to "blow down" through the LOX repress system and possibly overpressurize the LOX tank.

Table B-4. IU Significant Configuration Changes

SYSTEM	CHANGE	REASON
Environmental Control System	Material used for thermal radiation shroud has been modified to incorporate a stronger nylon core and a new Tedlar back-up film.	Increased reliability of shroud.
	The Methanol/Water (M/W) coolant used in the Environmental Control System has been changed to Oronite Flo-Cool 100.	Oronite Flo-Cool 100 eliminates operational problems associated with M/W coolant.
Networks	Added capability to inhibit Command and Communication System (CCS) 1.024 MHz.	Signal interference on AS-508 resulted from IU/CCS and LM/USB having same nominal center frequencies.
	Added capability to turn the Flight Control Computer (FCC) off before loss of the second IU battery.	Unexpected velocity change on AS-508 which resulted from IU battery decay which caused erroneous control system response.
	Add redundant power to IU switch selector, mission critical discretes to LVDA, FCC Switch Points, Spacecraft control of Saturn and FCC S-II burn mode. Provide voting circuit for FCC S-II burn mode.	Increase probability of completing the prime mission in case of 6D10 or 6D30 battery failure.
Instrumentation and Communications	Three platform accelerometer measurements were added to the DF-1 telemetry link: H17-603 Z accelerometer H21-603 X accelerometer H25-603 Y accelerometer	Accommodation for these measurements became available when the following S-IVB measurements were deleted from the DF-1 link: A15-424 D1-401 XD3-403 E99-411 E100-411
Flight Program	Time Base 6c (TB6c) can now be initiated by the detection of any two of the four no thrust indications as well as the TLI inhibit discrete.	To allow the program to return to TB5 from TB6 if S-IVB mainstage thrust is not achieved.
	Time Base 6d added. (Initiated by DCS command.)	Eliminates issuance of high density generalized switch selector commands in an S-IVB chilldown sequence failure contingency.

Table B-5. Spacecraft Significant Configuration Changes

SYSTEM	CHANGE	REASON
Electric Power Systems	A third cryogenic oxygen storage tank was installed in sector 1 of the Service Module (SM) to be used simultaneously with tanks 1 and 2 located in sector 4.	To provide an additional oxygen supply for the fuel cells.
	An isolation valve was installed between SM cryogenic oxygen tanks 2 and 3.	Prevents oxygen flowing from tank 3 to the fuel cells in the event of a leak in any of the cells, but allows flow to the Environmental Control System.
	Auxiliary 400 ampere-hour battery installed on the SM aft bulkhead in sector 4.	To provide source of electrical power in the event of a cryogenic subsystem failure.
SM Cryogenic Oxygen Tanks	1. Destratification fans eliminated. 2. Quantity gauging probe material changed from aluminum to stainless steel. 3. Heater changed from two parallel-connected elements to three parallel-connected elements with separate control of one element. 4. Filter relocated from the tank discharge to an external line. 5. Heater thermal switches were removed. 6. Internal wiring insulated with magnesium oxide and sheathed with stainless steel.	To reduce potential ignition sources in the high pressure system.

APPROVAL

SATURN V LAUNCH VEHICLE FLIGHT EVALUATION REPORT

AS-509, APOLLO 14 MISSION

By Saturn Flight Evaluation Working Group

The information in this report has been reviewed for security classification. Review of any information concerning Department of Defense or Atomic Energy Commission programs has been made by the MSFC Security Classification Officer. The highest classification has been determined to be unclassified.

Stanley L. Fragge
Security Classification Officer

This report has been reviewed and approved for technical accuracy.

George H. McKay, Jr.
Chairman, Saturn Flight Evaluation Working Group

Herman K. Weidner
Director, Science and Engineering

Richard G. Smith
Saturn Program Manager

END

DATE

FILMED

DEC 14 1973